FACTORS THAT AFFECT THE EXTENSION OF DENDRITES AND THE EXPRESSION OF NICOTINIC ACETYLCHOLINE RECEPTORS BY RAT PERIPHERAL NEURONS.

By

Paul De Koninck

Department of Biology
McGill University
Montréal, Québec, Canada

June 1995

A Thesis Submitted to the
Faculty of Graduate Studies and Research
in partial fulfilment of the requirements
for the degree of Doctor of Philosophy

ISBN 0-612-08091-9

Canada

à Catherine

ABSTRACT

The establishment of neuronal polarity constitutes a central phase in neuronal development and synaptogenesis. In my thesis, I study factors that regulate the development of neuronal polarity and its relationship with neurotransmitter receptor expression. For my experiments, I have investigated the development of sensory neurons from neonatal rat nodose ganglia in culture. Sensory neurons have a pseudo-unipolar morphology, do not extend dendrites, and are devoid of synaptic connections on their somata. However, nodose neurons form synapses *de novo* in cultures, and I show that the neurons have retained the ability to extend dendrites. Extrinsic factors control dendrite extension by these neurons: the ganglionic satellite cells inhibit the growth of dendrites and induce the neurons to develop a unipolar morphology. In the absence of satellite cells, nodose neurons establish a new multipolar morphology and, in response to nerve growth factor (NGF), extend several dendrites. However, brain-derived neurotrophic factor (BDNF) and neurotrophin-3 (NT-3) do not induce the neurons to extend dendrites, but promote the expression of properties typical of nodose neurons *in vivo*.

As nodose neurons acquire a new dendritic-axonal polarity in the presence of NGF, they increase the density of functional neuronal nicotinic acetylcholine receptors (nAChRs) on their somato-dendritic domains. To learn more about the relationship between dendrites extension and nAChR gene expression, I have examined the changes in transcript levels of nAChR subunits in neonatal rat sympathetic neurons developing in culture. I show that the developmental pattern of nAChR subunit expression in the cultured neurons follows closely that of sympathetic neurons developing *in vivo*, with the exception of one specific subunit, α_7. I show that the increase in α_3 mRNA levels correlates well with an increase in the density of functional nAChRs on the neurons. In addition, my results suggest that these increases are regulated by mechanisms intrinsic to neonatal sympathetic neurons. On the other hand, the changes in α_7 gene expression, which correlate with changes in α-bungarotoxin binding, are activity-dependent and regulated by a calcium/calmodulin-dependent protein kinase pathway. The results presented in this thesis provide insights on how neurons are influenced in their extension of dendrites and how this extension affects neurotransmitter receptor expression.

RÉSUMÉ

L'établissement de la polarité neuronale représente une étape critique du développement neuronal et de la synaptogénèse. Dans ma thèse, j'étudie les facteurs qui contrôlent le développement de la polarité neuronale et son lien avec l'expression des récepteurs de neurotransmetteurs. Les neurones sensoriels ont une morphologie pseudo-unipolaire, ne développent pas de dendrites et sont dénués de contacts synaptiques sur leur corps cellulaire. Pour mes expériences, j'ai suivi en culture le développement de neurones sensoriels provenant du ganglion nodose chez le rat nouveau-né, car ces neurones forment des synapses *de novo* lorsqu'ils se développent en culture. En fait, je démontre qu'ils ont la capacité de croître des dendrites, et que des facteurs externes contrôlent cette croissance. Les cellules ganglionnaires satellites inhibent la croissance dendritique et incitent les neurones à acquérir une morphologie unipolaire. Cependant, en l'absence de cellules satellites, les neurones du nodose acquièrent une nouvelle morphologie multipolaire et, en réponse à la neurotrophine, NGF, développent plusieurs dendrites. En revanche, les neurotrophines BDNF et NT-3 n'induisent pas ces neurones à croître des dendrites, mais stimulent plutôt l'expression de caractéristiques propres aux neurones sensoriels du ganglion nodose *in vivo*.

Lorsque les neurones du nodose développent une nouvelle polarité dendritique-axonale, en présence de la NGF, ils augmentent la densité fonctionnelle de récepteurs nicotiniques de l'acétylcholine (nAChRs) sur leur membrane somato-dendritique. Pour mieux comprendre le lien entre la croissance dendritique et l'expression des gènes du nAChR, j'ai examiné les changements de niveau des ARN messagers (ARNm) pour les sous-unités du nAChR dans les neurones sympathiques du rat nouveau-né en culture. Je montre que le patron d'expression des gènes du nAChR dans les neurones en culture suit de près celui qui prévaut dans les neurones sympathiques se développant *in vivo*, à l'exception d'un gène, α_7. Je montre également que l'augmentation du niveau d'ARNm pour α_3 est en corrélation avec l'augmentation de la densité fonctionnelle de nAChRs sur les neurones. De plus, mes résultats suggèrent que ces augmentations sont contrôlées par des mécanismes intrinsèques aux neurones sympathiques post-nataux. Cependant, les changements de niveaux de l'ARNm α_7, qui sont en corrélation avec les changements de niveaux du récepteur nicotinique de la α-bungarotoxine, dépendent de l'activité neuronale et sont contrôlés par un mécanisme impliquant l'activité de la protéine kinase calcium/calmoduline-dépendente. Les résultats présentés dans ma thèse mettent en lumière certains mécanismes qui contrôlent la croissance des dendrites et la façon dont celle-ci influence l'expression des récepteurs de neurotransmetteurs.

REMERCIEMENTS

Je dois beaucoup à mon co-directeur de thèse, le Dr. Ellis Cooper. Je remercie Ellis pour m'avoir transmis une curiosité et une rigueur scientifique et pour m'avoir appris (du moins essayé) à rechercher la simplicité. J'ai eu la chance de jouir d'une grande liberté durant mes six années dans le laboratoire, ce qui a rendu mon doctorat, à la fois, très agréable et formateur. Je remercie Ellis pour sa disponibilité, sa franchise, son amitié et les longues heures passées à corriger mon anglais trébuchant. Bref, je considère avoir reçu, de la part d'Ellis, une supervision exemplaire pour une préparation à une carrière de scientifique, et je lui en suis très reconnaissant. Enfin, Ellis m'a appris une autre chose: éviter de remercier trop de gens, car cela amenuise ceux qui comptent vraiment! J'essayerai donc de me limiter.

Je tiens à remercier mon second co-directeur, le Dr. Salvatore Carbonetto, qui m'a beaucoup supporté dans la démarche que j'ai entreprise lors de mon doctorat tout en me conseillant de façon juste et éclairée. J'ai de plus, développé une amitié avec Sal que je chéris beaucoup.

Dans le laboratoire du Dr. Cooper, j'ai reçu beaucoup d'aide, en particulier de la part de Brigitte Pié, qui a toujours manifesté une énergie et un enthousiasme particuliers lorsqu'il fallait me venir en aide. Brigitte, merci pour ton expertise, ta rigueur, ton support, ton sourire et surtout ton coeur. Merci à Tom, qui a toujours montré beaucoup de disponibilité et qui a passé de longues soirées à m'aider à terminer cette thèse.

Je voudrais remercier les autres membres du laboratoire pour leur collaboration, discussions et amitié, en commençant d'abord par Sarah avec qui j'ai eu de bons moments et qui, à sa façon, m'a beaucoup appris à mon arrivée dans le laboratoire. Je ne saurai oublier Allan, qui m'a rapidement inculqué un sens de la modestie et qui, avec les années, s'est avéré un très bon et rigolo compagnon. Merci à Michel pour de longues heures de discussion autour d'une tasse de café. Merci à Misha, Andrew, Pejmun et Damian pour leur collaboration et pour avoir corrigé mes textes. Merci à Pejmun aussi pour son aide avec les grenouilles! Merci à Lucie pour son aide avec la synaptophysine. Un gros merci à Adam qui m'a dépanné plus d'une fois avec les ordinateurs et avec son logiciel Patchkit.

Merci aussi à Frank, qui m'a bien conseillé avec la biologie moléculaire.

Je tiens à remercier le Dr. Alvin Shrier pour son support et son amitié et les Drs. John Orlowski, John White et Robert Levine pour leurs judicieux conseils.

Je tiens aussi à remercier tous mes amis hors de McGill qui m'ont encouragé, supporté et amusé pendant ces années et qui m'ont amené camper pour m'empêcher de trop travailler. Je dois, bien sûr, beaucoup à mes parents qui, en plus de leur support et leurs encouragements, m'ont transmis la richesse de leurs valeurs.

Enfin je termine avec les plus importants remerciements, puisqu'ils s'adressent à la personne la plus importante dans ma vie, Catherine, mon épouse. Je te dédie cette thèse, Catherine, pour ton amour, ce qui résume tous les efforts et sacrifices que tu as faits pour m'aider à terminer cette thèse. Sans oublier un gros merci pour ton travail colossal à préparer ma bibliographie.

CONTRIBUTION TO ORIGINAL SCIENCE

In chapter 3, I demonstrate, for the first time, that neonatal rat sensory neurons have the ability to extend dendrites in culture, and that two extrinsic influences control dendritic outgrowth from these neurons. Ganglionic satellite cells inhibit their growth, whereas NGF stimulates their growth. I show that satellite cells induce nodose neurons to acquire a unipolar morphology through a direct contact mechanism. These results indicate that neuronal polarity is regulated, in part, by extrinsic factors, and provide clues to the mechanisms that control neuronal polarity.

In chapter 4, I show a correlation between the extension of dendrites by nodose neurons and an increase in the functional expression of nAChRs, and demonstrate that the neurons express functional nAChRs on their somatodendritic domains. In addition, I show that nodose neurons develop clusters of synaptophysin immunoreactivity in axonal-terminal-like or varicosities-like structures as they develop in culture. These results suggest that sensory neurons can develop a fully differentiated dendritic-axonal polarity.

In chapter 5, I demonstrate that P1 rat nodose neurons can grow in culture in the absence of exogenous sources of neurotrophins. However, I show that nodose neurons contain significant transcript levels for the 4 known neurotrophin receptors, $p75^{LNGFR}$, *trk*A, *trk*B and *trk*C. I demonstrate that neurotrophins have distinct effects on the differentiation of nodose neurons: while NGF promotes dendrite outgrowth and functional nAChR expression by the neurons, BDNF and NT-3 promote capsaicin sensitivity, a characteristic of C-type sensory neurons. My results provide preliminary evidence for co-expression of multiple *trk* receptors within individual nodose neurons and for distinct effects mediated by different neurotrophins on individual neurons.

In chapter 6, I demonstrate that the expression of 4 nAChR transcripts (α_3, α_5, β_2 and β_4) in cultured neonatal rat superior cervical ganglion neurons occurs independent of innervation and membrane depolarization. In addition, I provide evidence for the lack of regulation by protein kinase C and A, and tyrosine kinases on the expression of nAChR transcripts. On the other hand, I demonstrate that the expression of α_7 transcripts and α-BTX-nAChRs are up-regulated by membrane depolarization. I identify part of the

signalling pathway that regulates α_7 in showing that Ca^{2+} influx through L-type Ca^{2+} channels and CaM kinase activity are mediating the effects of membrane depolarization. These results provide evidence that nAChR subunit expression is differentially regulated. One novel aspect of this study is that it links membrane depolarization with neurotransmitter receptor expression through a CaM kinase pathway. The identification of a CaM kinase mechanism in regulating expression of a neurotransmitter receptor offers a potential mechanism for some forms of synaptic plasticity.

In Chapter 7, I show a correlation between the specific increase in α_3 transcript levels and an increase in ACh-evoked current densities on cultured SCG neurons. In contrast, I show that changes in α_7 transcript levels have no consequences on the macroscopic ACh-evoked currents on SCG neurons.

All of the experiments presented in this thesis were performed by myself. The experiment presented in Figure 7.6 was done in collaboration with Ali Haghighi.

TABLE OF CONTENTS

Chapter 1

Introduction

INTRODUCTION

The complex morphologies of nerve cells have fascinated many investigators for over 150 years. In the early age of neuroscience, the unusual shapes of neurons had, in fact, represented an obstacle to the appreciation of the cellular nature of the nervous system. Neurons make use of their complex morphology to establish thousands of connections with other distant neurons. These connections, or synapses, generally form between the specialized processes of two neurons: the axon terminals and the dendrites. During development, neurons extend these processes in various, but specific, directions; these processes, then, encounter numerous axons and dendrites from other nerve cells. Remarkably, neurons appear to have the ability to choose to form synapses only with a specific subsets of other neurons. Among the numerous elements that determine the specificity of neuronal connections, a major one is the chemical compatibility between nerve cells. Indeed, neurons use various neurotransmitters and neurotransmitter receptors to transmit information from one to another. Furthermore, each neuron releases a particular set of neurotransmitters and possesses a few specific types of neurotransmitter receptors. Therefore, for neurons to communicate with each other, the presynaptically released neurotransmitter molecule must recognize its specific chemical receptor on the postsynaptic membrane.

It is unknown why neurons adopt a given shape or synthesize a particular set of neurotransmitters or neurotransmitter receptors. The synthesis of these molecules is often initiated by the transcription of their genes in the nucleus, but these molecules typically act far away from that nucleus, in the remote axonal terminals and dendritic branches. Thus, the morphologies that neurons adopt during development will greatly influence the development of synaptic connections and the transmission of signals from neuron to neuron.

In my thesis, I have studied factors that control the morphologies of neurons. More specifically, I have investigated the extrinsic influences that govern the initiation of dendrites and examined the relationship between the extension of dendrites and the expression of neurotransmitter receptors. My experiments address several topics in developmental and cellular neurobiology; to keep this introduction from being too long, I have restrained myself to discuss only the topics that are immediately relevant to my experiments. Unfortunately, many interesting and important subjects receive only brief attention, although some are discussed later in the following chapters or in one of the 3 appendices. Furthermore, in attempt to write an introduction for non-experts on these different topics, I have made several generalizations and simplifications that experts will easily recognize.

I have organized this introduction as follows: First, I discuss the essence of neuronal polarity by highlighting the differences between axons and dendrites at the cellular and physiological level. Second, I briefly review experiments that have addressed the intrinsic mechanisms and extrinsic influences that govern the establishment of neuronal polarity. Third, I briefly review what is known about factors that regulate the expression of neurotransmitter receptors on neurons. As my experiments addressed the expression of neuronal nicotinic acetylcholine receptors (nAChRs) on peripheral neurons, I have largely restricted this section to the expression of these members of the ligand-gated ion channel family on peripheral neurons.

NEURONAL POLARITY

With his remarkable sketch of a large motor neuron, Dieters was the first, in 1865, to identify the neuron's axon and dendrites, in what he described as the "axis cylinder" and the "protoplasmic prolongations" (Shepherd, 1994). Three decades later, Cajal formulated the "Law of Dynamic Polarization" which stipulated that "the transmission of the nervous impulse is always from the dendritic branches and the cell body to the axon or functional process". The cell body and its dendritic prolongations would be the "receptor apparatus" whereas the axon would be the "emission apparatus" and the nerve terminals the "apparatus of distribution" (Cajal, 1989). His proposition provided the basis of what is

now the concept of "neuronal polarity". With the discovery of dendro-dendritic and axo-axonic synapses, initially referred to as "unconventional" or "unusual" synapses, the law of dynamic polarization had to be modified (Shepherd, 1994). However, for most neurons, the axon is primarily concerned with conduction and transmission of information, while dendrites are primarily concerned with receiving information. From a cell biological point of view, neurons are highly polarized, and axons and dendrites have fundamentally different structures. Accordingly, the establishment of neuronal polarity is a critical stage of neuronal development, and has important consequences on the construction of complex neuronal circuitry.

Dendrites

Dendrites appear like extensions of the perikaryon. Generally, multiple dendrites originate from the cell body as thick tapering unmyelinated processes that have irregular contours and specialized appendages. They ramify by branching at acute angles, usually subdividing into branches smaller than the parent stem. Typically, their ramifications are confined to the vicinity of the cell body (Peters *et al.*, 1991). The surface area of dendrites is commonly greater than that of the perikaryon; for instance, the surface area of the dendrites of the dentate granule cells is approximately 12 times greater than that of the cell body (Desmond and Levy, 1982). In the central nervous system (CNS), the majority of synapses form on dendrites.

The classical view of dendrites has been that they are electrically passive structures that funnel synaptic potentials to the soma and axon hillock, the site of action potential initiation. (Eccles, 1964; Rall, 1970). However, dendrites are now believed to be active structures, capable of actively propagating action potentials, controlling internal free calcium (Ca^{2+}) levels, modulating synaptic transmission, and even hosting protein synthesis (Steward and Banker, 1992; Bliss and Collingridge, 1993; Stuart and Sakmann, 1994; Regehr and Tank, 1994). In order to assimilate synaptic inputs and translate them into short- and long-term responses, dendrites possess elements that can adapt quickly to changes in synaptic activity. They have voltage-dependent ion channels that sense and control the neuron's state of excitability. Dendrites have organelles and proteins that can

buffer or release Ca^{2+} almost instantaneously, and enzymes that respond to rapid changes in Ca^{2+} levels thereby modifying locally the receptive properties of the postsynaptic membrane.

Cytoplasmic content

The original denomination of dendrites by Dieters as protoplasmic prolongations is accurate in that dendrites appear metabolically continuous with the cell body; it is sometimes impossible to delineate, even with electron microscopy (EM), where the cell body ends and where dendrites begin (Peters *et al.*, 1991). Indeed, the rough endoplasmic reticulum (RER), ribosomes and the Golgi complex extend into dendrites for some distance (Bartlett and Banker, 1984a,b; Peters *et al.*, 1991). The dendritic cytoskeleton is particularly enriched in microtubules. These microtubules are polarized in both orientations and linked together by the microtubule-associated protein 2 (MAP2) (Bernhardt and Matus, 1984; Caceres *et al.*, 1984; Baas *et al.*, 1988; Burton, 1988; Peters *et al.*, 1991). An intriguing observation in dendritic cytoplasm is the presence of RNA and even some mRNAs, which have been shown to be actively transported relatively far into distal dendrites (Davis *et al.*, 1987, 1990). Notable examples of dendritic mRNAs are those of MAP2, the α subunit of the multifunctional Ca^{2+}/calmodulin-dependent protein kinase (CaM kinase II), the immediate early gene *Arc*, and a small non-coding RNA, Neural BC1 (Garner *et al.*, 1988; Bruckenstein *et al.*, 1990; Kleinman *et al.*, 1990; Tiedge *et al.*, 1991; Chicurel *et al.*, 1993; Lyford *et al.*, 1995). The presence within dendrites of these mRNAs, which code for proteins associated with neuronal polarity or synaptic function, suggests that 1) protein synthesis occurs within dendrites and 2) that local control of protein synthesis is used as a mechanism to modulate synaptic interactions. The possibility of dendritic translation is supported by the presence of a synthetic machinery within dendrites, including polyribosomes, Golgi apparatus and the "spine apparatus" or "cisternae" that are often observed with EM at the base of dendritic spines (Steward and Falk, 1986; Steward and Reeves, 1988). In addition, Steward and colleagues have provided further evidence of dendritic translation of mRNA to protein by demonstrating

the incorporation of radiolabelled amino acids within dendrites of cultured hippocampal neurons and within preparations of hippocampal synaptosomes (Rao and Steward, 1991; Torre and Steward, 1992; Steward and Banker, 1992).

Dendritic spines and surface domains

Dendrites can be covered with protuberances or spines that are typically "mushroom" shaped, but that can have a wide variety of other shapes, ranging from short and stubby, to long and thin. The density of spines varies for different neuronal types, as well as along the length of a given dendrite. For example, a layer 5 pyramidal cell in the visual cortex may have up to 15000 spines, averaging about two spines per micrometer length of dendrite (Larkman, 1991). Each of these spines commonly receive a single excitatory synapse. The spine contains a diffuse electron dense structure stretching from the plasma membrane into the cytoplasm that is referred to as the postsynaptic density (Peters *et al.*, 1991). This dense structure of proteins develops in close apposition to presynaptic terminals, and contains the basic elements for the reception and transmission of synaptic signals. It contains ligand-gated ion channels that mediate synaptic currents, and enzymes such as CaM kinases that modulate synaptic transmission. Postsynaptic densities are also localized outside dendritic spines, throughout somatodendritic domains, and are anchored by structural proteins, such actin, spectrin and tubulin.

Although spines appear to increase the surface area of dendrites significantly, their role seems not simply to provide more postsynaptic membrane but rather to help modulate synaptic transmission (Koch and Zador, 1993). Their shape have led some to propose that the high resistance of the spine stem might sculpt the electrical signal generated by the synapse (Chang, 1952). Thus, the spine stem resistance may be used physiologically to control the relative weights of synaptic inputs from different afferent sources (Rall, 1970). The presence of actin filaments at the spine base suggests that its shape may be changed to control the resistance of the spine neck (Crick, 1982). However, our current understanding of the plasticity of synaptic transmission, with the key role of Ca^{2+} and its linked effectors, suggests that dendritic spines may rather serve to concentrate the biochemical elements that modulate synaptic activity. Indeed, the size of a dendritic spine

approaches the molecular scale: the estimated volume of a rat CA1 pyramidal cell spine is roughly 0.06 μm^3 (Harris and Stevens; 1989); in such volume, the resting levels of free Ca^{2+} (e.g. 80-100 nM) is reached with approximately only 4 Ca^{2+} ions.

Modulation of synaptic transmission in dendrites

A common link to synaptic modulation events in dendrites appears to be the generation of intracellular waves of free Ca^{2+} (Kennedy, 1989; Schulman, 1993; Regehr and Tank, 1994; Clapham, 1995). The primary source of Ca^{2+} during synaptic activity comes from the extracellular solution. Ca^{2+} flows inside neurons mainly through 2 classes of ion channels: voltage-gated Ca^{2+} channels and ligand-gated ion channels that are permeable to Ca^{2+}, particularly the N-methyl-D-aspartate (NMDA) and nicotinic acetylcholine (nACh) receptors. Internal stores of Ca^{2+}, such as the smooth endoplasmic reticulum, also play a significant role in dendritic Ca^{2+} dynamics (Regehr and Tank, 1994). A local rise in Ca^{2+} concentration ($[Ca^{2+}]$) can trigger and regulate the activities of a variety of enzymes, receptors, ion channels, regulatory proteins and structural proteins. This broad scope of effects by Ca^{2+} requires an assortment of Ca^{2+} effector systems, including ATPases, ion channels, proteases, phospholipases, kinases and phosphatases, that can respond to changes in Ca^{2+} levels within milliseconds to minutes (Kennedy, 1989; Schulman, 1993). Ca^{2+}-linked signalling cascades within dendrites can produce long-term changes in neuronal function that underlie synaptic plasticity.

The best characterized phenomena of synaptic plasticity are those of long-term potentiation (LTP) and long-term depression (LTD), which represent changes in synaptic efficacy that may underlie learning and memory (Bliss and Collingridge, 1993; Linden, 1994; Bear and Malenka, 1994). LTP and LTD are respectively elicited by high- or low-frequency stimulation of a presynaptic neuron. Although these changes in synaptic efficacy are opposite, they both require, in the brain, the activation of postsynaptic NMDA receptors, as well as a rise in $[Ca^{2+}]$ in the dendritic spine. The decoding of these Ca^{2+} influxes by Ca^{2+}-linked protein kinases and phosphatases, such as CaM kinase II and calcineurin, may determine the elicited changes in synaptic efficacy (Lisman, 1994). CaM kinase II is one of the most abundant protein in postsynaptic densities. Its biochemical

properties (see appendix 3) make it an attractive candidate for decoding synaptic signals and translating them into biochemical signals, that ultimately lead to gene expression. Indeed, transynaptic signals inducing long-term responses in neurons are bound to involve changes in gene expression (Goelet *et al.*, 1986; Frey *et al.*, 1993; Nguyen *et al.*, 1994). During synaptic activity, oscillations in $[Ca^{2+}]$ are also generated at the base of dendrites and in the perikaryon. These waves of Ca^{2+} are, in part, triggered by the activity of L-type Ca^{2+} channels, which preferentially target to those membrane domains (Ahlijanian *et al.*, 1990; Westenbroek *et al.*, 1990; Regehr and Tank, 1994). The slowly inactivating Ca^{2+} influxes through L-type Ca^{2+} channels at depolarized potentials may provide a link between activity in distal dendrites and changes in gene expression (Murphy *et al.*, 1991; Ghosh and Greenberg, 1995). Little is known about the relationship between synaptic activity and the expression of proteins involved in synaptic transmission. In chapter 6, I propose a novel link between neuronal activity and neurotransmitter receptor expression. Potential mechanisms of activity-mediated changes in gene expression in neurons are briefly discussed in appendix 2.

Axons

A single axon originates generally from the perikaryon or, occasionally, from a dendrite. The axon can be discerned morphologically from dendrites by its cylindrical shape and smooth contours. At its site of origin, the axon is commonly thinner than dendrites. The length of axons varies substantially; certain axons project to structures located centimeters away from the cell body, while others extend only a few microns, remaining in the vicinity of the perikaryon. The axon is not a unique process; it ramifies extensively by branching at obtuse angles, usually giving rise to collaterals of the same diameter as the parent stem. Some axonal collaterals are "recurrent" and grow back to the perikaryon, while most collaterals ramify in the terminal field of the axon, giving rise to a dense arborization of very fine branches that form synaptic contacts with their cellular targets. The axon and its collaterals can be wrapped with a sheath of myelin of various thickness that is produced by the glial cells (Hammond and Tritsch, 1990; Peters *et al.*,

1991).

The principal characteristic of the axon is its ability to act as a "transmission cable" by propagating all or none action potentials over long distances up to its terminals to evoke transmitter release. However, the axon has additional functions: it can modulate synaptic transmission, release various factors, retrogradely transport signals from its targets and also receive synaptic contacts from other neurons.

Cytoplasmic content

The cytoskeletal filamentous elements in axons are packed more densely than those in dendrites. Axons are enriched in actin filaments and neurofilaments (Peters *et al.*, 1991), the latter being heavily phosphorylated (Sternberger and Sternberger, 1983; Lein and Higgins, 1989). Unlike in dendrites, the microtubules of axons all have the same orientation with their plus-end distal (Baas *et al.*, 1988; Burton, 1988), and these microtubules are associated with abundant tau and MAP 3/4 (Huber *et al.*, 1985; Bernhardt *et al.*, 1985; Goslin *et al.*, 1988, 1990; Kosik and Finch, 1987; Dotti *et al.*, 1987; Binder *et al.*, 1985). A lipid linked protein termed GAP-43 (growth-associated protein-43), whose function is not fully understood, is enriched in the axon, particularly in its growth cones (Goslin *et al.*, 1988; 1990).

The axon appears to exclude organelles involved in protein synthesis and it is generally accepted that mRNAs are not transported in the axon beyond its proximal segment (Bartlett and Banker, 1984a,b; Peters *et al.*, 1991; Craig and Banker, 1994; see Litman *et al.*, 1993, 1994). However, the axon's cytoplasm is highly specialized in the bidirectional transport of vesicles that contain various proteins and peptides. Vesicles filled with neurotransmitter synthetic enzymes or neuropeptides can be transported up to hundreds of millimeters a day by mechanisms of fast axonal anterograde transport. On the other hand, cytoskeletal proteins such as tubulin, actin and neurofilaments are transported slowly and move at a rate of a few millimeters per day. The axon also retrogradely transports molecules, such as nerve growth factor (NGF), that are taken up at the nerve terminals. Retrograde transport is achieved at rates similar to fast anterograde transport. The force-

generating proteins that mediate these transports include kinesin and dynein; these proteins bind to microtubules and travel along their length using energy derived from ATP hydrolysis. Kinesin binds to vesicles and carries them along the plus-end of microtubule tracks toward the axonal terminals. In contrast, dynein moves toward the minus-end of microtubules and serves as a retrograde carrier (Vallee and Bloom, 1991; Vale *et al.*, 1992).

Axonal terminals, varicosities and surface domains

The axonal membrane has numerous specialized domains distributed in specific regions along its length. Many axons begin with a cone-shaped axon hillock that contains clusters of voltage-dependent Na^+ channels (Westenbroek *et al.*, 1989); these clusters generate the action potentials. The nodal portions of myelinated axons, known as nodes of Ranvier, also contain dense clusters of Na^+ channels which serve to propagate the action potentials along the axon to the nerve terminals (Westenbroek *et al.*, 1989).

The axonal terminal is a distinct domain of the axon. Terminals are filled with synaptic vesicles that are anchored to a cytoskeletal matrix. They also contain large-dense core vesicles, mitochondria, endosomes and coated vesicles (Peters *et al.*, 1991). Elements of the smooth endoplasmic reticulum in the terminals act as intracellular Ca^{2+} stores. The synaptic vesicle membranes and the plasma membrane contain a collection of proteins, such as synapsins, synaptophysin and syntaxin, that control synaptic vesicle trafficking, docking or fusion (Benneth and Scheller, 1994). These processes are highly regulated by phosphorylation events achieved by protein kinases, such as CaM kinases and protein kinase C (PKC). The differential activities of these enzymes contribute to the modulation of synaptic vesicle release and to the plasticity of synaptic transmission (Bliss and Collingridge, 1993; Schulman, 1993; Chapman *et al.*, 1995).

An electron dense domain at the membrane serves as the site of vesicle contact for exocytosis and is termed the active zone. Ca^{2+} influx is the primary signal that initiates the synaptic release mechanism (Dodge and Rahamimoff, 1967; Katz and Miledi, 1968); at the neuromuscular junction, N-type Ca^{2+} channels and Ca^{2+}-gated K^+ channels are

clustered in line with the postsynaptic neurotransmitter receptors to provide rapid activation of postsynaptic receptors upon fusion of vesicles (Robitaille *et al.*, 1990, 1993; Cohen *et al.*, 1991). Unmyelinated axons of autonomic neurons form a dense plexus of fibers on target smooth muscle and release neurotransmitters from axonal varicosities which appear like protrusions of the axon spaced every 3 to 5 μm. These varicosities do not contain electron dense active zones, suggesting no preferential orientation of synaptic vesicle exocytosis (Peters *et al.*, 1991).

In summary, axons and dendrites have fundamental differences in their cytoskeletal organization, membrane domains and physiological properties. The extension of dendrites provides a neuron with a greater postsynaptic surface area, but more importantly, with a subcellular domain that is specialized in receiving synapses and in modulating synaptic information. The complexity of dendritic patterns contributes to the particular function of a neuron in the circuits to which it belongs. Consequently, determining the mechanisms that control dendrite initiation, elongation, branching patterns and maturation is vital to the understanding of brain functions.

THE ESTABLISHMENT OF NEURONAL POLARITY

To develop a dendritic-axonal polarity, neurons need highly efficient mechanisms of sorting and targeting of proteins. An appropriate targeting of cytoskeletal or membrane proteins is critical for the establishment and maintenance of neuronal polarity. Learning how cellular constituents come to be differentially distributed within neurons will help to elucidate how neuronal polarity develops.

A major advance in the study of neuronal polarity was the demonstration by Banker and colleagues that many of the morphological and molecular distinctions between axons and dendrites of hippocampal neurons are reproduced when embryonic hippocampal neurons develop in culture (Bartlett and Banker, 1984a,b; Dotti *et al.*, 1988). Soon after plating, these neurons extend several minor processes; after 1-2 days, one of those processes becomes longer, accelerates its growth and develops into an axon. At day 4, the minor processes differentiate into dendrites. By then, both types of processes have

segregated their specific cytoskeletal constituents, such as MAP2 or GAP-43. The fact that embryonic hippocampal neurons readily establish a dendritic-axonal polarity in culture suggests that an endogenous program governs their development (Craig and Banker, 1994). Sympathetic neurons from embryonic or neonatal rat superior cervical ganglia (SCG) develop a similar dendritic-axonal polarity in culture (Landis, 1976; Peng *et al.*, 1986; Higgins *et al.*, 1991). *In vivo*, both hippocampal and SCG neurons exhibit primarily "classical" synaptic interactions; in culture, their axons are consistently presynaptic and their dendrites postsynaptic (Bartlett and Banker, 1984b; Furshpan *et al.*, 1986). Neurons obtained from other regions of the nervous system, including the cerebellum and the mesencephalon have also been shown to develop neuronal polarity in culture (Kosik and Finch, 1987; Autillo-Touati *et al.*, 1988; Ferreira and Caceres, 1989; Caceres and Kosik, 1990; Lafont *et al.*, 1992).

Because of the advantages of cell culture for cell biological studies, these culture systems have thus become the method of choice to study the mechanisms that govern neuronal polarity. The ability to visualize living cells, to alter their intrinsic properties, or to manipulate their environment has provided a preliminary understanding of the intrinsic mechanisms and extrinsic factors that control the establishment of neuronal polarity (Craig *et al.*, 1992; Craig and Banker, 1994).

Intrinsic mechanisms of neuronal polarity

The cytoskeletal properties of axons and dendrites contribute to their differential growth, maintenance and molecular targeting. The orientation of microtubules is different in axons versus dendrites: while in the axon they are all oriented plus-end distal, in dendrites both microtubule orientations exist (Baas *et al.*, 1988). Consequently, proteins and organelles that preferentially travel on microtubules oriented towards the minus end could target specifically to dendrites. Little is known, however, about the specific signals that proteins use to travel on microtubules. Molecules such as dynein, which moves toward the minus end of microtubules, could specifically carry vesicles within dendrites. Differentially targeted proteins may contain amino acid sequences that allow them

selective incorporation into distinct populations of transport vesicles.

Neuro-specific microtubule-associated proteins, such as MAP2 and tau are believed to contribute to the support of neuronal processes by making microtubules longer, more stable and stiffer than in non-neuronal cells. MAP2 and tau cause microtubules to bundle and may stabilize the emerging microtubules behind the growth cone (Kelly and Grote, 1993; Matus, 1994). Caceres and Kosik (1990) have shown that inhibition of tau expression by cultured cerebellar neurons with antisense oligonucleotides prevents the initiation of axonal growth, or causes the retraction of a mature axon. "Dendrite-like" minor processes appeared unaffected by this treatment, suggesting that tau promotes primarily axonal growth. Similar antisense experiments were performed for MAP2 on these neurons; in this case, the growth of all processes was prevented (Caceres *et al.*, 1992; see also Dinsmore and Solomon, 1991), suggesting that both axons and dendrites need MAP2 for their development. In fact, neurons have been shown to express MAP2 in all processes early on in culture, and to segregate MAP2 to somatodendritic compartments later on (Kosik and Finch, 1987; Craig and Banker, 1994). These results suggest that MAP2 is essential for the initiation of neurite outgrowth, while later, during neuronal maturation, it acts to stabilize dendritic microtubules (Matus, 1988, 1994). However, observations presented in Chapter 3 would seem to indicate that MAP2 may, in fact, not be essential for the initiation of axonal growth from sensory neurons.

The cross bridging of microtubules by MAP2 or tau causes a differential spacing between microtubules, which is likely to affect targeting. The space between microtubules polymerized with tau is approximately 20 nm, while it is roughly 100 nm with MAP2, which is a 4-5 fold larger protein than tau (Hirokawa *et al.*, 1988a,b; Goedert *et al.*, 1991). One possible consequence of the narrow spacing between microtubules cross-linked by tau may be the exclusion of ribosomes from the axon (Baas *et al.*, 1987).

Another mechanism of protein targeting may involve targeting of specific transcripts to dendrites and local translation (Steward and Banker, 1992). However, it is virtually unknown how local translation in dendrites is regulated; equally unknown is whether membrane proteins, such as neurotransmitter receptors, which require RER- and Golgi-like structures for translation, are synthesized in dendrites. In chapter 6, we will further discuss

this problem, after presenting evidence suggesting that ligand-gated ion channel transcripts are not targeted to dendrites.

The targeting of proteins incorporated in different surface domains can arise in two main ways. One way is by intracellular transport and insertion at specific sites. The other way is by random insertion of membrane proteins that diffuse within the lipid moiety and are trapped at specific sites by elements of the cytoplasmic cytoskeleton (Elson, 1993). The distinct cytoskeletons of dendrites and axons may provide differential anchoring of membrane proteins. Postsynaptic receptors on somatodendritic domains have been shown to cluster at synapses (Jacob *et al.*, 1984; Triller *et al.*, 1985; Loring and Zigmond, 1987; Loring *et al.*, 1988; Sargent and Pang, 1989; Craig *et al.*, 1993; Sargent and Wilson, 1995); while this process appears to be in part controlled by presynaptic contacts (Sargent and Pang, 1988, 1989; Moss and Role, 1993; Craig *et al.*, 1993), intracellular anchors are likely to contribute to the formation of postsynaptic receptor clusters. By analogy, the clustering of muscle nAChRs at the endplate is mediated, in part, by the 43K protein and the spectrin/dystrophin family of proteins (reviewed by Froehner, 1993); similar anchors could be involved in clustering neuronal ion channels.

Why is it that some neurons do not establish a dendritic-axonal polarity?

While almost all neurons in mammals establish a typical dendritic-axonal polarity, a notable exception is the sensory neuron. Mammalian sensory neurons do not extend dendrites from their cell body; sensory neuroblasts extend two axonal-like processes that fuse together during embryogenesis (Tennyson, 1965). The portion of cytoplasm remaining between the two neurites then elongates into a short and thick trunk forming a unipolar process from which the two axonal processes bifurcate (Cajal, 1955). Sensory neurons have thus a "pseudo-unipolar" morphology, with one axon growing peripherally and the other growing centrally (see Figure 1.1). The neuronal somata in sensory ganglia are totally engulfed by peri-somatic glial cells (satellite cells) and are completely devoid of synapses (Lieberman, 1976; Pannese, 1981). The satellite cells are believed to influence this developmental transition between bipolar to unipolar neurons: cultured embryonic dorsal root ganglion (DRG) neurons recapitulate this developmental transition only in the

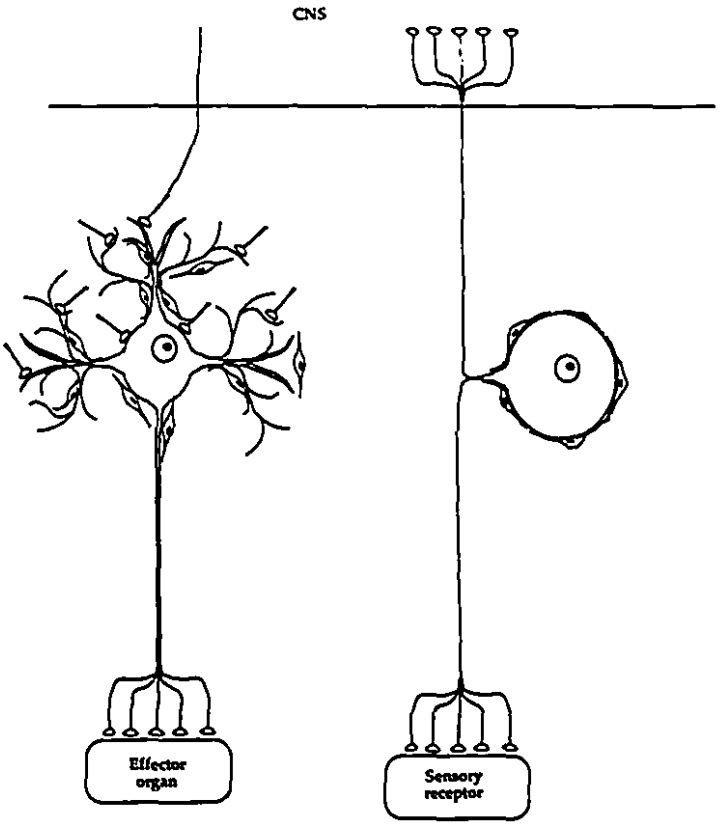

Figure 1.1. *Distinct polarities of sympathetic and sensory neurons*

Sympathetic neurons develop a typical dendritic-axonal polarity: they extend several dendrites that contain nAChRs and receive synapses; they extend one axon that innervates various effector organs. Sensory neurons do not extend dendrites from their cell body, and do not receive synapses; instead, they extend two axonal-like processes that fuse together during development, giving rise to a pseudo-unipolar morphology, with one axon growing peripherally and one growing centrally.

These striking differences in morphology provide each class of neurons with very distinct functions. Sympathetic neurons integrate synaptic potentials induced, in part, by the release of ACh onto their dendrites from pre-ganglionic neurons in the CNS. These potentials are then transmitted to the proximal axon where an all or none action potential is triggered and sent along the axon to the terminals or varicosities to evoke transmitter release onto effector organs. In contrast, in sensory neurons, a receptor potential is generated at the peripheral nerve endings, which evokes action potentials; these action potentials are then conducted along the axon to the terminals within the CNS. In sensory neurons, the cell body is, in fact, displaced from the main route of information flow and appears to play no immediate role in transferring signals from the periphery to the CNS.

presence of their satellite cells (Mudge, 1984).

The importance of satellite cells in the development of sensory neuron morphology raises the question of whether they are responsible for the lack of dendrites on these neurons. On the other hand, sensory neurons may be intrinsically incapable of elaborating dendrites. However, their common neural crest cell origin with sympathetic neurons, which elaborate a complete dendritic-axonal polarity, suggests that extrinsic influences play a role in determining the polarity of sensory neurons and their lack of dendrites. Determining the mechanisms that control the polarity of sensory neurons should provide clues to the understanding of the initial events that lead to dendrite extension and to the establishment of neuronal polarity. In Chapter 3, I demonstrate that extrinsic influences greatly affect the polarity of sensory neurons.

Extrinsic factors that influence neuronal polarity

In spite of the intrinsic ability that hippocampal or sympathetic neurons have to establish a dendritic-axonal polarity, their environment contributes significantly to the refinement of a fully differentiated polarity. For hippocampal neurons, their maturation stage in culture (>day 7), which involves dendritic branching, synaptogenesis and the formation of dendritic spines, is believed to be highly regulated by extrinsic influences, particularly cell-cell interactions (Bartlett and Banker 1984b; Fletcher *et al.*, 1991; Craig *et al.*, 1993; Fletcher *et al.*, 1994). Extrinsic influences on neuronal polarity have been particularly well characterized in cell culture, and include the extracellular matrix (ECM), cell-cell contacts, growth factors, neurotransmitters and neuronal activity. Below, I briefly review the roles that these influences play on the establishment of neuronal polarity and dendritic outgrowth.

Extracellular matrix and cell adhesion molecules

The roles that adhesion molecules play on the extension of neurites have been extensively studied (Sanes, 1989), but the number of studies that have addressed the differential effects of these molecules on axonal growth versus dendritic growth remains modest. Cell-substratum contacts, orchestrated by integrins (i.e. transmembrane receptors

that integrate extracellular and intracellular structures) or other cell-adhesion molecules, are believed to mediate differential attachment to the substrate (Burridge *et al.*, 1988; Gumbiner, 1993). Axons and dendrites are likely to use different types of focal contacts for their growth. Specific adhesion molecules, such as the L1 cell-adhesion molecule (Persohn and Schachner, 1987, 1990) and the α_8 integrin subunit, have already been shown to localize preferentially on axonal membranes (Bossy *et al.*, 1991). More of these molecules specifically located on axonal or dendritic membranes will probably be identified in the future.

Higgins and colleagues have investigated the role of ECM molecules on axonal and dendritic growth by embryonic and neonatal rat SCG neurons developing in culture. In serum-free medium, SCG neurons usually extend a single axon on a polylysine substrate, whereas laminin induces the extension of several axons that grow more rapidly (Lein and Higgins, 1989). In contrast, collagen IV and thrombospondin accelerate axonal growth without promoting multiple axons (Lein *et al.*, 1991; Osterhout *et al.*, 1992). When SCG neurons develop on a mixture of ECM proteins, in the form of a basement membrane extract, called Matrigel, they develop multiple dendrites (Lein and Higgins, 1989). These results suggest that SCG neurons possess various ECM protein receptors that mediate differential growth of neuronal processes. Lein *et al.* (1991) showed that the collagen IV-accelerated axonal growth by SCG neurons could be blocked by an $\alpha_1\beta_1$ integrin antibody (Turner *et al.*, 1989) without any effect on the laminin-induced axonal growth. Furthermore, short term axonal growth (e.g. 6 hours) on laminin can occur independent of protein synthesis, whereas collagen IV-mediated outgrowth requires protein synthesis (Lein *et al.*, 1991). However, the effects of laminin on axonal growth differ among distinct neuronal types: while it increases both the number of axons and their rate of growth in SCG neurons, it does not affect axonal number in hippocampal neurons, but only accelerates their growth (Lein *et al.*, 1992). These findings illustrate the potential diversity of interactions between ECM proteins and their receptors as well as the differential signals that these receptors may transduce to promote distinct patterns of process outgrowth.

Prochiantz and colleagues also investigated the role of ECM proteins on rat mesencephalic and striatal neurons (Chamak and Prochiantz, 1989; Prochiantz *et al.*, 1990; Lafont *et al.*, 1992), and have proposed that dendritic growth by these neurons is dependent on a tight adhesion to the substrate, whereas axonal growth is not. A similar postulate was made from experiments with cultured hippocampal neurons that elongated longer axons on substrates of decreased adhesive strength, such as laminin and tenascin, while more adhesive substrates, such as poly-ornithine or concanavalin A, promoted dendrite outgrowth (Lochter and Schachner, 1993).

Glial cells

A major source of ECM proteins and other adhesion molecules that interact with neurons *in vivo* comes from surrounding glial cells. The importance of glial cells in determining the morphology of nerve cells is well documented. Astrocytes from various regions of the brain have been shown to differentially support dendritic and axonal growth (Denis-Donini *et al.* 1984; Chamak *et al.*, 1987; Autillo-Touati *et al.*, 1988; Rousselet *et al.*, 1988, 1990; Prochiantz *et al.*, 1990; Qian *et al.*, 1992; Le Roux and Reh, 1994). In culture, postnatal day 1 (P1) rat SCG neurons do not extend dendrites in the absence of serum (Bruckenstein and Higgins, 1988a). Addition of ganglionic satellite cells (peri-somatic glia) or Schwann cells (peri-axonal glia) to these cultures induces dendritic growth by the neurons (Tropea *et al.*, 1988). Unlike P1 rat SCG neurons, P21 neurons develop dendrites in serum-free medium, indicating that, over the first 3 weeks of postnatal development *in vivo*, SCG neurons acquire an intrinsic ability to develop dendrites in culture (Bruckenstein *et al.*, 1989). The acquisition of this ability appears to be influenced by the SCG satellite cells, whose proliferation occurs mainly during the first 2-3 weeks postnatally (see Figure 1.2; Hendry and Campbell, 1976). Indeed, by growing P1 rat SCG neurons with satellite cells for 3 weeks in serum-free medium, and re-plating these neurons in the absence of satellite cells, Bruckenstein *et al.* (1989) showed that the neurons can then elaborate dendrites.

Prochiantz and colleagues have shown that astrocytes from different regions of the

brain differentially promote dendritic and axonal growth from rodent mesencephalic and striatal neurons. They proposed that homotypic astroglial cells promote dendritic growth while target-derived astrocytes promote axonal growth (Denis-Donini *et al.* 1984; Chamak *et al.*, 1987; Autillo-Touati *et al.*, 1988; Rousselet *et al.*, 1988, 1990; Prochiantz *et al.*, 1990; see also Qian *et al.*, 1992). However, others have shown that the differences in the ability of glial cells to promote axonal or dendritic growth may not be confined to either homotypic or target-derived glia (Le Roux and Reh, 1994). Furthermore, astrocytes have been shown to promote dendritic growth from SCG neurons (Johnson *et al.*, 1989), as do sciatic nerve Schwann cells or satellite cells derived from sensory ganglia; however, fibroblasts and heart cells do not (Tropea *et al.*, 1988; Johnson *et al.*, 1989). In contrast, Schwann cells induce sensory neurons to acquire a unipolar morphology in culture (Mudge, 1984). In summary, these results indicate that most glial cells express factors that affect neuronal morphologies and polarities; however, these factors produce different effects on different neuronal types.

Growth factors

The nature of the glial cell factors that affect neuronal polarity is largely unknown. In addition to adhesive interactions, diffusible factors released by glial cells are also important. For example, conditioned media from astroglial cells have been shown to promote dendritic outgrowth from various CNS neurons (Rousselet *et al.*, 1988, 1990; Le Roux and Reh, 1994). Growth factors, such as neurotrophins and cytokines, are likely candidates for mediating the effects of glial cell released factors.

Cytokines

Cytokines, which were originally identified as signalling factors in the immune system, also have important effects on developing nerve cells (Jonakait, 1993; Rothwell and Hopkins, 1995a,b). For example, cultured rat SCG neurons switch their neurotransmitter phenotype from adrenergic to cholinergic in response to leukemia inhibitory factor (LIF), a factor identical to the cholinergic differentiation factor released by heart muscle cells

(Patterson and Chun, 1977; Yamamori *et al.*, 1989). It has been shown that the presence of either serum, glial cells or basement membrane extract is essential for dendritic outgrowth from embryonic rat SCG neurons (Bruckenstein and Higgins, 1988b; Tropea *et al.*, 1988; Lein and Higgins, 1989). Lein *et al.* (1994) have identified a potential candidate that could mediate these interactions; they have shown that, in the absence of the above 3 influences, osteogenic protein-1 (OP-1), a member of TGF-ß family (Ozkaynak *et al.*, 1990), induces SCG neurons to develop dendrites to the same extent as they do *in vivo*. Cytokine receptor complexes, such as those of ciliary neurotrophic factor (CNTF) or LIF, interact with cytoplasmic tyrosine kinases that navigate below the surface membrane (known as Jak/Tyk kinases) and mediate signalling after cytokine binding (Stahl and Yancopoulos, 1994).

Neurotrophins

More than 4 decades ago, Levi-Montalcini discovered a factor that caused sympathetic and sensory neuron neurites to grow, and was therefore termed nerve growth factor (NGF). In the late 1950s, the combined efforts of Levi-Montalcini, Hamburger and Cohen led to the remarkable experiment of injecting antibodies to NGF in neonatal mice, which resulted in the massive death of sympathetic neurons (Levi-Montalcini, 1987). This experiment demonstrated the crucial role of NGF in neuronal survival, and since then, NGF and now other neurotrophins have become key players in the neurotrophic hypothesis. The hypothesis stipulates that during development neurons actively compete for the limiting quantities of target derived factors, by establishing optimum contact with their targets. Those neurons that fail to make contacts with their targets in time undergo programmed cell death. As different targets may release different factors, this mechanism provides a means of enforcing appropriate connections between neurons and their intended terminal targets.

In addition to their neurotrophic action, neurotrophins produce a vast array of effects on neuronal functions and even on some non-neuronal cell functions (reviewed in Korsching, 1993; Davies, 1994; Bothwell, 1995). Furthermore, in the last decade, there has been an enormous increase in our understanding of how these neurotrophins operate,

in part due to the identification of their receptor tyrosine kinase *trk*s and to the development of useful neuronal cell line models such as the PC12 rat pheochromocytoma cell line (reviewed in Greene, 1991; Barbacid, 1994; Chao, 1994; Kaplan and Stephens, 1994). However, the amount of new information is too large to review in this introduction. Therefore, I have restricted the following section mainly to the role of NGF on dendritic outgrowth. As a complement, I included in appendix 1 a summary of the molecular diversity of the neurotrophin family and the neurotrophin receptors.

The promoting effects of NGF on axonal growth and on neurite outgrowth from PC12 cells are well documented (Greene and Tischler, 1982; Campenot, 1994). Experiments with compartmented cultures of SCG neurons have demonstrated that NGF supplied to axonal terminals is necessary and sufficient to promote axonal elongation and branching, whereas NGF supplied only to neuronal somata does not promote axonal growth. These results indicate that the effects of NGF on axonal growth are local and that no anterograde NGF-mediated signals affect axonal growth (reviewed in Campenot, 1994).

Although few studies have investigated the effects of neurotrophin on dendritic growth, NGF has been proposed to play a critical role in the development of dendrites by sympathetic neurons. Axotomy of adult mice SCG neurons causes a significant reduction in the length and complexity of their dendrites in a reversible fashion until peripheral re-innervation occurs (Yawo, 1987). As the major source of NGF acting on neurons is believed to be the innervated target (Korsching and Thoenen, 1983b; Shelton and Reichardt, 1984; Purves *et al.*, 1988), this observation suggests that NGF promotes dendrite outgrowth from SCG neurons. In fact, daily injections of NGF to neonatal rats or mice caused a substantial increase in the growth of SCG neuron dendrites (Snider, 1988; Purves *et al.*, 1988; Ruit and Snider, 1991).

SCG neurons in young adult mice continue to increase their dendritic arbour as the targets of these neurons expand (Purves *et al.*, 1986a). Presumably, the amount of NGF available is determined by the target size which then regulates the density of innervation as well as the size of the dendritic field (Korsching and Thoenen, 1983a; Purves *et al.*,

1986b, 1988). In fact, synapses on SCG neurons are formed mainly on the dendrites (Osterberg *et al.*, 1976; Forehand, 1985), and it has been shown that NGF treatment in neonatal rats results in a significant increase in the number of synapses in the SCG (Schafer *et al.*, 1983).

It is unknown whether the effects of NGF on axonal outgrowth and dendritic outgrowth operate through similar mechanisms. NGF activates tyrosine phosphorylation of its receptor *trk*A and also binds to a second receptor termed $p75^{LNGFR}$ (whose function is poorly understood; see appendix 1, and see appendix 2 for a brief description of signalling pathways that are activated by NGF). These receptors are expressed throughout the surface of neurons (Kim *et al.*, 1979; Carbonetto and Stach, 1982; Okazawa *et al.*, 1993); however, the major supply of NGF is believed to be from retrograde transport (Korsching and Thoenen, 1983b; Richardson and Riopelle, 1984; Shelton and Reichardt, 1984; Purves *et al.*, 1988). If target sources of NGF stimulate dendritic outgrowth, while the action of NGF on axonal growth is local (Campenot, 1994), then it is likely that NGF acts on axonal and dendritic growth through different mechanisms.

Innervation and activity

Several studies, *in vivo* and in culture, have indicated that innervation, neurotransmitters and neuronal activity alter the growth patterns of dendrites (Rakic and Sidman, 1973; Berry and Bradley, 1976; Benes *et al.*, 1977; Bradley and Berry, 1978; Deitch and Rubel, 1984; Mattson, 1988; Lipton and Kater, 1989; Vaughn, 1989; Wong *et al.*, 1991; Schilling *et al.*, 1991; Wingate and Thompson, 1994). In rodent cerebellum, mutations and treatments that affect afferent input to Purkinje cells result in dramatic alterations in the morphology of their dendritic tree (Rakic and Sidman, 1973; Berry and Bradley, 1976; Bradley and Berry, 1978). The primary effect of afferent innervation is an induction of dendritic branching by Purkinje cells. In culture, synaptic activity in these cells has been shown to produce similar effects: the emerging dendrites of Purkinje cells stop growing once functional synapses form and begin to branch. One of the initial events that produces this effect is the influx of Ca^{2+} (Schilling *et al.*, 1991).

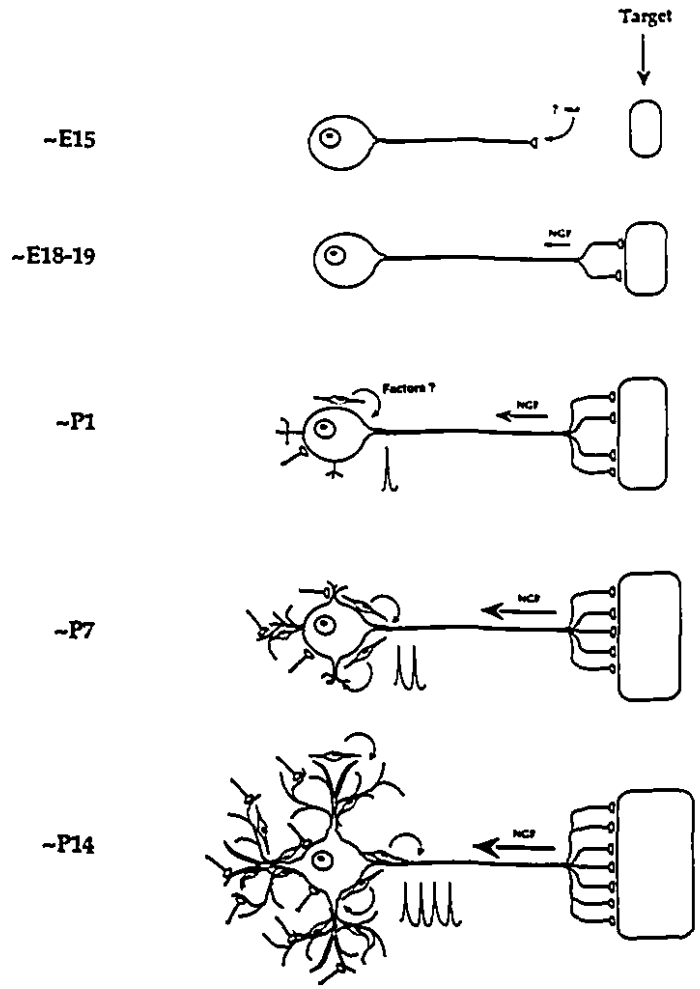

Figure 1.2. *Development of the rat superior cervical ganglion.*

This cartoon illustrates in a simplified manner some of the stages of development for rat sympathetic neurons during late embryogenesis and early postnatal life. By birth, SCG neurons have reached their targets, which supply NGF to the neurons and thereby support neuronal survival. At this stage of development, SCG neurons have few small dendrites and receive few synapses. During the first two weeks of postnatal development major changes occur in the SCG. Satellite cells proliferate, SCG neurons elaborate dendrites, and a considerable number of synapses form between nerve terminals of preganglionic neurons and dendrites of SCG neurons. During that time, SCG neuron axonal terminals branch further and innervate larger surface of target cells, and consequently transport retrogradely increasing amounts of NGF. In addition, during this early postnatal development, SCG neurons increase the density of their nAChRs on their somatodendritic membranes.

The coincidence of these events raises the question of whether some of those are linked together or coordinately regulated. For instance, is the larger supply of NGF from retrograde transport stimulating dendrite outgrowth? Is the satellite cell proliferation promoting dendrite extension? Are the incoming synapses inducing more dendritic outgrowth? Or, is it the elongating dendrites that "capture" more incoming terminals to form synapses? What causes the density of nAChRs to increase on these neurons? Is it due to NGF supply? Satellite cell influence? Innervation? Increase in neuronal activity? Does the extension of dendrites affect nAChR expression?

In contrast, innervation and electrical activity seem to play a small role on the dendritic geometry of sympathetic neurons, even though over 90% of synapses form on dendrites (Forehand, 1985). Indeed, Voyvodic (1987) showed that denervation of neonatal SCG neurons caused no effect on the subsequent growth or branching of dendrites. Likewise, addition of elevated potassium (high K^+) or TTX on cultured SCG neurons had no effect on dendritic growth by the neurons in serum-free condition (Bruckenstein and Higgins, 1988b).

Several studies performed in culture investigated the effects of neurotransmitters, such as glutamate, serotonin, dopamine and ACh, on neuritic outgrowth. These experiments showed that neurotransmitters can greatly affect neuritic outgrowth through the influx of Ca^{2+}. However, diverse effects have been observed, from neurite retraction to neurite sprouting and branching (Mattson, 1988; Lipton and Kater, 1989; Pugh and Berg, 1994; Zheng *et al.*, 1994; Small *et al.*, 1995). Part of this diversity of effects is due to the different types and amounts of neurotransmitter used, the time course of their applications, as well as the neuronal types that were studied. Furthermore, most of these studies did not make the distinction between axons and dendrites. Nevertheless, these results emphasize the notion that a fine tuning of $[Ca^{2+}]$ in growth cones is critical for controlling its movements (Lipton and Kater, 1989). Therefore, it appears that innervation and neuronal activity cause a variety of effects on dendritic outgrowth and neuronal polarity. These differential effects are, in part, related to the neural circuits involved, and may contribute to the differential effects that synaptic activity has on adaptive changes.

RELATIONSHIP BETWEEN DENDRITE OUTGROWTH AND POSTSYNAPTIC RECEPTOR EXPRESSION

Beyond the establishment of a basic morphological polarity, neurons undergo further maturation of their axonal and dendritic arbours and form synapses. Synaptogenesis involves several complex processes in both the presynaptic and postsynaptic neuron. In order to provide an efficient assembly of the numerous proteins involved in the establishment of functional synapses, neurons must have the necessary mechanisms for targeting these molecules to the appropriate location.

How is the expression of molecules involved in synaptogenesis regulated during the establishment of neuronal polarity? The initiation and the further elaboration of dendrites will require additional supply of elements of the postsynaptic densities. How are these molecules coordinately expressed? Do the same extrinsic factors that regulate dendrite outgrowth regulate the expression of molecules needed for synapse formation, such as the postsynaptic neurotransmitter receptors? Little is known about the factors that influence the expression of neurotransmitter receptors on neurons; much of what is known comes from studies on the nAChRs on autonomic neurons. Below, I review the main findings on the regulation of nAChR expression on autonomic neurons, but first, I briefly introduce the family of neuronal nAChRs.

Neuronal nicotinic acetylcholine receptors

Fast synaptic transmission in autonomic neurons is mediated by nAChRs, which are part of the gene superfamily of ligand-gated ion channels that includes 5-HT_3, $GABA_A$ and glycine receptors (reviewed in Ortells and Lunt, 1995). The neuronal nAChR gene family is composed of 11 genes that code for proteins with homologies to the muscle nAChR genes (Sargent, 1993; Elgoyhen *et al.*, 1994). These genes have been grouped in two classes of subunits, α (α_2-α_9) and ß ($ß_2$-$ß_4$), based respectively on the presence or the lack of two adjacent cysteines in a region homologous to the putative ACh binding site of the muscle nAChR α subunit (α_1). The homologies of the predicted sequences among the cloned neuronal nAChR subunits in the rat range from 40 to 68%, with no preferential homology among α or ß subunit groups (Sargent, 1993). In rats, no α_8 gene has been identified; the recently discovered α_9 subunit appears to be a more distant member of the nAChR family, with 36-39% homology with all rat neuronal and muscle α subunits (Elgoyhen *et al.*, 1994).

Neuronal nAChRs are believed to be pentamers containing 2 α and 3 ß subunits (Cooper *et al.*, 1991; Anand *et al.*, 1991). Unlike muscle nAChRs, which incorporate 4 different gene products, the products of only one α subunit gene and one ß subunit gene can give rise to a functional receptor in *Xenopus* expression system. Thus far, 3 α subunits (α_2, α_3, α_4) and 2 ß subunits ($ß_2$, $ß_4$) have been found to co-assemble in various

functional combinations in *Xenopus* oocytes (Patrick *et al.*, 1993; Papke, 1993). In addition, 3 other nAChR genes, α_7, α_8 and α_9, have been shown to give rise to functional homomeric nAChRs when expressed in *Xenopus* oocytes (Couturier *et al.*, 1990b; Séguéla *et al.*, 1993; Elgoyhen *et al.*, 1994; Gerzanich *et al.*, 1994). In contrast, expression of α_5 and α_6 in combination with any ß subunit, or expression of $ß_3$ with any of the α subunits did not give rise to functional nAChRs (Boulter *et al.*, 1990; Couturier *et al.*, 1990a). However, these subunits, particularly α_5, may incorporate into functional nAChRs that are composed of more than two different subunits (Vernallis, 1993; McGehee and Role, 1995). As of yet, the potential for combinations of 3 different subunits incorporating into a functional nAChR in *Xenopus* oocytes has been largely unexplored (but see McGehee and Role, 1995). Several experiments have indicated that most functional receptor subtypes expressed in *Xenopus* oocytes have different functional properties in terms of ligand affinity, open time, conductance and ion selectivity (Deneris *et al.*, 1991; Patrick *et al.*, 1993; Papke, 1993; McGehee and Role, 1995). Such functional diversity opens the possibility of a large number of functionally distinct nAChRs; yet the subunit composition of nAChRs on neurons has not been fully resolved. Several lines of evidence suggest that the prevalent high-affinity nicotine binding receptor in the CNS is an $\alpha_4/ß_2$ receptor (Wada *et al.*, 1989; Flores *et al.*, 1992; Clarke, 1993; Sargent, 1993). In autonomic neurons, synaptic receptors are likely to incorporate α_3 and $ß_4$ subunits, perhaps in combination with other subunits, like $ß_2$ and α_5 (Vernallis *et al.*, 1993; Conroy *et al.*, 1994; Mandelzys *et al.*, 1994, 1995).

Nicotinic AChRs have been shown to cluster at synaptic membranes of autonomic neurons (Jacob *et al.*, 1984; Loring and Zigmond, 1988; Loring *et al.*, 1988; Sargent and Pang, 1989; Sargent and Wilson, 1995). Zigmond and colleagues measured the density of nAChRs at synapses by EM autoradiography using [^{125}I]-neuronal-Bungarotoxin, a toxin that blocks synaptic transmission on autonomic neurons (Sah *et al.*, 1987; Loring and Zigmond, 1988). They estimated approximately 600 sites/μm^2 in the synaptic membrane of chick ciliary neurons and 4800 sites/μm^2 in that of cultured rat sympathetic neurons. These estimates were 10-20 and 50-100 fold higher, respectively, than for non-synaptic

membranes. However, these densities of nAChRs at neuronal synapses are lower than those at the neuromuscular junction (up to 20000 sites/μm^2 of [^{125}I]-α-Bungarotoxin). If a quantum of ACh released from pre-ganglionic neuron nerve terminals is similar to that released from motor neuron nerve terminals, it is possible that these lower densities of nAChRs in neuron-neuron synapses limit the size of synaptic potentials (Dryer and Chiappinelli, 1987). If so, modifying the number and localization of nAChRs on neurons may be a strategy for synaptic plasticity.

Neuronal nAChRs appear to gate significant amount of Ca^{2+}, although precise measurements of Ca^{2+} permeability through neuronal nAChRs have been difficult to obtain (Patrick *et al.*, 1993; Vernino *et al.*, 1992, 1994). Vernino *et al.* (1994) recently estimated that approximately 4% of the inward current through nAChRs in chromaffin cells was carried by Ca^{2+}. This permeability to Ca^{2+} by nAChRs may be important for the modulation of nicotinic cholinergic synaptic activity in the nervous system, as it has been shown for NMDA receptor-mediated synapses in CNS neurons (Bliss and Collingridge, 1993; Bear and Malenka, 1994; Linden, 1994).

α-BTX-nAChRs

Alpha-bungarotoxin (α-BTX) binds to many nerve cells in the CNS and PNS. However, unlike for nerve-muscle synapses, α-BTX does not block synaptic transmission on neurons that express α-BTX binding proteins (α-BTX-nAChRs) (Clarke, 1992). The first α-BTX-nAChR to be purified was shown to contain an α_7 gene product (Schoepfer *et al.*, 1990). α-BTX has been shown to bind homomeric receptors expressed in *Xenopus* oocytes (i.e. α_7, α_8 and α_9 homomeric receptors) and to block their agonist-gated currents (Couturier *et al.*, 1990b; Séguéla *et al.*, 1993; Elgoyhen *et al.*, 1994; Gerzanich *et al.*, 1994). Based on their homomeric nature, α-BTX-nAChRs have been suggested to represent primitive ancestors of the ligand-gated ion channel superfamily of receptors (Ortells and Lunt, 1995). These receptors have distinct patterns of distribution compared to conventional nAChRs, both in the CNS and PNS (Jacob and Berg, 1983; Clarke *et al.*, 1985; Loring *et al.*, 1985; Clarke, 1993; Deltoro *et al.*, 1994; Elgoyhen *et al.*, 1994). In

autonomic ganglia, α-BTX-nAChRs appear less clustered than other nAChRs and are distributed primarily on extra-synaptic membranes (Jacob and Berg, 1983; Loring *et al.*, 1985; Sargent and Wilson, 1995). However, these receptors have also been detected near synaptic sites and have been proposed to have a peri-synaptic localization (Jacob and Berg, 1983; Sargent and Wilson, 1995). Their role in synaptic transmission is poorly understood (Clarke, 1992), except for the α_9/α-BTX-nAChR that is believed to mediate the cholinergic synapses between the cochlear efferents and outer hair cells of the guinea pig and short hair cells of the chick cochlea (Housley and Ashmore, 1991; Fuchs and Murrow, 1992; Elgoyhen *et al.*, 1994). Alpha-BTX-nAChRs appear to have a remarkably high permeability to Ca^{2+}, suggesting that they activate Ca^{2+}-dependent cellular events, such as those involved in synaptogenesis or synaptic plasticity (Séguéla *et al.*, 1993; Patrick *et al.*, 1993; Elgoyhen *et al.*, 1994; Castro and Albuquerque, 1995). Interestingly, α-BTX-nAChRs have been observed on growth cones of cultured chick sympathetic neurons (Carbonetto and Fambrough, 1979), and nicotine applications on growth cones of chick ciliary neurons cause them to retract, unless α-BTX-nAChRs or Ca^{2+} influx through voltage-dependent Ca^{2+} channels are blocked (Pugh and Berg, 1994). These results suggest that the α-BTX-nAChR plays a role in neurite outgrowth through direct or indirect control of Ca^{2+} levels in growth cones.

Expression of nAChRs in autonomic neurons

Autonomic ganglia express primarily 5 identified nAChR transcripts: α_3, α_5, α_7, $ß_2$ and $ß_4$ (Corriveau and Berg, 1993; Mandelzys *et al.*, 1994; Devay *et al.*, 1994). Based on comparisons between the functional properties of nAChRs expressed in *Xenopus* oocytes and those of nAChRs on rat SCG neurons, there is evidence to indicate that SCG neuron nAChRs incorporate α_3 and $ß_4$, and perhaps $ß_2$ (Covernton *et al.*, 1994; Mandelzys *et al.*, 1995). On the other hand, nAChRs on chick ciliary neurons have been shown to contain also an α_5 subunit (Vernallis *et al.*, 1993). Autonomic neurons express an α-BTX-nAChR that incorporates the α_7 subunit; whether other subunits are included in the α-BTX-nAChR is unknown (Vernallis *et al.*, 1993). During development of autonomic ganglia,

nAChR transcripts first appear at a period that corresponds to neuronal differentiation (Zoli *et al.*, 1995). Subsequently, some transcripts disappear (Devay and Role, 1994; Zoli *et al.*, 1995), while others increase significantly (Corriveau and Berg, 1993; Devay and Role, 1994; Mandelzys *et al.*, 1994; Schwartz Levey *et al.*, 1995; Zoli *et al.*, 1995).

In chick ciliary neurons, the expression of nAChRs has been investigated at the protein level using various antibodies of different subunit specificities. The most commonly used antibody has been the MAb35, which was raised against the α subunit of the *Electrophorus* nAChR. This antibody specifically recognizes the chick α_5 subunit on immunoblots, but binds to neuronal-BTX binding sites on cultured ciliary neurons and to some nAChRs in chicken brain (Whiting and Lindstrom, 1986; Halvorsen and Berg, 1987; Schoepfer *et al.*, 1989; Conroy *et al.*, 1992; Vernallis *et al.*, 1993). Chick ciliary neurons contain abundant MAb35 binding sites on their membrane as well as intracellularly; the ratio of intracellular versus membrane MAb35 binding was estimated to be 3 to 1 (Jacob *et al.*, 1986; Jacob, 1991). Surprisingly, only 5% of the intracellular MAb35 binding sites were shown to incorporate in the membrane (Stollberg and Berg, 1987). This finding suggests that the turnover rate of intracellular MAb35 binding proteins is much higher than that of the surface ones. This situation is reminiscent of muscle where the half-life of nAChRs is greatly increased at the synapse (Hall and Sanes, 1993). Taken together, these findings suggest that ciliary neurons contain an intracellular pool of MAb35 binding sites that correspond to 1) a reserve of readily accessible nAChRs, and/or 2) improperly assembled receptors, and/or 3) single nAChR subunits (e.g. α_5) expressed in excess compared to their rate of incorporation into functional receptors. It is possible that unassembled nAChR subunits or improperly assembled receptors are more rapidly degraded than fully assembled pentamers. The prevalence of an intracellular pool of nAChR subunit immunoreactivity has also been observed in the CNS with a $ß_2$ specific antibody (Hill *et al.*, 1993).

Experiments using various subunit-specific antibodies revealed that ciliary neurons express proteins for all 5 nAChR subunit transcripts, but only two receptor subtypes were distinguished on their surface: one that incorporates α_3, α_5 and $ß_4$ subunits and one that

incorporates α_7 subunit. The α_7-containing receptor binds α-BTX specifically (Conroy *et al.*, 1992; Vernallis *et al.*, 1993; Sargent and Wilson, 1995).

Several studies also investigated the expression of functional nAChRs. During development of autonomic neurons, there is a substantial increase in the ACh-evoked current densities (Margiotta and Gurantz, 1989; Engisch and Fischbach, 1990; Mandelzys *et al.*, 1994; Schwartz Levey *et al.*, 1995), which appears to correlate with an increase in nAChR transcript levels (Corriveau and Berg, 1993; Devay *et al.*, 1994; Mandelzys *et al.*, 1994; Schwartz Levey *et al.*, 1995). However, on cultured chick ciliary neurons, the size of macroscopic ACh-evoked currents does not seem to correspond to the number of MAb35 binding sites (Margiotta *et al.*, 1987a). The authors have postulated that the majority of nAChRs on cultured ciliary neurons are non-functional or desensitized. Incubating these neurons with cAMP analogues increased the size of the ACh-evoked currents by 2-3 fold, without affecting single channel conductance or the number of [^{125}I]MAb35 binding sites, suggesting that a cAMP-dependent mechanism influences the number of functional receptors on these neurons (Margiotta *et al.*, 1987b; Vijayaraghavan, *et al.*, 1990).

Based on these results obtained from experiments with chick ciliary neurons, it has been postulated that these neurons express far more nAChR subunit transcripts and proteins than needed for the expression of ACh-evoked currents, and that post-transcriptional mechanisms contribute significantly to their functional expression (Margiotta *et al.*, 1987a,b; Jacob, 1991; see also Corriveau and Berg, 1994).

Extrinsic influences regulate nAChR expression in autonomic neurons

Extracellular matrix and cell-cell contacts

By analogy with muscle nAChRs, there is good reasons to believe that the targeting of nAChRs is regulated by cell-cell interactions or by the ECM proteins (Froehner, 1993; Hall and Sanes, 1993). Surprisingly, little is known about cell-cell contact- or ECM molecule-mediated mechanisms that regulate neurotransmitter receptor localization or expression on neurons. The pre-ganglionic nerve appears to regulate nAChR clustering at

the synapse (Sargent and Pang, 1988, 1989; Moss and Role, 1993); this process may involve the release of an agrin-like molecule from the nerve (McMahan, 1990). It is unknown whether ECM proteins and cell-cell contacts regulate the expression of nAChR genes. Sensory neurons from the rat nodose ganglion express little or no ACh-evoked currents on their somata *in vivo* or when co-cultured with their ganglionic satellite cells. However, when satellite cells are removed, the neurons begin to express large ACh-evoked currents, suggesting that ganglionic satellite cells repress the appearance of these currents (Baccaglini and Cooper, 1982; Cooper, 1984; Cooper and Lau, 1986).

Growth factors

Axotomy experiments in post-hatched chick ciliary neurons have been shown to cause a reduction in ACh-evoked currents, suggesting that the target of these neurons (the eye) promotes nAChR expression (Brenner and Martin, 1976; Jacob and Berg, 1987; 1988; McEachern *et al.*, 1989). However, the possibility of an injury response by the neurons was proposed as a possible explanation for the decrease in currents (Schwartz Levey *et al.*, 1995). Engisch and Fischbach (1990) removed the eyes of embryonic chicks (E2) before the ciliary neurons could contact them, and measured their ACh sensitivity during development *in ovo*. Their results indicate that the developmental increase in ACh-evoked currents is largely unaltered by the removal of the eye. Schwartz Levey *et al.* (1995) repeated this experiment, but measured the effects of target deprivation on the mRNA levels of 3 nAChR transcripts, α_3, α_5 and $ß_4$, as well as on ACh-evoked currents. In contrast to the study of Engisch and Fischbach (1990), the ACh sensitivity of target-deprived neurons was smaller than control neurons, and a corresponding reduction in α_3 and $ß_4$ mRNA levels was observed (Schwartz Levey *et al.*, 1995). The reasons for these different results is unclear; problems such as ectopic re-innervation of ciliary neuron axons, or selective survival of neuronal subpopulations could have contributed to the apparent conflicts in these results.

Consistent with a target-derived factor regulating nAChR expression is the finding that an eye extract increases nAChR number when added to cultures of chick ciliary neurons

(Halvorsen *et al.*, 1991). However, no effect was observed on the expression of nAChR transcripts (Corriveau and Berg, 1994), suggesting that a post-transcriptional mechanism controls ACh sensitivity on these neurons.

There is also evidence that neurotrophins can affect nAChR expression. NGF increases the ACh-evoked current densities on nodose neurons developing in culture in the absence of satellite cells (Mandelzys *et al.*, 1990; Mandelzys and Cooper, 1992). Also, NGF has been shown to differentially regulate the expression of nAChR genes in PC12 cells (Rogers *et al.*, 1992); whether such regulation occurs in neurons is unknown; this issue is addressed in Chapters 5 and 6.

Growth factors from pre-ganglionic innervation may also regulate nAChR expression. Role and colleagues found that a soluble factor released by pre-ganglionic neurons induces functional nAChR expression by cultured chick sympathetic neurons. These changes in ACh sensitivity could be accounted for by changes in single channel properties, as well as an increase in functional receptor incorporation at the surface membrane (Role, 1988; Gardette *et al.*, 1991). These results differ somewhat from those obtained with denervation experiments on chick ciliary neurons *in vivo*, where no difference in the currents was observed between denervated and control neurons (see below; McEachern *et al.*, 1989; Engisch and Fischbach, 1990; Schwartz Levey *et al.*, 1995). This suggests that local environmental factors affect functional expression of nAChRs *in vivo*.

These factors may be related to the growth and differentiation factor ARIA (AChR inducing activity) which is a leading candidate as a motor-derived inducer of nAChR expression from skeletal muscle synaptic nuclei (Jessel *et al.*, 1979; Martinou *et al.*, 1991; Falls *et al.*, 1993). ARIA is found at the motor endplate and up-regulates gene expression of the ε nAChR subunit (Chu *et al.*, 1995). In addition, it has recently been shown to be expressed by all cholinergic neurons in the CNS and to cause the tyrosine phosphorylation of a 185 KDa protein in central and peripheral targets of these cholinergic neurons (Corfas *et al.*, 1995). These results suggest that ARIA or other related molecules play a similar role to that on muscle nAChRs on neuronal nAChR expression.

In summary, several lines of evidence indicate that growth factors regulate functional

expression of nAChRs; it remains unknown whether any growth factors control nAChR gene expression in neurons.

Innervation and activity

The role of activity *per se* on neuronal nAChR gene expression has not been closely studied. Most of what is known on activity-mediated regulation of nAChR expression comes from studies on muscle extra-junctional nuclei (Changeux, 1991; Hall and Sanes, 1993). Indeed, Ca^{2+} influx through L-type Ca^{2+} channels and PKC activity (Klarsfeld *et al.*, 1989) or protein kinase A (PKA) activity in rat (Walke *et al.*, 1994) down-regulate the expression of nAChR subunits from extrasynaptic nuclei.

Several studies on the developmental expression of neuronal nAChRs have suggested that innervation plays a key role in nAChR expression, based on the coincidence between the time of innervation and the period of large increases in nAChR transcripts, proteins and ACh-evoked currents (Jacob, 1991; Moss and Role, 1993; Devay *et al.*, 1994). For example, the postnatal developmental increase in both nAChR transcripts and ACh-evoked current densities in SCG neurons (Mandelzys *et al.*, 1994) occurs during the period of synapse formation.

Surprisingly, innervation appears not to play a predominant role in the expression of neuronal nAChRs. Pre-ganglionic denervation or removal of pre-ganglionic neurons prior to innervation have little effect on the developmental increase in both the number of surface nAChRs (measured by MAb35 or neuronal-BTX binding) and the size of the ACh-evoked currents on autonomic neurons (McEachern *et al.*, 1989; Engisch and Fischbach, 1992; Sargent *et al.*, 1991; Streichert and Sargent, 1992; Mandelzys *et al.*, 1994). However, a number of studies examining the influence of innervation on intracellular MAb35 binding or nAChR transcript levels have indicated that removal of innervation slows the increase in nAChR transcripts and intracellular pool of MAb35 binding sites (Jacob and Berg, 1987; 1988; Boyd *et al.*, 1988; McEachern *et al.*, 1989; Arenella *et al.*, 1993; Schwartz Levey *et al.*, 1995). Mandelzys *et al.* (1994) compared the effects of neonatal rat SCG pre-ganglionic denervation on the expression of both the ACh-

evoked currents and the levels of nAChR transcripts. The results indicated that, similar to the ACh-evoked currents, the developmental increase in nAChR transcript levels was little affected. However, much of the developmental increase in α_7 mRNA was prevented by denervation.

Thus, the precise role of innervation in the regulation of nAChR expression is not completely resolved. In order for functional synapses to form rapidly when neuronal processes come in contact, the synaptic machinery should be ready for fast assembly. Therefore, it may be essential that expression of postsynaptic receptors is already activated prior to innervation. This situation has been well described for synaptogenesis on muscle where there are ample nAChRs on the muscle membrane before synaptogenesis (Cohen *et al.*, 1979). Once the functional synaptic connections are established, activity-dependent refinement of the synaptic machinery may take place to modify the synaptic interactions (Haydon and Drapeau, 1995).

One way that synaptic activity can modify synaptic interactions is by causing changes in gene expression of molecules involved in synaptic transmission. Neuronal activity is believed to activate a series of immediate early genes, which in turn may control the expression of delayed response genes. Little is known, however, about the relationship between neuronal activity and expression of proteins involved in synaptic transmission. To learn more about the role that activity plays on nAChR expression, we have used the approach of culturing rat sympathetic neurons under conditions that mimic neuronal activity, and measured the effects on nAChR transcript levels. Our findings are consistent with the concept that activity plays little role in the expression of the nAChRs that are involved in synaptic transmission, while they demonstrate that activity regulates the expression of α-BTX-nAChRs (Chapter 6).

Statement of problem and overview

The data accumulated thus far on the developmental appearance of nAChR transcripts and on the regulation of their expression in autonomic neurons raise the possibility that after neurogenesis the neurons are intrinsically programmed to express nAChRs. Furthermore, there is not direct evidence that nAChR genes are regulated by extrinsic

influences. What regulates the developmental increases in nAChR transcript levels and ACh-evoked currents? Could they be controlled by mechanisms related to neuronal maturation, such as the extension of dendrites?

To investigate this problem, an additional class of neurons are useful: the sensory neurons from the rat nodose ganglion. The mammalian nodose ganglion is a cranial sensory ganglion whose axons run in the vagus nerve to provide sensory innervation to most of the viscera, including heart, lungs, trachea and gut (Paintal, 1973). Sensory neurons do not elaborate dendrites or receive synapses on their cell body. Interestingly, nodose neurons have been shown to form cholinergic synapses among each other when they develop in culture under certain conditions, suggesting that these neurons can express new postsynaptic elements involved in synaptogenesis. An important component of synapses is the dendrite. Could these neurons be extending dendrites in these cultures? If so, this could provide information on the initial events that determine dendrite outgrowth.

For my thesis work, I first asked: what determines the polarity of sensory neurons? Is it an intrinsic determination or do extrinsic influences control sensory neuron polarity? Can nodose neurons develop dendrites in culture? I investigated whether glial cells play a role in nodose neuron polarity and whether neurotrophins are involved in the differentiation of nodose neurons in culture. Next, I asked whether there is a relationship between nAChR expression and the establishment of polarity by nodose neurons.

To determine whether the establishment of neuronal polarity influences the expression of nAChR genes and whether they are controlled by similar influences, I began to investigate the regulation of nAChR gene expression in cultured sympathetic neurons. I asked more specifically what role activity plays in nAChR expression. Finally, I investigated how changes in mRNA levels for specific nAChR subunits affect changes in ACh-evoked currents on neurons.

In Chapter 3, I examine the establishment of polarity by newborn rat nodose neurons and show that they have retained the ability to extend dendrites in newborn rats. I demonstrate that two extrinsic influences control dendritic outgrowth on nodose neurons: satellite cells and NGF.

In Chapter 4, I show a correlation between the extension of dendrites by nodose neurons and the expression of functional nAChRs, and I show that nodose neurons express nAChRs on their dendrites.

In Chapter 5, I investigate the roles that various neurotrophins play in nodose neurons development. I demonstrate that nodose ganglia express multiple neurotrophin receptors and that BDNF and NT-3 influence nodose neurons to undergo a distinct differentiation compared to NGF-treated neurons: while NGF promotes dendrite extension and functional nAChR expression, BDNF and NT-3 influence nodose neurons to express attributes of their sensory phenotype.

To learn more about mechanisms that regulate nAChR gene expression, I investigate, in Chapter 6, the expression of nAChRs in sympathetic neurons, as they develop in culture under various conditions. I demonstrate that activity plays a differential role in nAChR expression and identify one signalling pathway that leads to the expression of one single nAChR subunit. My findings provide a link between neuronal activity, CaM kinase II activity and neurotransmitter receptor expression. Such link suggests a potential mechanism for synaptic plasticity. In this chapter, I also provide some clues to the role of NGF on the expression of nAChR genes. Finally, I begin to investigate the expression of nAChR genes in nodose neurons.

In Chapter 7, I demonstrate a correlation between increases in transcript levels for one single nAChR subunit and increases in ACh-evoked current densities. In addition, I examine the contribution of the α-BTX-nAChRs on the macroscopic ACh-evoked currents on SCG neurons.

Chapter 2

General Methodology

This chapter describes the general methods and the materials used for the experiments described in the following chapters. In the "experimental procedures" sections of each of the following chapters, relevant additional information is included.

2.1. NEURONAL CULTURES

Nodose and superior cervical (SC) ganglia were dissected under sterile conditions from P1 to P14 rats (Sprague Dawley, C.D. strain, Charles River, Canada) that were killed by cervical dislocation. The dissected ganglia were placed in a petri dish containing plating medium (see below).

2.1.1. Dissociation and plating

The ganglia were dissociated and the neurons cultured as originally described by Mains and Patterson (1973), Hawrot and Patterson (1979) and Hawrot (1980). The dissociation was done at 37°C in the following enzyme containing medium: modified HBSS (see below), 8% (v/v) FVM (see below), 4 mM HEPES (pH 7.4), collagenase (1 mg/ml, type 1: Sigma) and a neutral protease, dispase (grade 2, 2.4 mg/ml, Boehringer Mannheim). After a 15 min incubation period, the ganglia were gently triturated (pipetted up and down) with a 5 ml serological pipette to soften the capsule surrounding the neurons. When the ganglia had settled to the bottom of the tube, the solution was removed and replaced with a similar enzymatic solution as above, except that the collagenase was omitted. Dispase was used because it is a mild proteolytic enzyme that causes minimal damage to neurons. The dissociation continued at 37°C for another 3-4 hrs, while triturating the ganglia several times every 15-20 min with a fire polished pasteur pipette coated with plating medium.

When cells were fully dissociated, 5 ml of plating medium were added to the cell suspension to inactivate the enzymes, and the cells were centrifuged with a clinical

centrifuge (International Equipment Co.) at 1335 RPM for 5 min. Cells were then resuspended in 0.5 ml of plating medium and added on the top of 5.7 ml of a 35% percoll solution (see below). The percoll solution was centrifuged for 20 min at 1335 RPM to establish a gradient of cells: more than 95% of the neurons pelleted to the bottom of the tube, while ≈80% of non-neuronal cells remained in suspension. The top 3.5 ml of the solution was either discarded or kept for non-neuronal cell cultures (see below); the pelleted neurons were washed twice by centrifugations in plating medium, resuspended in plating medium (0.1 ml/culture dish), and added to the center well of modified petri dishes (see below) which had been previously coated with laminin (see below) and that contained 1.5 ml of growth medium (see below). The cell suspension was restricted to the center well of the culture dish by a sterile glass ring. The glass ring was removed 24 hrs later, a time at which all neurons have attached to the substrate and extended neurites. In spite of the percoll separation (above) a few non-neuronal cells remained in the neuronal suspension of SCG, while significantly more remained in the nodose neuronal suspension. For relatively pure neuronal cultures, 5-10 μM cytosine arabino-furanoside (Ara-C, Sigma) was added to the growth medium for the first 3–4 days of culture.

2.1.2. Isolation of ganglionic non-neuronal cells and satellite cell-neuron co-cultures

The non-neuronal cells of dissociated nodose and SC ganglia were obtained from the percoll separation step (above): after the centrifugation, the non-neuronal cell fraction remains on top of the percoll solution, while the neurons pellet to the bottom. Therefore, we collected the top layer (3 ml) of the solution and transferred it to another 15 ml centrifuge tube, and washed the cells twice by centrifugation in plating medium. The non-neuronal cells from nodose ganglia were occasionally cultured alone to prepare monolayers of satellite cells, which then served as substrates for subsequent neuronal platings. Alternatively, the non-neuronal cells were mixed with neurons before plating and both cell types were co-cultured. In addition, non-neuronal cells from nodose and SC ganglia were used for RNA isolation (see section **2.4.1.**). Over 95% of the cells isolated in this manner are non-neuronal as measured by cell counts under phase contrast microcopy. The nodose non-neuronal cell population is composed of satellite cells

(peri-somatic glia), Schwann cells (peri-axonal glia) and fibroblasts (Pannese, 1981). In culture, the first two types are indistinguishable; we have not attempted to differentiate satellite cells and Schwann cells, which are very closely related (Lieberman, 1976; Pannese, 1981; Le Douarin and Ziller, 1993). In this thesis, I refer to spindle shaped cells (10-12 µm long and 3-4 µm at their widest portion) as satellite cells. Fibroblasts flatten on the substrate and cover a large area (>100 µm diameter). When plated in culture, satellite cells proliferate much more rapidly than the fibroblasts, so they can rapidly form a confluent monolayer (3-4 days). As they divide more rapidly, satellite cells can be killed with 3-4 days of Ara-C treatment. In contrast, fibroblast-like cells divide slowly in these nodose cultures and many do not die with a 4 day Ara-C treatment. Although they are low in number in enriched neuronal cultures (<5%), they flatten on the coverslips and cover large areas under the neurons within a few days in culture, and become difficult to detect by phase microscopy. In this thesis, when I refer to satellite-cell free neuronal cultures, these fibroblasts may be present.

2.1.3. Incubation

The cultures were incubated in a humid atmosphere of 95% air and 5% CO_2 at 37°C, and were fed with growth medium every 2, 3 or 4 days depending on the experimental paradigms.

2.1.4. Solutions and media

Modified L15 medium: Leitzbovitz 15 (L15; Gibco) was used as a base for all media (plating and growth). The powder (14.9 g) was dissolved in 1080 ml of double distilled water (ddH_2O). To the mixture was added: 60 mg imidazole, 15 mg glutamic acid, 15 mg proline, 10 mg inositol, 15 mg aspartic acid, 15 mg cystine, 5 mg ß-alanine, 2 mg vitamin B12, 10 mg choline chloride, 0.5 mg lipoic acid, 0.02 mg biotin, 5 mg ß-aminobenzoic acid, 25 mg fumaric acid (all from Sigma), and 0.4 mg coenzyme A (P-L Biochemicals, Inc.). The pH was adjusted to 7.4 with 1 M HCl, and the medium was filtered through a 0.2 µm filter (Nucleopore). This modified L15 medium is termed L15-Air.

L15-CO_2: to 850 ml of L15-Air, 170 ml of 150 mM $NaHCO_3$ was added before filtration. The pH of this solution, used in growth media, was kept at pH 7.4 by exposing it to an atmosphere containing 95% air and 5% CO_2.

These media were stored at 4°C for up to 6 months.

Growth medium: Generally consisted of L15-CO_2, supplemented with FVM, 5% rat serum and neurotrophins.

Modified HBSS (Hank's balanced salt solution): 140 mM NaCl, 5.4 mM KCl, 0.33 mM NaH_2PO_4, 0.44 mM KH_2PO_4, 0.18 mM $MgCl_2$, 10 mM *N*-2-hydroxyethylpiperazine-*N'*-2-ethanesulfonic acid (HEPES), 5.6 mM glucose, 5 µg/ml phenol red (pH adjusted to 7.4 with 1 N NaOH).

Fresh vitamin mix (FVM): 1.25 mg/ml ascorbic acid, 65 µg/ml glutathione and 12 µg/ml 6,7-Dimethyl-5,6,7,8-tetrahydropterine [Sigma], supplemented with 100 mg/ml glucose (Fisher), L-glutamine (50 mM, Gibco) penicillin (12000 Units/ml, Gibco), streptomycin (12000 µg/ml, Gibco)

Plating Medium: consist of 45 ml of L15-Air, 5 ml horse serum (Gibco) and 2 ml FVM.

Percoll solution (35%): 2 ml percoll (Pharmacia), 3.7 ml L15-Air and 0.1 ml of 1 M HEPES (pH 7.4).

Rat serum: The rat serum was prepared by bleeding male retired breeders (Sprague Dawley, C.D. strain, Charles River Canada Inc.) that were asphyxiated in a CO_2 saturated bell jar. The blood was allowed to clot on ice and centrifuged at 16,000 rpm at 4°C for 30 min to pellet the blood cells. The supernatant (serum) was kept at 4°C overnight, recentrifuged, filtered through a 0.22 µm filter and stored in 2.5 ml aliquots at -20°C.

Neurotrophins: Two types of NGF were used in our experiments. First, 7S NGF was isolated and purified from mouse salivary glands using column chromatography through Sephadex G-100 and DEAE-cellulose (by Brigitte Pié and Allan Mandelzys) based on the method of Bocchini and Angeletti (1969). The NGF stock (1 mg/ml in ddH_2O) was filtered through a 0.22 µm membrane and stored at -70°C until use. We

tested the activity of this 7S NGF by growing SCG neurons in increasing concentrations. We used the dose (usually 1 µg/ml) that provided maximal survival and neurite outgrowth from SCG neurons cultured for 1 week. Second, we used recombinant 2.5S NGF at 25 ng/ml. We also used BDNF and NT-3 (provided by Amgen) at 25 ng/ml.

2.1.5. Modified culture dishes

Holes (5-15 mm in diameter) were cut in the center of plastic petri dishes (Corning, 35mm) and covered with an aclar (Allied Plastics) coverslip fixed to the outside with a silicon elastomer (sylgard; Dow Corning). This creates a shallow (2 mm) well in the center of the petri dish, which allows changing the growth media without exposing the neurons to the air. The day before a culture, the petri dishes were sterilized with ultraviolet light (20 min), and 50-100 µl laminin (prepared by Steve Gee and Yves Gagné, in Dr. S. Carbonetto's laboratory, Center for Research in Neuroscience) at a concentration of 30 µg/ml (diluted in L15-Air) was added to the center wells and left at 4°C overnight. Prior to plating the neurons, the dishes were washed twice with HBSS to remove unbound laminin, before growth medium was added. These culture dishes also served as recording chambers for the electrophysiological experiments, and incubation chambers for immunocytochemistry and *in situ* hybridization.

2.2. STAINING AND BINDING

2.2.1. Immunocytochemistry

Freshly prepared fixative solution (see below) was added (≈1 ml) to culture dishes for 15 min. The fixed neurons were rinsed 3 times with Tris-buffered saline (TBS; see below), permeabilized with 100% ethanol at -20°C for 15 min, rehydrated with 3 rinses of TBS, and incubated in blocking buffer (see below) for 30 min. In the same solution, primary antibodies were added for 1 hr at room temperature. After 3 rinses with TBS, the secondary antibodies (goat anti-mouse FITC and goat anti-rabbit RITC [1:500 or 1:1000], or horse anti-mouse biotin and donkey anti-rabbit biotin [1:200 or 1:500]) were added for

1 hr (Boehringer Mannheim, ICN immunobiologicals, Sigma). When biotinylated secondary antibodies were used, strepavidin-FITC or strepavidin-alkaline phosphatase (AP) was added for 45 min. after rinsing. When strepavidin-AP was used, cells were rinsed once more with AP reaction buffer (see below), and incubated in AP reaction buffer plus NBT (180 µg/ml; see below) and BCIP (360 µg/ml; see below) to allow AP enzymatic reaction. When a strong brown staining appeared (≈30 min), the reaction was terminated with stopping buffer (see below). All incubations and rinses were done in the modified culture dishes (see 2.1.5.), in which the neurons were grown in the center well; in this way, small volumes of antibody solution (25-50 µl) could be used to incubate the neurons, while large volumes (≈2 ml) of TBS were used for rinsing out antibodies. After the last rinse, the coverslips were pealed off from under the culture dishes with small forceps and mounted on slides using Immuno Fluore mounting medium (ICN Immunobiologicals). The cells were examined by epifluorescence on a Zeiss (Axiovert 35) microscope, or with bright field microscopy (for AP labelling).

2.2.1.1. Preparation of fixative solution:

The fixative solution consisted of 4% paraformaldehyde in 0.1 M phosphate buffer (pH 7.4). 25 ml of ddH_2O was warmed up to 50-60°C in a clean beaker containing a stirring bar. 4 g of paraformaldehyde (16% solution: w/v) was added to the warmed ddH_2O. While stirring, ≈10 pasteur pipette drops of 10 M NaOH were added until almost all the paraformaldehyde was dissolved. A drop of phenol red was added to approximate the pH (i.e. pink solution). Drops of 10 M HCl were then added until the colour changed to red-orange (the accuracy of the pH is not critical at this step). The solution was filtered (0.22 µm) to remove traces of undissolved paraformaldehyde and kept cold afterward until needed (within 24 hrs). At the time of fixation, the paraformaldehyde stock (16%) was mixed with phosphate buffer (pH 7.4; 0.5 M stock). Occasionally, glutaraldehyde (0.02%; from 25% stock; Fisher) was added to retain better neuronal morphology. The fixative solution was warmed up to 37°C before use.

2.2.2.2. Solutions and reagents for immunocytochemistry:

AP (alkaline phosphatase) reaction buffer: 100 mM NaCl, 5 mM $MgCl_2$, 100 mM Tris-HCl (pH 9.5).

BCIP (bromochloroindolyl phosphate): 50 mg of BCIP dissolved in 1 ml of 100 % dimethylformamide; vortexed well and stored at 4°C, protected from light for up to a year (Boehringer Mannheim).

Blocking buffer: TBS containing 5% normal serum (either from goat, rabbit or horse depending on the secondary antibody origin).

NBT (nitro blue tetrazolium): 50 mg of NBT in 1 ml 70% dimethylformamide; stored at 4°C, protected from light for up to a year (Boehringer Mannheim).

Phosphate buffer: for 1 liter of 0.5 M phosphate buffer pH 7.4: 387 ml of 1 M Na_2HPO_4 and 113 ml of 1 M NaH_2PO_4, completed to 1 liter with ddH_2O. Sterilized by autoclaving.

Phosphate buffer saline (PBS): 0.1 M phosphate buffer (pH 7.4) with NaCl 0.9%. Sterilized by autoclaving.

Tris-buffered saline (TBS): 5 mM Tris-HCl, NaCl 0.9%, (pH adjusted to 7.4 with HCl).

Stopping buffer: PBS (pH 7.4) and 20 mM NaEDTA.

2.2.3. Lucifer yellow injection

A stock of lucifer yellow (lithium salt; Sigma) was prepared by dissolving 5 mg of lucifer yellow in 100 µl of distilled water (5%). This solution was then mixed with LiCl 200mM (1:1). Microelectrodes filled with the lucifer yellow solution (resistance of 20-70 MΩ) were used to impale neurons. The microelectrode was connected to a tank of pressurized nitrogen and the release of pressure was controlled by a solenoid valve. When a resting potential of at least -30 mV was observed, lucifer yellow was injected with brief pulses (0.1-1 sec) of pressure (5-15 psi). Lucifer yellow (potassium salt; Sigma) was also used to label neurons while performing whole-cell voltage clamp experiments (see chapter 4). In these experiments, the lucifer yellow was included in the pipette solution and diffused passively into the cell during the recordings.

2.2.3. Measurements of MAP2 labelled dendrites

The proportion of neurons forming dendrites was measured by counting the number of neurons with and without dendrites in cultures that were immunostained for MAP2 after 1, 2 and 3 weeks in culture. In this thesis, I refer to thick, tapering, MAP2 positive processes that end locally (but that have a length of at least one cell body diameter [>35μm]) as dendrites (Dotti *et al.*, 1988; Bruckenstein and Higgins, 1988a,b). The number of primary dendrites per neuron was determined for all neurons that had dendrites in a given culture. The mean dendritic length was measured by projecting the image from an inverted Zeiss (axiovert 35) microscope on a digitizing tablet and analyzed with Sigmascan software (Jandel Scientific). The lengths of each primary dendrite, including the branches, were measured on 30 neurons with dendrites in a given culture. We expressed the total dendritic growth as the product of the percentage of neurons with dendrites, the number of primary dendrites per neuron, and the mean length of dendrites. We also traced MAP2 positive processes onto paper by camera lucida drawing; to do this, we used AP-labelling and bright-field microscopy.

2.2.4. α-BTX binding

SCG neurons were plated at 5000-6000 neurons/cm^2 on 3 cm^2 aclar coverslips. Before performing α-BTX binding, all cultures were washed twice with plating medium, followed by a 90 min pre-incubation with or without 1 μg/ml of cold α-BTX in plating medium at 37°C. [^{125}I]α-BTX (1.5 nM; 130 Ci/mmol; NEN; kindly provided by Dr. M. Quik, Department of Pharmacology, McGill University) dissolved in plating medium was then added to every dish for a 90 min incubation at 37°C. The cells were subsequently washed 6 times with plating medium over a 60 min period to remove all unbound [^{125}I]-α-BTX. The neurons were finally extracted in 0.5 ml of 0.5 M NaOH, and the radioactivity was measured with a γ-counter (from Department of Pharmacology).

2.3. ELECTROPHYSIOLOGY

2.3.1. Patch-clamping recording conditions

We used the modified culture dishes (see 2.1.5.) as recording chambers. The thin aclar coverslips permit visualization of neurons at 400X on a Zeiss (axiovert 35) microscope. The ground electrode was connected using an agar bridge (small tubing filled with perfusion solution containing 2% agar). During the recording, the chamber was continually perfused at a rate of 0.5-1 ml/min using a peristaltic pump (Extracorporeal) and the fluid was withdrawn via a suction tube positioned at the opposite side of the chamber. The fluid volume in the recording chamber was approximately 500-800 µl. All recordings were done at room temperature (21-24°C).

Membrane currents were measured with whole-cell patch-clamp techniques (Hamill *et al.* 1981) using a LIST EPC-7 amplifier. Currents were usually filtered at 3 KHz with an eight-pole Bessel filter (Frequency Devices, Inc.), and then sampled, displayed and stored on line with a 386-based PC computer (AT class with an EISA bus running at 33 MHz and a 64K cache and an A/D card [Omega]): we used Patchkit (Alembic Software, Montréal) for data acquisition and analysis. In some experiments, the currents were digitized at 44 kHz by a pulse code modulation unit (PCM 701, Sony Corp.) and stored on a Beta video cassette recorder (Betamax, Sony Corp.). The pipette resistances were 2-6 MΩ (Narishige PP-83 patch pipette puller) and the current signal was balanced to zero in the extracellular perfusion fluid (see below).

2.3.2. Ligand sensitivity assays

To measure ligand sensitivity on neurons, we used three different methods of ligand application.

First, ligands dissolved in extracellular medium were applied for 1 to 4 sec onto the cell body by pressure ejection from an electrode with a ≈10-20 µm diameter tip. The pipette tip was positioned at 20-30 µm from the cell body, so that, on application of light pressure (≈10-30 KPa from a tank of pressurized nitrogen) the entire cell body and proximal processes were perfused. The cultures were continuously perfused at a rate of

1 ml/min so that no buildup of ligand occurred in the recording chamber during the experiment.

Second, ligands were also applied by pressure ejection, but from double barrel pipettes (see below) to test for sensitivity of two different ligands on the same neuron. The tip openings were also ≈10-20 µm, and the pressure was applied in one pipette at a time.

Third, we used a method of rapid agonist application: the agonist solution is applied to a neuron from double-barrel pipette (see below), each barrel having a tip opening of 150-200 µm in diameter. The double-barrel pipette is attached to an electromechanical switching device (built by John Knowles, Department of Physiology, McGill), and its tips are positioned ≈30-50 µm from the neuron, with the central axis of one barrel in line with the neuron: initially the neuron is perfused by the solution from this barrel (control solution), but, by triggering the electromechanical device, the second barrel rapidly moves into position and perfuses the neuron with its solution (agonist). The flow rate from each barrel is usually 8-12 µl/sec; higher rates are difficult because they detach the neurons from the substrate. The flow from each barrel is controlled by a valve so that the flow of agonist is not continuous, but limited to recording period (usually 2-5 s for each trial); in addition, the recording chamber is perfused at 1-2 ml/min with perfusion solution (see below) to minimize the build up of agonist. To assess the speed of our agonist application technique, we filled each barrel with a different salt concentration and measured the time course for the change in electrode tip potential to occur upon switching from one barrel to the other. From this test, we demonstrated that our switching device changes the concentration in the vicinity of the electrode within 2 ms (Figure 2.1).

When rapid agonist application was used, we found that it was imperative to add 500 nM Tetrodotoxin (TTX; Sigma) in the perfusion solution as well as in the agonist solution to block unclamped voltage-dependent Na^+ currents (see Figure 7.1).

For measurements of ligand sensitivity, neurons with clear nuclei were selected at random and voltage-clamped at -60 or -50 mV during drug application. All currents were normalized to whole-cell membrane capacitance by integrating the capacity current evoked by a 5 mV hyperpolarizing voltage step from a holding potential of -60 or -50 mV.

Figure 2.1 Rapid agonist application. A patch electrode containing regular intracellular medium (section 2.3.4.) was perfused by one barrel containing 50 mM NaCl. By triggering an electro-magnetic device at the time indicated by the arrow, a second barrel perfusing 250 mM NaCl moved rapidly in front of the patch electrode tip. The resulting shift in the liquid junction potential produced a current that reached its peak within approximately 2 ms.

For measurements of ACh-evoked current densities on nodose neurons, 50 µM ACh was used: at this dose, little desensitization of the nAChRs occurred. The ACh-evoked currents on nodose neurons are blocked by nicotinic antagonists hexamethonium or curare (Mandelzys and Cooper, 1992). With whole-cell voltage clamp technique, a current of 5 pA could be resolved: such current is likely to arise from the simultaneous opening of only 2-3 nAChRs. Thus, neurons scored as "non-sensitive" to ACh are presumed not to express functional nAChRs. When a larger dose (e.g. 100 µM) was used in parallel (double-barrel), it was shown not to detect more ACh-sensitive neurons (Mandelzys and Cooper, 1992), indicating that 50 µM ACh is sufficient to measure the proportion of neurons expressing functional nAChRs.

Double-barrel electrode puffers: Two microelectrodes were inserted together in a Narishige PF-2 vertical microelectrode puller: heat was applied without vertical tension and the two microelectrodes were twisted by 360 degrees. The heat was then turned off to allow the two twisted microelectrodes to cool down: then vertical tension was applied with heat to pull two identical double-barrel puffers. For experiments using pressure

ejection of ligands, the tips were cut to have openings of 10-20 µm, using sharp dissection forceps. For fast application experiments, tips were cut to be 150-200 µm in diameter, and the edges were smoothed with a sharpening rock.

2.3.3. Voltage-gated Ca^{2+} current recording

For recording Ca^{2+} currents, we used 2 depolarizing protocols, one to focus on the tail currents (e.g. L-type Ca^{2+} currents) and one to focus on more rapidly inactivating Ca^{2+} currents (including N-type Ca^{2+} currents) (see Chapter 6 for details). The perfusion solution was the same as that shown below except that it contained 5 mM $CaCl_2$, 10 mM tetraethylammonium (TEA)-bromide (Sigma) and 2 mM 4-aminopyridine (4-AP)-Cl (grade II, Sigma). In most recordings, the dihydropyridine agonist (+)-202-791 (1 µM; stock: 1 mM in ethanol, Sandoz Pharma) was added to the perfusion solution to allow better resolution of the tail currents.

2.3.4. Solutions and reagents for electrophysiological recordings

Pipette solution (regular): 65 mM KF, 55 mM KAc, 5 mM NaCl, 1 mM $MgCl_2$, 10 mM ethylene glycol-bis (b-aminoethyl ether)-*N,N,N',N'*-tetraacetic acid (EGTA), 10 mM HEPES, and 0.2 mM $CaCl_2$ (final concentration of $\approx 10^{-7}$M); pH was adjusted to 7.4 with 2 M KOH (final≈20 mM). In some experiments, the pipette also contained 0.5% lucifer yellow (potassium salt; Sigma).

Pipette solution for recording Ca^{2+} currents: 65 mM CsF, 50 mM CsAc, 4 mM $MgCl_2$, 4 mM Na_2ATP, 0.2 mM NaGTP, 14 mM phosphocreatine (Sigma), 10 mM HEPES, 10 mM EGTA; pH was adjusted to 7.4 with 2 M KOH (final≈25 mM). The solution was kept on ice during the experiments.

Extracellular perfusion solution (regular): 140 mM NaCl, 5.4 mM KCl, 0.33 mM NaH_2PO_4, 0.44 mM KH_2PO_4, 2.8 mM $CaCl_2$, 0.18 mM $MgCl_2$, 10 mM HEPES, 5.6 mM glucose, 2 mM glutamine, 5 µg/ml phenol red; pH was adjusted to 7.4 with 1 M NaOH (final≈2 mM). For fast agonist application experiments, 0.5 µM Tetrodotoxin (TTX; Sigma) was added.

Extracellular perfusion solution for recording Ca^{2+} currents: same as above except that $CaCl_2$ was at 5 mM, and 10 mM tetraethylammonium (TEA)-bromide (Sigma), 2 mM 4-aminopyridine (4-AP)-Cl (grade II, Sigma) and 1 µM TTX were added.

2.4. MOLECULAR BIOLOGY

2.4.1 RNA extraction

RNA was extracted from nodose and SC ganglia or from cultured neurons, by a method based on Chomczynski and Sacchi (1987). The ganglia were dissected and kept in a petri dish containing ice-cold L15-Air until the end of the dissection. The ganglia were then transferred to a 15 ml polypropylene tube (Falcon 2059), and the L15 air was removed and replaced by 3 ml of ice-cold solution D (see below). The ganglia were then homogenized using a polytron. For many experiments, the ganglia were dissociated and neurons were separated from non-neuronal cells as described above (**2.1.1.**) prior to RNA extraction. In that case, the dissociated neurons were rinsed once with plating medium (**2.1.4.**) and once with ice-cold modified HBSS (**2.1.4.** containing DEPC-H_2O [see below]) and resuspended in solution D (usually 200–400 µl) by pipetting up and down 10 times with a "pipetman" (no polytron was necessary). For cultured neurons, the petri-dishes were rinsed twice with ice-cold modified HBSS (plus 1 mM $CaCl_2$). Then, 2–4 petri dishes from one given condition were typically pooled together and 300–400 µl of solution D was used to collect the RNA. To maximize yield of RNA extraction, 100 µl of solution D was added to the center well of one petri dish, pipetted up and down 5 times and the solution was transferred to a second well. A second 100 µl of solution D was used to rinse the same center well.

The following solutions were added sequentially to the solution D containing neuronal extracts while vortexing between each one: sodium acetate 2 M (pH 4.1) at a 1:10 ratio with solution D; phenol (see below) at a 1:1 ratio with solution D; chloroform:isoamyl (24:1) at a 2:10 ratio with solution D. This mixture was kept on ice for 15 min, centrifuged for 20 min at 4°C (10 000g), and the aqueous phase was recovered and mixed with equal volume of isopropanol and stored at -20°C for 1 hr or overnight (24–48 hrs for

cultured neuron RNA). The precipitated RNA was then centrifuged, resuspended in 0.1 to 0.5 ml of solution D (depending on the amount of RNA) and reprecipitated with equal volume of isopropanol at -20°C for 1 hr or overnight (24-48 hrs for RNA from cultured neurons). The precipitated RNA was rinsed with 70% ethanol, air dried and resuspended in DEPC-H_2O (100-400µl) and the optical densities (OD_{260} and OD_{280}) were measured on a spectrophotometer to quantify the amount of RNA (OD_{260} of 1=40µg/ml RNA) as well as the ratio RNA:DNA. A ratio OD_{260}/OD_{280} of 1.8-2.1 was considered satisfactory for RNase protection assays. The RNA from cultured neurons was resuspended in only 100 µl, and its OD was measured using an RNase free microcuvette (100 µl; Beckman) that was pre-cleaned with DEPC-H_2O containing 100 mM NaOH and 1 mM EDTA. In this manner, the ODs could be measured for the entire RNA samples, without extra dilutions. The RNA was then re-precipitated and kept at -20°C until use for RNase protection assays. Our average yield of total cellular RNA from 4 petri dishes with each ≈6000 SCG neurons cultured for 7 days was 2.0 ± 0.2 µg.

2.4.2. Riboprobe synthesis

Riboprobe syntheses, for RNase protection assays and *in situ* hybridization experiments, were performed according to that described by Krieg and Melton (1987). [^{32}P] radiolabelled antisense RNA probes were transcribed *in vitro* from linearized plasmids containing subcloned portions of the cDNAs of interest. For the transcription reaction, the following reagents were added sequentially in a microcentrifuge tube: 1 µl of ATP, GTP and CTP (10 mM stock; final=500 µM; Promega), 8.5 µl nuclease free ddH_2O (Promega), 2 µl 10X transcription buffer (see below), 4 µl ^{32}UTP (800 Ci/mmol; Dupont), 1 µl (30 Units) RNase inhibitor (Pharmacia), ≈0.5 µg of linearized template cDNA (≈1 µl) and 0.2 to 1.0 µl of RNA polymerase (either SP6, T3 or T7, 5-10 Units). The final volume was ≈20 µl; after mixing well, the solution was incubated at 37°C for 50-60 min. Occasionally, fresh polymerase was added for another 50-60 min of transcription reaction. The template DNA was then digested with 10 Units of DNase I (Pharmacia) for 20 min at 37°C. To help precipitating the probes, 10 µg tRNA (Sigma) was added, before 100 µl DEPC-H_2O and 100 µl water-saturated phenol:chloroform

(50:50) was added and vortexed well in order to remove all proteins. After 5 min centrifugation (10 000g), the aqueous phase was collected and mixed with 9 µl of 10 M ammonium acetate and 322 µl ethanol. The probes were precipitated for 30 min and centrifuged for 20 min at 10 000g.

In order to eliminate any smaller radiolabelled RNA resulting from incomplete transcription, which could interfere with the full length riboprobes in the hybridization reactions, we "gel purified" the probes. The pelleted probes were resuspended in loading buffer (see below) and separated by electrophoresis on a 5% polyacrylamide-8M Urea gel (see below) for 1 hr at constant voltage (240 V) with 1X TBE (see below) as the running buffer. Following electrophoresis, the gel was adsorbed to Watman paper and covered with plastic wrap, and exposed to Kodak X-ray film (in the dark room) for approximately 1 min to reveal the probe signals. The outline of the film was drawn with a marker onto the Watman paper during the exposure period: the developed X-ray film could then be placed back on top of the gel to excise the probes (through the film) with a razor blade. The highly radioactive piece of gel was then put in a microcentrifuge tube containing elution buffer (see below). The probes were eluted (vigourous shaking at 37°C) for 2-18 hrs. The eluate was mixed with equal volume of 100% ethanol to precipitate the probes. The precipitated probes were kept at -20°C until use (up to 3 days).

2.4.3. RNase protection assay

RNase protection assays were performed according to protocols described in Krieg and Melton (1987), Sambrook *et al.* (1989) and Ausubel *et al.* (1989), with minor modifications. Typically, 0.5-2 µg of total cellular RNA was combined with 1 to 3 radiolabelled riboprobes (usually 200 000 cpm each), both as ethanol precipitates. The mixture was centrifuged at 10 000g for 20 min, the ethanol removed and the radioactive pellet resuspended in 30 µl hybridization buffer (see below), by 30 triturations. We found that this method gave us much more reproducible results than resuspending the pellet by vortexing. The RNA mixture was denatured at 85-90 °C for 10 min and incubated overnight at 60°C. The following day, the non-hybridized riboprobes (or all single stranded RNAs) were digested by a 30 min incubation at 37°C with RNase T1 (1000

Units, Sigma), in 350 ml of digestion buffer (see below). To stop the digestion reaction, 50 µg of proteinase K (Sigma) and 10% sodium dodecyl sulfate (SDS) were added for a 15 min incubation at 37°C. Then, 10 µg of tRNA was added to help precipitate the RNA/riboprobe duplexes which were first extracted with phenol:chloroform (50:50). After vortexing and centrifuging (5 min, 10000g), the aqueous phase was recovered and combined with 1 ml of 100% ethanol to precipitate the RNA/riboprobe duplexes, which took 30 min at room temperature. After centrifugation (20 min, 10 000g) the ethanol was removed and the pelleted RNA/riboprobe duplexes were resuspended in 30 µl loading buffer by 30 "triturations", separated by incubating at 85-90°C for 5 min, and electrophoresed on a 5% polyacrylamide-8 M Urea gel for 2-3 hrs at 230 volts. The gel was then placed on Watman paper, covered of plastic wrap and vacuum-dried for 45-60 min. The dried gel was first exposed to a phosphor imaging plate for 1-2 hrs at room temperature to quantify the hybridization signals. Then the gel was exposed to X-ray film at -70°C with an intensifying screen for 1-4 days.

The thermal stabilities for all probes, as calculated from their melting temperatures, differed by less than 1°C. The specific activity of each riboprobe was calculated from the number of adenine bases. To quantify the levels of mRNA among different transcripts, the relative intensities of the hybridization signals were divided by the specific activity of the corresponding riboprobe.

2.4.4. *In situ* hybridization

For *in situ* hybridization, neurons were grown in small (5 mm^2) coverslips to minimize the amount of riboprobes. Two labelling techniques were used: [^{32}P]-labelled riboprobes revealed by emulsion photography and digoxigenin (DIG)-labelled riboprobes revealed by immunocytochemistry with a DIG antibody conjugated with alkaline phosphatase (DIG-Ab-AP).

2.4.4.1. Fixation of cells

Cells were fixed according to that described in section 2.2.1., except that the fixative was prepared with DEPC-H_2O. Glutaraldehyde (0.01%) was also used facultatively (better

fixation quality, but weaker hybridization signals). Neurons also were permeabilized with 100% ethanol at -20°C for 15 min, or alternatively with 70% ethanol (30% DEPC-H_2O) and stored at -20°C until use (up to 2 weeks).

2.4.4.2. Pre-hybridization

Cells were re-hydrated by 3 rinses with DEPC-PBS. Salmon sperm DNA (final: 250 µg/ml; see below) and tRNA (final: 500 µg/ml) were boiled for 5 min and chilled on ice, and then mixed with pre-hybridization buffer (see below), containing RNase inhibitor, vanadyl sulphate ribonucleoside complex (VSRC; 20 mM; Boehringer Manheim). The mixture was rapidly added to the neurons in the center well of each dish (e.g. 20-30 µl) and the cells were incubated for 1-3 hrs at 43°C in a humid incubator.

2.4.4.3. Riboprobe hybridization

Precipitated cRNA probes (either [^{32}P] or DIG -labelled probes; see below) were pelleted by 20 min centrifugation, rinsed with 70% ethanol, and air dried for 10 min. Salmon sperm DNA and tRNA (same final concentrations as above) were added to the pellet and thoroughly mixed by 30 triturations. The mixture was boiled 5 min after which the hybridization buffer, VSRC (20 mM final), and DTT (60 mM final) were added. After removing the pre-hybridization buffer from the center well of each culture dish, the cRNA probe-containing hybridization buffer was added (30 µl). The cells were incubated with the probes for ≈16 hrs at 43°C in a humid incubator: 1 X 10^6 cpm of [^{32}P]-labelled riboprobes or 20 ng of DIG-labelled riboprobes were mixed with 30 µl of hybridization buffer.

2.4.4.3. Rinsing procedure and digestion of non-hybridized RNA

After hybridization, the cells were rinsed twice with ≈1 ml of warm (≈43°C) 4X SSC (see below) while gently shaking on a rotatory plate in a 43°C incubator for 10-15 min. Two more rinses were repeated with 2X SSC and then the neurons were rinsed once with RNase buffer (see below), followed by a 30 min incubation at 37 °C with RNase T1 (2µl/ml; Sigma) in RNase buffer, in order to digest any non-hybridized cRNA probes. This

was followed by 3 rinses with 1X SSC for 10-15 min. and 1 rinse with 0.1X SSC for 15 min at 43°C.

2.4.4.4. [^{32}P]-riboprobes: emulsion coating, development and slide mounting

The emulsion coating of [^{32}P]-labelled specimen was carried out in the dark room. The emulsion solution (50:50 Kodak NTB2:ddH_2O) was melted by incubation in 37°C water bath. The aclar coverslips were pealed off from the petri dishes and, one by one, dipped vertically into the emulsion without tilting. After dipping for 2-3 sec. the coverslips were withdrawn, the excess emulsion drained into tissue paper, and the coverslips were allowed to dry by standing vertically in a light proof plastic box containing a Drierite bag to remove humidity. The boxes were sealed with tape and stored at 4°C for 1 to 2 weeks, before processing for development. To develop the emulsion, coverslips were dipped (in the dark room) in Kodak D-170 developer (15°C) for 6 min. Development was stopped by rinsing with ddH_2O for 30 sec. and the emulsion was fixed with 24% sodium thiosulphate for 3 min. After rinsing for 10 min with tap water and 30 sec in ddH_2O, coverslips were dehydrated by sequential rinses with 50%, 75%, 95% and 100% ethanol solutions, and air-dried for 15 min. Coverslips were then mounted on slides with Entellan (Fisher), and examined with phase contrast and dark field microscopy.

2.4.4.5. DIG-riboprobes: DIG-antibody incubation and alkaline phosphatase reaction

Cells were rinsed once with DIG-Ab-AP buffer (see below) and incubated with DIG-Ab-AP blocking solution (see below) for 30 min at room temperature. Then, the cells were incubated for 1 hr with DIG-Ab-AP (sheep antibody; Boehringer Mannheim; 1/200 dilution in DIG-Ab-AP blocking solution), followed by 3 rinses with DIG-Ab-AP buffer for 10-15 min on shaking table at room T°C. The alkaline phosphatase reaction was performed as described in section 2.2.1.. Cells were incubated with the reaction mixture for 1 to 24 hrs depending on the intensity of the signal (brown color).

2.4.4.6. Riboprobe synthesis for *in situ* hybridization

[^{32}P]-labelled cRNA antisense probes were synthesized, gel purified and eluted as

described in section **2.4.2.**

DIG-labelled cRNA antisense probes were synthesized according to the method described in section **2.4.2.** with some modifications:

The following reagents were added sequentially in a microcentrifuge tube: 6 µl of ATP, GTP and CTP (10 mM stock: final=1.5 mM), 6 µl of UTP:DIG-UTP mix (75%:25%; both 10 mM stocks: UTP-DIG from Boehringer Mannheim), 4 µl 10X transcription buffer, 10 µg linearized template DNA, 2 µl (60 Units) RNase inhibitor (Pharmacia), 0.5-2 µl RNA polymerase (SP6, T7 or T3), completed to 40 µl with nuclease free ddH_2O. Probes were synthesized for 1 hr, and fresh polymerase was added for a second round of synthesis.

As described in section **2.4.2.**, the template DNA was digested, the probes were extracted with phenol-chloroform, and then precipitated with ethanol. Precipitated probes were resuspended in DEPC-H_2O and reprecipitated again with ethanol and ammonium acetate. Finally, the pelleted probes were rinsed with 70% ethanol and resuspended for OD measurements, after which they were re-precipitated and kept a -20°C until use (good for several months).

2.4.5. cDNA plasmids

Plasmids (containing cloned cDNA and ampicillin resistance gene) were grown in E. Coli, on 2YT agar plates (see below) or in 2YT medium (see below) containing ampicillin (20-100 µg/ml). The plasmid DNA was extracted and purified using alkali lysis of bacterial cultures, phenol-chloroform extraction, and polyethylene glycol precipitation as described by Sambrook *et al.* (1989).

Plasmids containing nAChR subunit cDNA inserts of α_2, α_3, α_4, α_5, α_7, β_2, β_3 and β_4 were supplied by Dr. E. Deneris (Case Western reserve University) and used as templates for the transcription reaction (Mandelzys *et al.*, 1994). The sizes of the synthesized riboprobes (in base pairs) were α_2=194, α_3=268, α_4=602, α_5=547, α_7=510, β_2=581, β_3=492 and β_4=441. Most of the probes were made against the carboxy terminus and the 3' non-coding region, except for the probes for α_4 and β_3 which were made against the amino termini. All chosen sequences exhibit very little homology among one

another.

Plasmids containing subcloned portions of neurotrophin receptors were supplied by Dr. P. Barker (Montreal Neurological Institute, McGill university) for *trk*A (pSP*trk* 5-7) and $p75^{LNGFR}$ (p5a), Dr. Tony Jelsma (Center for Research in Neuroscience, McGill University) and Dr. E. Shooter (Stanford University) for $p75^{LNGFR}$ (pNGFR1), Dr. G. Yancopoulos (Regeneron) for *trk*B (pSK-*trk*B) and *trk*C (pSK-*trk*C). The sizes of the synthesized riboprobes (in base pairs) were: *trk*A=397, *trk*B=730 or 335, *trk*C=324, $p75^{LNGFR}$ (p5a)=300.

The plasmid pSK-*trk*B contained the full length clone of *trk*B. To make a template cDNA for a riboprobe that would allow us to distinguish both major splice isoforms of *trk*B (i.e. $trkB^{TK+}$ and $trkB^{TK-}$), we cut the clone at site 2530 and in the polylinker of pSK with DraII to remove a portion of the DNA. The cut DNA was migrated on a 1% agarose (with ethidium bromide) to separate the linear plasmid from the released undesired piece of DNA. The linear plasmid (larger band) was excised from the gel under a UV light, extracted from the gel by centrifugation through micro-spin filter (0.45 µm; DiaMed) and religated using T4 DNA ligase. By linearizing this modified *trk*B clone [pSK-*trk*B⁻] with Hinc II we transcribed an antisense riboprobe that spans part of the intracellular tyrosine kinase domain (only in $trkB^{TK+}$) as well as the transmembrane region (common to both isoforms). The riboprobe length was 730bp, and the length of the fragments after protection were: $trkB^{TK+}$ =715bp, $trkB^{TK-}$ =210bp.

Plasmid containing subcloned portion of GAPDH (pTRI-GAPDH-mouse plasmid) was purchased from Ambion. Probe length=300bp; protected length of riboprobe=150bp.

All restriction enzymes, DNA modifying enzymes and transcription enzymes were purchased from New England Biolabs (NEB).

2.4.6. Solutions and reagents for molecular biology:

2x YT Medium: for 1 liter of ddH_2O, 16g bacto-tryptone, 10g bacto-yeast extract (Fisher), and 5g NaCl; pH adjusted to 7.0 with NaOH 5N; sterilized by autoclaving 20 min.

Agar plates: 2x YT medium plus 15 mg/ml bacto-agar; autoclaved 20 min, cooled down

to 50°C and 20 µg/ml of ampicillin was added before liquid (30-35 ml) was poured in 10 cm plates. Kept at 4°C protected from light up to a month.

Denhardt's solution 100X: 2% (w/v) Ficoll (Sigma-mol biol grade), 2% (w/v) polyvinylpyrollidine (mol. biol. grade: Sigma), 2% (w/v) BSA (fraction V: Sigma), in ddH_2O; filtered through 0.45 µm, aliquoted (≈1 ml) and stored at -20°C.

DEPC-H_2O: diethyl pyrocarbonate-treated ddH_2O. The ddH_2O was stirred with 0.1% of DEPC for several hrs and autoclaved for 1 hr to hydrolyse the DEPC (from Fisher).

DIG-Ab-AP buffer (Digoxigenin-antibody-alkaline-phosphatase buffer): 150 mM NaCl, 100 mM Tris-HCl (pH 7.5)

DIG-Ab-AP Blocking solution: DIG-Ab-AP buffer + 3% Fetal Calf Serum (v/v) and 1% blocking reagent (Boerhinger Mannheim).

Digestion buffer: 300 mM NaCl, 10 mM Tris-Cl (pH 7.5) and 5 mM NaEDTA in ddH_2O.

DTT (Dithiothreitol): 5 M DTT (mol. biol. grade: Sigma), dissolved in 0.01 M sodium acetate (pH 5.2); filtered through 0.45 µm, aliquoted (≈1 ml) and stored at -20°C.

Elution buffer: 2 M ammonium acetate, 1% SDS, 33 µg/ml tRNA, and DEPC-H_2O

Hybridization buffer for in situ hybridization: same as pre-hybridization buffer plus 10% dextran sulphate

Hybridization buffer for RNase protection assays: 80% deionized formamide (Fisher), 10% 10X hybridization buffer (400 mM PIPES [piperazine-N,N'-bis[2-ethanesulfonic acid]] buffer, pH 6.4, 4 M NaCl and 10 mM EDTA), and 10% DEPC-H_2O.

Loading buffer: 80% formamide, 1 mM EDTA, 0.02% (w/v) xylene cylanol, 0.02% (w/v) bromophenol blue, and DEPC-H_2O.

Phenol for DNA preparation: The phenol (Fisher) was saturated with 0.1 M Tris pH 8.0 according to the method of Sambrook *et al.*, 1989. Hydroxyquinoline (0.1% w/v) was added to reduce oxidation, RNase activity, and to facilitate the distinction between the aqueous and organic phases.

Phenol for RNA preparation: The phenol was saturated with ddH_2O (+ 0.1% hydroxyquinoline).

Phenol:chloroform: 1 volume of phenol (DNA or RNA type: see above) was mixed with

1 volume of chloroform:amyl (24:1).

Polyacrylamide-8 M Urea gel (5%): (for 50 ml) 24g of urea (BRL), 5 ml of 10X TBE, 6.25 ml of 24:1 acrylamide:bis-acrylamide (38:2% stock, Fisher) and DEPC-H_2O. Once the ingredients were dissolved, the solution was filtered through Watman paper. 500 µl of 10% ammonium persulfate (BRL) and 10 µl of TEMED (N,N,N',N'-tetramethylethylenediamine, Fisher) were added to catalyse gel polymerization, which took approximately 1 hr.

Pre-hybridization buffer for in situ hybridization: 50% formamide (super pure grade, Fisher), 4X SSC, 1X "denhardt's", 20 mM phosphate buffer (pH 7.0), 20% (w/v) sarcosyl; filtered through 0.45 µm filter, aliquoted (≈1 ml) and stored at -20°C.

RNase buffer: 300 mM NaCl, 100 mM Tris-HCl, 5 mM NaEDTA, ddH_2O

Salmon sperm DNA: prepared according to Sambrook *et al.* (1989).

Solution D: 4 M guanidine isothiocyanate, 25 mM sodium citrate, 0.5% sarcosyl (v/v), 0.75 % (v/v) ß-mercaptoethanol

SSC: 20X solution: NaCl (175.3 g) and sodium citrate (88.2 g) in 1 liter of ddH_2O, pH adjusted to 7.0 with 10 N NaOH; sterilized in autoclave (20 min).

Stopping buffer: PBS (pH 7.4) and 20 mM NaEDTA.

TBE: 892 mM Tris-HCl, 890 mM boric acid and 25 mM EDTA, pH adjusted to 8.3 with HCl; Sterilized by autoclaving.

Transcription buffer: 400 mM Tris-HCl [pH 7.9], 60 mM $MgCl_2$, 20 mM spermidine, 10 mM DTT; from NEB.

2.5. Data analysis

When scoring the percentage of neurons that extended dendrites or that were sensitive to capsaicin, the confidence limits of these percentages were estimated from the binomial distribution (Walpole, 1982). Standard t-tests and Duncan's multiple-range tests were used, where indicated, to determine statistical differences (Walpole, 1982).

Chapter 3

NGF Induces Neonatal Rat Sensory Neurons To Extend Dendrites in Culture After Removal of Satellite Cells

INTRODUCTION

Vertebrate neurons typically have several dendrites that originate from their cell bodies, and most afferents establish synapses on these dendrites. Little is known, however, about the mechanisms that stimulate or inhibit the initiation of dendrites, or what controls the arborization of dendrites once they have been initiated. Studies have indicated that the initiation of dendrites are, in part, governed by mechanisms intrinsic to neurons (Dotti *et al.*, 1988; Black and Baas, 1989). In addition, there is ample evidence that extrinsic factors influence neuronal polarity and dendritic arborization (Mudge, 1984; Purves *et al.*, 1988; Snider, 1988; Tropea *et al.*, 1988; Bruckenstein and Higgins, 1988a,b; Lein and Higgins, 1989; Chamak and Prochiantz, 1989; Johnson *et al.*, 1989; Clendening and Hume, 1990; Rousselet *et al.*, 1990; Schilling *et al.*, 1991; Le Roux and Reh, 1994).

While almost all vertebrate neurons extend dendrites, a notable exception is the peripheral sensory neuron. Morphologically, sensory neurons are pseudo-unipolar, and their ovoid somata, which are devoid of synapses, are covered by satellite cells (peri-somatic glia) and lack dendrites (Lieberman, 1976; Pannese, 1981). The axons of sensory neurons bifurcate shortly after emerging from the cell body; one branch grows peripherally and its terminals develop into a sensory transducer; the other branch grows centrally forming synaptic connections within the CNS. The fact that sensory neurons do not express typical dendritic-axonal polarities, like those established on most neurons, suggests that either part of the mechanisms that initiate dendritic growth are not functioning in sensory neurons, or mechanisms exist which actively suppress sensory neurons from extending dendrites. Deciding between these two possibilities should provide some clues as to the mechanisms that control the establishment of neuronal polarity.

Previously, it was shown that when neonatal sensory neurons from rat nodose ganglia

were cultured in the absence of satellite cells, they formed synapses among one another (Cooper, 1984), suggesting that these neurons were expressing new postsynaptic elements necessary for synapse formation. One example is the neuronal nAChR: *in vivo*, few nodose neurons express ACh-evoked currents, yet in these cultures, many have high density ACh-evoked currents and the synapses are cholinergic (Cooper, 1984; Mandelzys and Cooper, 1992). Other possible postsynaptic specializations that could be expressed on these neurons, and play a role in promoting these novel synapses among sensory neurons, are dendrites. If dendrites were being expressed *de novo* on these neurons, this preparation would provide an attractive model to investigate various mechanisms that control dendritic outgrowth, as well as targeting and localization of postsynaptic elements (e.g. nAChRs) and nerve terminals in neuron-neuron synapses.

To investigate whether nodose neurons have dendrites, one needs a reliable marker to distinguish dendrites from axons as the neurons develop in culture. There are several notable differences in cytoskeletal protein and organelle content between axons and dendrites. For example: (1) ribosomes and Golgi elements are present in dendrites but not in axons (Bartlett and Banker, 1984a,b; Peters *et al.*, 1991); (2) the microtubule polarity orientation differs in axons and dendrites (Black and Bass, 1989); (3) a much greater number of neurofilaments are phosphorylated in axons compared to dendrites (Peng *et al.*, 1986); and, (4) the types of microtubule-associated proteins differ in axons and dendrites (Kosik and Finch, 1987; reviewed by Matus, 1988). In particular, microtubule-associated protein-2 (MAP2), and the mRNA that codes for it, are found exclusively in cell bodies and dendrites (Caceres *et al.*, 1984; Caceres *et al.*, 1986; Kosik and Finch, 1987; Garner *et al.*, 1988), whereas, tau proteins are predominantly distributed in axons (Kosik and Finch, 1987; Craig and Banker, 1994).

In this chapter, we have used lucifer yellow injections to examine the establishment of neuronal polarity by neonatal nodose neurons in culture and used antibodies to MAP2 to investigate whether these neurons extend dendrites as they develop in culture.

EXPERIMENTAL PROCEDURES

Cell cultures

Neurons were dissociated, separated from their non-neuronal cells and cultured as described in section **2.1.** In satellite cell free cultures, Ara-C (10 μM) was added to the culture medium for the first 4 days to eliminate any remaining dividing cells. As described in section **2.1.2.** some slow dividing fibroblast-like cells remain in these cultures. Satellite cells and Schwann cells divide rapidly in culture and can be virtually eliminated with a 4 day Ara-C treatment. Both cell types are undistinguishable in these cultures, and are essentially similar *in vivo* (Lieberman, 1976; Le Douarin and Ziller, 1993); therefore, we include both types when we refer to satellite cells. To co-culture neurons and satellite cells, we used two different methods. First, for most cultures, the percoll step (for separation of neurons from satellite cells; see section **2.1.1.**) was omitted and no Ara-C was added to the growth medium. Second, for some cultures, particularly those involving short term cultures combined with lucifer yellow injections, the satellite cells suspension obtained from the percoll step was washed and plated on laminin coated coverslips, allowed to grow 2-3 days (until confluence) before neurons (from another litter of neonatal rats) were plated on top of them. In some cases, the satellite cell layer was pre-fixed with 0.5% paraformaldehyde (overnight at 4°C), and thoroughly washed with HBSS before plating the neurons on top (Hawrot, 1980).

In this study, we used 10 nM 7S NGF (see section **2.1.4.**). In cultures grown without NGF, sheep antiserum to mouse NGF (kindly provided by Dr. J. Diamond, McMaster University) was added to the cultures at a dilution of 3:10000 (a dilution of 1:10000 blocks the trophic effect of 10 nM 7S NGF when added to SCG cultures).

Immunocytochemistry

All immunostaining procedures were performed as described in section **2.2.1.** HM-2 (Sigma), a mouse monoclonal antibody against MAP2, was used to label dendrites. SMI31 (Sternberger-Meyer Immunochemicals), a mouse monoclonal antibody against phosphorylated forms of the M and H neurofilaments subunits, was used to label axons. For double labelling experiments (for MAP2 and phosphorylated neurofilaments), we used

a rabbit polyclonal antibody against MAP2 (R4, kindly provided by K. Kosik) together with the SMI31 antibody. In some experiments we immunostained our cultures with an antibody against MAP2a and b isoforms (AP-20; Sigma); the staining pattern was similar to the HM-2 and R4 antibodies suggesting that MAP2c, which has been observed in axons (Tucker *et al.*, 1988), is not present in neonatal nodose neurons or at least not in their axons. We also tested the antibody SMI32 (Sternberger-Meyer Immunochemicals) to stain non-phosphorylated neurofilaments in neuronal cell bodies and dendrites (Sternberger and Sternberger, 1983). Although we observed most of the immunoreactivity with this antibody in the cell bodies and dendrites, we could detect weak labelling in some axons; therefore, we preferred to use MAP2 antibodies as dendritic markers. The primary antibodies dilutions were: HM-2, 1:5000; R4, 1:10000; AP-20, 1:500; SMI31 and SMI32, 1:20000. Both dendritic morphologies and the localization of HM-2, R4, AP-20, SMI31 and SMI32 staining were similar in nodose and SCG neurons. However, we occasionally observed faint staining with the MAP2 antibodies in SCG axons particularly before the extension of dendrites from SCG neurons. This is consistent with previous observations (Caceres *et al.*, 1986; Kosik and Finch, 1987; Higgins *et al.*, 1988). In contrast, nodose neurons had no apparent staining in their axons beyond their proximal 20-30 μm, at all times in culture.

Lucifer yellow injection

To visualize complete neuronal morphologies, neurons were injected with lucifer yellow as described in section **2.2.3.**.

RESULTS

Nodose neurons co-cultured with ganglionic satellite cells have morphologies typical of sensory neurons

In vivo, nodose neurons develop in close association with their ganglionic satellite cells and do not extend dendrites (Pannese, 1981). Figure 3.1A shows a typical phase contrast photomicrograph of nodose neurons co-cultured with their satellite cells for three

FIGURE 3.1. Nodose neurons cultured with their ganglionic satellite cells.

(A) Phase contrast photomicrograph of neonatal nodose neurons in culture for 3 weeks with satellite cells. (B) lucifer yellow injection of two nodose neurons from sister cultures. The upper neuron is unipolar and is illustrated in a montage of two photographs at different exposures to allow a better visualization of the single axon branching into two axons. The lower neuron is bipolar: it has two axons emerging from the cell body. (C) Fluorescent MAP2 (HM-2) staining of the same neurons as in A. Neurons lack MAP2 positive processes and many neurons have weakly immunostained cell bodies. Scale bar, 40 μm.

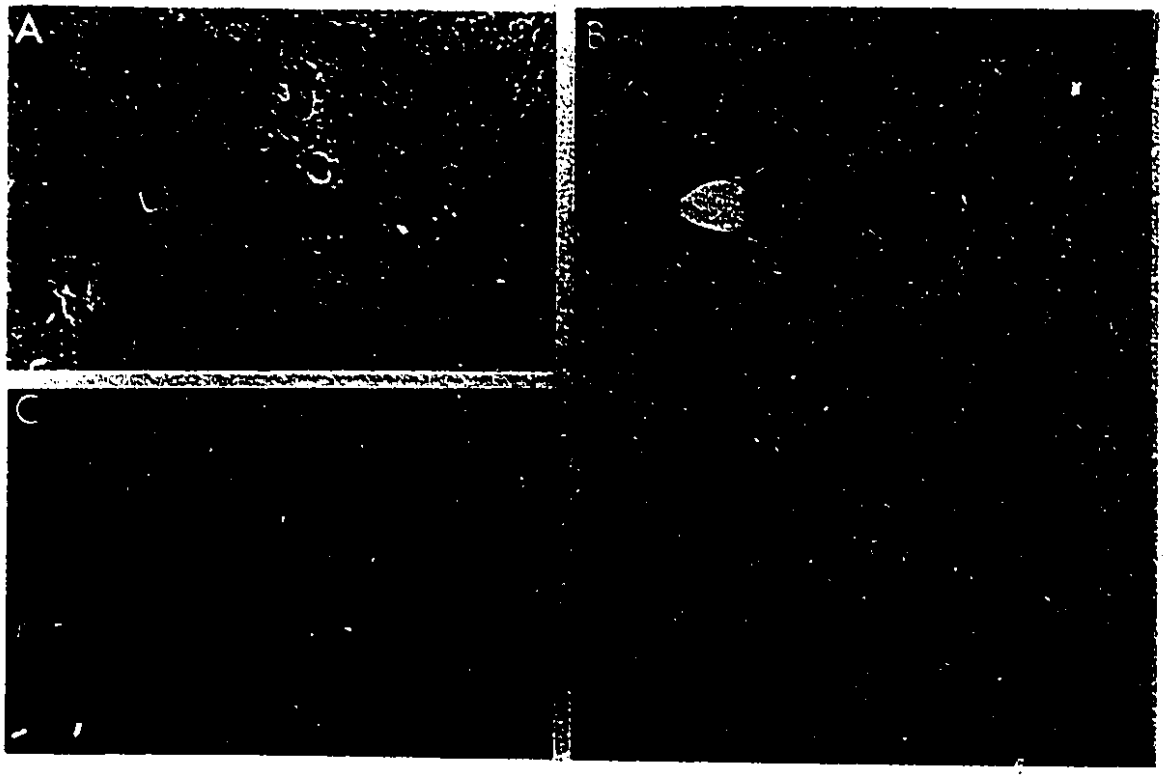
A
B
C

weeks with NGF. The cell bodies of most neurons remained spherical or ovoid, although many appeared to have flattened onto the satellite cells. Most processes from these neurons are covered by the satellite cells and are difficult to resolve with phase optics. To investigate the morphologies of these neurons, the neurons were injected with lucifer yellow. Forty-six percent (29/63) of these neurons were unipolar after 2-3 weeks in culture (Figure 3.1B; top). This unipolar morphology is similar to sensory neurons *in vivo* (Cajal, 1955; Tennyson, 1965). Twenty-nine percent (18/63) of the neurons had a bipolar morphology (Figure 3.1B; bottom); this morphology is typical of undifferentiated sensory neuroblasts (Tennyson, 1965). Sixteen percent (10/63) of the neurons had 3 or more axons. Six percent (4/63) of the neurons had one or two short (≤35μm) thick processes emerging from the cell body, and 2 neurons, however, had thick processes that were 35 to 60 μm in length suggestive of dendrites. To investigate whether these processes had properties typical of dendrites, cultures were immunostained with antibodies to MAP2. Figure 3.1C shows the same field as Figure 3.1A but immunostained for MAP2. Of 1740 neurons examined, over 97% lacked processes with detectable MAP2 labelling.

Nodose neurons cultured alone are multipolar and develop dendrites

Unlike nodose neurons co-cultured with satellite cells, virtually all nodose neurons cultured without satellite cells acquire multipolar morphologies. Figure 3.2A and 3.2B show two typical examples of neurons injected with lucifer yellow that had developed for three weeks in culture in the absence of satellite cells and in the presence of NGF. The neuron in Figure 3.2A has 3 thick tapered processes emerging from the cell body that are typical of dendrites, and has at least 2 thin processes of constant calibre typical of axons. In contrast, all 3 processes emerging from the neuron in Figure 3.2B appear axonal.

To distinguish further dendrites from axons in these cultures, we immunostained them with antibodies to MAP2 and to phosphorylated neurofilaments (SMI31), as MAP2 is localised to somatodendritic domains, while neurofilaments are primarily phosphorylated in axons (Sternberger and Sternberger, 1983). Figure 3.3A is a typical phase contrast photomicrograph of three neonatal rat nodose neurons that have developed in culture for 3 weeks in the absence of satellite cells and in the presence of NGF. Figure 3.3B shows

FIGURE 3.2. Nodose neurons cultured without their ganglionic satellite cells.

Lucifer yellow injection of two typical nodose neurons that have developed for three weeks in the absence of satellite cells. The neuron in (A) has three thick tapering processes that end locally, typical of dendrites, and at least two long thin processes of constant calibre, typical of axons (which extend well beyond the field). The neuron in (B) has a spherical cell body with three axonal processes but no dendrite-like processes. Scale bar, 40 μm.

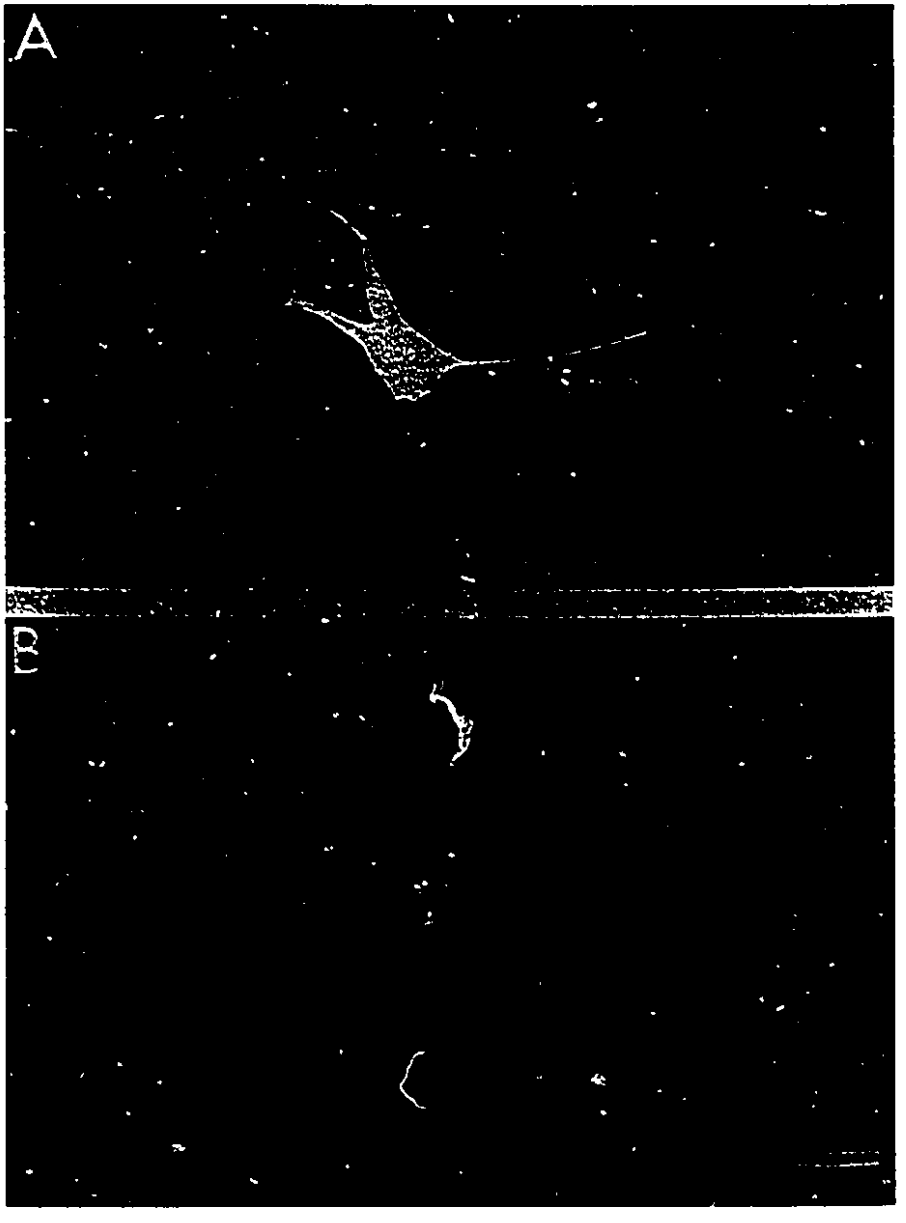
A
B

FIGURE 3.3. Double labelling for MAP2 and phosphorylated neurofilaments on nodose neurons after three weeks in culture without satellite cells and with NGF.

(A) Phase contrast photomicrograph showing three neurons (one is out of the plane of focus). (B) Fluorescent photomicrograph (rhodamine labelling) showing MAP2 staining with rabbit anti-MAP2 (R4). One neuron has three MAP2 positive processes while the other two have no MAP2 positive processes. (C) Fluorescent photomicrograph (fluoresceine labelling) showing phosphorylated neurofilament staining with mouse antibody SMI31. The network of axons seen in A is brightly labelled whereas the cell bodies and dendrites (arrow) have little if any staining. Note the thin axons running along and on top of the dendrites (arrowhead). Scale bar. 40 µm.

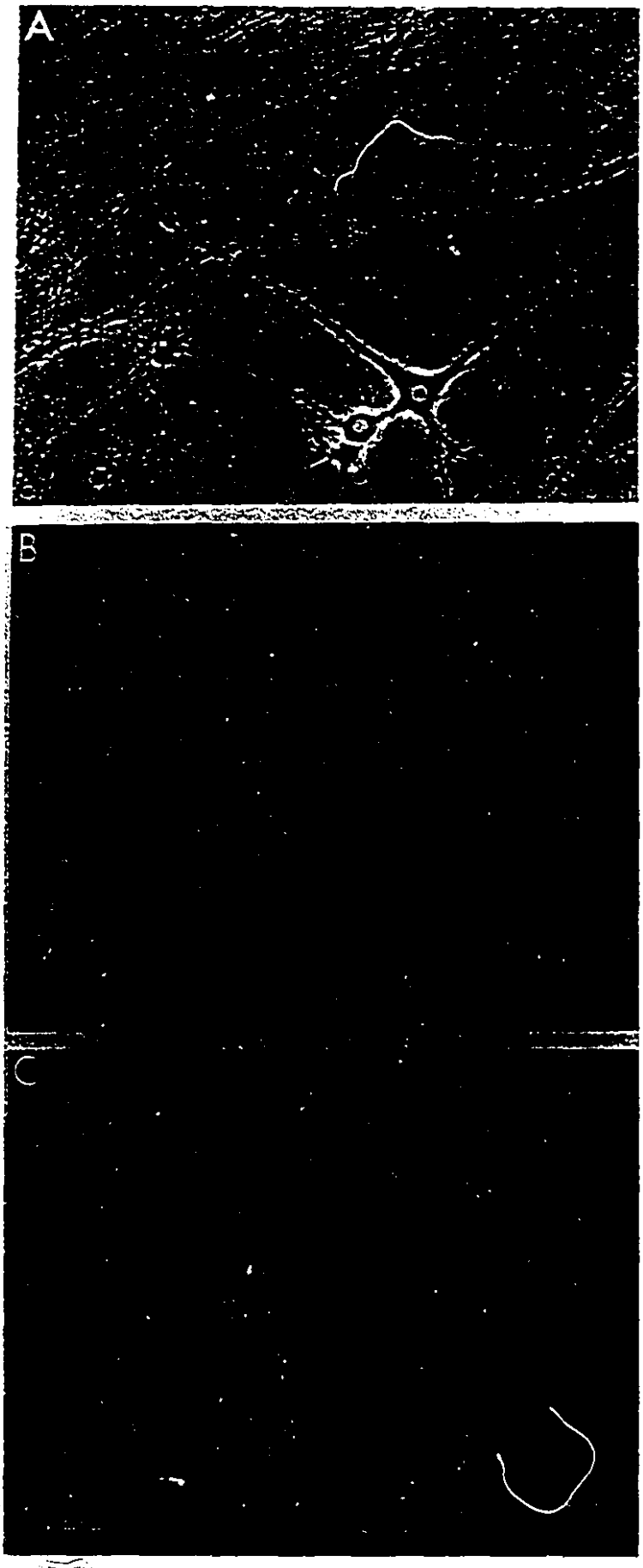
A
B
C

the same 3 neurons immunostained for MAP2. Two neurons have faint MAP2 labelling in their cell bodies but no MAP2 positive processes; the other neuron has 3 thick, MAP2 positive processes, typical of dendrites. Figure 3.3C shows the same field immunostained with the SMI31 antibody. SMI31 labels most of the processes observed with phase optics except for the dendrites which typically have axonal processes running over or along the side of them. Almost 25% (Table 3.1) of the neurons in these cultures had dendrites after three weeks; Figure 3.4 is a montage from one such culture that illustrates this proportion.

In addition to the proportion of neurons that had dendrites, we also measured the number of primary dendrites (dendrites extending directly from the cell bodies) of these neurons and the lengths of each primary dendrite to quantify further the extent of dendritic outgrowth in these cultures. Each parameter was measured at one, two, and three weeks after plating the neurons. Table 3.1 shows that, between one and three weeks in culture, 1) the proportion of neurons extending dendrites increased approximately 2.5 fold 2) the average number of primary dendrites per neuron increased nearly two fold, and 3) the mean dendritic length doubled.

Table 3.1. Development of dendrites and axons in the absence of satellite cells and with NGF.

Time in culture (weeks)	Percentage of neurons with dendrites[1]	Number of primary dendrites per neuron[2]	Mean length of dendrites[3]	Number of axons per neuron[4]
1	10.6 ±0.2 (2314)	1.4 ±0.1 (246)	86 ±8 (66)	2.9 ±0.1 (14)
2	18.7 ±0.3 (2503)	2.0 ±0.2 (469)	108 ±7 (92)	2.7 ±0.1 (31)
3	24.1 ±0.4 (1753)	2.4 ±0.2 (422)	155 ±9 (93)	2.7 ±0.1 (48)

[1] Mean ± SEM (n=total number of neurons from 4 different platings)
[2] Mean ± SEM (n=all the neurons that had dendrites)
[3] Mean ± SEM (n=all the dendrites from 30 neurons selected randomly in a given culture)
[4] Mean ± SEM (n=all the neurons injected with lucifer yellow)

FIGURE 3.4. Nodose neurons cultured with NGF.

(A) Phase contrast photomicrograph of nodose neurons that have developed in culture for three weeks in the absence of satellite cells and in the presence of NGF. (B) Fluorescent MAP2 (HM-2) staining of the same neurons as in A. Note that 2 neurons have long MAP2 positive processes, 1 neuron has a short MAP2 positive process (< 35μm), 4 neurons have MAP2 staining (of variable intensities) only in their cell bodies and 1 neuron shows no staining for MAP2 (arrow). Scale bar, 80 μm.

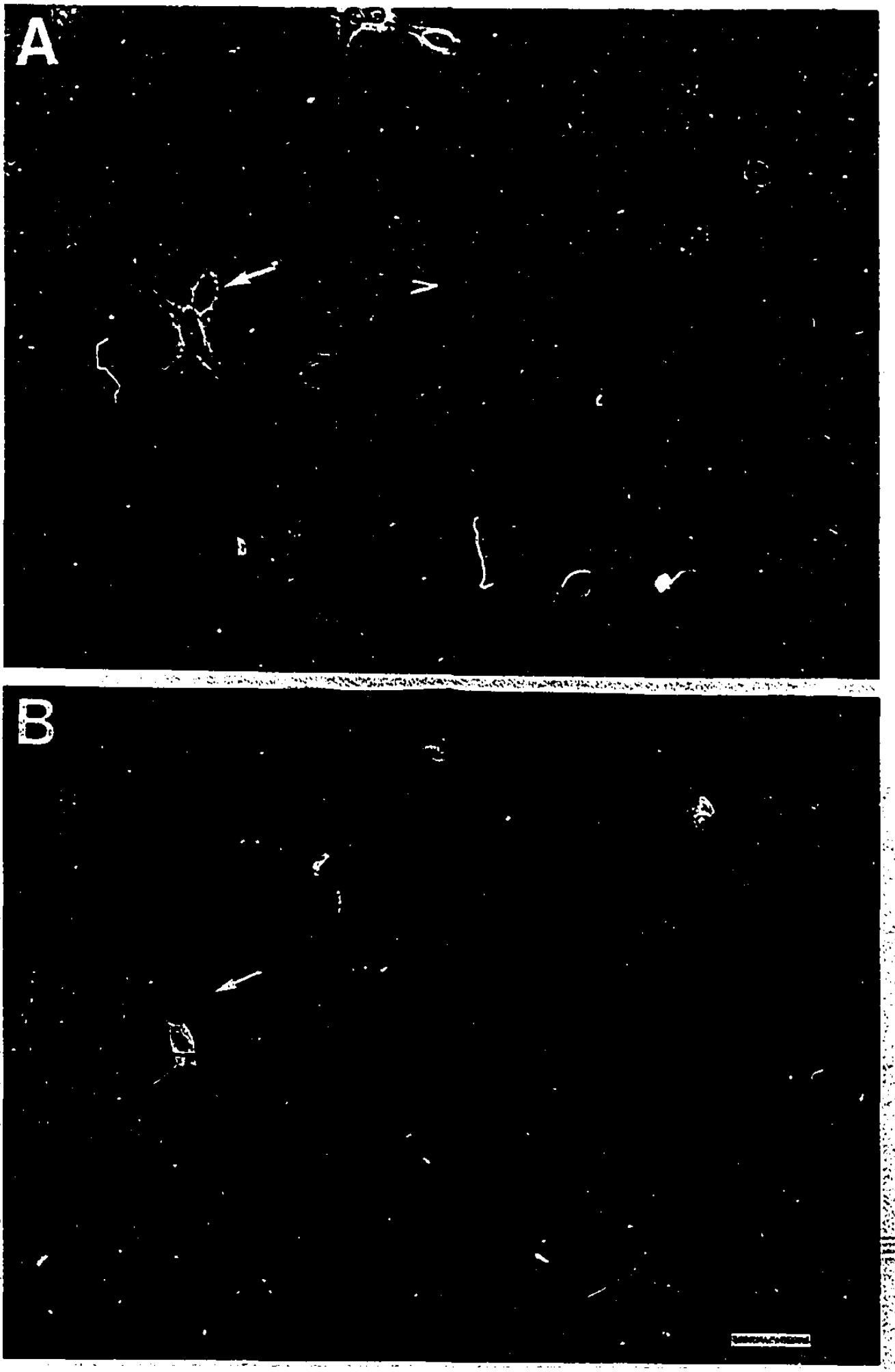
A
B

NGF stimulates dendrite formation

The above results indicate that the control of dendrite initiation is subject to the removal of satellite cells; however, NGF was continually present in these cultures, and NGF has been shown to induce dendritic arborization on sympathetic neurons *in vivo* (Purves *et al.*, 1988; Snider, 1988). NGF also promotes the expression of ACh-evoked currents on nodose neurons in culture (Mandelzys *et al.*, 1990; Mandelzys and Cooper, 1992). Therefore, we tested whether NGF had an effect on dendrite outgrowth once the satellite cells were removed from the cultures.

Figure 3.5A shows a typical phase contrast photomicrograph of nodose neurons that have developed in culture essentially devoid of satellite cells and without NGF for three weeks. With phase optics, these cultures appear qualitatively similar to cultures grown in the presence of NGF (c.f. Figure 3.4A), as neonatal rat nodose do not need NGF for growth and survival in culture, even though they possess high-affinity NGF receptors (Mandelzys *et al.*, 1990; see also Figure 5.1). Figure 3.5B shows the same field immunostained with an antibody to MAP2. In contrast to what was observed with cultures grown with NGF, these cultures showed significantly fewer MAP2 positive processes. The quantification of dendritic outgrowth in these cultures without NGF is presented in Table 3.2. This Table shows that after three weeks without NGF, less than 6% of the neurons extended dendrites and that the average number of primary dendrites per neuron, as well as the mean dendritic length, are both two fold less than those of neurons stimulated by NGF. Total dendritic growth, calculated as the product of the three dendritic parameters in Table 3.1 and 3.2, was more than 15 fold greater in cultures with NGF (Figure 3.6).

To test whether NGF selectively rescued NGF-dependent neurons capable of extending dendrites, we removed NGF and added anti-NGF to some cultures that had received NGF for their first 2 weeks of development and allowed the cultures to develop for an additional 2 weeks. The removal of NGF did not result in neuronal death. In contrast, when we removed NGF from cultures of SCG neurons, the neurons died within a few days.

FIGURE 3.5. Nodose neurons cultured without NGF.

(A) Phase contrast photomicrograph of neurons in culture for three weeks without satellite cells and without NGF. (B) Fluorescent MAP2 (HM-2) staining of the same neurons as in A. Note that fewer MAP2 positive processes are present (compare with Figure 3.4) in these cultures. Same scale as Figure 3.4.

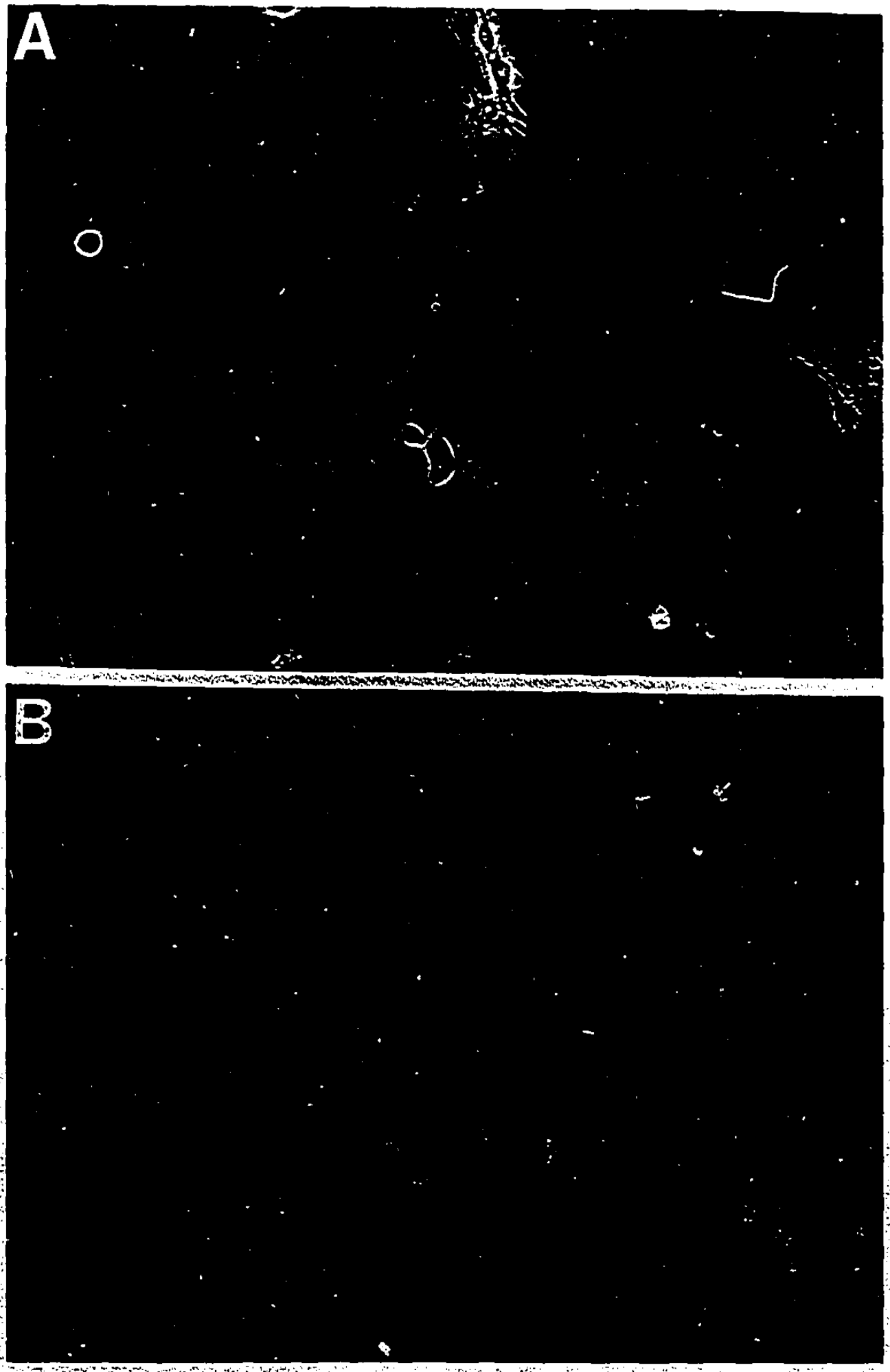
A
B

Table 3.2. Development of dendrites and axons in the absence of satellite cells and without NGF.

Time in culture (weeks)	Percentage of neurons with dendrites[1]	Number of primary dendrites per neuron[2]	Mean length of dendrites[3]	Number of axons per neuron[4]
1	4.3 ±0.1 (1839)	1.3 ±0.1 (79)	77 ±6 (40)	ND
2	5.2 ±0.1 (3023)	1.2 ±0.1 (158)	81 ±6 (42)	2.9 ±0.1 (20)
3	5.8 ±0.1 (999)	1.2 ±0.1 (47)	75 ±8 (40)	2.6 ±0.1 (35)

[1] Mean ± SEM (n=total number of neurons from 4 different platings)
[2] Mean ± SEM (n=all the neurons that had dendrites)
[3] Mean ± SEM (n=all the dendrites from 30 neurons selected randomly in a given culture)
[4] Mean ± SEM (n=all the neurons injected with lucifer yellow)
ND= not determined

To test whether these effects of NGF on process outgrowth were specific for the initiation of dendrites (and not axons), we filled individual neurons with lucifer yellow and measured the number of axons emerging from the somata after 1, 2 and 3 weeks in culture. We classified thin processes of constant calibre that could be followed for a long distance as axons, whereas dendrites were classified as thick, tapered, processes that ended locally (Tropea *et al.*, 1988; Bruckenstein and Higgins, 1988a,b; Peters *et al.*, 1991). The results from these experiments indicate that the number of axons emerging from the somata did not increase significantly from 1 week to 3 weeks in culture, independent of the presence of NGF (see Table 3.1 and 3.2). These results indicate that the effects of NGF are specific for dendrite initiation and emphasize that the initiation of dendrites on these neurons occurs after much longer times in culture than the initiation of axons (c.f. Dotti *et al.*, 1988).

The ability of nodose neurons to develop dendrites is developmentally regulated

The above results indicate that nodose neurons from P1 rats retain the ability to extend dendrites. To determine whether this ability is developmentally regulated, we

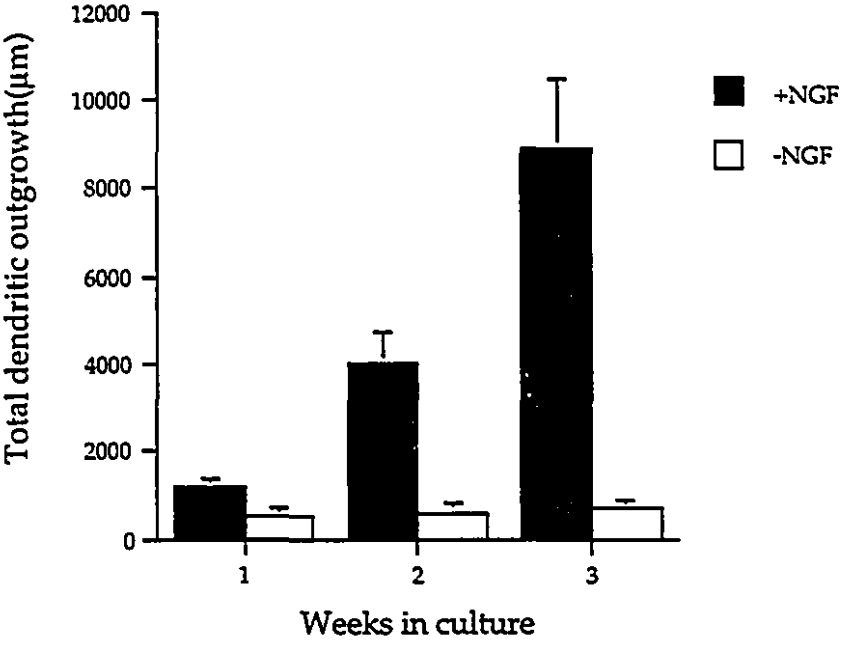

FIGURE 3.6. Total dendritic outgrowth by nodose neurons over time in culture. Total dendritic outgrowth was determined by the product of percentage of neurons with dendrites, number of primary dendrites per neuron, and mean length of dendrites, as given in Table 3.1 and 3.2. The values are normalized for 100 neurons. The bars represent SEM.

cultured P14 nodose neurons in the absence of satellite cells and with NGF. The results obtained from staining 3 week old cultures indicate that the neurons have lost most of their ability to extend dendrites (Table 3.3). Although we did not inject these neurons with lucifer yellow, most neurons appeared multipolar under phase microcopy, suggesting that the removal of satellite cells still alters the pseudo-unipolar morphology of these P14 neurons.

Table 3.3. Limited development of dendrites by P14 nodose neurons.

Time in culture (weeks)	Percentage of neurons with dendrites[1]	Number of primary dendrites per neuron[2]	Mean length of dendrites[3]
3	6.0 ±0.5 (1347)	1.5 ±0.2 (75)	63 ±4 (47)

[1] Mean ± SEM (n=total number of neurons from 4 different platings)
[2] Mean ± SEM (n=all the neurons that had dendrites)
[3] Mean ± SEM (n=all the dendrites from 30 neurons selected randomly in a given culture)

The expression of MAP2 immunoreactivity is low in neonatal nodose neurons

In Figures 3.4 and 3.5, it is noticeable that many of the neurons without dendrites have weak or no detectable MAP2 staining in their cell bodies, suggesting that these neurons express little MAP2. To examine whether P1 nodose neurons express MAP2, we fixed neurons 12-18 hrs after plating and immunostained the neurons for MAP2. We simultaneously immunostained freshly plated SCG neurons to compare levels of MAP2 staining. Figure 3.7 shows phase contrast photomicrographs of 3 P1 nodose neurons (A) and 2 P1 SCG neurons (B) grown overnight in culture. Figures 3.7C and 3.7D demonstrate that P1 nodose neurons contain far less MAP2 immunoreactivity than SCG neurons. The majority of P1 nodose neurons had faint or undetectable MAP2 immunoreactivity; some showed moderate staining, whereas all SCG neurons had strong MAP2 labelling. These observations suggest that P1 nodose neurons express little MAP2.

FIGURE 3.7. MAP2 immunoreactivity in freshly plated P1 nodose and SCG neurons.

Phase contrast photomicrographs of 3 nodose (A) and 2 SCG (B) neurons grown in culture for 18 hrs. Fluorescent photomicrographs (C and D) of the same neurons as above. Note that SCG neurons have bright MAP2 immunoreactivity in their somata, while nodose neurons have faint MAP2 staining. Scale bar, 10 μm.

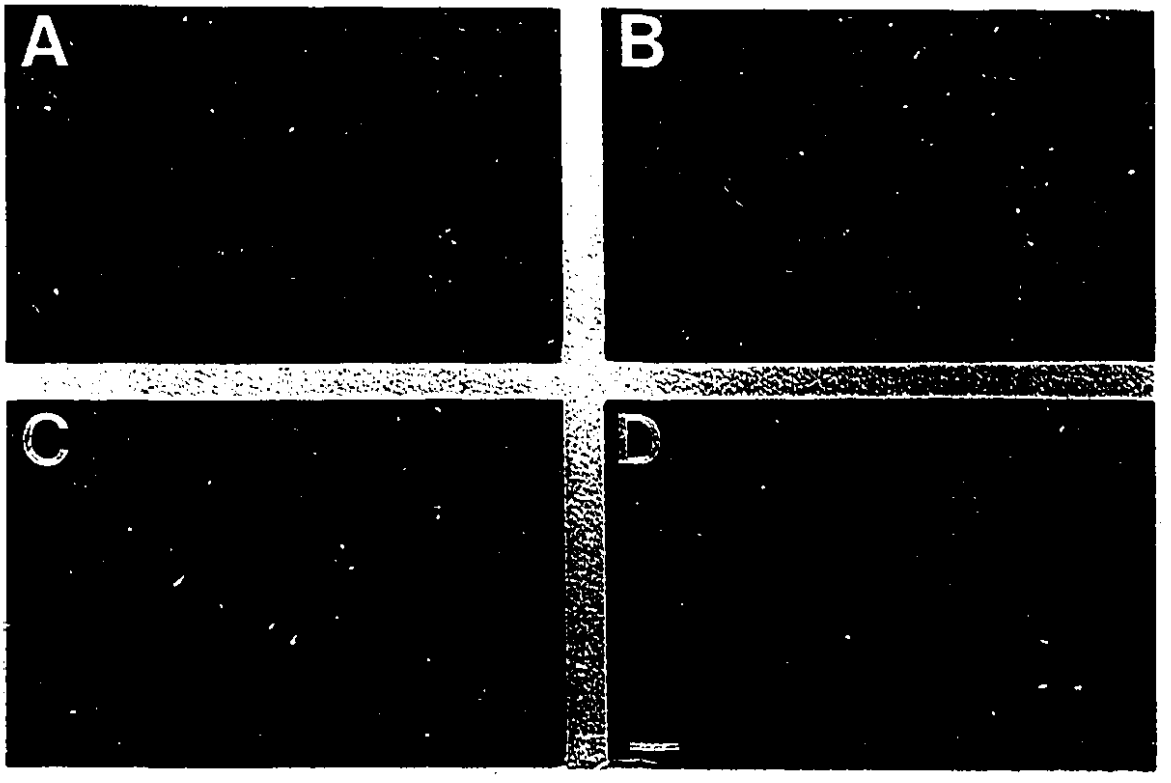
A
B
C
D

conceivably because they do not extend dendrites *in vivo*. After 3 weeks in culture, many neurons still had faint or undetectable MAP2 immunoreactivity (see Figure 3.4); none of these neurons had thick tapered processes. On the other hand, several neurons had moderate or strong MAP2 immunoreactivity in their cell bodies but did not extend dendrites. Finally, all neurons that extended thick, tapering processes had strong MAP2 staining in their cell bodies as well as in their dendrites (we did not quantified precisely the proportions of "faintly", "moderately" and "strongly" MAP2-labelled neurons, because of the variability of labelling intensities between experiments). These results suggest that 1) MAP2 is involved in dendrite extension by nodose neurons, but not sufficient (Higgins *et al.*, 1988), and 2) that MAP2 is not essential for axonal outgrowth.

Nodose neurons acquire their unipolar morphology early when co-cultured with satellite cells

During sensory neuron development, the two axons of bipolar sensory neuroblasts fuse at their origin to give rise to one single primary process that bifurcates into two axonal processes (e.g. pseudo-unipolar: Tennyson, 1965). After 2-3 weeks in cultures with satellite cells, nearly half of nodose neurons have one single primary process, while almost one third are bipolar (see Figure 3.1). These results raise the question as to whether these neurons, when co-cultured with satellite cells, undergo the same pattern of differentiation as observed *in vivo*. Alternatively, could these unipolar neurons (seen after 2-3 weeks) be extending only one process right from the onset of development in culture? To answer these questions, we plated freshly dissociated P1 nodose neurons on either a laminin substrate or on a confluent monolayer of nodose satellite cells that had been plated 2-3 days earlier on laminin. The next day, we injected neurons in both culture conditions with lucifer yellow to visualise neuronal morphologies. Figure 3.8 shows examples of neurons injected with lucifer yellow under phase contrast or fluorescence optics. When plated on a laminin substrate, most neurons acquire a multipolar morphology (Figure 3.8A and 3.8B); in contrast, when plated on satellite cells, approximately 50% of the neurons were unipolar (Figure 3.8C and 3.8D; Table 3.4). Interestingly, this effect seems to occur only when the satellite cells are in high density (i.e. forming a monolayer

on the substrate); indeed, as noticeable in Figure 3.8A, the enriched neuronal fraction from dissociated nodose ganglia (see section **2.1.2.**) still contains a substantial number of non-neuronal cells (either satellite/Schwann cells or fibroblasts). However, their density is much lower compared to Figure 3.8C, indicating that low density satellite cells may not induce nodose neuron to re-acquire unipolarity. Because nodose neurons seem to re-acquire their unipolar morphology rapidly (less than 24 hrs) when growing on satellite cells, it suggests that nodose neurons do not recapitulate the developmental switch from bipolar to unipolar morphologies that has been observed for sensory neuroblasts *in vivo* (Tennyson, 1965). Instead, the neurons appear to extend only one axon, thereby re-acquiring "immediately" their unipolar morphology when they develop with satellite cells.

The influence of satellite cells on nodose neuron polarity involves a direct contact mechanism

The mechanism by which satellite cells induce sensory neurons to acquire their pseudo-unipolar morphology is unknown. A simple scheme is that the satellite cell produce their effect via either a diffusible released factor(s) or a direct contact mechanism. To test whether satellite cells promote unipolar morphology via a direct contact mechanism, we plated freshly dissociated neurons under 3 conditions: 1) on monolayers of living satellite cells; 2) on monolayers of paraformaldehyde-fixed satellite cells (Hawrot, 1980); or 3) on laminin-coated coverslip treated with paraformaldehyde. Then, 18-24 hrs after plating, we injected the neurons with lucifer yellow. The fixed satellite layers appeared intact 18 hrs post-fixation, when viewed with phase contrast microscopy (compare Figure 3.8E and 3.8C). Interestingly, 4/9 injected neurons were unipolar on fixed satellite cells (Table 3.4), whereas 0/5 neurons were unipolar on fixed laminin. These results suggest that a direct contact mechanism between satellite cells and neurons is, at least in part, responsible for the unipolar morphology of sensory neurons.

FIGURE 3.8. Satellite cells induce nodose neurons to re-acquire a unipolar morphology early on in culture via a cell-cell contact mechanism.

Phase contrast photomicrographs (A, C, E) of 2 P1 nodose neurons that were plated on 18 hrs before on (A) laminin, (C) satellite cell monolayer, (E) fixed satellite cell monolayer. Fluorescent photomicrographs (B, D, F) of the same neurons as on the left injected with lucifer yellow. In (A) note the presence of a few satellite cells as well as some large fibroblast-like flat cells. (B) shows a neuron that extended 3 axons after being plated on laminin. (D) shows a neuron that extended only 1 axon after being plated on a monolayer of satellite cells. (F) shows a neuron that extended only 1 axon after being plated on a monolayer of fixed satellite cells. This figure indicates that living or fixed satellite cells induce nodose neurons to extend only one axon. Scale bar, 20 μm.

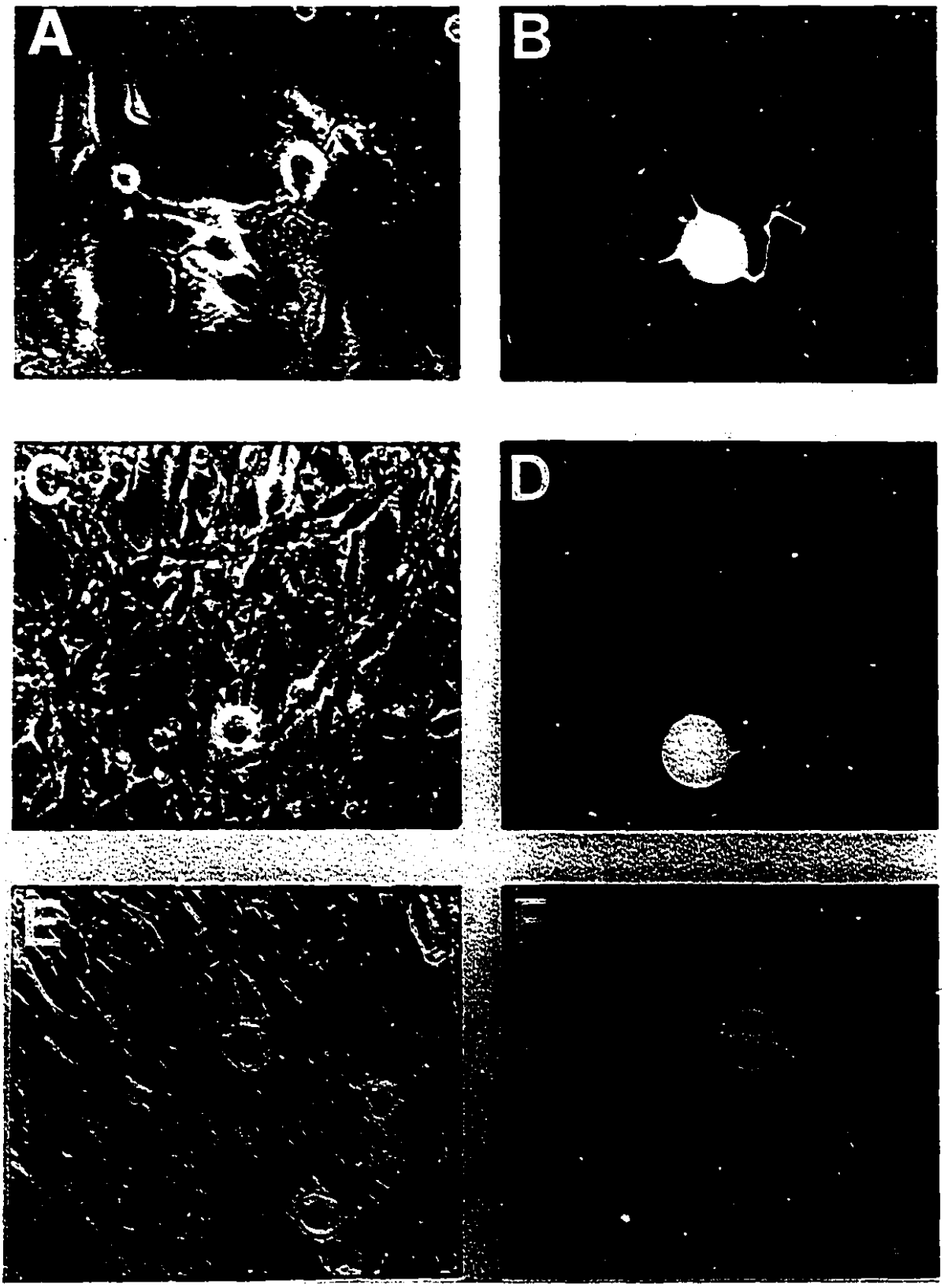
A
B
C
D
E
F

Table 3.4. Differential polarities of nodose neurons on laminin and satellite cell substrate

Substrate	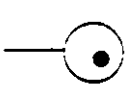	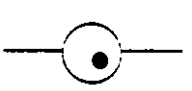	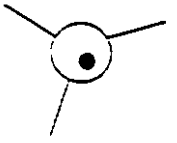
Laminin (11)	9%	18%	73%
Satellite cells (12)	50%	42%	8%
Fixed satellite cells (9)	44%	33%	22%

Percentage of lucifer yellow-injected neurons that were either unipolar (left), bipolar (middle) or multipolar (right; 3 or more axons), when plated on laminin or on living or pre-fixed satellite cells. The number of injected neurons is in parentheses for each condition.

DISCUSSION

In this chapter we have investigated factors that determine the polarity of sensory neurons of neonatal nodose ganglion. Our main finding is that these P1 nodose neurons are capable of extending dendrites in culture, in spite of their unipolar morphology *in vivo*. We showed that removal of satellite cells is essential to permit these neurons to develop a multipolar morphology and that NGF promotes their extension of dendrites.

Role of satellite cells on neuronal polarity

When neonatal sensory neurons from rat nodose ganglia develop in culture with their ganglionic satellite cells, many of these neurons acquire pseudo-unipolar morphologies similar to that of sensory neurons *in vivo*. Furthermore, it appears that the satellite cells repress dendrite outgrowth from nodose neurons, as the removal of satellite cells in culture allows them to develop dendrites, particularly in the presence of NGF. Interestingly, this satellite cell influence on sensory neurons is opposite to the glial cell influence on neurons which normally extend dendrites *in vivo* (Tropea *et al.*, 1988; Clendening and Hume, 1990; Johnson *et al.*, 1989; Rousselet *et al.*, 1990); in these latter studies, the presence of

glial cells induces dendrite outgrowth. For instance, satellite and Schwann cells promote dendritic outgrowth from cultured SCG neurons (Tropea *et al.*, 1988). However, as discussed in Chapter 1, Schwann cells from sciatic nerve or from sensory ganglia also promote dendritic outgrowth by SCG neurons (Tropea *et al.*, 1988). These results indicate that influences from non-neuronal cells have differential effects on neuronal morphology, whether they act on sensory or sympathetic neurons (see also Mudge, 1984). Possibly, the two neuronal types have distinct surface receptors that respond differently to satellite cells influence. Alternatively, similar receptors on both neuronal lineages are linked to different signalling molecules and thereby produce different signals. Consequently, with respect to dendrites and neuronal polarity, glial cells influence cultured neurons to acquire properties that they would normally have *in vivo* (Mudge, 1984; Tropea *et al.*, 1988).

Our results are reminiscent of those of Mudge (1984) who reported that embryonic (E 9-10) chick sensory neurons undergo a developmental transition from bipolar to pseudo-unipolar within 5-7 days when Schwann cells are added to cultures that had developed without non-neuronal cells. We show that when rat neonatal nodose neurons are plated directly on satellite cells, many of them seem to have acquired a unipolar morphology by less then 24 hrs. Unless nodose neurons undergo a rapid switch from bipolar to unipolar (less than 24 hrs), our results differ from those of Mudge (1984), which showed a transition from bipolar to unipolar when DRG neurons develop with Schwann cells. Two explanations can be proposed to account for these differences. First, most rat nodose neurons are already pseudo-unipolar by P1 (Altman and Bayer, 1982), unlike E 9-10 chick DRG neurons that are still bipolar (Mudge, 1984). Conceivably, when unipolar nodose neurons are dissociated and come in contact with satellite cells, they only regenerate that single process, thus re-acquiring a unipolar morphology. Second, in our experimental paradigm, the neurons did not develop alone prior to addition of satellite cells, but were instead in continuous contact with satellite cells. However, it seems unlikely that delayed satellite cell proliferation would induce nodose neurons to acquire a unipolar morphology. Indeed, in some instances, a few satellite cells would remain alive after the initial 4 days of Ara-C treatment in a given culture dish, and 10-14 days later,

a confluent monolayer would form. Nonetheless, in that situation the neurons often had MAP2 positive dendrites and most had multiple processes, suggesting that satellite cells may not reverse nodose neuron morphology back to unipolar.

Thus, it appears that nodose neurons develop in culture, in part, differently than DRG neurons. In fact, when we cultured P1 rat DRG neurons without satellite cells and on laminin, they failed to extend dendrites. The reasons for this difference are unknown. Nodose neurons originate from the ectodermal placodes, whereas DRG neurons come from the neural crests (d'Amico-Martel and Noden, 1983; Le Douarin, 1986). It is possible that this difference in origin is responsible for this difference in the morphological plasticity of these neurons. However, when we plated trigeminal neurons (of which 50% originate from the ectodermal placodes; d'Amico-Martel and Noden, 1983), only 2% developed dendrites. Another possibility is that nodose neurons are less committed to their *in vivo* morphology at this stage of development compared to other peripheral sensory neurons. In this context, when we cultured P14 rat nodose neurons without satellite cells, we observed limited dendritic outgrowth, suggesting that by P14 nodose neurons have become more committed to their sensory phenotype.

Another difference between our results and the ones of Mudge (1984) is noteworthy: embryonic chick DRG neurons were shown to remain bipolar when grown without Schwann cells, whereas many nodose neurons develop multiple processes in the absence of satellite cells. These DRG neurons were plated on collagen, while nodose neurons were plated on laminin. Higgins and colleagues showed that laminin induces SCG neurons to extend more axons than does collagen IV (Lein and Higgins, 1989; Lein *et al.*, 1991). Therefore, it is possible that laminin induced nodose neurons to extend more axons than they would have on a collagen substrate. This result also suggests another explanation for the fact that late proliferation of ganglionic satellite cells did not reverse nodose neuron polarity: the neurons have become multipolar (3 or more axons), and this may prevent them from being able to re-acquire a pseudo-unipolar morphology as bipolar neuroblasts can (Tennyson, 1965; Mudge, 1984).

The mechanism(s) by which the satellite cells produce their effect on polarity is

unknown. As a first approach we took advantage of the fact that the neurons re-acquire their unipolar morphology rapidly when plated on a monolayer of satellite cells. By plating neurons on fixed satellite cells, we found that nearly as many neurons were unipolar, providing good evidence that a direct contact is essential for nodose neurons to acquire sensory morphology. This result is consistent with the finding that Schwann cell condition media did not induce DRG neurons to become pseudo-unipolar (Mudge, 1984). In addition, a low density of satellite cells neither inhibited dendrite extension from nodose neurons nor promoted their unipolarity. *In vivo*, sensory neurons are tightly surrounded by satellite cells (Pannese, 1981); in culture, a similar situation occurs when satellite cells are in high density, causing many neurons to flatten on the substrate. Perhaps numerous contacts with their satellite cells affect the sensory neurons' cytoskeletal elements, which then cause the neurons to acquire this unipolar morphology.

We did not determine the nature of the contact involved. It appears unlikely that a satellite cell layer does not allow nodose neurons to become multipolar because the neurons are not in contact with the laminin substrate. Indeed, satellite cells produce large amounts of laminin that can be easily detected on their surface (Bunge and Wood, 1987). On the other hand, it seems more likely that a molecule(s) on the surface of satellite cells represses the extension of multiple axons and/or dendrites. This raises the question as to whether the satellite cell interaction that causes the neurons to become unipolar is also responsible for the lack of dendrites on these neurons.

The number of candidate molecules for this satellite cell effect remains rather large at this point. Cell-adhesion molecules, such as N-CAMs or integrins represent obvious possibilities to consider. Receptor tyrosine kinase activity plays an essential role in nerve cell differentiation (Schlessinger and Ullrich, 1992). These receptors are activated either by diffusible factors (e.g. NGF, EGF, FGF, CNTF, insulin) or by cell-cell interactions, in the case of the *eph*-related receptor tyrosine kinases. The *eph* receptors belong to the largest known family of receptor tyrosine kinases, with many members displaying specific patterns of expression in the developing and adult nervous system. Many of the genes coding for *eph*-related tyrosine kinases are expressed primarily in nerve cells (Hirai *et al.*, 1987; Lai and Lemke, 1991; van der Geer *et al.*, 1994; Davis *et al.*, 1994). Conceivably,

a receptor of this kind may be expressed specifically on the surface of sensory neurons and respond to a ligand expressed on the surface of glial cells.

Role of NGF on the extension of dendrites by nodose neurons

For neonatal nodose neurons developing in culture without satellite cells, we showed that NGF causes over a 15 fold increase in total dendritic outgrowth. Snider (1988) showed that treatment of neonatal rats with NGF for 1 to 2 weeks increased the number of primary dendrites on SCG neurons, as well as the length and branching of existing dendrites, an effect that persisted for many months (Ruit and Snider, 1991). Our results on the effects of NGF are consistent with Snider's observations *in vivo*: we found that NGF caused an increase in the number of primary dendrites, as well as in the length of each dendrite. Importantly, we observed that NGF also caused a 5 fold increase in the number of neurons extending dendrites, so that after 3 weeks in culture, almost 25% of the neurons extended dendrites. These results suggest that NGF causes neurons to initiate dendrites *de novo*.

It seems unlikely that these results are due to selective survival of a sub-population of NGF-dependent neurons because: (1) 85-90% of neonatal rat nodose neurons do not need NGF for survival in culture (Mandelzys *et al.*, 1990; see also Figure 5.1); (2) addition of anti-NGF to the cultures after two weeks had no effect on the number of neurons. It is also very unlikely that NGF induced mitosis of neuronal precursors present in the postnatal nodose ganglion that would have then differentiated differently than typical sensory neurons and extended dendrites. Indeed, Altman and Bayer (1982) showed, using [^{3}H]thymidine incorporation experiments, that nodose neurons undergo last cell division between embryonic day 11 and 15. Furthermore, Cooper (1984) showed that the number of neurons in the nodose ganglion does not change in the ganglion after birth.

In contrast to chick nodose neurons which do not have high-affinity NGF receptors (Lindsay and Rohrer, 1986), Mandelzys *et al.* (1990) showed that neonatal rat nodose neurons express high-affinity NGF receptors in culture in the absence of satellite cells. In adult rats, it appears that a significant proportion of nodose neurons have relatively high-

affinity NGF receptors, but few appear to express detectable levels of *trk*A mRNA (Verge *et al.*, 1992). Furthermore, in embryonic mice (Martin-Zanca *et al.*, 1990; Barbacid, 1994) and rats (Ernfors *et al.*, 1992), *in situ* hybridization experiments detected few neurons with *trk*A mRNA. However, it has been shown that many embryonic (E 13.5- 14.5) rat nodose neurons can be rescued by NGF in culture, suggesting that significant levels of *trk*A protein may be expressed in many of these neurons at that stage of development (Katz *et al.*, 1990). Therefore, it is possible that the levels of *trk*A mRNA have been underestimated in previous studies (Martin-Zanca *et al.*, 1990; Ernfors *et al.*, 1992; Barbacid, 1994). For instance, initial *in situ* hybridization studies revealed that *trk*A mRNA was not present in SCG ganglia (Martin-Zanca *et al.*, 1990), whereas nearly all SCG neurons were shown later to express *trk*A (Ernfors *et al.*, 1992; Barbacid, 1994). Furthermore, a recent report indicated that *trk*A is expressed in more CNS regions than previously appreciated (Holtzman *et al.*, 1995). Alternatively, as the expression of *trk* receptors has been shown to be highly regulated during development of peripheral neurons (Ernfors *et al.*, 1992; Mu *et al.*, 1993; Barbacid, 1994; Verdi and Anderson, 1994), it is possible that *trk*A is expressed at higher levels in P1 rat nodose neurons, compared to embryonic nodose neurons (see Chapter 5). Another possibility, not mutually exclusive of the previous ones, is that *trk*A expression is up-regulated in cultured nodose neurons.

In addition, rat nodose neurons contain abundant mRNA and protein levels of the so-called low-affinity NGF receptor ($p75^{LNGFR}$) (Yan and Johnson, 1988; Verge *et al.*, 1992; see Chapter 5), more so than sympathetic neurons. The significance of this abundant expression of $p75^{LNGFR}$ in nodose neurons and the putative role that $p75^{LNGFR}$ may play in the NGF effect on nodose neurons will be discussed in Chapter 5.

The specificity of NGF for *trk*A makes it unlikely that its effects are mediated through another *trk* receptor (but see also Chapter 5). If the effects of NGF operate via a *trk*A-driven tyrosine kinase signalling cascade, it may involve post-translational modifications of proteins important for dendrite outgrowth (e.g. MAP2, see below) or through *de novo* expression of genes that were previously repressed and that code for proteins essential for

the initiation and growth of dendrites. Such repression may have been released by the removal of satellite cells which override the dendrite induction by NGF on nodose neurons (unless satellite cells repress *trk*A expression). It is likely that nodose neurons encounter NGF *in vivo*, but based on the results presented here, the satellite cells surrounding the neurons in the ganglia should prevent NGF from inducing nodose neurons to extend dendrites.

NGF promotes axonal growth and nerve terminal branching. The action of NGF on axonal growth is local and independent of the amount of NGF supplied to the cell body (reviewed by Campenot, 1994), indicating that NGF's action on axonal growth cones is, at least in part, independent of protein synthesis. In contrast, the initiation of dendritic growth by sympathetic neurons in culture has been shown to depend on protein synthesis (Lein and Higgins, 1991). It is widely believed that a major source of NGF for neurons is their innervated targets (Korsching and Thoenen, 1983a; Richardson and Riopelle, 1984; Shelton and Reichardt, 1984; Purves *et al.*, 1988); thus, the promoting effect of NGF on sympathetic neuron dendritic growth *in vivo* may occur through retrogradely transported NGF (or a retrograde signal modulated by NGF). However, local supply of NGF is necessary for neurite outgrowth of sympathetic neurons in culture (Campenot, 1994). Does NGF promote the growth of dendrites at the level of dendritic growth cones? If so, the supply of NGF would have to be provided by other sources than neuronal targets, possibly from the satellite cells. If dendrites require a local supply of NGF as well as protein synthesis in order to extend, a concerted action of NGF from local sources and from retrograde sources may be necessary for their development. During retrograde transport of NGF and of its internalized receptor, *trk*A, the latter could remain autophosphorylated and thereby recruit SH2-domain-containing molecules in the cell body. Some of these molecules are involved in signalling cascades that lead to activation of gene expression (appendix 2). NGF has been shown to activate a program of neuronal differentiation in PC12 cells through the activation of ras-MAP kinase (MAPK) pathway (appendix 2) leading to neuro-specific gene expression. Conceivably, the effect of NGF on dendritic outgrowth could involve activation of a similar cascade of events leading to the expression

of neuro-specific genes essential for dendritic outgrowth.

The role of NGF and other neurotrophins on nodose neuron development will be discussed further in chapter 5.

Role of MAP2 in nodose neuron polarity

The MAP2 gene is alternatively spliced into 3 different transcripts encoding for two high molecular weight forms, MAP2a and MAP2b, and a low molecular weight form, MAP2c (Garner and Matus, 1988). MAP2a,b are almost exclusively localized in the cell bodies and dendrites (Goedert *et al.*, 1991), whereas, MAP2c is found in axons during development (Tucker *et al.*, 1988). It appears likely that MAP2a,b play an essential role for the growth and maintenance of dendrites, presumably by stabilizing microtubules or by cross-bridging them to neurofilaments (Hirokawa *et al.*, 1988b; Matus, 1988, 1994; Goedert *et al.*, 1991). The degree of phosphorylation of MAP2a,b, could affect the cross-bridging of microtubules to other cytoskeletal elements allowing dendritic growth (Olmsted, 1986). A good correlation has been observed between the degree of MAP2 phosphorylation and the extension of dendrites by hippocampal neurons in culture (Diez-Gaza and Avila, 1993). NGF may regulate MAP2 phosphorylation via activation of intracellular kinases such as MAPK (Schanen-King et al., 1991) which itself phosphorylates MAP2 (Landreth *et al.*, 1990; Miyasaka *et al.*, 1990) (see appendix 2).

An intriguing observation is the fact that most P1 nodose neuron somata had weak or undetectable staining for MAP2. Similar observations were made for adult rat DRG neurons (De Camilli *et al.*, 1984). As sensory neurons do not extend dendrites *in vivo*, these finding suggests that sensory neurons do not need to express MAP2 for their normal development. If so, it raises questions about the relationship between the expression of MAP2 and the extension of dendrites: in the cascade of events that lead to the initiation of dendrites, does MAP2 expression precede the development of dendrites and is it essential? Or instead, is MAP2 expression concomitant with dendrite initiation, or perhaps even delayed until the dendrite emerges from the soma? Qualitative observations suggest that the number of MAP2 positive neurons increased in culture over time, even though

many of these neurons did not extend dendrites. Furthermore, every neurons that extended thick tapered processes strongly stained for MAP2 in their cell body and dendrites. This suggests that MAP2 expression precedes dendrite initiation and provides additional evidence that MAP2 is essential for dendrite growth and maintenance (Matus, 1988, 1994). However, we observed many neurons that had strong MAP2 labelling in their cell body but that did not extend dendrites. Furthermore, Higgins *et al.* (1988) found that rat SCG neurons, cultured without other cell types and without serum, do not extend dendrites, even though they all express MAP2. These results imply that MAP2 expression is not sufficient for dendrite extension, and that other factors, in addition to MAP2, are involved in the initiation of dendrites. These are likely to include extracellular matrix or cell-adhesion molecules (Bruckenstein and Higgins, 1988b; Tropea *et al.*, 1988; Lein and Higgins, 1989).

Our suggestive evidence that sensory neurons may not need to express MAP2 for their normal development is worth further discussion. Two groups have inhibited the expression of MAP2, using antisense technology, either in P19 EC cells (Dinsmore and Solomon, 1991) or in cerebellar neurons (Caceres *et al.*, 1992). The results of these studies indicated that MAP2 expression was essential for the extension of all neurites (thus including axons). Our observation would imply that, on the contrary, MAP2 is not essential for axonal outgrowth from sensory neurons. We cannot exclude, however, that low levels of MAP2 expression occurs in all nodose neurons and that they are not detected by immunocytochemistry. As the cell types used in these studies are different from sensory neurons, our results do not necessarily contradict these studies, but they inevitably raise the question of whether these antisense experiments can cause additional uncontrollable effects.

Chapter 4

Expression of Nicotinic Acetylcholine-Evoked Currents on Nodose Neurons Extending Dendrites.

INTRODUCTION

In chapter 3, we demonstrated that P1 nodose neurons have the ability to extend dendrites when they develop in culture in the absence of satellite cells and in the presence of NGF. This formation of dendrites, which were identified on the basis of their morphology and staining for MAP2 (Caceres *et al.*, 1984; Caceres *et al.*, 1986; Kosik and Finch, 1987; Dotti *et al.*, 1988), indicates that nodose neurons have established a new dendritic-axonal polarity. An advanced stage in the establishment of neuronal polarity involves the segregation of elements implicated in synapse formation, such as the clustering of synaptic vesicles in presynaptic terminals and the clustering of postsynaptic receptors on somatodendritic domains (Craig and Banker, 1994). Cooper (1984) showed that nodose neurons form *de novo* functional synapses among each other when they develop under similar culture conditions, and that the pharmacology of these synaptic interactions is nicotinic. Furthermore, unlike *in vivo*, many nodose neurons express large nicotinic ACh-evoked currents when they develop in culture in the absence of non-neuronal cells (Baccaglini and Cooper, 1982; Cooper, 1984; Cooper and Lau, 1986), providing that NGF is present (Mandelzys *et al.*, 1990; Mandelzys and Cooper, 1992).

Therefore, it appears that the extension of dendrites by nodose neurons correlates well with the expression of nicotinic ACh-evoked currents on these neurons and with the formation of cholinergic synapses. However, these findings raise the following questions: 1) Is the expression of ACh-evoked currents on nodose neurons restricted to neurons extending dendrites? 2) Are nAChRs located on these dendrites? 3) Do synapses form on these dendrites?

In this chapter, we have combined morphological and electrophysiological techniques to determine the expression of functional nAChRs on nodose neurons with or without

dendrites. In addition, we examine the segregation of synaptic vesicles in these cultures as the neurons develop dendrites.

EXPERIMENTAL PROCEDURES

Neuronal cultures

Nodose neurons were cultured as described in section 2.1., in the presence of NGF and in the absence of satellite cells.

ACh sensitivity and lucifer yellow injection

ACh-evoked currents were measured electrophysiologically using whole-cell patch-clamp techniques as described in section 2.3.. Lucifer yellow (1%, potassium salt; Sigma) was added to the pipette solution; the fluorescent dye rapidly diffused throughout the entire cell body and proximal processes (up to 150-200 µM), while performing whole-cell recordings. ACh (50 µM) was applied by pressure ejection (see section 2.3.2.) onto neurons that were voltage-clamped at -50 mV. Two types of "puffers" were used: 1) to record whole-cell ACh-evoked current densities we used a puffer with an opening of 10-20 µm (microelectrode with a broken tip) to ensure that cell body and proximal processes were perfused by the ACh; 2) to record ACh-evoked currents on dendrites, we used a puffer with an opening of <1 µm (patch-clamp pipette of high resistance) to restrict the application of ACh to a small area. In most of the experiments described in Figure 4.1, the neurons were visualized by epi-fluorescence after the electrophysiological recordings on a different microscope (Leitz Ortholux II, with the kind permission of Dr. Wayne Lapp, Department of Physiology, McGill University). In these cases, the neurons were fixed with 4% paraformaldehyde and mounted on glass slides with immunofluor mounting media (see section 2.2.1.). In order to match appropriately the recorded ACh-evoked currents with the labelled neurons, we marked the aclar coverslip from beneath with a sharp glass electrode. Furthermore, we recorded from only 2-3 neurons per culture dish before fixation to avoid mismatches and to ensure that recorded neurons did not lose their fluorescence, as some neurons die after whole-cell recordings. Fortunately, we later

installed a fluorescent attachment on the electrophysiological setup which allowed us to visualize the neurons during the recordings. This was imperative for the experiments shown in Figure 4.2, where the ACh was applied locally onto dendrites. For these experiments, once a neuron had been filled with lucifer yellow, we drew its silhouette on paper and noted where the ACh "puffs" were applied. Afterward, the fluorescent neuron was photographed, and a more accurate sketch of the neuron was done by laying a transparent paper on the picture of the fluorescent neuron and outlining its silhouette. This drawing was then scanned to produce a computer generated image as seen in Figure 4.2C.

Immunocytochemistry

Neurons we fixed, permeabilized and immunostained as described in section 2.2.1. after different periods of time in culture. To label synaptic vesicle protein synaptophysin we used a mouse monoclonal antibody (SVP-38, Sigma) and goat anti-mouse-FITC secondary antibody. Due to the limited amount of polyclonal MAP2 antibody (R4, Chapter 3) supplied, double staining experiments for MAP2 and synaptophysin could not be performed.

RESULTS

The extent of dendrite growth correlates with ACh sensitivity

To investigate whether ACh-evoked current densities were different on neurons extending dendrites from those lacking dendrites, we simultaneously filled neurons with lucifer yellow while recording from them electrophysiologically with whole-cell voltage clamp techniques. We held the neurons at -50 mV and applied 50 μM ACh from a "puffer" pipette with large opening (see experimental procedures and section 2.3.2). We classified thick, tapering processes that end locally as dendrites and thin processes of relatively constant calibre that extend for long distances as axons (Bruckenstein and Higgins, 1988a,b; Chapter 3). Figure 4.1A shows 3 neurons grown for 3 weeks and filled with lucifer yellow; below each one is shown their respective whole-cell ACh-evoked currents. *Neuron A* has 2 long dendrites and a large (2300 pA) ACh-evoked current;

FIGURE 4.1. ACh sensitivity of nodose neurons with and without dendrites.

(A) shows three lucifer yellow-filled neurons that have developed in culture for two weeks. Neuron A has two long dendrite-like processes; neuron B has two short dendrite-like processes; neuron C has no dendrite-like processes. Under each neuron is shown its respective ACh-gated inward current evoked by pressure application of 50 μM ACh for 2 sec (horizontal bar). (B) shows the ACh-evoked current densities (pA/pF) on the three classes of neurons shown in (A): class A (n=12), B (n=9), and C (n=12). The values represent the means ± SEM. Currents were filtered at 3 KHz and sampled at 5 KHz. Scale bar, 40 μm.

A

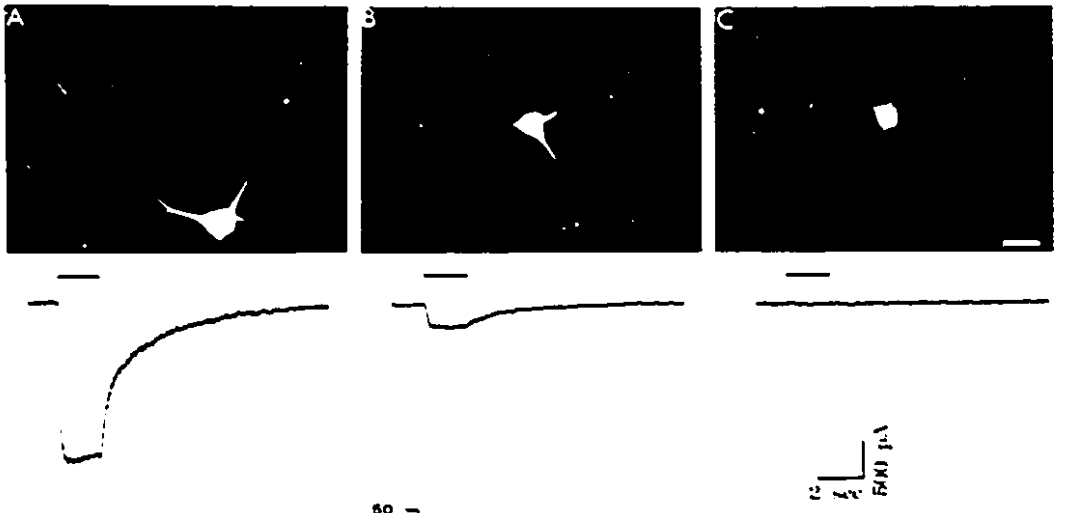

B

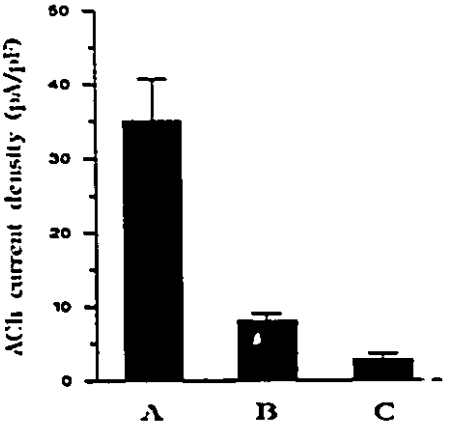

neuron B has 2 short dendrites and a smaller (300 pA) ACh-evoked current; *neuron C* has no dendrite and has no detectable ACh-evoked current. We recorded from over 30 identified neurons and their morphologies fell into the 3 categories illustrated in Figure 4.1A: *class A neurons*, with 2 or more long dendrites (>60 μm), *class B neurons*, with 1 or 2 small dendrites (35-60 μm), and *class C neurons*, with no dendrites. Figure 4.1B shows the quantification of ACh-evoked current densities, which represent the peak evoked currents normalized for the size of the neurons (whole-cell capacitance). Neurons with long dendrites had larger functional nAChR density than neurons with small dendrites or without dendrites. The *class A neurons* have ACh-evoked current densities similar to sympathetic neurons (Mandelzys and Cooper, 1992; see Chapter 7). These results demonstrate that the ACh-evoked current densities correlate with the extent of dendritic growth on nodose neurons.

Nodose neuron dendrites have functional nAChRs on their surface

The above results strongly suggest that nodose neurons express functional nAChRs on their dendrites. To obtain more direct evidence of this, we applied ACh locally along dendrites, axons and cell bodies of neurons using a puffer pipette with small opening (<1 μm). By including lucifer yellow in the patch electrode, we could visualize the entire dendrites and the proximal axons. Figure 4.2 shows the results obtained by recording from a neuron grown for 3 weeks. Figure 4.2A is a phase contrast photomicrograph taken after the whole-cell recordings were performed, and Figure 4.2B shows the same neuron as in A under fluorescence optics. This neuron has 3 thick dendrites and 2 smaller dendrite-like processes; axonal-like processes appear to emerge from the base of one dendrite. Figure 4.2C shows a sketch of the same neuron with the superimposed ACh-evoked currents obtained by application of 50 μM ACh. Each arrow points to the region of ACh application. The ACh response on the cell body was 140 pA (*trace 1*), while the ACh-evoked currents ranged from 50 to 250 pA on the dendrites (*traces 2-5, 7-10*). Applications of ACh on axonal-like processes evoked no detectable current (*traces 11 and 12*). In addition, application of ACh at regions where no processes were apparent produced no detectable current (*traces 6 and 13*), indicating that the ACh-evoked currents

FIGURE 4.2. ACh-evoked currents on nodose neuron dendrites.

(A) Phase contrast photomicrograph of nodose neurons grown for 3 weeks in the absence of satellite cells and with NGF. (B) Fluorescent photomicrograph of the same field as in A showing a neuron filled with lucifer yellow and the patch electrode containing lucifer yellow. Note the three thick dendrites and the 2 smaller dendrite-like processes emerging from the cell body. Axonal processes appear to emerge from the base of the dendrite that is growing toward "4 O'clock". (C) Silhouette of a the same neuron as in B with ACh-evoked currents superimposed near the locations of ACh applications (arrows). The currents were recorded from the cell body which was held at -50 mV with whole-cell voltage-clamp, after 250 ms applications of 50 μM ACh from a "puffer" electrode with a small tip opening (<1 μm), positioned a few μm away from the surface of the neuron. The peak ACh-evoked current on the cell body (trace 1) was 140 pA, while the peak ACh-evoked currents on dendrites ranged from 50 to 250 pA (traces 2-5, 7-10). ACh applications on axonal-like processes (traces 11 and 12) or on regions without processes (traces 6 and 13) evoked no detectable currents. Currents were sampled at 5 KHz and filtered at 3 KHz. Scale bar, 40 μm.

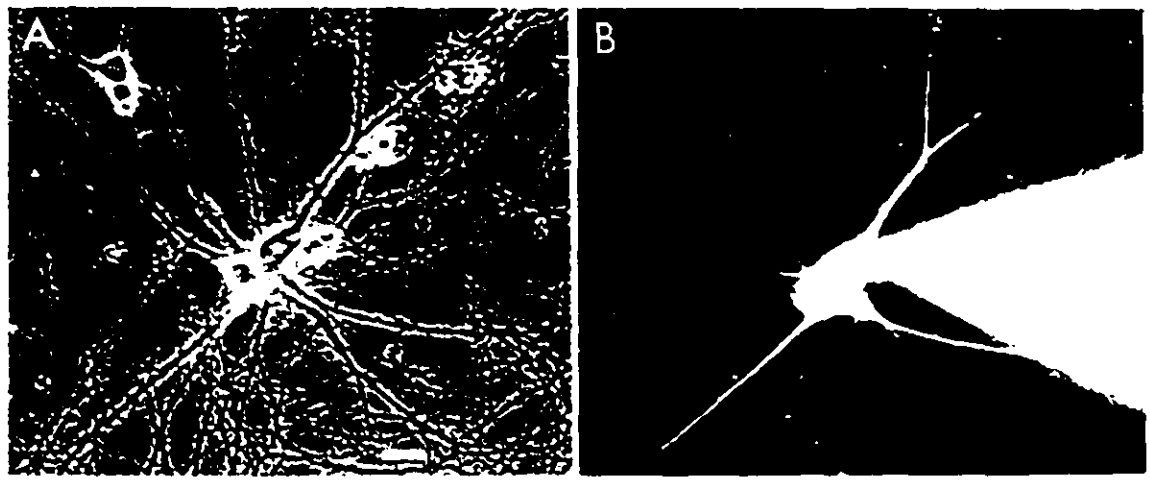

C

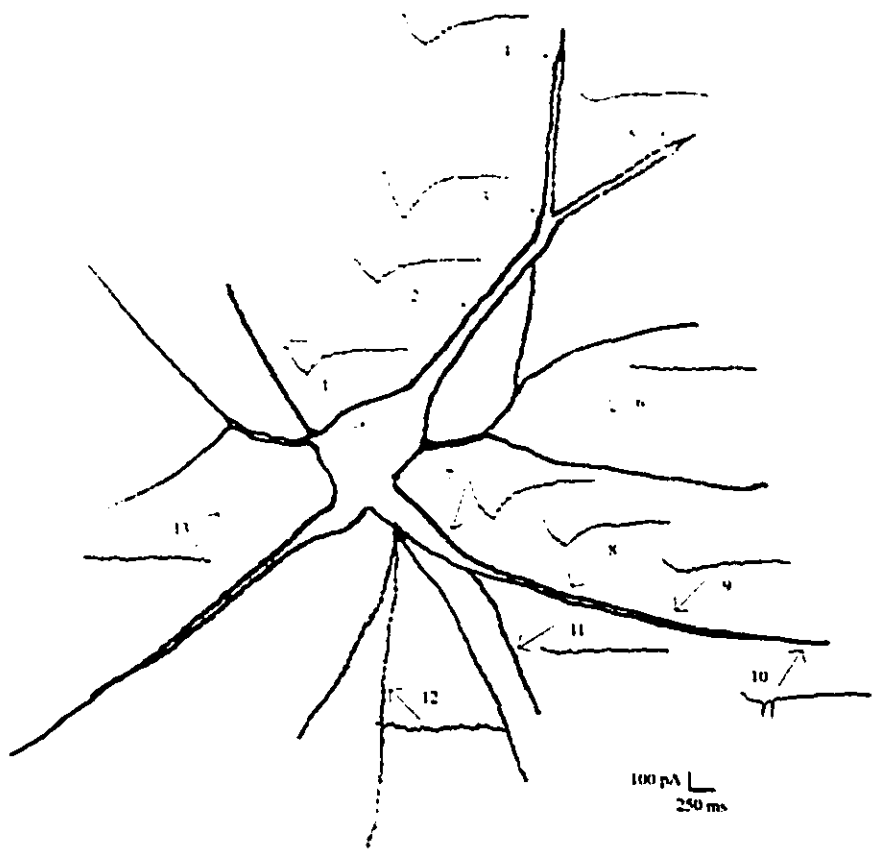

recorded on dendrites are not due to diffusion of agonist to the cell body. Experiments such as the one shown in Figure 4.2 were performed on 6 neurons which had identifiable dendrites (judged first by phase contrast microscopy, and confirmed by fluorescent microscopy). In all cases, the neurons had measurable ACh-evoked currents on their dendrites. These results demonstrate that dendrites from nodose neurons express functional nAChRs.

Observation of functional synapses in cultures of nodose neurons

By recording from pairs of neurons with microelectrodes, Cooper (1984) demonstrated that nodose neurons can form functional cholinergic synapses under similar culture conditions. The probability of finding pairs of neurons that were synaptically coupled was around 15-20%. However, in approximately 50% of the recorded neurons, spontaneous excitatory postsynaptic currents (EPSCs) could be observed (Cooper, 1984). In this study, we did not attempt to repeat these experiments with patch clamping, but occasionally, while recording from these neurons to measure their ACh sensitivity, we observed spontaneous EPSCs. Figure 4.3 shows examples of spontaneous EPSCs recorded from 3 neurons; each had large ACh-evoked currents consistent with the nicotinic pharmacology of these synapses (Cooper, 1984).

Presence of synaptophysin clusters along nodose neuron dendrites

Banker and colleagues described the time course of synaptic vesicle accumulation in axonal terminals during the establishment of neuronal polarity by hippocampal neurons (Fletcher *et al.*, 1991, 1994). Early on in culture, synapsin I and synaptophysin are expressed by these neurons, but their immunoreactivity is diffuse and mainly restricted to the cell bodies and proximal axons. When axons contact appropriate targets, synaptic vesicles rapidly redistribute to form dense accumulations of vesicles within presynaptic specializations, as demonstrated by electron microscopy (Fletcher *et al.*, 1991). These clusters of vesicles can also be detected as large puncta of synaptic vesicle protein immunoreactivity (Fletcher *et al.*, 1991, 1994; Craig *et al.*, 1993). Interestingly, Fletcher *et al.* (1994) demonstrated that the limiting factor in the time course of this presynaptic

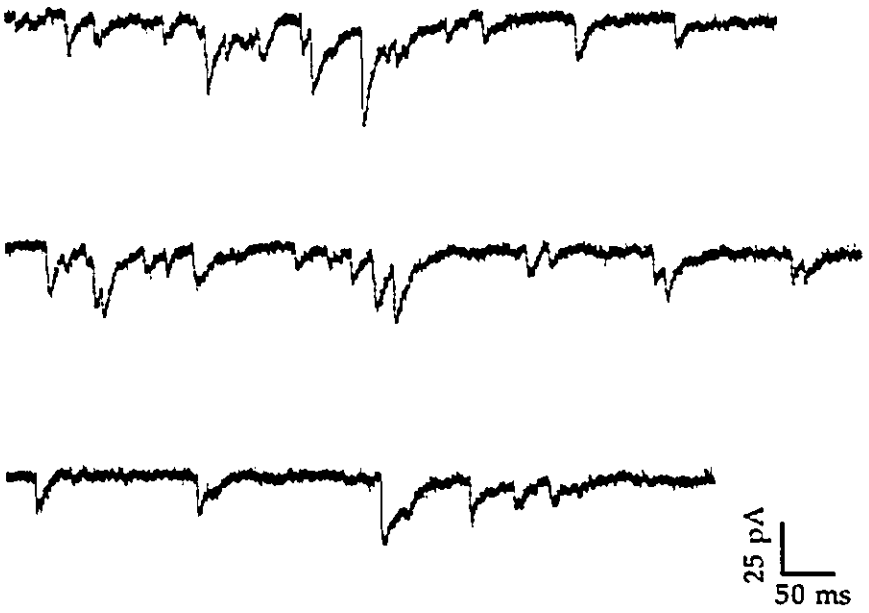

FIGURE 4.3. Synaptic currents in nodose neurons developing in culture.

Representative recordings of EPSCs with whole-cell patch-clamping from 3 neurons voltage-clamped at -50 mV. These neurons were grown in culture for 3 weeks with NGF, and had large ACh-evoked current densities. Currents were filtered at 3 KHz and sampled at 20 KHz.

FIGURE 4.4. Formation of synaptophysin immunoreactive puncta in cultured nodose neurons.

Phase contrast photomicrographs of nodose neurons grown in the absence of satellite cells and in the presence of NGF for 3 (A), 7 (C), 20 (E), and 26 (G) days. Fluorescent photomicrographs (fluorescein) of the same fields as on the left showing synaptophysin immunoreactivity. After 3 days (B) synaptophysin immunoreactivity is diffuse an primarily visible in the cell bodies (arrow). After 7 days (D), few puncta of synaptophysin immunoreactivity are visible, primarily apposed to cell bodies (arrows), while the diffuse immunoreactivity within the cell bodies has decreased. (F) After approximately 3 (F) to 4 (H) weeks, several puncta of synaptophysin labelling are visible, both on somata (arrowheads) and dendrites (arrows). In addition, several puncta of synaptophysin immunoreactivity appear along axons, usually at the intersection of two axons. These puncta may correspond to axonal varicosities. Scale bar, 35 μm.

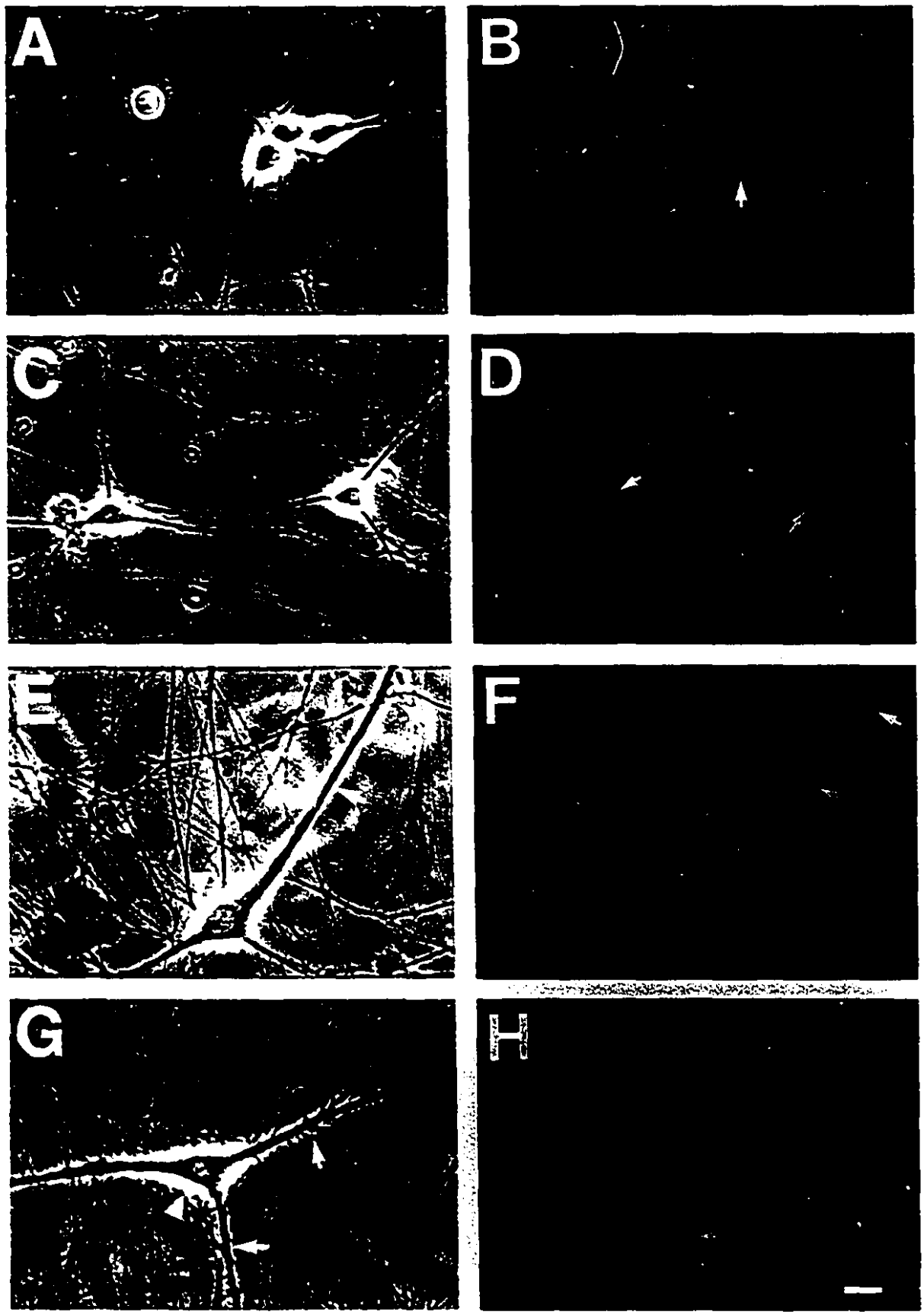
A
B
C
D
E
F
G
H

organization, in hippocampal cultures, was the state of maturity of the postsynaptic membrane.

Given that nodose neurons develop dendrites, express functional nAChRs on their surface as well as on their cell body, and form nicotinic cholinergic synapses among one another, we immunostained nodose neuron cultures for synaptophysin, to examine whether synapse may form on their dendrites.

Figure 4.4 shows the localization of synaptophysin immunoreactivity in cultured nodose neurons after 3, 7, 18 and 27 days in culture. By day 3, only faint synaptophysin immunoreactivity is detectable in the cell bodies (Figure 4.4A and 4.4B, arrow). By 7 days, a few puncta of synaptophysin immunoreactivity are detectable and are mainly concentrated around cell bodies (Figure 4.4C and 4.4D, arrow), suggesting the formation of presynaptic specializations apposed to neuronal somata. After 3-4 weeks in culture, puncta of synaptophysin immunoreactivity are abundant. Most of them are localized around the somata (Figure 4.4E-4.4H, arrowheads), although a significant number of puncta also appear along dendrites (arrows). In addition, a significant number of immunoreactive clusters appear at the intersections of axons (Figure 4.4E-4.4H), suggestive of axonal varicosities. These results suggest that 1) cultured nodose neuron axons develop presynaptic accumulations of synaptic vesicles; 2) this accumulation occurs during the maturation of postsynaptic membrane; 3) synapses form on both cell bodies and dendrites.

DISCUSSION

Correlation between nAChR expression and dendrite extension

In vivo, nodose neurons do not extend dendrites nor do they exhibit much ACh sensitivity on their cell body (Mandelzys and Cooper, 1992). A similar situation occurs in co-cultures of nodose neurons with their ganglionic satellite cells. In contrast, when they develop without satellite cells they develop sensitivity to ACh (Baccaglini and Cooper, 1982; Cooper, 1984; Cooper and Lau, 1986; Mandelzys and Cooper, 1992) and extend dendrites. The addition of NGF to satellite cell-free nodose cultures greatly

enhances both the ACh-evoked current densities (Mandelzys and Cooper, 1992) and dendritic outgrowth, whereas the addition of NGF to satellite cell-neuron co-cultures has no inductive effect on both the ACh sensitivities and dendrite outgrowth. In addition, when the neurons develop for an additional 2 weeks *in vivo*, they lose this ability to extend dendrites in culture as well as to develop ACh-evoked currents (Mandelzys and Cooper, 1992). These results suggest that the acquisition of both of these new properties are intimately related. However, not all nodose neurons develop these new properties in cultures. Therefore, in spite of these correlations, the possibility remained that the neurons extending dendrites and the neurons expressing functional nAChRs in these cultures were distinct neuronal populations. In this chapter, we demonstrate in combined morphological and electrophysiological experiments that neurons extending several long dendrites have high ACh-evoked current densities, whereas neurons that lacked dendrites had small or no detectable ACh-evoked currents. The *class A neurons* (Figure 4.1) represent approximately 20-30 % of the neurons in these cultures, the *class B neurons* approximately 20 %, while the *class C neurons* constitute approximately half of the neurons in these cultures.

These results link together the developmental expression of dendrites, a major structural component of a postsynaptic neuron, with the expression of a postsynaptic neurotransmitter receptor. The temporal expression of these two synaptic elements suggests that they are coordinately regulated, and suggest that nAChRs are expressed on dendrites.

Expression of functional nAChRs on nodose dendritic membrane

The establishment of neuronal polarity involves the segregation of molecules to the various domains specialized for synaptic functions. Targeting of neurotransmitter receptors to dendritic domains within dense clusters is likely to represent one of the most advanced stages of neuronal maturation (Craig and Banker, 1994). Dendrites need neurotransmitter receptors on their surface to receive synaptic inputs. We demonstrate here that the newly extended dendrites of nodose neurons possess functional nAChRs on their surface, suggesting that the neurons have established an advanced stage of neuronal polarity.

Our experiments did not address whether nAChRs are concentrated in clusters on the dendritic membrane. Although the size of the puffer tip was kept very small (<1 μm), the ACh could have easily diffused to reach relatively large patches of membrane. However, the ACh responses recorded on dendrites cannot be explained by a diffusion of the ACh to the cell body for the following 3 reasons: 1) the kinetics of the responses were similar when ACh was applied onto the cell body or on the dendrites; 2) the sizes of the responses were comparable on both surfaces, and 3) when ACh was applied on axonal-like processes or near the cell body where no processes were apparent, no ACh-evoked currents were detected. The second point suggests that the density of nAChRs on certain regions of dendrites is at least as high as on the cell body. The third point suggests that axonal-like processes do not have functional nAChRs on their surface, although we cannot rule out that dispersed clusters of receptors may have been missed or that currents were not observed because of the small surface area of axons.

Evidence for synaptic contacts onto nodose neuron dendrites

The observation that clusters of synaptophysin immunoreactivity develop in culture of nodose neurons suggests that accumulation of synaptic vesicles occurs in their nerve terminals or axonal varicosities. Early on in culture, few clusters are apparent, while faint, diffuse labelling is visible in cell bodies. Interestingly, the formation of these clusters appears delayed (>6 days) compared to cultured hippocampal neurons, where cluster formation starts within 3 days after plating (Fletcher *et al.*, 1994). In hippocampal neurons, this delay in cluster formation has been shown to depend on the period needed for postsynaptic membrane maturation. Indeed, Fletcher *et al.* (1994) used co-cultures of mature and young neurons ("heterochronic" co-cultures) to demonstrate that presynaptic terminals from newly plated neurons contacting mature postsynaptic neurons were rapidly induced to accumulate synaptic vesicle proteins, whereas contacts with immature postsynaptic neurons failed to induce such cluster formation. Their results suggest that axons have the capacity to develop presynaptic specializations soon after they emerge, provided they encounter appropriate targets. Furthermore, they suggest that the maturation stage of the postsynaptic cell bodies and dendrites determines, or at least, influences the

onset of presynaptic specializations (Fletcher *et al.*, 1994). In nodose neuron cultures, few dendrites are observed after one week and the density of functional nAChRs is still low. Therefore the longer delay in synaptophysin immunoreactivity clustering observed in nodose neuron cultures is consistent with this concept of a role in postsynaptic membrane maturity. While the temporal expression of dendrites and nAChRs suggests that they are coordinately regulated, a similar temporal correlation appears to take place for the clustering of synaptic vesicles, suggesting an additional component of synapses that is coordinately regulated in these neurons.

We observed the highest concentration of puncta of synaptophysin immunoreactivity around cell bodies (Figure 4.4); we also observed several clusters along dendrites. In addition, puncta were detectable along axons often at intersections with other axons. The latter clusters may correspond to the formation of axonal varicosities by these neurons, as those seen in sympathetic neurons (Landis, 1976; Peters *et al.*, 1991). Occasionally, when nodose neurons were injected with lucifer yellow, small "swellings" in their axons were observed, reminiscent of varicosities.

That higher density of synaptophysin clusters forms along cell body membranes, compared to dendritic membranes, after 2-3 weeks of culture development is not surprising; the first appearance of immunoreactive puncta is detectable on cell bodies (Figure 4.4C and 4.4D) when dendrites are just emerging; if synaptic contacts form at random on both types of postsynaptic membranes, more presynaptic contacts should accumulate along cell bodies, while some are accumulating along newly extending dendrites.

When sympathetic neurons develop in culture with skeletal myotubes, they become cholinergic and form functional cholinergic synapses with each other and with the myotubes (Nurse and O'Lague, 1975). Single sympathetic neurons grown in microcultures form synapses onto themselves ("autapses"); these synapses can be either cholinergic or adrenergic, although only the cholinergic synapses can be detected electrophysiologically (Furshpan *et al.*, 1976; Landis, 1976). Interestingly, Landis (1976) found that, in these microcultures, cholinergic synapses were preferentially located on dendrites, while

adrenergic synapses were located on cell bodies. Nodose ganglia contain several neurotransmitters including acetylcholine, serotonin, dopamine, glutamate, as well as substance P, vasoactive intestinal polypeptide and somatostatin (Matsumura and Koelle, 1961; Fujiwara *et al.*, 1978; Talman *et al.*, 1980; Gaudin-Chazal *et al.*, 1983; Katz *et al.*, 1983; Kessler *et al.*, 1983; Mathieu *et al.*, 1984; Palouzier *et al.*, 1987; Ternaux *et al.*, 1989). Cooper (1984) showed that functional synaptic interactions between nodose neurons were cholinergic. It would be interesting to determine whether the clusters of synaptophysin immunoreactivity seen on dendrites correspond preferentially to cholinergic synapses in these cultures, as observed in sympathetic neurons microcultures (Landis, 1976). In addition, it will be interesting to examine the potential clustering of nAChRs into "hot spots" and co-localization with synaptophysin immunoreactivity, and, if this happens, to see which one appears first.

Chapter 5

BDNF and NT-3 Promote Sensory Differentiation by Neonatal Rat Nodose Neurons

INTRODUCTION

A critical phase in the development of the PNS is the period of large scale cell death. This period is believed to be an important determinant in the achievement of appropriate connections in neural circuitry. Neurotrophins are key players in this process as they selectively rescue neurons that express their cognate receptors. In the CNS, however, neurons appear less dependent on neurotrophins for survival during development (Klein *et al.*, 1993, 1994; Barbacid, 1994), and studies have indicated that neurotrophins play additional roles to their neurotrophic action (Korsching, 1993; Campenot, 1994; Davies, 1994; Kang and Schuman, 1995). In fact, neurotrophins and their receptors (see appendix 1) are still expressed in the postnatal nervous system (Klein *et al.*, 1990b; Barbacid, 1994), suggesting that neuronal functions in postnatal life are regulated by neurotrophins. While there is considerable information on the survival role of neurotrophins, less is known about their specific effects on other neuronal functions.

Some distinctions are beginning to unravel between the signalling cascades activated by the NGF receptor, *trk*A, and other receptor tyrosine kinases, such as the EGF receptors (see appendix 2); however it is largely unknown whether different *trk* receptors activate distinct signalling cascades in neurons. There is evidence that different *trk* receptors may be co-expressed within the same sensory neurons (McMahon *et al.*, 1994), and the marked overlap in *trk* receptor expression in the CNS suggests that co-expression of *trk*s occurs in some CNS neurons as well (Ernfors *et al.*, 1992; Barbacid, 1994; Holtzman *et al.*, 1995). This raises the question as to whether different neurotrophins can produce distinct responses by neurons that co-express their receptors, and consequently whether different neurotrophins can stimulate distinct pathways of neuronal differentiation in a neuron. If so, this would imply that each class of *trk* receptors activate different downstream

signalling events within a given neuron.

Neonatal nodose neurons represent a good preparation to investigate the differential roles that neurotrophins play on neuronal differentiation as these neurons can grow well in culture in the absence of exogenous neurotrophins. As of yet, however, there has been no quantitative measurements of *trk* expression in rat nodose neurons. Experiments with *in situ* hybridization indicate that in developing rodents most nodose neurons express *trk*B, many express *trk*C, and only few express *trk*A (from E13-E18; Klein *et al.*, 1990b; Martin-Zanca *et al.*, 1990; Ernfors *et al.*, 1992; Barbacid, 1994). However, Verge *et al.* (1992) reported that adult nodose ganglia contain many more neurons with high-affinity NGF binding sites compared to neurons expressing detectable levels of *trk*A by *in situ* hybridization; furthermore, P1 rat nodose neurons grown in culture also possess abundant high-affinity NGF binding sites (Mandelzys *et al.*, 1990). The presence of high-affinity NGF binding and the lack of *trk*A mRNA in a given neuron may seem contrary to what one would expect; however, the majority of nodose neurons express high mRNA and protein levels of $p75^{LNGFR}$ (Yan and Johnson, 1988; Verge *et al.*, 1992). Although the relationship of $p75^{LNGFR}$ to *trk*A is still unclear, recent evidence indicates that $p75^{LNGFR}$ favours high-affinity NGF binding when co-expressed with *trk*A, particularly when a high ratio of $p75^{LNGFR}$ versus *trk*A is expressed (e.g. 10:1) (Benedetti *et al.*, 1993; Lee *et al.*, 1994; Verdi *et al.*, 1994; Chao, 1994). Therefore, one interpretation of the above findings is that nodose neurons that have high-affinity NGF binding sites express *trk*A at low levels (below detection in previous *in situ* hybridization studies) in combination with high levels of $p75^{LNGFR}$.

As it is clear that most nodose neurons express *trk*B (Klein *et al.*, 1990b; Ernfors *et al.*, 1992; Barbacid, 1994), if *trk*A is also expressed at low levels by many of these neurons, then a significant proportion of neurons may co-express multiple *trk*s. This raises the question of whether NGF and BDNF would produce the same effects on the differentiation of nodose neurons co-expressing their receptors. As shown in Chapter 3 and 4, NGF promotes the establishment of a dendritic-axonal polarity on nodose neurons developing in culture and stimulates the neurons to express a higher density of functional nAChRs on their somatodendritic domains. These effects of NGF can only occur in the

absence of ganglionic satellite cells which appear to repress this NGF-induced differentiation, while they induce nodose neurons to acquire a pseudo-unipolar morphology. On the other hand, BDNF has been shown to promote neuronal precursors to acquire properties of sensory neurons in culture (Kalchiem and Gendreau, 1988; Sieber-Blum, 1991). In addition, BDNF and, to a lesser extend, NT-3 have been shown to support embryonic nodose neuron development (Davies, 1994; Ernfors *et al.*, 1994a,b; Farinas *et al.*, 1994; Jones *et al.*, 1994). Based on these observations, we hypothesized that BDNF and perhaps NT-3 promote the sensory differentiation of nodose neurons. To test these predictions, we compared the effects of these neurotrophins on nodose neurons polarity, dendrite outgrowth, nAChR expression and capsaicin sensitivity. Capsaicin (the active ingredient in hot pepper) is a highly selective marker for sensory neurons that extend C fibers and thinly myelinated Aδ fibers (Fitzgerald, 1983; Marsh *et al.*, 1987; Bevan and Geppetti, 1994), and the majority of neurons (70-75%) in the nodose ganglion extend unmyelinated C fibers (which notably innervate the tongue; Paintal, 1973).

In addition, in this chapter, we first examine the effects of neurotrophins on the growth and survival of cultured nodose neurons and quantify the expression of neurotrophin receptor transcripts in neonatal nodose neurons.

EXPERIMENTAL PROCEDURES

Neuronal cultures

P1 nodose and SC ganglia were dissociated and the neurons were plated and cultured according to that described in section **2.1.** From 400 to 600 neurons were plated in the center wells (6 mm in diameter) of modified petri dishes (section **2.1.5.**). Each neurotrophin was added at 25 ng/ml, even when combined together in the growth medium. As described in the result section, most cultures were grown initially with all 3 neurotrophins (4 days). At day 4, the dishes were rinsed twice with L15-Air and fresh growth media were added, containing either NGF, BDNF, NT-3, no neurotrophins, or all 3 neurotrophins combined.

Neuronal counts

Approximately equal number of neurons (400-600) were plated in each condition (4 petri dishes per condition). A few hours after plating, nodose neurons can easily be distinguished from non-neuronal cells under phase contrast microscopy as they remain spherical while non-neuronal cells quickly flatten down and spread on the substrate. All neurons were counted in each culture dish, 12-18 hrs after plating, and 4, 7 and 14 days later. The counts were repeated on 3 separate platings.

Immunocytochemistry

Neurons were fixed, permeabilized and immunostained for MAP2 (HM-2 antibody), as described in section **2.2.1.** and Chapter 3, after approximately 3 weeks of development in culture.

Electrophysiology

Whole-cell voltage clamp was performed as described in section **2.3.**. ACh and capsaicin (8-methyl-*N*-vanillyl-6-nonenamide) (both 50 μM) were applied sequentially on a given neuron by pressure ejection from a double-barrel puffer with tip openings of approximately 20 μm, prepared as described in section **2.3.2.**. In most experiments, ACh was applied first because the capsaicin-evoked currents took several minutes to recover. To make sure that prior application of ACh did not affect capsaicin sensitivity, we applied capsaicin first on some neurons followed by an ACh application 5-10 minutes later, and then re-applied capsaicin 2 min later. The second response to capsaicin was not significantly different from the first one, whether the cell was sensitive or not to ACh (n=5).

RNA extraction and RNase protection assays

Total cellular RNA was extracted from freshly dissociated P1 nodose and SCG neurons which had been separated from their satellite cells (see section **2.1.1.**) as described in section **2.4.1.** RNase protection assays were performed as described in section **2.4.3.** with riboprobes for *trk*A, *trk*B, *trk*C, and $p75^{LNGFR}$. We used two different probes

for *trk*B (see section **2.5.4.**): one probe (730 bp) is protected either by *trk*B^{TK+} (715 bp) or by *trk*B^{TK-} (210 bp) transcripts; the other probe is protected only by the *trk*B^{TK+} transcript (315 bp). The *trk*C riboprobe (324 bp) can only hybridize with the *trk*C^{TK+} transcripts (protected length=315 bp). Either 1 or 2 µg of total cellular RNA were used for hybridization with each riboprobe. The assays were repeated 5 times (each in duplicate reactions) on different extracted RNAs. The hybridization signals were quantified as described in section **2.4.3.** after correction for the specific activity of each riboprobe.

***In situ* hybridization**

The *in situ* hybridization experiments were performed as described in section **2.4.4.** using digoxigenin (DIG)-labelled riboprobes, and immuno-alkaline phosphatase reaction. P1 Nodose and SCG neurons were plated and fixed 12 hrs after plating. The neurons were incubated with a DIG-labelled antisense *trk*A riboprobe synthesized from the same template as that used for the RNase protection assays. The controls consisted of 1) neurons incubated only in the pre-hybridization buffer (section **2.4.4.2.**) but not with *trk*A riboprobes, and subsequently processed for alkaline phosphatase immunoreaction; 2) neurons treated with RNase T1 for 30 minutes, prior to regular hybridization with DIG-labelled *trk*A riboprobes; 3) neurons incubated with sense DIG-labelled *trk*A riboprobes; 4) neurons pre-incubated with 5X unlabelled *trk*A antisense riboprobe for 3 hrs and subsequently co-incubated with 5X unlabelled antisense *trk*A and DIG-labelled antisense *trk*A. To make sure that our 5X unlabelled *trk*A competition control (#4) was specific, we pre-incubated neurons with an unrelated, unlabelled antisense riboprobe (α_7 nAChR; see Chapter 6) for 3 hrs and co-incubated this riboprobe with DIG-labelled antisense *trk*A (see Figure 5.4C and 5.4D). Our controls #1 and 2 were completely negative, while our sense control (#3) showed low levels of labelling after long alkaline phosphatase reaction. Our control #4 showed very little signal in nodose neurons and low levels of labelling in SCG neurons (see Figure 5.4F) which express higher levels of *trk*A than nodose neurons (see Figure 5.3b). This control indicates that the 5X unlabelled *trk*A competed most of the DIG-labelled *trk*A antisense riboprobe. In Figure 5.4, we show two of these controls (#2: Figure 5.4G and 5.4H, and #4: Figure 5.4E and 5.4F). The alkaline phosphatase reactions

were all stopped at the same time in a given experiment, usually after approximately 5 hrs.

RESULTS

Growth and survival of nodose neurons developing in culture with or without different neurotrophins

Neonatal rat nodose neurons can grow for many weeks in culture without satellite cells and without adding any neurotrophin (Chapter 3; Mandelzys *et al.*, 1990). However, soon after plating, a significant proportion of neurons die within the first 2-3 days, with or without NGF. This cell death may be due to the manipulations and dissociation of the neurons, or perhaps because other neurotrophins, such as BDNF or NT-3, are needed for their survival. To test whether these neurons require neurotrophin for survival, we plated freshly dissociated neurons under 5 conditions: with 1) NGF, 2) BDNF, 3) NT-3 , 4) NGF+BDNF+NT-3, and 5) without any neurotrophin (each neurotrophin at 25 ng/ml), and counted the proportions of neurons that survived over a 2 week period. Figure 5.1A shows that in the absence of neurotrophin, approximately 60% of the neurons have remained from day 1 to day 4 in culture. Adding NGF resulted in a 10% increase in the number of neurons after 4 days in culture compared to no neurotrophin. In contrast, most neurons remained after 4 days in the presence of BDNF (94%) or NT-3 (89%). Finally, in the presence of all neurotrophins, almost no neuronal loss was measured after plating (Figure 5.1A). Interestingly, past 4 days in culture, nearly all neurons remained and grew in the cultures independent of the condition (Figure 5.1A). These results indicate that a large proportion of rat neonatal nodose neurons can grow independent of neurotrophin in culture, suggesting that these neurons have developed, at P1, beyond the period of neurotrophin dependence.

Next, we asked whether growing the neurons with a combination of all 3 neurotrophins for the first 4 days was sufficient to make them all neurotrophin-independent thereafter. To do this, we changed the growth medium at day 4 to one containing either NGF, BDNF, NT-3, no neurotrophin, or the 3 combined. Figure 5.1B

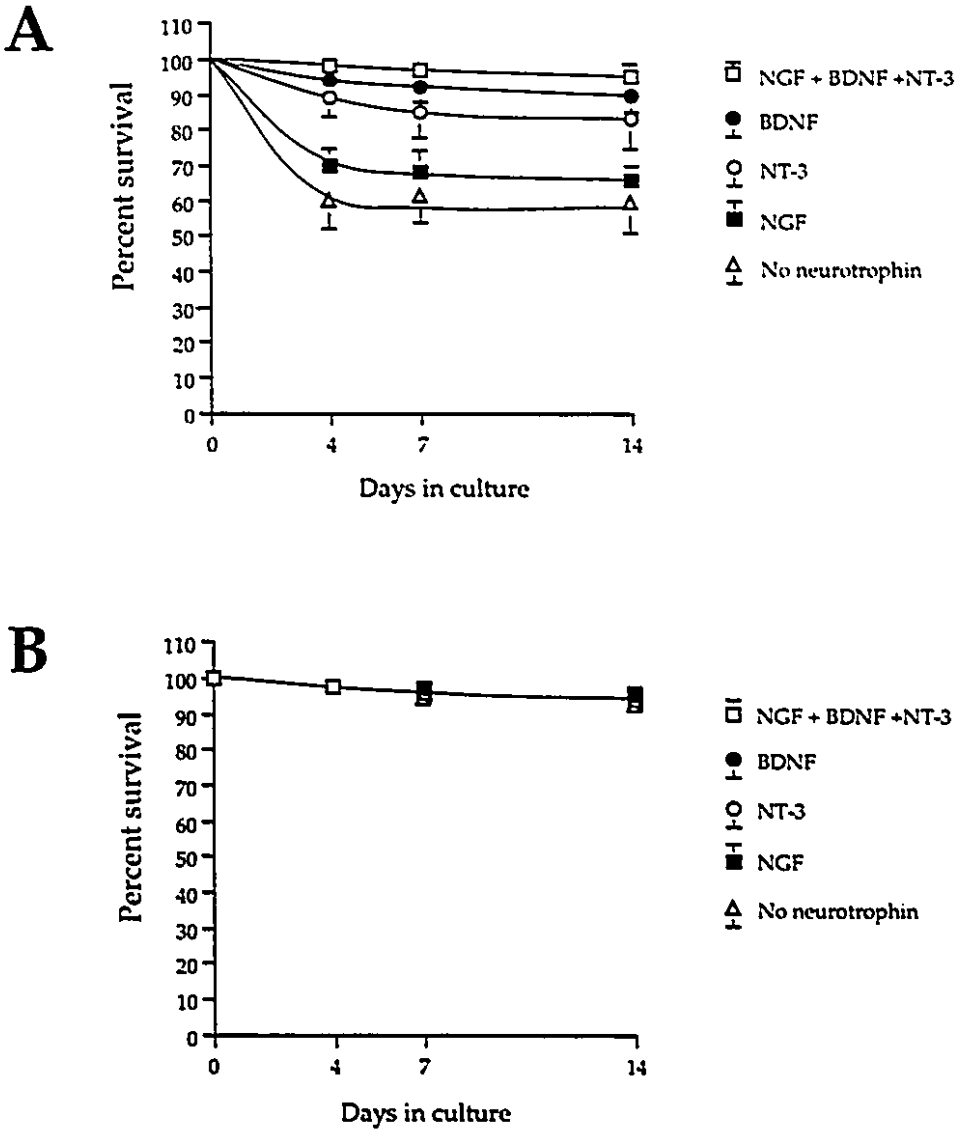

FIGURE 5.1. Effects of neurotrophins on nodose neuron survival in culture. (A) Mean (±SEM) counts of neurons grown in the absence of neurotrophin, or in the presence of NGF, BDNF, NT-3, or NGF+BDNF+NT-3 (all neurotrophins at 25 ng/ml). Neurons were counted 12 hrs after plating, and 4, 7 and 14 days later. The number of neurons after 12 hrs were normalized to 100%. (B) Mean (±SEM) counts of neurons grown in presence of NGF+BDNF+NT-3 for the first 4 days, and subsequently grown in presence of either no neurotrophin, NGF, BDNF, NT-3 or NGF+BDNF+NT-3. Under this paradigm, most neurons survive for 2 weeks in culture.

FIGURE 5.2. Effect of neurotrophins on nodose neuron growth in culture.

Phase contrast photomicrographs of nodose neurons grown for 4 days with NGF+BDNF+NT-3, and subsequently without neurotrophin, or with NGF, BDNF or NT-3, or with NGF+BDNF+NT-3, for a following 17 days. The number of neurons and the total amount of process outgrowth were similar under each condition.

NGF

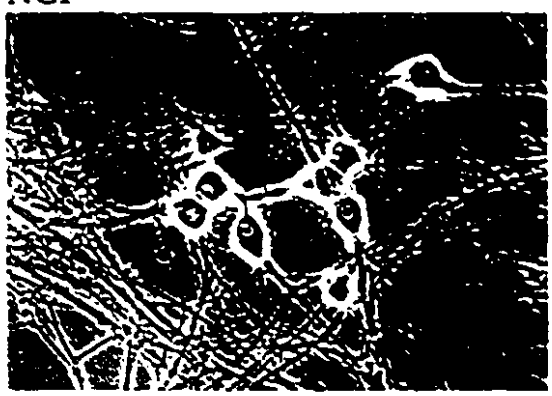

BDNF

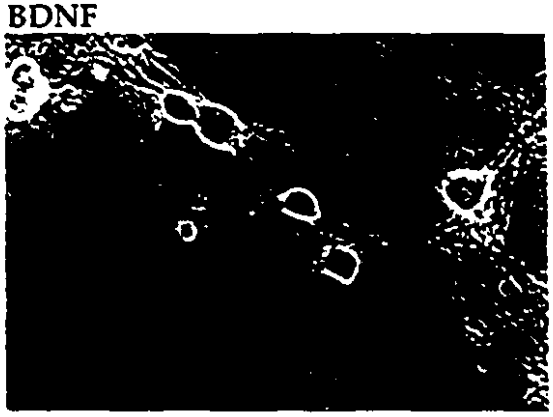

NT-3

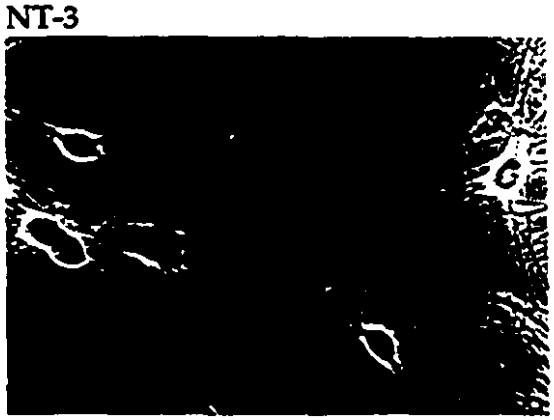

NGF + BDNF + NT-3

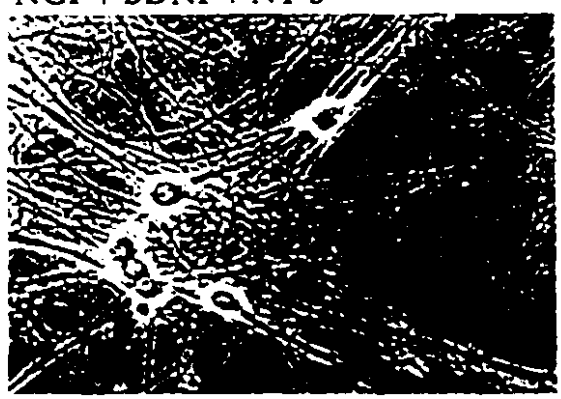

Without neurotrophin

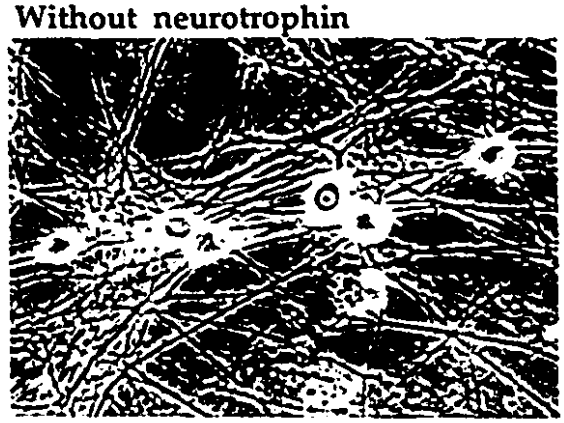

shows that after 4 days in culture nearly all nodose neurons no longer depend on any exogenous neurotrophin for survival. Figure 5.2 shows phase contrast photomicrographs of these cultures which were grown for the first 4 days with NGF+BDNF+NT-3 and for a following 17 days in the presence of either NGF, BDNF, NT-3, all 3 neurotrophins or without neurotrophin. This Figure shows that the amount of process outgrowth is roughly the same under each condition.

Expression of neurotrophin receptors in P1 nodose neurons

To determine which neurotrophin receptors are expressed by newborn rat nodose neurons, we measured the transcript levels of *trk*A, *trk*B, *trk*C and $p75^{LNGFR}$ with RNase protection assays. For comparison, we measured simultaneously the levels of these transcripts on newborn SCG neurons.

Figure 5.3a shows the results from an RNase protection assay for the 4 neurotrophin receptor transcripts in nodose and SCG neurons that were dissociated and separated from their ganglionic satellite cells (see section 2.1.1). Figure 5.3b shows the quantification of the levels of these neurotrophin receptor transcripts in both neuronal types, expressed relative to $p75^{LNGFR}$ in nodose neurons (=100%). This figure demonstrates that among *trk* receptor transcripts, *trk*B mRNA is expressed at highest levels in nodose neurons, but only by 2-3 fold compared to *trk*A and *trk*C mRNAs. $p75^{LNGFR}$ transcripts are expressed 10-14 fold more than *trk*A mRNA in nodose neurons. In contrast, *trk*A mRNA is 2-3 fold more abundant than $p75^{LNGFR}$ in SCG neurons. SCG neurons contain undetectable levels of *trk*B transcripts and little *trk*C mRNA. Nodose neurons contain approximately 5 fold less *trk*A mRNA than SCG neurons.

The riboprobes used to hybridize *trk*B and *trk*C mRNAs were directed against regions that encode the tyrosine kinase domains of the receptors. Therefore, these 2 riboprobes cannot detect mRNAs that encode the truncated spliced variants of these two receptors that lacked the tyrosine kinase domains ($trkB^{TK-}$ and $trkC^{TK-}$; see appendix 1). To test whether the $trkB^{TK-}$ receptor is expressed in nodose neurons, we used a longer riboprobe of 715 bp that spans from part of the tyrosine kinase intracellular loop to the transmembrane region which is common to both spliced variants (see section 2.4.5.). The

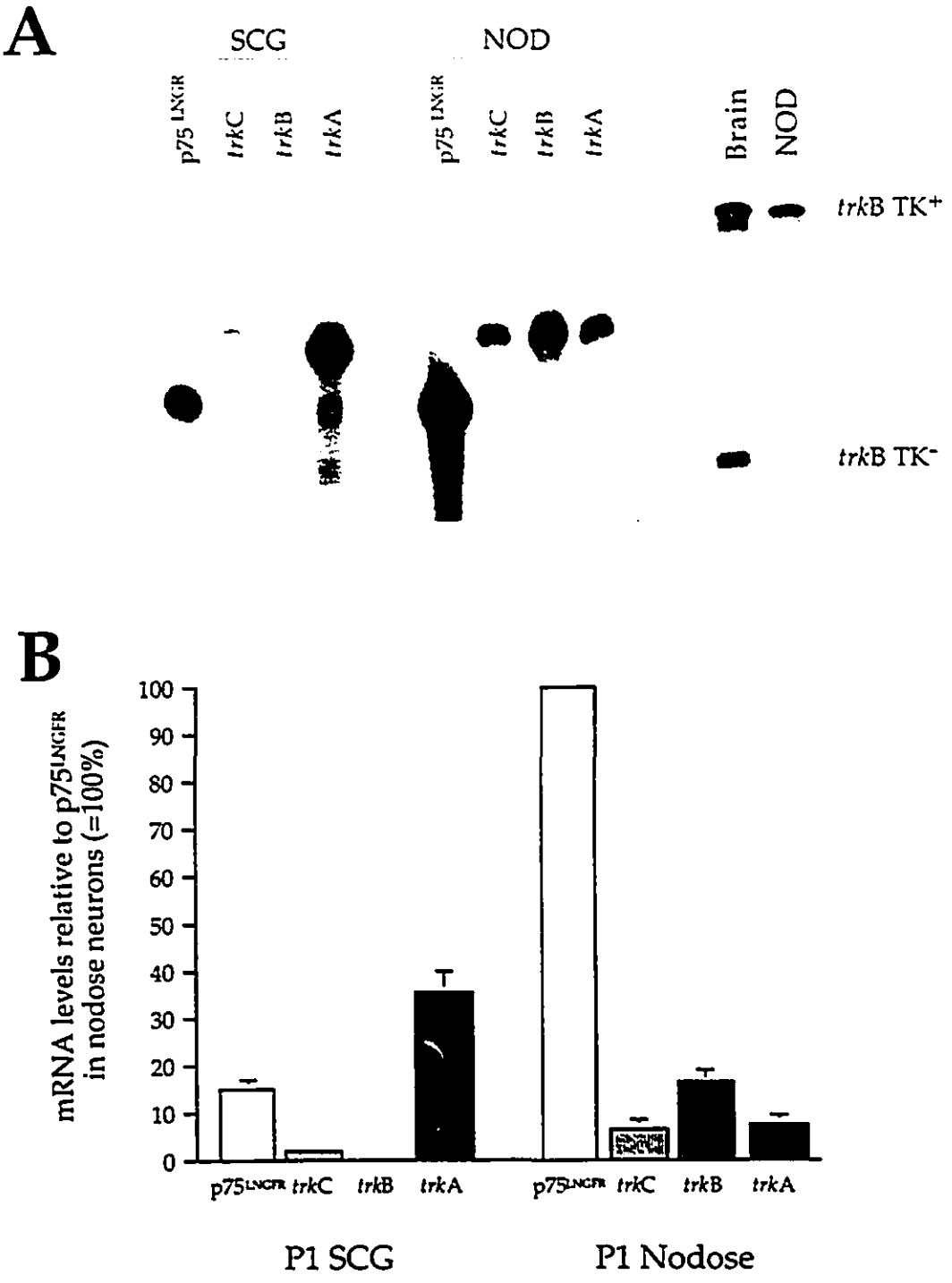

FIGURE 5.3. Expression of neurotrophin receptor transcripts in P1 nodose and SCG neurons.

(A) Left: RNase protection assay for *trk*A, *trk*B^{TK+}, *trk*C^{TK+} and p75^{LNGFR} transcripts on P1 nodose and SCG neuron RNA. The sizes (bp) of the protected antisense riboprobes on the left panel are: *trk*A=300 *trk*B=315 *trk*C=315 and p75^{LNGFR}=270. Right: RNase protection assay for *trk*B^{TK+} and *trk*B^{TK-} on nodose neuron and total brain RNA. The 730 bp *trk*B riboprobe was protected by either the *trk*B^{TK+} transcript (715bp) or the *trk*B^{TK-} transcript (210bp). 1 mg of total cellular RNA and 200 000 cpm of riboprobe was added in each reaction. (B) Mean (±SEM) transcript levels of neurotrophin receptors in nodose and SCG neurons normalized to p75^{LNGFR} transcript levels in nodose neurons (n=5).

right panel of Figure 5.3a shows that very little if any *trk*B^{TK-} is expressed in nodose neurons, while it is abundantly expressed in the brain. *trk*B^{TK-} is believed to be mainly expressed in glial cells (Beck *et al.*, 1993; Frisen *et al.*, 1993; Jelsma *et al.*, 1993; Valenzuela *et al.*, 1993); when we performed RNase protection assays on whole ganglia, this splice variant became apparent suggesting that nodose satellite cells express some *trk*B^{TK-}.

These results demonstrate that all 4 neurotrophin receptor transcripts are expressed by nodose neurons. If we compare our results on *trk* mRNA levels in nodose neurons with those obtained from *in situ* hybridization experiments (Martin-Zanca *et al.*, 1990; Verge *et al.*, 1992; Ernfors *et al.*, 1992; Barbacid, 1994), it suggests that *trk*A is expressed at low levels in the majority of the neurons. Such conclusion would imply that previous *in situ* hybridization studies did not detect those low levels of *trk*A transcripts. Alternatively, as these *in situ* hybridization experiments were performed on embryonic or adult nodose ganglia, it is possible that P1 rat nodose neurons express higher levels of *trk*A than earlier and later in development. Our measurements of neurotrophin receptor transcripts on SCG neurons are consistent with previous studies which have indicated that 1) *trk*A mRNA is expressed at high levels in embryonic and neonatal SCG neurons; 2) *trk*C is expressed very early in embryonic development and its transcript levels decrease thereafter; 3) *trk*B is expressed at very low levels if at all expressed; 4) p75^{LNGFR} expression is still low by birth, but it largely increases postnatally (Ernfors *et al.*, 1992; DiCicco-Bloom *et al.*, 1993; Barbacid, 1994; Verdi *et al.*, 1994).

To estimate the proportion of nodose neurons that express *trk*A, we needed to develop a sensitive protocol for *in situ* hybridization to be able to resolve low levels of *trk*A mRNA in neurons. Our preliminary approach has been to use uniformly labelled antisense riboprobes (300 mers) that have been labelled on every four uracil with a digoxigenin molecule (DIG), which is then revealed with an immuno-alkaline phosphatase reaction (see section **2.4.4.**). As a first step, we performed the *in situ* hybridization on freshly plated neurons to minimize background signals. Figure 5.4 shows the result from one

FIGURE 5.4. *In situ* hybridization for *trk*A in nodose and SCG neurons, with DIG-labelled antisense *trk*A riboprobe.

Phase contrast photomicrographs of nodose (A) and SCG (B) neurons grown for 12 hrs in culture, fixed and incubated with DIG-labelled *trk*A antisense riboprobes, revealed with an immuno-alkaline phosphatase reaction. (C) and (D) Bright field photomicrographs of the same field as above showing *trk*A mRNA labelling in neurons. (C) The majority of nodose neurons were labelled at various intensities for *trk*A mRNA. The large arrow points to a neuron that showed little or no signal for *trk*A mRNA, the arrowhead to a neuron with faint signal for *trk*A mRNA, and the small arrow to a neuron with moderate signal for *trk*A mRNA. (D) Virtually all SCG neurons showed strong signal for *trk*A mRNA (large arrow points to one example). No *trk*A mRNA signal above background was found in non-neuronal cells (small arrow). The DIG-*trk*A riboprobe hybridization in C and D was performed with a 5X amount of unlabelled riboprobes of an unrelated mRNA (α_7 nAChR subunit); this provided a control for the specificity of the competition with unlabelled *trk*A antisense riboprobe shown in E and F. (E) to (H) show control experiments with differential interference optics to allow better visualization of unlabelled neurons. In (E) and (F) the hybridization with DIG-*trk*A riboprobe was competed with 5X unlabelled *trk*A antisense riboprobe. No signal above background was observed in nodose neurons (E), while faint signal was observed in SCG neurons (examples pointed by arrowheads in E and F). This suggests that most, but not all DIG-*trk*A signal is competed with the unlabelled *trk*A antisense riboprobe. In (G) and (H) the fixed neurons were pre-incubated with RNase T1 (20 U/μl) for 30 min before incubation with DIG-*trk*A riboprobe. No signal above background was observed under this condition in both neuronal populations. Similar results as those in G and H were obtained with sense DIG-labelled *trk*A riboprobe incubation, or without DIG-labelled riboprobe incubation. Scale bar, 40 μm.

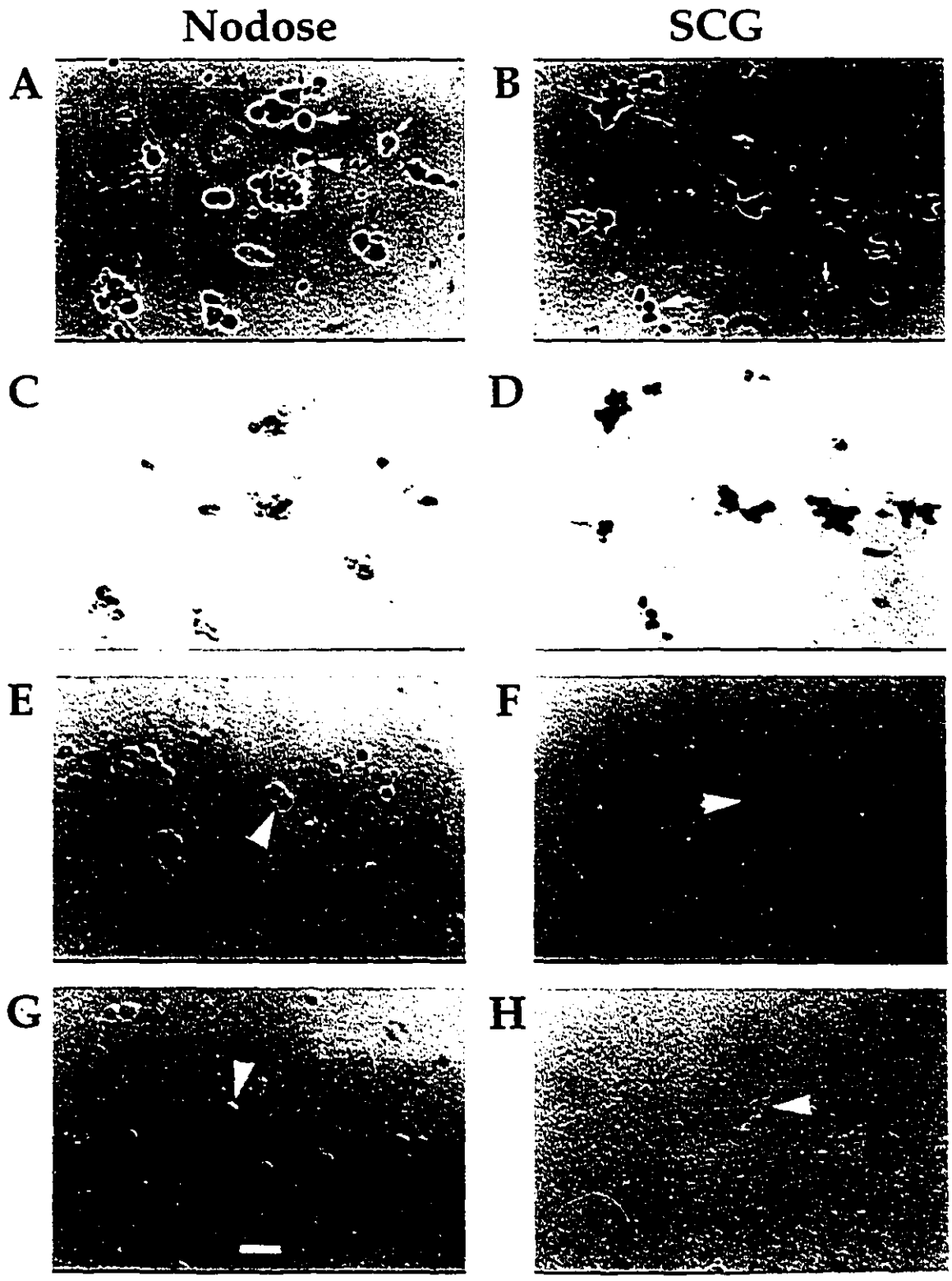
Nodose
SCG
A
B
C
D
E
F
G
H

experiment performed on P1 nodose and SCG neurons. This figure shows that while nearly all SCG neurons are labelled strongly for *trk*A mRNA (Figure 5.4B and 5.4D), the majority of nodose neurons are moderately labelled, although the labelling appears more uneven between nodose neurons in the same culture (Figure 5.4A and 5.4C). Furthermore, some nodose neurons appear unlabelled (Figure 5.4A and 5.4C; large arrow). These preliminary results suggest that *trk*A mRNA is present in a much larger proportion of nodose neurons than previously appreciated, though at low levels.

NGF specifically induces dendrite formation

After three weeks in culture, many nodose neurons have extended MAP2 positive dendrites when grown in the absence of satellite cells and in the presence of NGF (Chapter 3). To test whether BDNF and NT-3 influence the polarity of nodose neurons, we grew sister cultures of neurons in the presence of these neurotrophins and immunostained them for MAP2. Neurons were grown in the presence of all 3 neurotrophins for the first 4 days; at day 4, the growth medium was changed to one containing either NGF, BDNF, NT-3, or no neurotrophin. Figure 5.5 shows that nodose neurons extend more elaborate dendrites in the presence of NGF compared to BDNF, NT-3, or without neurotrophins. In addition, only approximately 6 or 7% of the neurons had dendrites in the presence of BDNF or NT-3, respectively, whereas in the presence of NGF, nearly 20% of the neurons had dendrites after 3 weeks in culture. BDNF appeared not to promote any dendritic outgrowth, while NT-3 seemed to cause a small increase in the dendritic length (Figure 5.6).

The estimated total dendritic outgrowth, under the different conditions, as calculated by the product of the proportion of neurons with dendrites, the number of dendrites per neuron, and the mean dendritic length, is shown in Figure 5.6B. This histogram demonstrates that among these neurotrophins, only NGF induces substantial dendritic outgrowth; in the presence of NT-3 the amount of total dendritic growth is significantly higher than without neurotrophin, mainly because the few dendrites present are more elaborated than the ones present in the absence of neurotrophins.

As illustrated in Figure 5.2, the overall amount of process outgrowth appeared

FIGURE 5.5. MAP2 immunostaining in nodose neurons developing in culture with either NGF, BDNF, NT-3, or without neurotrophin.

Fluorescent photomicrographs of neurons immunostained with monoclonal antibody HM-2 against MAP2. In the presence of NGF many neurons extend long elaborated dendrites; in the presence of BDNF, few neurons had short dendrites; in the presence of NT-3, few neurons have short dendrites, although occasionally longer than in the presence of BDNF; in the absence of neurotrophin, few neurons had short dendrites.

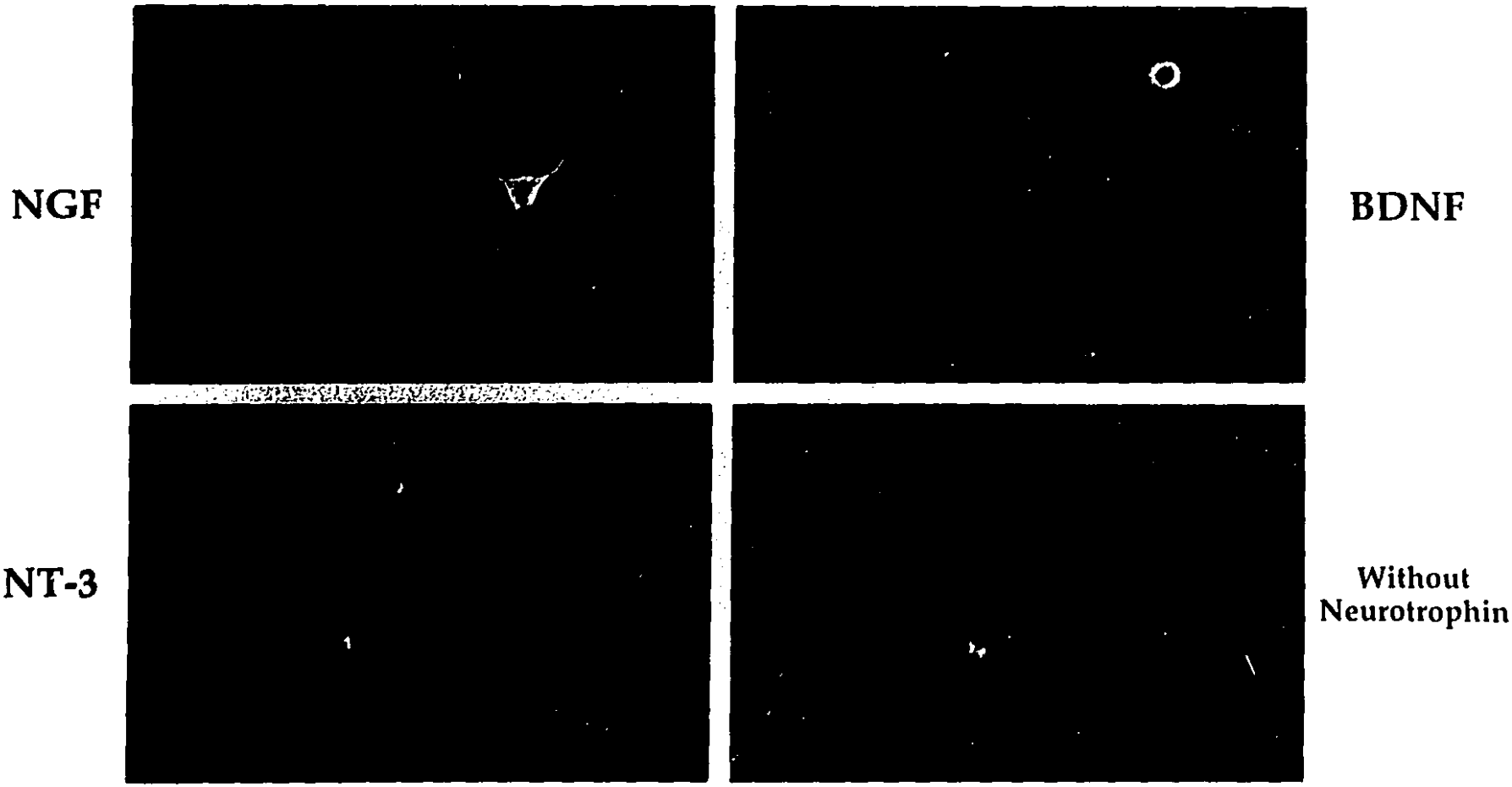
NGF
BDNF
NT-3
Without
Neurotrophin

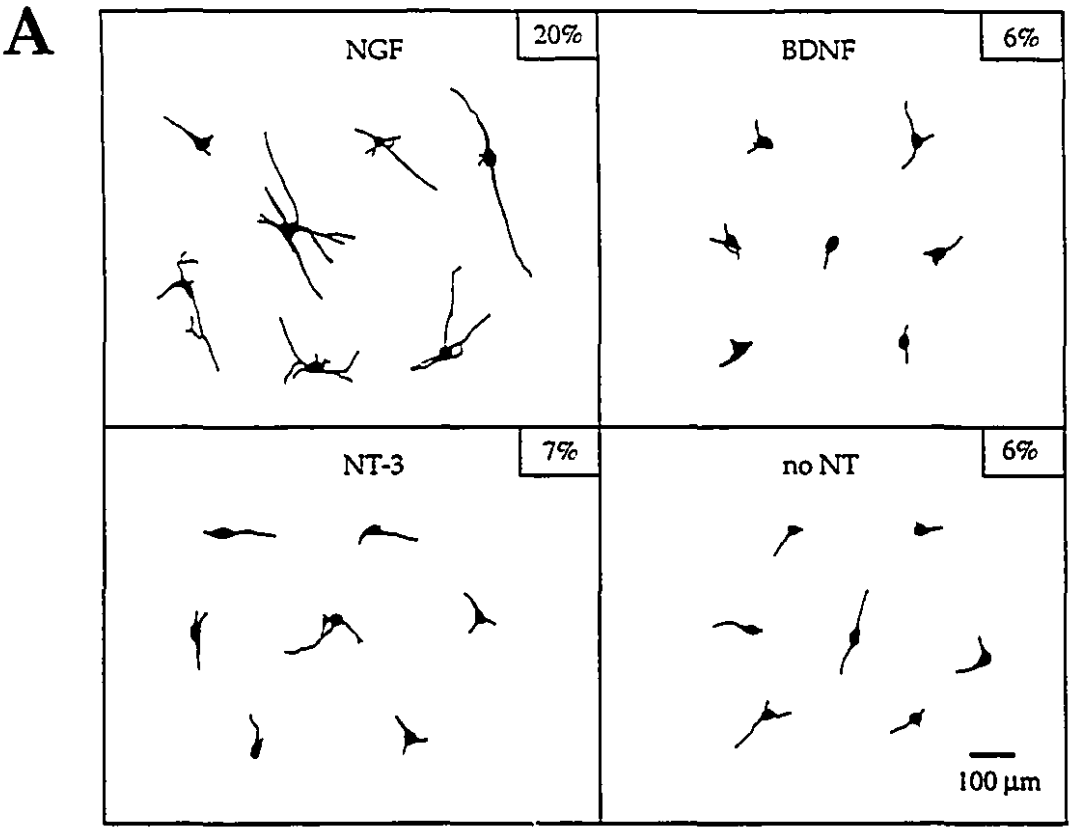

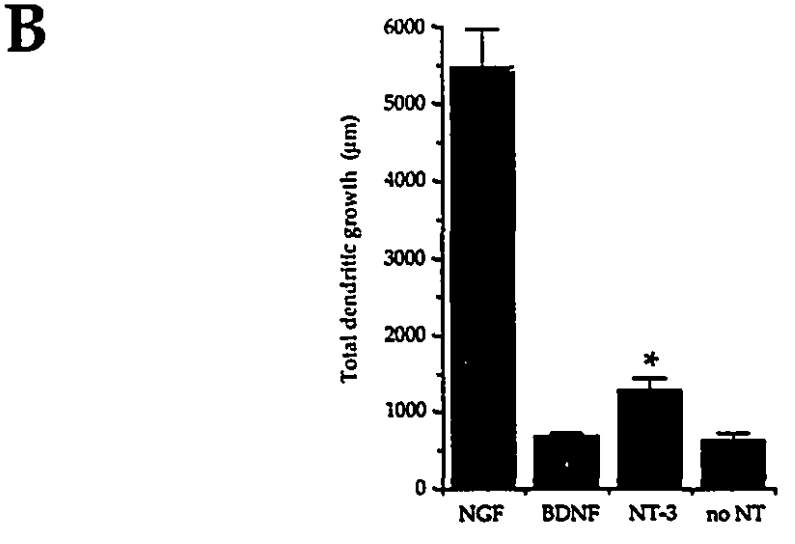

FIGURE 5.6. Camera lucida drawings and quantification of dendritic outgrowth by nodose neurons in the presence or absence of neurotrophins. **(A)** Selected neurons with MAP2 labelled dendrites were traced by camera lucida drawing. The neurons were grown for 3 weeks in culture in the presence of NGF, BDNF, NT-3 (25 ng/ml) or without neurotrophin (no NT). In the presence of NGF, 20% of the neurons had several elaborated MAP2 positive dendrites. In the presence of BDNF, 6% of the neurons had short dendrites. In the presence of NT-3, 7% of the neurons had short dendrites, occasionally longer compared to neurons grown with BDNF or without neurotrophins. In the absence of neurotrophin, 6% of the neurons had short MAP2 positive dendrites. **(B)** Total dendritic outgrowth by nodose neurons, as calculated by the product of the percentage of neurons with dendrites, the number of dendrites per neuron, and the mean dendritic lengths. The mean total dendritic outgrowth (±SEM) is expressed per 100 neurons. *In the presence of NT-3, the total dendritic growth was significantly different from that in the absence of neurotrophin ($p<0.001$, t-test).

relatively similar between each neurotrophin condition, suggesting that axonal outgrowth was not differentially affected by any of these neurotrophins. Although we did not measure the number of primary axons per neuron in this chapter (see Chapter 3), it was clear that the neurons were multipolar under each condition. Similar observations were made when the neurons were grown in the presence of either NGF, BDNF, NT-3 or without neurotrophin at the onset of plating. These observations suggest that the number of axons that nodose neurons extend in these cultures is independent of neurotrophins and is only determined by the presence or the absence of satellite cells (Chapter 3).

Capsaicin-evoked currents on nodose neurons

The above results indicate that BDNF and NT-3 do not induce much dendritic outgrowth from nodose neurons; perhaps instead, these neurotrophins influence P1 nodose neurons to acquire properties of sensory neurons. To examine this possibility, we investigated whether neurotrophins influence the neurons to acquire their typical sensitivity to capsaicin, using whole-cell voltage clamp recording (Bevan and Geppetti, 1994). Figure 5.7A shows an example of a capsaicin-evoked inward current on a freshly dissociated P1 nodose neuron: the current activates relatively slowly (e.g. 2-4 sec; see inset) and is sustained for a long period of time (e.g. 3-4 min). We found that 26/40 (65%) P1 nodose neurons were sensitive to capsaicin, with a mean evoked-current of 40 ± 6 pA/pF (SEM). This compares well with a proportion of 70-75% measured *in vivo* in nodose ganglia (Marsh *et al.*, 1987). In contrast, when we measured capsaicin sensitivity on freshly dissociated P1 SCG neurons, 0/12 neurons were sensitive.

Capsaicin sensitivity is retained by BDNF but not by satellite cells

The ganglionic satellite cells of the nodose ganglion induce the neurons to re-acquire a unipolar morphology typical of sensory neurons. However, satellite cells by themselves do not sustain nodose neuron's capsaicin sensitivity in culture (Figure 5.7B). In contrast, capsaicin sensitivity is influenced by neurotrophins: when neurons grow in the presence of BDNF with or without satellite cells, 50-70% of them retain their sensitivity to capsaicin, whereas neurons developing with NGF, either in the presence or absence of

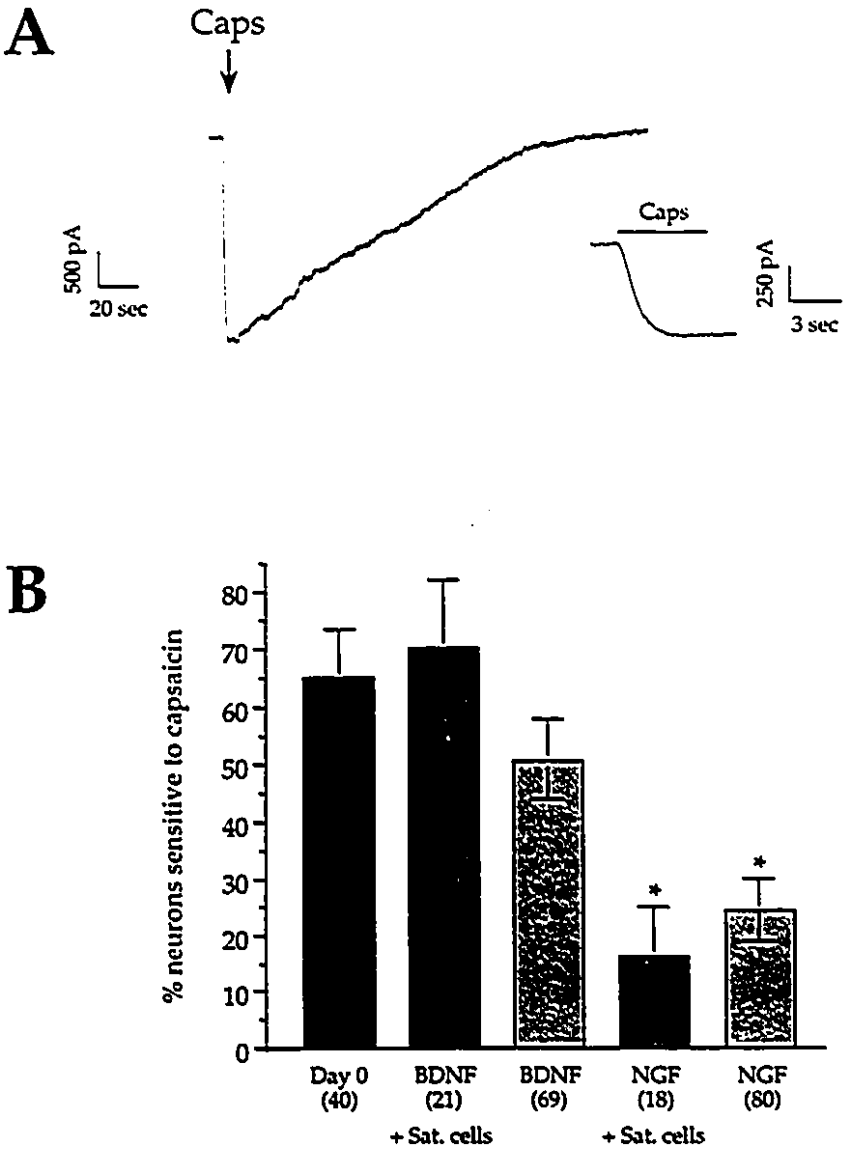

FIGURE 5.7. Capsaicin sensitivity of nodose neurons.

(A) Whole-cell patch clamp recording of a typical capsaicin-evoked current on a nodose neuron voltage clamped at -50 mV. Upon a 4 sec application of 50 μM capsaicin by pressure ejection, a large, slowly activating inward current is evoked and takes a few minutes to return to baseline. The inset shows the time of full activation (3-4 sec). The current was filtered at 3 KHz and sampled at 100 Hz. (B) Percentage of capsaicin-sensitive nodose neurons *in vivo* (freshly dissociated) and after development in culture. Approximately 65% of freshly plated nodose neurons are sensitive to capsaicin. In the presence of BDNF, cultured nodose neurons retain their capsaicin sensitivity with or without satellite cells (no significant difference between + or - satellite cells; $p>0.05$, t-test). In the presence of NGF, cultured nodose neurons lose their sensitivity to capsaicin, with or without satellite cells (* significantly different from day 0; $p< 0.001$, t-test)

satellite cells, lose their capsaicin sensitivity (Figure 5.7B). These results indicate that in spite of their induction effect on sensory neuron polarity, satellite cells do not sustain capsaicin sensitivity on nodose neurons.

BDNF and NT-3 promote capsaicin sensitivity, while NGF promotes ACh sensitivity on nodose neurons.

As shown above, NGF does not sustain capsaicin sensitivity on nodose neurons, but instead it promotes dendritic outgrowth and causes an increase in ACh-evoked current densities (Mandelzys and Cooper, 1992). To test whether the neurons that acquire high ACh sensitivity lose their sensitivity to capsaicin, we applied both ACh and capsaicin on the same neurons using double-barrel electrode puffers, with one barrel containing 50 μM capsaicin and one barrel containing 50 μM ACh.

Figure 5.8 shows the ACh- and capsaicin-evoked currents from three neurons grown for 3 weeks with NGF. The neuron in (A) has a large ACh-evoked current (2800 pA) but is insensitive to capsaisin; the neuron in (B) has a smaller ACh-evoked current (500 pA), but has a large capsaicin-evoked current (2600 pA); the neuron in (C) has no ACh-evoked current and a large capsaicin-evoked current (2700 pA). Figure 5.9A shows the ACh-evoked current densities plotted against the capsaicin-evoked current densities for 35 nodose neurons grown with NGF for 2-3 weeks. The distribution of points is skewed to the bottom right of the plot indicating that most neurons with large ACh-evoked currents (>10 pA/pF) had no capsaicin-evoked currents. In contrast, a higher proportion of neurons with small or no ACh-evoked currents were capsaicin-sensitive. We found that 20% of the neurons were insensitive to both ACh and capsaicin (Figure 5.9A; right).

As BDNF promotes capsaicin sensitivity of nodose neurons in culture (Figure 5.7B) and does not promote dendritic outgrowth, one would predict that in the presence of BDNF, nodose neurons do not express ACh-evoked currents. Figure 5.9B shows that in the presence of BDNF, the distribution of capsaicin-evoked currents plotted against the ACh-evoked currents is skewed to the left, indicating that most capsaicin-sensitive neurons had small ACh-evoked currents. However, this figure shows that a large proportion of neurons were sensitive to ACh, albeit the currents were small, generally ≤10pA/pF. Based

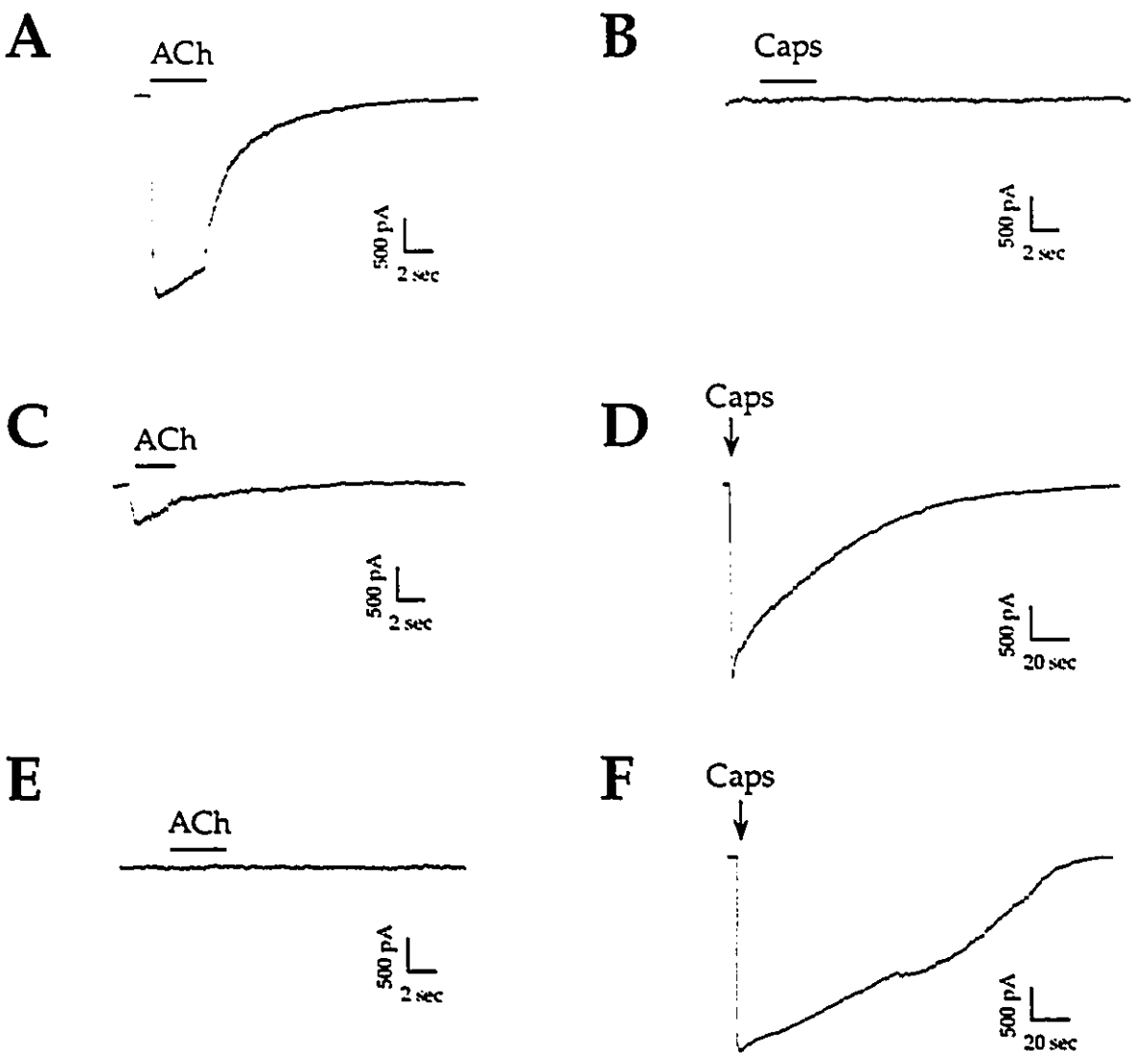

FIGURE 5.8. ACh- and capsaicin-evoked currents on nodose neurons grown for 17 days in culture without satellite cells and with NGF (after an initial 4 days with all 3 neurotrophins). ACh (50 μM) and capsaicin (50 μM) were co-applied sequentially on the same neuron with a double- barrel puffer electrode. The capsaicin application (3 sec) was done 2 min after the ACh application (3 sec). (A) This neuron had a large ACh-evoked current and a large capsaicin-evoked current (B). (C) This neuron had a small ACh-evoked current and a large capsaicin-evoked current (D). (E) This neuron had no ACh-evoked current and was sensitive to capsaicin. ACh-evoked currents were filtered at 3 KHz and sampled at 5 KHz. Capsaicin-evoked currents were sampled at 100 Hz.

on our results in Chapter 4 (Figure 4.1), an ACh-evoked current density of approximately 10 pA/pF may represent an indicator of neurons that extend dendrites. We found that only 2-3% of the neurons had ACh-evoked current densities ≥10pA/pF in the presence of BDNF (Figure 5.9B; right), while approximately 6% had dendrites (Figure 5.3). In contrast, we found that 30-35% of the neurons had ACh-evoked currents ≥10pA/pF in the presence of NGF (Figure 5.7A; right), while 20-25% had dendrites (Figure 5.3; chapter 3). These proportions are consistent with a correlation between dendrite outgrowth and ACh-evoked current densities (Chapter 4).

In addition, we found that NT-3 essentially produces the same effects as BDNF on nodose neurons, as it sustains their capsaicin sensitivity, and few neurons have ACh-evoked currents ≥10pA/pF (2-3%; Figure 5.9C).

To test whether NGF actually inhibits capsaicin sensitivity on nodose neurons, we grew the neurons without neurotrophin. Figure 5.9D shows that only 20% of the neurons were sensitive to capsaicin in the absence of neurotrophin, indicating that NGF does not inhibit capsaicin sensitivity on nodose neurons. Surprisingly, Figure 5.9D also shows that fewer neurons had ACh sensitivity in the absence of neurotrophin compared to neurons grown with BDNF or NT-3, indicating that these neurotrophins promote low density nAChR expression on nodose neurons.

If individual nodose neurons co-express multiple *trk* receptors, one might expect that by adding all 3 neurotrophins together the neurons will be induced to express both large capsaicin- and ACh-evoked currents, unless conflicting signals are mediated by different *trk* receptors on the same neurons. To determine whether more than one neurotrophin can produce effects on individual neurons, we grew nodose neurons in the presence of all 3 neurotrophins. Figure 5.9E shows that 50% of the neurons were sensitive to capsaicin, indicating that BDNF and NT-3 did not have additive effects on the proportion of neurons that express capsaicin-evoked currents (c.f. Figure 5.9B and 5.9C). However, surprisingly, in the presence of all 3 neurotrophins fewer neurons (16%) had ACh-evoked currents ≥10 pA/pF (Figure 5.9E; right) compared to neurons grown with NGF (33%; Figure 5.9A; right).

Table 5.1 shows the mean ACh- and capsaicin-evoked current densities from all

FIGURE 5.9. Effects of neurotrophins on ACh- and capsaicin-evoked currents in culture in the absence of satellite cells.

ACh (50 μM) and capsaicin (50 μM) were co-applied sequentially on neurons (see Figure 5.8) that were grown for 2-3 weeks with either (A) NGF, (B) BDNF, (C) NT-3, (D) no-neurotrophin or (E) all 3 neurotrophins. All neurons were grown for the first 4 days with the 3 neurotrophins combined. On the left hand graph of (A) to (E), the capsaicin-evoked current densities are plotted against the ACh-evoked current densities for individual neurons (filled circles). On the right hand histogram of (A) to (E) is shown the percentage of neurons 1) non-responsive to both capsaicin and ACh, 2) sensitive to capsaicin, and 3) that had ACh-evoked current densities ≥10 pA/pF. This value of 10 pA/pF may represent a rough indicator of neurons with dendrites (see Figure 4.1). (A) In the presence of NGF, the distribution of current densities are skewed to the bottom-right of the plot, indicating that many neurons had large ACh-evoked currents (33% with current densities ≥10 pA/pF), but few (23%) were sensitive to capsaicin. (B) In the presence of BDNF, the current densities are skewed to the middle-left of the plot, indicating that few neurons had large ACh-evoked currents (3%) and many were capsaicin-sensitive (50%). (C) In the presence of NT-3, neurons had similar ACh and capsaicin sensitivities compared to neurons grown with BDNF. (D) In the absence of neurotrophin few neurons had ACh-evoked current densities above ≥10 pA/pF (1-2%) and few were sensitive to capsaicin (20%); a large proportion of neurons were, in fact, insensitive to both ACh and capsaicin (50%). (E) In the presence of all 3 neurotrophins, the same percentage of neurons were sensitive to capsaicin as in the presence of BDNF, however fewer neurons (16%) had ACh-evoked current densities above ≥10 pA/pF compared to neurons grown with NGF (33%). n: NGF=74, BDNF=69, NT-3=52, no neurotrophin=37, NGF+BDNF+NT-3=35. For the current density plots, 35 neurons were selected at random for each condition. The proportion of unresponsive neurons is not reflected on these distribution plots and was therefore shown on the histogram.

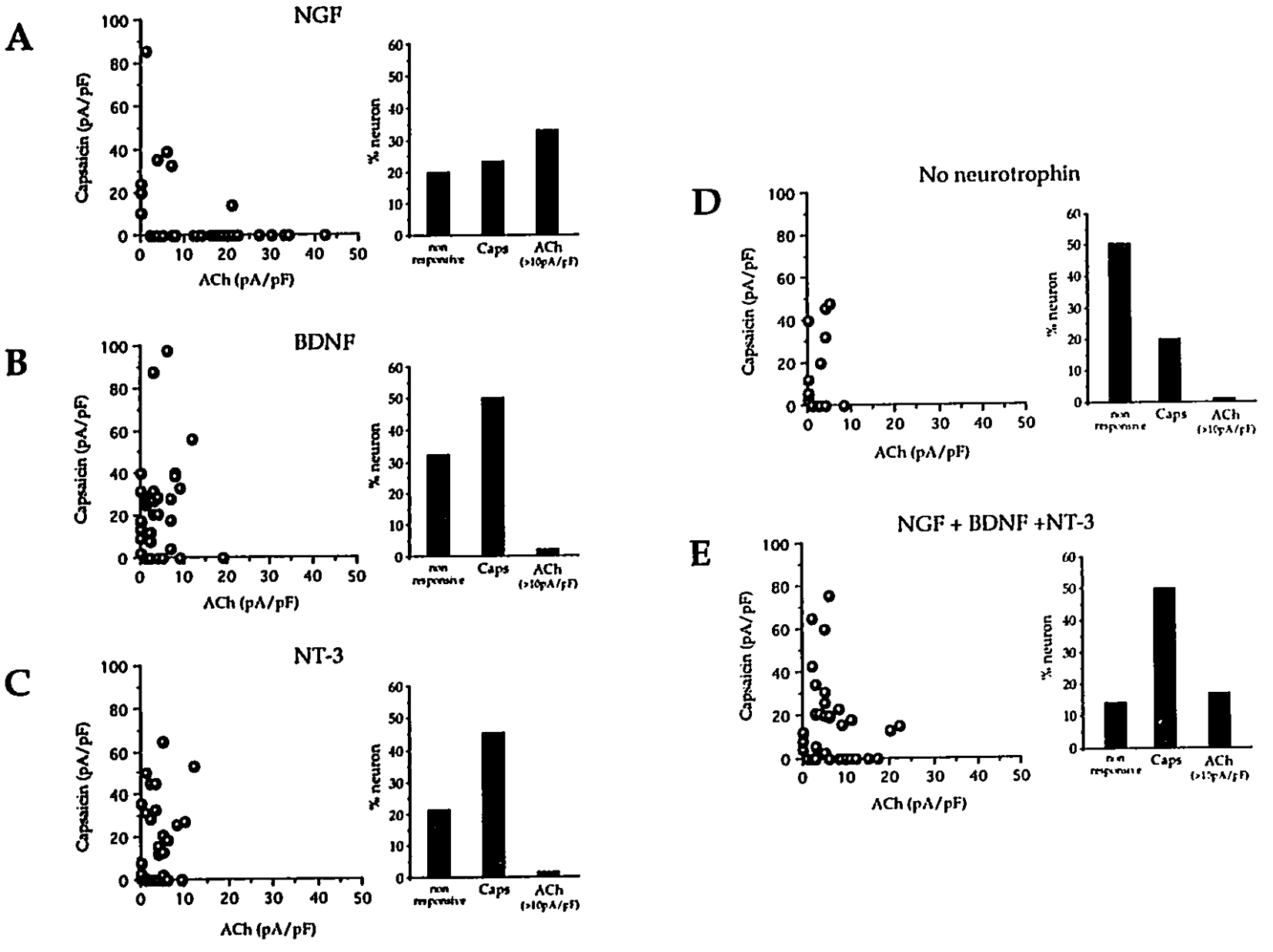
A
NGF
Capsaicin (pA/pF)
ACh (pA/pF)
% neuron
non responsive
Caps
ACh (>10pA/pF)
B
BDNF
C
NT-3
D
No neurotrophin
E
NGF + BDNF +NT-3

neurons growing under each condition. This table demonstrates that in the presence of all neurotrophins, the mean ACh-evoked current densities are smaller than with NGF alone, suggesting that BDNF and/or NT-3 partially repress the effects of NGF on functional nAChR expression. In addition, it shows that the mean ACh-evoked currents in the presence of BDNF or NT-3 are higher than in the absence of neurotrophin, suggesting that these neurotrophins promote the expression of low density nAChRs. Finally, the few neurons that were sensitive to capsaicin in the presence of NGF had 2 fold larger capsaicin-evoked currents than in the absence of neurotrophin.

Table 5.1 Effects of neurotrophins on mean ACh- and capsaicin-evoked currents on nodose neurons

	NGF (74)	BDNF (69)	NT-3 (52)	NGF + BDNF + NT-3 (35)	without neurotrophin (37)
ACh (pA/pF)	8.7 ±1.2$^{\#+}$	2.1 ±0.4$^{*\#+}$	2.8 ±0.5$^{*\#+}$	5.3 ±1.0^{*-}	1.1 ±0.3$^{*\#}$
Caps (pA/pF)	6.8 ±2.0	13.2 ±2.4§	11.1 ±2.4§	13.7 3.8§	3.4 ±1.9§

Mean (±SEM) ACh- and capsaicin-evoked current densities (pA/pF) measured with whole-cell voltage-clamp recording on nodose neurons grown for 2-3 weeks with or without various neurotrophins. Significant differences ($p<0.05$, Duncan's multiple-range test) for mean ACh-evoked current densities compared to neurons grown with *NGF, or compared to neurons grown with $^{\#}$NGF+BDNF+NT-3, or compared with neurons grown $^{-}$without neurotrophins. Significant differences ($p<0.001$, t-test) for capsaicin-evoked current densities compared to neurons grown with §NGF. (n in parentheses)

DISCUSSION

Nodose neurons provide sensory innervation to the viscera, including the heart, the lungs, the trachea, the gut, and to the tongue, and thereby participate in autonomic reflex responses, such as a change in blood pressure, heart rate, respiration, or suckling in neonates (Paintal, 1973). The main finding in this chapter is that BDNF and NT-3 influence nodose neurons to retain some of the attributes of sensory neurons, while NGF influences these neurons to acquire new properties more typical of sympathetic neurons.

Neonatal rat nodose neurons grow in culture without addition of exogenous neurotrophins.

An interesting observation in this chapter is that only 40% of P1 rat nodose neurons depend on neurotrophins for survival initially after plating. Furthermore, this neurotrophin-dependence nearly disappears as the neurons grow for an additional 4 days in culture. These results contrast with those obtained with embryonic chick nodose neurons which highly depend on BDNF and, to a lesser extend, on NT-3 for survival (Hofer and Barde, 1988; Lindsay *et al.*, 1985; Vogel and Davies, 1991; Davies, 1994; Fariñas *et al.*, 1994). Furthermore, *trk*B^{TK-} (-/-) and BDNF (-/-) neonatal mutant mice have very small nodose ganglia, suggesting that many of these neurons depend on BDNF for survival (Klein *et al.*, 1993; Ernfors *et al.*, 1994a; Jones *et al.*, 1994). One likely explanation for our results is that P1 rat nodose neurons have developed beyond the period of large-scale cell death that occurs during the development of most peripheral ganglia (Barde, 1989). Consistent with this interpretation is the fact that the number of neurons in the nodose ganglion does not change from newborn to adult rats (Cooper, 1984). Marked changes in neurotrophin dependence during development have been shown in peripheral neurons (Oppenheim, 1991; Birren *et al.*, 1993; Buchman and Davies, 1993; Buj-Bello *et al.*, 1994; Gaese *et al.*, 1994).

Recent evidence have indicated that sensory neurons, as well as CNS neurons, may "feed" themselves with neurotrophins in an autocrine fashion (Ghosh *et al.*, 1994; Acheson *et al.*, 1995). Several studies have shown that sensory neurons express neurotrophins (Schecterson and Bothwell, 1992; Ernfors *et al.*, 1992; Acheson *et al.*, 1995), and Ernfors *et al.* (1992) reported the presence of BDNF mRNA in embryonic rat nodose ganglia. Thus, it is possible that some nodose neurons survived in these cultures by producing their own neurotrophins. If so, such production of neurotrophins was not sufficient to induce the neurons to extend dendrites, express ACh-evoked currents or remain capsaicin-sensitive. Precedent evidence exist for a differential effect of neurotrophin concentration on neuronal survival versus expression of genes involved in neuronal function. For instance, low concentration of NGF (e.g. 2 ng/ml) is sufficient to sustain rat SCG neurons,

although high concentrations of NGF (e.g. 100-200 ng/ml) cause a large increase in Tα1 α-tubulin and tyrosine hydroxylase mRNA (Ma *et al.*, 1992). The fact that P1 rat nodose neurons no longer depend on neurotrophins for survival after 4 days in culture provided us with a good preparation to investigate the distinct roles of neurotrophins on neuronal differentiation.

Capsaicin-sensitive sensory neurons

In this chapter, we used capsaicin as a marker for the sensory neuron phenotype of nodose neurons. The gene coding for the capsaicin receptor has not yet been identified. The capsaicin receptor is linked to a non-selective cation channel and is believed to correspond to a proton sensor that activates at acidic pH (Bevan and Geppetti, 1994). Capsaicin first excites and then functionally desensitizes visceral C-type afferents as well as a substantial proportion (40-50%) of somatic C-type afferents from the DRG; these afferents transmit noxious stimuli, and their activity can result in the sensation of pain (Fitzgeral, 1983; Marsh *et al.*, 1987; Bevan and Geppetti, 1994). Chronic treatment of animals with capsaicin causes a reduction in reaction to noxious chemical stimuli, as well as noxious thermal and mechanical stimuli (Fitzgerald, 1983). This subpopulation of DRG neurons has been shown to depend on NGF for survival during development, and *trk*A (-/-) mutant mice also lose much of their nociception and thermoception (Smeyne *et al.*, 1994). Likewise, Winter *et al.* (1988) showed that the response to capsaicin of cultured adult rat DRG neurons, which no longer depend on NGF for survival (Schwartz *et al.*, 1982), was sustained by NGF. In contrast, we show here that BDNF sustains capsaicin sensitivity on nodose neurons at a time when the neurons no longer depend on BDNF for survival. These results indicate that different neurotrophins can regulate similar functions on distinct populations of neurons depending on their context of development. This could mean that different *trk*s activate similar signalling pathways which lead to the expression of the same gene in different neurons. Such pathway could be related to the one that each *trk* receptor uses to promote neuronal survival, as in this case, NGF is a survival factor for the embryonic DRG neurons that express capsaicin sensitivity, while BDNF is a survival factor of most embryonic nodose neurons. However, it is also possible that

different signalling cascades activated by each *trk* lead to the expression of the same gene in distinct cellular contexts. In any case, it is interesting to consider that both receptors, *trk*A and *trk*B, appear not to mediate the same signals in nodose neurons, whether or not they are co-expressed in the same neurons (see below).

Model

Figure 5.10 describes our working model for the differentiation of nodose neurons in culture in response to satellite cells and neurotrophins, based on our results presented in Chapter 3, 4 and 5. First, the initial polarity that freshly dissociated nodose neurons (*Stage 1*) acquire is determined by the contact with satellite cells (*Stage 2*): 50% of the neurons re-acquire their unipolar morphology when plated with satellite cells, whereas in the absence of satellite cell contact (*Stage 4*), they elongate many axons giving rise to a multipolar morphology. This process is independent of neurotrophins. When the neurons develop in the presence of satellite cells (*Stage 2*), NGF does not induce them to extend dendrites or to express ACh-evoked currents, nor does it promote their capsaicin sensitivity. However, the neurons respond to BDNF (*Stage 3*) by maintaining their capsaicin sensitivity. In summary, in the presence of satellite cells and BDNF, nodose neurons appear to develop as sensory neurons *in vivo*.

When the neurons develop in the absence of satellite cells, they respond to NGF and to BDNF by expressing different properties. In the presence of BDNF (*Stage 5*), they express low density nAChRs, but retain their capsaicin sensitivity. However, with NGF (*Stage 6*), they acquire a fully differentiated dendritic-axonal polarity, express high density of nAChRs, and lose sensitivity to capsaicin: it appears that the neurons have then acquired a phenotype similar to sympathetic neurons.

In the presence of NT-3, the neurons had similar properties to those of neurons grown with BDNF, suggesting that *trk*C mediates mainly the same effects as *trk*B. However, as NT-3 has been shown to activate also *trk*B and *trk*A under some conditions (Cordon Cardo *et al.*, 1991; Ip *et al.*, 1993b; see appendix 1), it is possible that NT-3 mediates its effects through *trk*B (and *trk*A; but see below).

This model needs further discussion. Below I discuss the potential co-expression of

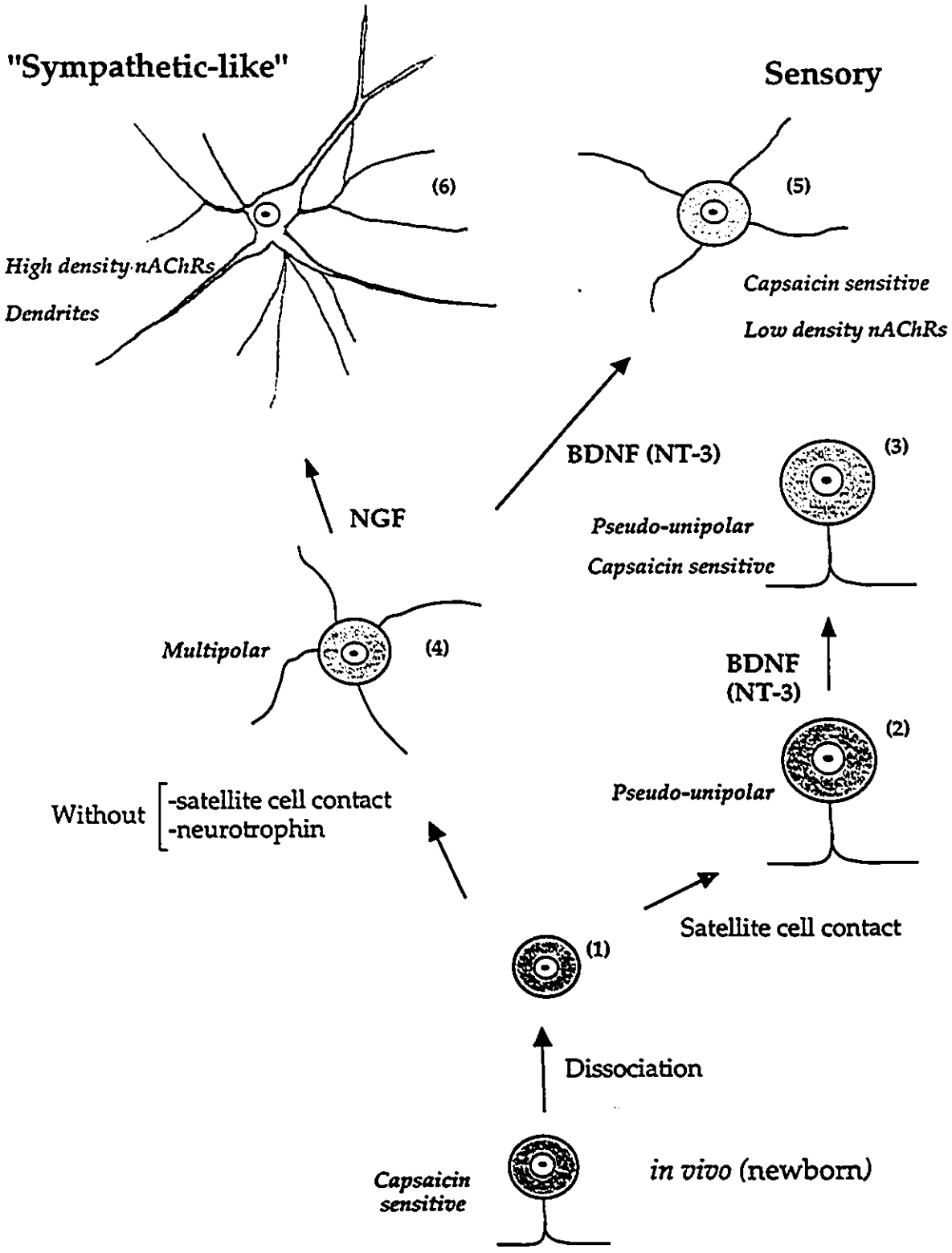

FIGURE 5.10. Model for P1 rat nodose neuron differentiation in culture in response to satellite cells and neurotrophins.

multiple *trk* receptors in nodose neurons and speculate on the possible specificities among *trk*-mediated signals. In addition, I discuss the potential participation of $p75^{LNGFR}$ in these effects. Finally, I address the role of nAChRs on sensory neurons and discuss the possible mechanisms that underlie the increase in ACh-evoked currents on nodose neurons.

Potential co-expression of multiple *trk*s in nodose neurons

An important question concerning our model is whether NGF, BDNF and NT-3 acted on separate populations of neurons each expressing their cognate receptors, or whether many of these neurons co-expressed both *trk*A and *trk*B (or *trk*A and *trk*C or the 3 *trk*s together), which thereby differentially affected nodose neurons' development. As mentioned above, for NT-3, it is possible that its effects were mediated by *trk*B, or even by *trk*A, in the case of the small induction of dendrite outgrowth (Figure 5.6B; appendix 1).

Our quantification of the transcript levels for the various neurotrophin receptors indicates that *trk*B mRNA is expressed at levels 2-3 fold greater than *trk*A and *trk*C. Based on the findings of previous *in situ* hybridization studies on *trk* receptor expression in embryonic rodents (Martin-Zanca *et al.*, 1990; Ernfors *et al.*, 1992; Barbacid, 1994), we were expecting a much greater difference between the amount of *trk*B mRNA and the amount of *trk*A mRNA, as well as more *trk*C than *trk*A. Our results then suggest that the levels of *trk*B and *trk*C have decreased in newborn nodose neurons compared to embryonic nodose neurons; this interpretation is consistent with the fact that many P1 nodose neurons survive in culture in the absence of BDNF and NT-3. Because the majority of embryonic rodent nodose neurons were shown to express *trk*B and *trk*C at high levels (Ernfors *et al.*, 1992; Barbacid, 1994), it is possible that a similar proportion of neurons express those *trk*s by birth, although at lower levels.

*trk*A is believed to be expressed by only a small fraction of nodose neurons in embryonic rodents, based on *in situ* hybridization experiments (Martin-Zanca *et al.*, 1990; Ernfors *et al.*, 1992; Barbacid, 1994); similar observations were made in adult rat nodose neurons (Verge *et al.*, 1992). However, this latter study demonstrated that a large fraction

of the ganglia bound NGF with relatively high-affinity, and similar observations were made on cultured nodose neurons (Mandelzys *et al.*, 1990). High-affinity NGF binding is believed to be optimized by a high ratio of $p75^{LNGFR}$:*trk*A expression (e.g. 10:1; Benedetti *et al.*, 1993; Lee *et al.*, 1994; Chao, 1994; see appendix 1), and we found 10-14 fold more $p75^{LNGFR}$ mRNA than *trk*A mRNA in nodose neurons. Taken together, these findings could be explained by the fact that many nodose neurons express both *trk*A and $p75^{LNGFR}$. Our finding that *trk*A is expressed at higher levels than previously appreciated may be due to the greater sensitivity of the RNase protection assays compared to *in situ* hybridization, or because the expression of *trk*A is higher in neonatal nodose neurons compared to embryonic or adult nodose neurons. In fact, profound developmental changes in neurotrophin receptor expression have been observed in peripheral neurons (Ernfors *et al.*, 1992; Mu *et al.*, 1993; Verdi and Anderson, 1994). A large increase in $p75^{LNGFR}$ has been shown in sympathetic neurons during late embryonic and postnatal development (Verdi and Anderson, 1994), and this increase could, in fact, be due to NGF's action on *trk*A (Ma *et al.*, 1992; Miller *et al.*, 1994; Verdi and Anderson, 1994). If so, the expression of *trk*A in nodose neurons may be essential for the high levels of $p75^{LNGFR}$ transcripts in these neonatal neurons (which would argue that *trk*A was already present in embryonic nodose neurons).

Our preliminary *in situ* hybridization experiments also suggest that a large proportion of nodose neurons express low levels of *trk*A, although we have not yet quantified this proportion precisely. In a given culture, we observed more variability in the intensities of the *trk*A mRNA signals between nodose neurons than between SCG neurons (Figure 5.4) which contained generally strong signals.

Taken together our results and those of others on neurotrophin receptor expression suggest that a significant proportion of nodose neurons co-express multiple *trk*s. Interestingly, McMahon *et al.* (1994) showed that nearly all visceral afferents of adult DRG neurons co-expressed *trk*A and *trk*B. This may indicate that visceral targets provide both BDNF and NGF to their afferent nerves. Another possibility is that NGF is provided by the targets, while BDNF is provided by the neurons themselves (Ernfors *et al.*, 1992;

Schecterson and Bothwell, 1992). We plan to repeat *in situ* hybridization experiments using riboprobes of all *trk*s and $p75^{LNGFR}$ on thin adjacent sections of P1 nodose ganglia to demonstrate more definitively co-expression of different *trk* receptor transcripts in nodose neurons. In addition, when specific *trk* antibodies become available, we will perform immunocytochemistry on these ganglia sections to verify that *trk* receptor proteins are also expressed.

Further evidence for co-expression of *trk*s in some nodose neurons comes from the results obtained in Figure 5.9E and Table 5.1, where the neurons were grown with all 3 neurotrophins. Indeed, under this condition, BDNF (or NT-3) seemed to have interfered with the effects of NGF on nodose neurons: 1) only 16% of the neurons had ACh-evoked currents above 10 pA/pF with all 3 neurotrophins (Figure 5.9E), while with NGF alone (Figure 5.9A), 33% had currents above 10 pA/pF; 2) the mean ACh-evoked currents on neurons grown with all 3 neurotrophins were only 60% of those on neurons grown with NGF alone (Table 5.1). If BDNF (and/or NT-3) and NGF were acting only on two separate populations of neurons, the induction of ACh-evoked currents by NGF should not have been affected by BDNF (and/or NT-3). These results suggest that activation of *trk*A and *trk*B (or *trk*C) can trigger distinct signalling cascades within one neuron, which produce conflicting signals to the neurons with respect to the expression of nAChRs and capsaicin receptors. In this context, it is noteworthy that the extension of dendrites by nodose neurons in this study appeared less extensive in the presence of NGF than that observed in Chapter 3. This difference could be explained by the fact that, in this chapter, we grew the neurons for the first 4 days with all neurotrophins. The presence of BDNF and/or NT-3 initially may have promoted survival of neurons that did not respond to NGF, or alternatively, as BDNF and NT-3 partially inhibited the effects of NGF on ACh-evoked currents (Figure 5.9E; Table 5.1), their presence initially, may have reduced the effects of NGF on dendritic outgrowth.

An alternative explanation can be offered for why fewer neurons expressed high ACh-evoked current densities in the presence of all 3 neurotrophins; this has to do with the possible involvement of $p75^{LNGFR}$ in this process and is discussed below.

Potential mechanisms for specificity among neurotrophin-mediated signals

How can 2 different neurotrophins mediate distinct signals in one neuron? Upon ligand binding, some of the tyrosine residues that are phosphorylated in the intracellular domains of *trk*s have been shown to bind specific SH2 domain-containing enzymes (or adaptor proteins; see appendix 2). Specificity in the binding of these SH2 domains appears to be provided by the structural arrangement of amino acids surrounding both the tyrosine residues on the receptors and the SH2 domain of the enzymes or adaptor proteins that bind to autophosphorylated *trk*s. Differences in the structural arrangement around the tyrosine residues of autophosphorylated *trk*A and *trk*B could link each of these *trk*s to distinct signalling molecules mediating separate functions.

Another difference in the activation of *trk*A and *trk*B in nodose neurons may have to do with the relative amount and/or distribution of each receptor on the surface membrane. The levels of expression of *trk*B transcripts is higher than that of *trk*A in nodose ganglia (Figure 5.3), and BDNF (and/or NT-3) seems to override, in part, the NGF influence on nAChR expression (Figure 5.9E; Table 5.1). It is possible that the intensity of autophosphorylation of a given *trk* mediates distinct signals; as *trk*B dominates, its activation may induce a different intracellular cascade of events than that of *trk*A. By analogy, the activations of *trk*A or the EGF receptor (EGFR) have been shown to cause very distinct effects on PC12 cells: NGF leads to mitotic arrest and neuronal differentiation, while EGF leads to cell proliferation (Greene and Tischler, 1982). However, both processes are believed to involve activation of the *ras*-MAPK pathway (see appendix 2). Recent evidence suggests that the intensity and the time course of activation of this *ras*-MAPK pathway encodes part of the differential effects of NGF and EGF on PC12 cells (Marshall, 1995). For example, PC12 expressing low levels of *trk*A can be induced to proliferate with NGF (Schlessinger and Bar-Sagi, 1995; Marshall, 1995), while PC12 cells over-expressing the EGFR can be induced to undergo neuronal differentiation with EGF (Traverse *et al.*, 1994). In this context, it is also possible that each of the neurotrophins up-regulated expression of their own receptors (Holtzman *et al.*, 1992); in this way, neurotrophins could potentiate their effect. To test this possibility, we plan to extract RNA from these cultures and measure mRNA levels for the various *trk*s under

each condition. Another possibility is that *trk*A and *trk*B are located in distinct surface domains or, once internalized, targeted to distinct intracellular regions, thereby recruiting and/or activating different signalling molecules.

Much remains to be learned about the specific signals that neurotrophin receptors mediate. In fact, we are just beginning to understand some of the specificity between *trk*- and other receptor tyrosine kinase-mediated signals (see appendix 2). Our results provide evidence that different *trk*s do produce distinct signals; more definitive evidence should arise from experiments that combine double labelling *in situ* hybridization with measurements of dendritic outgrowth, ACh- and capsaicin-evoked currents on identified neurons.

The role of $p75^{LNGFR}$

An important player in NGF's action on nodose neurons may be $p75^{LNGFR}$. Although little is known about the potential for $p75^{LNGFR}$ to mediate intracellular signals, there is good evidence that it cooperates with *trk*A for high-affinity NGF binding (Davies *et al.*, 1993; Barker and Shooter 1994; Lee *et al.*, 1994; Chao, 1994) and for signal transduction (Hantzopoulos *et al.*, 1994; Verdi *et al.*, 1994; Chao, 1994). The potentiation by $p75^{LNGFR}$ of high-affinity NGF binding and of *trk*A signalling was observed only when the ratio of $p75^{LNGFR}$:*trk*A was elevated (from 5 to 20 fold; Benedetti *et al.*, 1993; Lee *et al.*, 1994; Verdi *et al.*, 1994; Chao, 1994). In MAH cells, a neuronal progenitor cell line, *trk*A was transfected alone or with $p75^{LNGFR}$ at a ratio of 1:10-20 (*trk*A:$p75^{LNGFR}$; Verdi *et al.*, 1994). In $p75^{LNGFR}$ expressing cells, a 5 min NGF (50 ng/ml) treatment caused an 8 fold larger *trk*A autophosphorylation compared to cells expressing *trk*A alone. We find a $p75^{LNGFR}$:*trk*A ratio of 10-14 in nodose neurons (Figure 5.3). Therefore, it is possible that $p75^{LNGFR}$ potentiated NGF's action on nodose neurons in culture. Likewise, $p75^{LNGFR}$ may have potentiated BDNF and/or NT-3 effects on nodose neurons as well (Wright *et al.*, 1992; Hantzopoulos *et al.*, 1994); however, the relationship between $p75^{LNGFR}$ and *trk*A appears thus far more prevalent in neurons than between $p75^{LNGFR}$ and *trk*B or *trk*C (Chao, 1994). For instance, mutant mice lacking $p75^{LNGFR}$ show neuropathies in sensory neurons co-expressing *trk*A, but not in neurons co-expressing *trk*B or *trk*C (Lee *et al.*, 1992;

Crowley *et al.*, 1994). Trigeminal neurons from these mice require larger concentrations of NGF to survive in culture, but not BDNF nor NT-3 (Davies *et al.*, 1993).

In addition, $p75^{LNGFR}$ may promote specificity for activation of *trk*A by NGF. NT-3 has been shown to bind and activate *trk*A in cells expressing low levels of $p75^{LNGFR}$ (Cordon Cardo *et al.*, 1991; Ip *et al.*, 1993b), but Benedetti *et al.* (1993) demonstrated a dose dependent decrease in NT-3's ability to bind to *trk*A when $p75^{LNGFR}$ expression was increased in PC12 cells. If high levels of $p75^{LNGFR}$ favour selectivity, this could explain why NT-3 poorly mimicked NGF's action on nodose neurons. It is unknown, however whether NT-3 can bind to *trk*B in the presence of high levels of $p75^{LNGFR}$. We observed a similar effect on nodose neurons' capsaicin sensitivity by NT-3 and BDNF. If $p75^{LNGFR}$ also prevents NT-3 from activating *trk*B, our results would suggest that it is *trk*C that mediated the effect of NT-3 on nodose neurons.

It has been proposed that $p75^{LNGFR}$ promotes *trk*A autophosphorylation by favouring binding of NGF to *trk*A, through a phenomenon of local concentration of NGF (Barker and Shooter, 1994). Due to its rapid association and dissociation kinetics, combined with the fact that $p75^{LNGFR}$ is expressed in excess compared to *trk*A in neurons co-expressing these receptors, one role of $p75^{LNGFR}$ would be to concentrate NGF near *trk*A or to present NGF to *trk*A (Barker and Shooter, 1994). If so, adding, for example, BDNF and NGF together on neurons could lead to a screening effect by BDNF on the binding of NGF to $p75^{LNGFR}$. In this way, the addition of all 3 neurotrophins in Figure 5.9E could have reduced the action of NGF on *trk*A and thereby reduce its induction effects on the ACh-evoked currents. However, if such mechanism exists, it would imply that it is specific for the action of NGF on *trk*A, as the effects of BDNF as well as NT-3 on capsaicin sensitivity were not reduced by addition of all 3 neurotrophins together.

To determine further the role of $p75^{LNGFR}$ in neurotrophin's action on nodose neurons, we plan to repeat these experiments in the presence of an antibody to $p75^{LNGFR}$ that blocks neurotrophin binding to $p75^{LNGFR}$ (Barker and Shooter, 1994). In addition, we plan to test the effects of a mutated NGF molecule that binds and activates *trk*A, without being able to bind $p75^{LNGFR}$ (Barker and Shooter, 1994), to determine whether $p75^{LNGFR}$ is essential for NGF's action on nodose neurons.

nAChRs on sensory neurons

We find a good correlation between the extent of dendritic outgrowth and the density of functional nAChRs (i.e. most neurons with ACh-evoked current densities above 10 pA/pF have dendrites). In addition, nearly all neurons that had ACh-evoked current densities above 10 pA/pF were insensitive to capsaicin, indicating indirectly that nodose neurons with dendrites had no capsaicin receptors. Those neurons then resemble sympathetic neurons which extend dendrites, have ACh-evoked current densities above 10 pA/pF and are insensitive to capsaicin. However, approximately 30-40% of freshly dissociated P1 and P14 nodose neurons express small ACh-evoked currents (generally below 10 pA/pF; Mandelzys and Cooper, 1992), which were, for the most part, previously undetected by current clamp recordings with sharp microelectrodes (Mandelzys *et al.*, 1990). Figure 5.9 shows that in the presence of BDNF and/or NT-3, several neurons had both capsaicin-evoked currents as well as ACh-evoked current densities below 10 pA/pF. Chick DRG neurons have also been shown to express nAChR transcripts (Boyd *et al.*, 1991). As mammalian sensory neurons do not receive synaptic inputs onto their cell bodies (Lieberman, 1976), the putative role of these nAChRs in sensory function is more likely to be at the nerve terminals. The presence of nAChRs on sensory endings has been known for quite some times, but their role is yet unknown (see Diamond, 1955, 1959; Gray, 1959; Paintal, 1964). Electrophysiological recordings and immunohistochemical studies in the CNS support a presynaptic role for nAChRs (Esplin *et al.*, 1972; Rowell *et al.*, 1987; Swanson *et al.*, 1987; Mulle *et al.*, 1991). In fact, the terminal field of nodose afferents in the CNS, the nucleus tractus solitarius (Sumal *et al.*, 1983), shows immunoreactive signals for nAChRs (Swanson *et al.*, 1987). The functional role of nAChRs on sensory neuron nerve terminals may be to regulate axonal outgrowth and pathfinding or to modulate transmitter release from the terminals in the CNS (Diamond, 1959; Chesselet, 1984; Swanson *et al.*, 1987; Nordberg *et al.*, 1989).

If nAChRs are expressed in sensory neurons terminals, why do we detect ACh-evoked currents on their somata? Presumably, the targeting of the receptors is not strict and/or partially altered when the neurons are removed from their normal environment and allowed to develop in culture. If targeting of nAChRs is not precisely regulated, a low

density of receptors on the soma may be insignificant, while their accumulation in the small terminals may contribute to relevant presynaptic function and/or neurite outgrowth. If nAChRs expression in the terminals is indeed important for sensory function, this may explain why BDNF and NT-3 promote low density of functional nAChRs on these neurons (Figure 5.9; Table 5.1).

What induces high-density nAChRs on somatodendritic domains of nodose neurons?

The possibility that nodose neurons express nAChRs *in vivo* raises the question as to whether the large ACh-evoked currents induced by NGF are due to an increased expression of nAChR genes, or merely due to a change in nAChR targeting when the neurons undergo a change to dendritic-axonal polarities. Conceivably, more nAChR transcripts may not be needed to account for this NGF-mediated increase in functional nAChRs; the shipment of nAChRs to the terminals may be altered by the change in neuronal polarity causing more receptors to target to the somatodendritic domains. However, it is unclear whether such change in receptor targeting could account for the change in receptor density observed on the somatodendritic domains of the neurons, as their surface area should be larger than that of the neurons' nerve terminals.

Another possibility, not exclusive of the first one, is that the extension of dendrites, promoted by NGF, imposes on the neurons an increased expression of nAChR genes. In this manner, NGF may not *per se* regulate nAChR gene expression, but cause an indirect increase due to its effects on dendritic outgrowth. The fact that NGF does not induce more ACh-evoked currents on the somata of nodose neurons developing with their ganglionic satellite cells (i.e. when they are unipolar) is consistent with a link between the expression of ACh-evoked currents on the neurons' somata and nodose neuron polarity. In fact, the removal of satellite cells, which disrupts nodose neurons unipolar morphology, causes *per se* (in the absence of neurotrophins) a small increase in the proportion of neurons with ACh-evoked currents on their cell bodies (Mandelzys and Cooper, 1992).

If, on the other hand, NGF regulates directly the expression of nAChR genes on nodose neurons, this would imply that the ganglionic satellite cells repress this regulation. Satellite cells may regulate the expression of a "silencer factor" that negatively controls

nAChR gene expression. Alternatively, satellite cells may partially repress *trk*A expression on nodose neurons, so that upon their removal in culture, *trk*A expression increases and allows NGF to promote dendrites and nAChR expression on nodose neurons.

It is also conceivable that NGF regulates some post-translational modifications on nAChRs and thereby increases their gated currents or turns on pre-existing non-functional receptors (as it has been proposed for nAChRs on chick ciliary neurons via a cAMP-dependent mechanism: Margiotta *et al.*, 1987b). However, given the time course of the NGF effect (e.g. days; Mandelzys *et al.*, 1990; Mandelzys and Cooper, 1992) such mechanisms appear less likely.

Finally, another potential inducer of nAChR expression in these cultures is neuronal activity: in the absence of satellite cells and presence of NGF, functional synapses form between these neurons after 2-3 weeks. We did not investigate whether synapses formed in the presence of other neurotrophins: if synapse formation were to be induced preferentially by NGF, the increase in neuronal activity could potentially up-regulate nAChR expression.

Chapter 6

Differential Regulation of Neuronal Nicotinic ACh Receptor Subunit Genes in Cultured Neonatal Rat Sympathetic Neurons: Specific Induction of α_7 by Membrane Depolarization through a Ca^{2+}/Calmodulin-Dependent Kinase Pathway

INTRODUCTION

As nodose neurons acquire their new dendritic-axonal polarity, they increase the density of functional nAChRs on their surface. In Chapter 5 we discussed a number of possibilities of how this increase in functional nAChR density may be controlled on nodose neurons. To investigate these various possibilities one approach is to examine how nAChR gene expression changes in these neurons as they extend dendrites in culture.

However, before undertaking this type of study, we realized that it would be initially more advantageous to conduct these experiments on rat SCG neurons for the following reasons: 1) all SCG neurons express large ACh-evoked currents (Mandelzys and Cooper 1992) and 2) extend dendrites *in vivo* and in culture (Higgins *et al.*, 1991); 3) the nAChR genes expressed in SCG neurons have been identified (Mandelzys *et al.*, 1994). Moreover, 4) the SCG is a large peripheral ganglion that contains 6-8 fold more neurons than the nodose ganglion, and therefore provides more material for RNA measurements.

Interestingly, the ACh-evoked current densities on neonatal SCG neurons *in vivo* also increase (Mandelzys *et al.*, 1994) at a time when the neurons extend dendrites (Rubin, 1985a; Smolen and Beaston-Wimmer, 1986; Voyvodic, 1987), however, it is unknown what regulates nAChR gene expression in these neurons. Conceivably, the mechanisms that regulate nAChR gene expression in SCG neurons during development and establishment of polarity also control nAChR gene expression in nodose neurons extending dendrites in culture.

Therefore, to learn more about the regulation of nAChR gene expression on neurons, our first approach was to measure transcript levels of nAChR subunits in neonatal SCG

developing in culture.

SCG neurons express 5 nAChR genes: α_3, α_5, α_7, β_2 and β_4. As discussed in Chapter 1, autonomic neurons contain two types of nAChRs, one that incorporates α_3, β_4 and perhaps β_2 and/or α_5 (Vernallis *et al.*, 1993; Mandelzys *et al.*, 1995; McGehee and Role, 1995), and one that incorporates the α_7 subunit and that binds α-BTX (the α-BTX-nAChR; Schoepfer *et al.*, 1990; Couturier *et al.*, 1990b; Séguéla *et al.*, 1993). The expression of nAChR transcripts has been investigated over the first two weeks of postnatal development in rat SCG neurons (Mandelzys *et al.*, 1994), a period when these neurons extend dendrites as well as receive synaptic inputs (Smolen and Raisman, 1980; Schafer *et al.*, 1983; Rubin, 1985b). Mandelzys *et al.* (1994) found that α_3 and α_7 transcripts increased several fold over this period of development, while the two ß subunit transcripts and the α5 transcript showed little changed. In parallel to this differential change in nAChR transcript levels, the ACh-evoked current densities increased significantly. Interestingly, this developmental increase in ACh-evoked currents as well as the increase in dendrite outgrowth on SCG neurons were both found to be independent on presynaptic innervation (Voyvodic, 1987; Mandelzys *et al.*, 1994). Furthermore, in denervated SCG neurons, the developmental pattern of nAChR subunit gene expression occurred as in control neurons, with the exception of α_7, for which much of the developmental increase was prevented. As the α_7 gene codes for a protein that incorporates into an α-BTX-nAChR, these results suggest that each type of nAChRs on SCG neurons is regulated differently.

The α-BTX-nAChR is abundant on rat SCG neurons (Fumagalli *et al.*, 1976), but its function is poorly understood (Clarke, 1992). However recent studies have suggested that α-BTX-nAChRs promote Ca^{2+} influx and thereby influence various Ca^{2+}-mediated processes possibly linked to synapse formation or synaptic transmission (Vijayaraghavan *et al.*, 1992; Séguéla *et al.*, 1993; Pugh and Berg, 1994; Castro and Albuquerque, 1995).

To learn more about the factors that control the differential changes in nAChR transcript levels during sympathetic neuron development, we measured the levels of each nAChR subunit transcript present in these neurons as they develop in culture under

various conditions. In this chapter, we have focused primarily on the relationship between neuronal activity and nAChR expression. In addition, we have examined the role of Ca^{2+}-linked protein kinases in nAChR expression since related studies done on skeletal muscle have demonstrated that activity causes changes in nAChR gene expression as a consequence of Ca^{2+} influx and the activation of PKA in rat (Waike *et al.*, 1994) or PKC in chick (Klarsfeld *et al.*, 1989). However little is known about the role of activity on neurotransmitter receptor gene expression.

Finally, as a first approach in understanding what causes the increase in ACh-evoked currents on cultured nodose neurons, we have determined which nAChR transcripts are expressed by P1 rat nodose neurons *in vivo* and compared levels to those of P1 SCG neurons.

EXPERIMENTAL PROCEDURES

Neuronal Cultures

SCG ganglia were dissected from newborn rats, dissociated and cultured as described in section 2.1. The cultures were treated for the first 2-3 days with Ara-C to eliminate the few remaining non-neuronal cells. For explant cultures, we cut the ganglia in half and plated one half-ganglion per petri dish; no Ara-C was added.

Treatment of cultures. To depolarize the neurons, we mixed a stock solution of 350 mM KCl in a 1:9 ratio with growth medium, which already contains 5 mM KCl. Many of the agents that were added to our cultures were first dissolved in dimethyl sulfoxide (DMSO) or ethanol, which typically amounted to 0.1% of the culture media. Treating neurons for 48 hrs with any of the drugs listed below, with 0.1% DMSO or with an additional 35 mM KCl had no effect on neuronal survival, as measured by cell counts, or on the morphological appearance of the neurons, as judged by observing the cultures with phase contrast microscopy. Nifedipine, verapamil and KN-62 had no effect on the nAChR mRNA levels when added to control cultures (data not shown). We used the following agents: 50 µg/ml α-amanitin (stock: 1 mg/ml in H_2O), 5 µM nifedipine (stock: 10 mM in DMSO), 5 µM verapamil (stock: 20 mM in ethanol), 10-50 µM nicotine (hydrogen tartrate

salt, stock: 250 mM in H_2O), 10-100 µM carbachol (Cl salt, stock: 1 M in H_2O), 1-5 mM choline (Cl salt, stock: 1 M in H_2O), 100 mM hexamethonium (Cl salt, stock: 10 M in H_2O), 100-200 nM α-BTX (stock: 125 µM in H_2O) and 2 µM atropine (sulfate salt, stock: 1 mM in H_2O), all from Sigma; 0.5-10 µM KN-62 (stock: 20 mM in DMSO), 1-20 µM chelerythrin (stock: 10 mM in DMSO), 1-10 µM H-89 (stock: 10 mM in DMSO), 1-100 µM genistein (stock: 100 mM in DMSO), 100-300 nM PMA (stock: 300 µM in DMSO) and 1-10 µM forskolin (stock: 10 mM in DMSO), all from Biomol.

RNA extraction

The RNA was extracted from freshly dissociated neurons and from neurons that had grown from 1 to 7 days in cultures (occasionally 14 and 21 day old cultures), according to the method described in section **2.4.1.**.

RNase protection assays

RNase protection assays and riboprobe syntheses were performed as described in section **2.4.3.**. Antisense riboprobes for nAChR subunits and GAPDH were synthesized as described in section **2.4.2.** For each hybridization reaction, 0.5 µg of total cellular RNA was combined with 2 or 3 radiolabelled probes of 200,000 cpm each. Dried gels were first exposed to a phosphor imaging plate to quantify the radioactive bands and subsequently to X-ray film for 48-72 hrs. The specific activity of each riboprobe was calculated from the number of adenine bases in the protected region. To quantify the levels of mRNA among different transcripts, the relative intensities of the hybridization signals were divided by the specific activity of the corresponding riboprobe. For each culture, every RNA sample was tested in duplicate or triplicate. mRNA levels for all nAChR subunits were similar between whole ganglia and dissociated neurons (centrifuged through percoll), as the contribution of the non-neuronal cells in total ganglionic RNA from P1 rat SCG is less than 10 % (Mandelzys *et al.*, 1994). To estimate the number of nAChR transcripts expressed per neuron, we synthesized sense RNA for α_3 and β_2 and measured their OD_{260}. By comparing hybridization signals from known amounts of sense α_3 and β_2 RNA (e.g. 0.1, 0.5, 1, 2, 5, 10 pg) and hybridization signals from 0.5 µg of SCG RNA (≈6000

neurons: see section 2.4.1.), we estimated that an SCG neuron (average size = 30 μm in diameter) cultured for 7 days has on average 1000-1500 $ß_2$ transcripts and 5000-7000 α_3 transcripts. In some experiments, we normalized nAChR subunit hybridization signals with those for GAPDH to control for RNA loading. However, as both ß subunit transcript levels showed little change in culture and with any treatment, they also served as internal controls in many experiments. As shown previously for SCG neurons *in vivo*, transcripts for α_2, α_4 and $ß_3$ nAChR subunits were not detected in SCG neurons developing in culture (data not shown: see Mandelzys *et al.*, 1994).

In situ hybridization

The same [^{32}p]-labelled probes prepared for the RNase protection assays were used to perform the *in situ* hybridization on 2 week old cultures, as described in section 2.4.4..

Immunocytochemistry

Neurons cultured for 2-3 weeks were fixed and immunostained for MAP2 (HM-2 antibody) as described in section 2.2.1

α-BTX binding

Neurons were plated at 15 000-20 000 neurons/3 cm^2 aclar coverslip. At day 5, sister cultures were treated with 40 mM KCl. At day 7, α-BTX binding was performed as described in section 2.2.4.. In each experiment (n=3) 4 dishes per condition were used.

RESULTS

Expression of nAChR transcripts in cultured SCG neurons

P1 SCG neurons express 5 nAChR transcripts: the most abundant transcript is $ß_4$, followed by α_3 and α_7; $ß_2$ is expressed at approximately one third of $ß_4$, while α_5 is expressed at the lowest levels (i.e. 1/5 of α_3; see Figure 6.1 and Mandelzys *et al.*, 1994). Over the first two postnatal weeks, SCG neurons undergo a significant change in the expression of these transcripts: mRNA levels for α_3 increase nearly 4 fold, and levels for

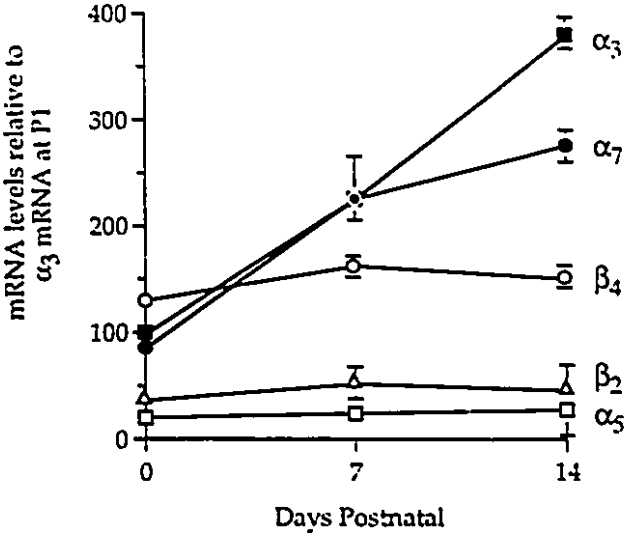

FIGURE 6.1. Developmental expression of nAChR subunit transcripts in neonatal rat SCG neurons *in vivo*.

Transcript levels of the 5 nAChR transcripts expressed in SCG neurons measured by RNase protection assays. The mRNA levels were normalized for the levels of α_3 (=100%). Adapted from Mandelzys, 1992.

α_7 increase 3 fold, whereas those for α_5, β_2 and β_4 show little change (see Figure 6.1 and Mandelzys *et al.*, 1994). The factors responsible for this differential expression of nAChR transcripts are unknown. To learn more, we have investigated nAChR expression by neonatal SCG neurons developing in dissociated cell cultures in the absence of satellite cells (Figure 6.2A). Figure 6.2B shows that SCG neurons developing in culture express 4 nAChR transcripts at levels similar to neurons developing *in vivo* (cf. Figure 6.1): mRNA levels for α_3 increase 2-3 fold over 7 days in culture, and levels of α_5, β_2 and β_4 remain essentially constant. These results suggest that the mechanisms that regulate gene expression of those 4 nAChR subunits in SCG neurons *in vivo* act similarly in cultured SCG neurons. However, the expression of α_7 is different: unlike the increase in mRNA levels during development *in vivo*, the α_7 mRNA levels in SCG neurons in culture decrease 3 fold within 2 days, and remain low for at least 3 weeks.

To test whether dissociation and removal of satellite cells affected nAChR transcript levels, we prepared explant cultures and extracted RNA from these cultures. We observed a similar differential change in nAChR mRNA levels with explant cultures, suggesting that the regulation of nAChR subunit expression is not influenced by SCG ganglionic satellite cells, and that the decrease in α_7 mRNA levels in these neurons is not a consequence of removing the non-neuronal cells.

To investigate whether the drop in α_7 mRNA level was a result of decreased stability of α_7 mRNA, we blocked mRNA synthesis by treating cultures at day 0 or at day 1 for 24 hrs with α-amanitin (50 μM), a transcription inhibitor. We found no significant difference in the rate of decrease in α_7 mRNA levels between control- and α-amanitin-treated cultures 24 hrs later, suggesting that the decreased α_7 mRNA levels reflect a reduction in α_7 mRNA synthesis and not an accelerated α_7 mRNA degradation (Figure 6.1C). In addition, we found that α_3 mRNA levels in α-amanitin-treated cultures decreased at a rate similar to that of α_7 mRNA (data not shown), suggesting that both transcripts have comparable stabilities.

Homogenous expression of nAChR transcripts

To determine whether all neonatal rat SCG neurons express nAChR transcripts, we

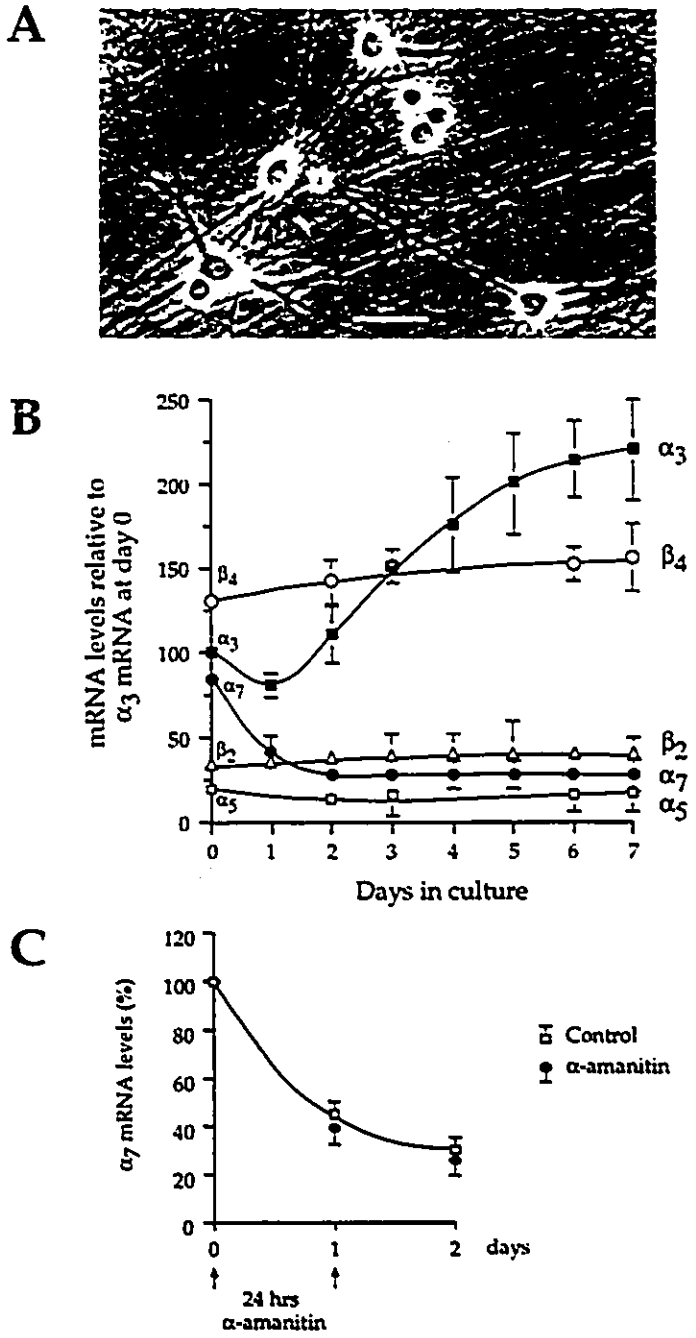

FIGURE 6.2. Developmental expression of nAChR transcripts by neonatal SCG neurons in culture.

(A) Phase contrast photomicrograph of SCG neurons that have developed in culture for 1 week. The horizontal bar is 60 μm. (B) Relative mRNA levels for the five nAChR subunits expressed in freshly dissociated rat SCG neurons (day 0) and over the first 7 days in culture. The mRNA levels for each subunit were measured by RNAse protection assays, quantified with a phosphor imager and expressed relative to the levels of α_3 subunit mRNA at day 0 (=100%). The measured α_3 transcript levels correspond approximately to 2000-3000 copies per neuron (see experimental procedures). Examples of the hybridization signals for the five nAChR subunits are shown in Figure 6.2A and 6.2C at day 0, 3 and 7. Each value represent an average of 4-6 cultures (±SEM). (C) Decay of mRNA levels for α_7 subunit in control and α-amanitin-treated cultures. α-amanitin (50 μM) was added for 24 hrs either at day 0 or at day 1. Values represent means (±SEM) of 4 cultures.

FIGURE 6.3. Homogenous expression of nAChRs in SCG neurons.

In situ hybridization with [^{32}P]-labelled antisense α_3 and β_4 subunit antisense riboprobes in SCG neurons cultured for 2 weeks. The same riboprobes as those used for the RNase protection assays were used for the *in situ* hybridization. Left hand panels (A, C, E, G): Phase contrast photomicrographs of fixed SCG neurons. Right panels (B, D, F, H): Dark field photomicrographs of the same fields as in the left hand panels. (B) shows the grain signals for antisense α_3 riboprobe. (D) shows the grain signals for antisense β_4 riboprobe. (F) High magnification of a neuron incubated with antisense α_3; this photograph shows the grains are restricted to neuronal somata and absent from dendrites (arrows). (H) shows a control pre-treated with RNase T1 and incubated with antisense radiolabelled α_3 riboprobe. Other controls, such as sense α_3 and β_4 radiolabelled riboprobes gave similar results as in H. Most if not all neurons had signals for α_3 and β_4 transcripts.

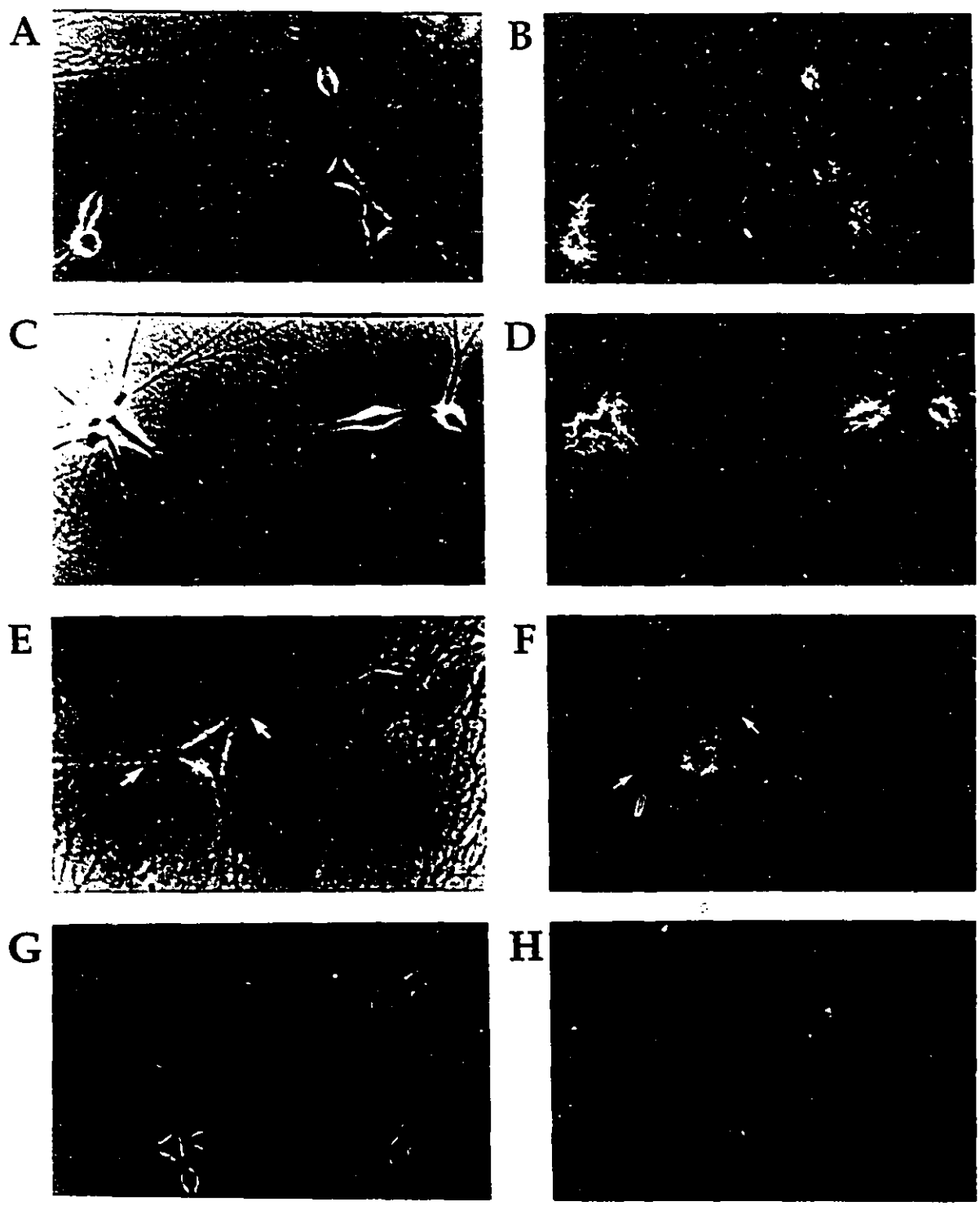
A
B
C
D
E
F
G
H

performed *in situ* hybridization on the cultured neurons. We used antisense [^{32}P]-labelled riboprobes for α_3 and β_4 subunits, which are believed to incorporate in the synaptic nAChRs (Vernallis *et al.*, 1993; Mandelzys *et al.*, 1995). Figure 6.3 shows an example of such an experiment. The results indicate that all neurons in the cultures express both α_3 and β_4 transcripts. Figure 6.3H shows a high power photomicrograph which demonstrates that the grains are restricted to neuronal somata. These results indicate that with respect to α_3 and β_4, the expression of nAChRs is homogenous in rat SCG; conceivably, the other subunit transcripts are also expressed by every neuron.

Membrane depolarization results in specific up-regulation of α_7 mRNA

The specific decrease in α_7 transcript levels in cultured SCG neurons is intriguing; *in vivo* the α_7 mRNA levels increase postnatally, and denervation experiments have indicated that much of this increase is regulated by pre-ganglionic innervation (Mandelzys *et al.*, 1994). One consequence of placing neonatal neurons in culture is that initially they have a reduced electrical activity, in part, because the neurons are denervated. To test whether membrane depolarization plays a role in the expression of nAChR subunits, we added 40 mM KCl to sister cultures (high K^+). Exposing the neurons to high K^+ at the time of plating had little effect on mRNA levels for α_5, β_2 or β_4 (Figure 6.4A) 48-72 hrs later. After 3 days, mRNA levels for α_3 were only 1.3 (±0.1) fold greater in high K^+-treated neurons compared to control neurons. However, high K^+ produced a significant change in α_7 mRNA levels: unlike in control neurons, α_7 mRNA levels remained at their initial value for several days in high K^+-treated neurons (Figure 6.4A, 6.4B). High K^+ appears to increase α_7 mRNA synthesis because addition of 50 µM α-amanitin to both control and high K^+ cultures resulted in similar decay rates for α_7 mRNA levels (data not shown); this suggests that high K^+ does not increase α_7 mRNA levels by affecting α_7 mRNA stability. Furthermore, by delaying the addition of high K^+ to day 5, we observed a 2-3 fold increase in α_7 transcripts, which reached 70% of its plateau value in 24 hrs and 100% by 48 hrs (Figure 6.4C). High K^+ added at day 5 caused little change in transcript levels of the other nAChR subunits, including α_3, indicating that the effects of membrane

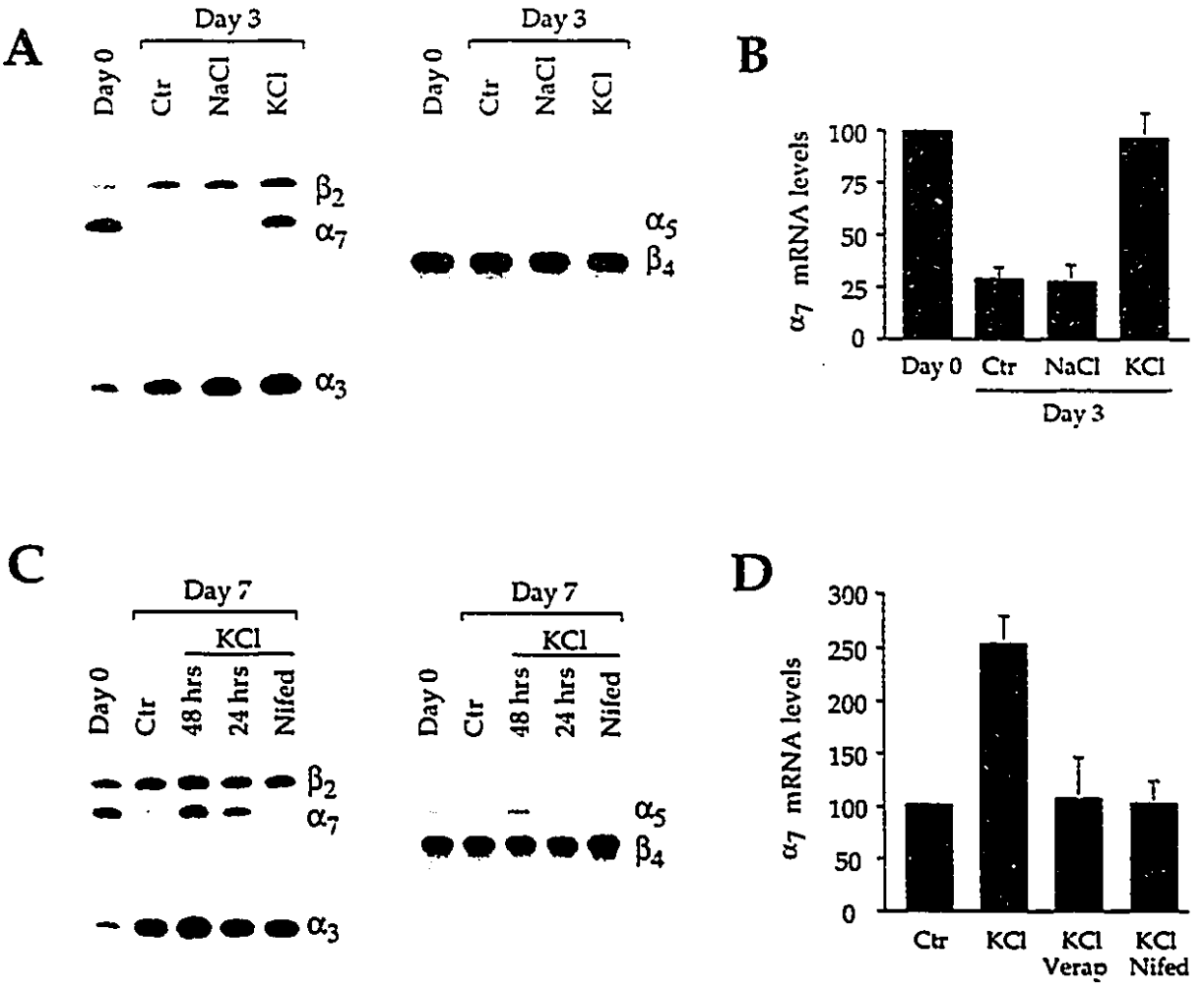

FIGURE 6.4. Membrane depolarization and Ca^{2+} influx induce α_7 gene expression.
(A) RNase protection assays for α_3, α_7, β_2 (left), α_5 and β_4 (right) nAChR subunit mRNAs. The protected riboprobe base pair sizes are: β_2= 571, α_7= 467, α_3= 258, α_5= 479, and β_4= 411. In both gels, the first lane (Day 0) is total cellular RNA from freshly dissociated SCG. RNA from neurons grown for 3 days in control medium (2nd lane; Ctr), with additional 35 mM NaCl (3rd lane; NaCl), as a control for osmolarity change, or with additional 35 mM KCl (3rd lane; KCl) to depolarize the neurons. α_7 mRNA levels drop in culture, but are sustained in high K^+. α_5, β_2 and β_4 mRNA levels change little in culture and are not affected by high K^+. α_3 mRNA levels increase in culture and are 1.3 ± 0.1 greater in high K^+. (B) Means (±SEM) of mRNA levels for α_7 subunit relative to Day 0 (=100%); n=3 cultures. (C) RNase protection assays, as in (A), for RNA extracted from freshly dissociated neurons (Day 0) or neurons that have been cultured for 7 days in control medium (Ctr), with additional 35 mM KCl for 24 hrs (added at day 6) or for 48 hrs (added at day 5), or for 48 hrs with both KCl and 5 µM nifedipine, an L-type Ca^{2+} channel blocker. High K^+ induces α_7 expression after its drop in culture; nifedipine blocks this high K^+ induction, but has no effect on other nAChR transcripts (see also Table 6.1). (D) Means (±SEM) of mRNA levels for α_7 subunit relative to Day 7 control (=100%); n=6 cultures. In some experiments, L-type Ca^{2+} channel blocker verapamil (5 µM) was added with high K^+ (n=3). Each reaction, in this figure and in figure 6.3, 6.4 and 6.6, contained 0.5 µg of total cellular RNA and 200 000 cpm for each riboprobe.

depolarization are specific for α_7 (Figure 6.4C and Table 6.1).

The role of Ca^{2+} influx

Several studies have shown that sustained membrane depolarization, produced by high K^+, induces the expression of many genes by increasing Ca^{2+} influx through 1,4-dihydropyridine (DHP)-sensitive L-type Ca^{2+} channels (Murphy *et al.*, 1991; Bading *et al.*, 1993; Rosen *et al.*, 1994; Bessho *et al.*, 1994). To test whether this is the case for α_7 gene expression, we added L-type Ca^{2+} channel blockers verapamil (5 μM) or DHP-antagonist, nifedipine (5 μM) to cultures treated with high K^+ from day 5 to day 7. Figure 6.4C and 4d show that both nifedipine and verapamil specifically block the increase in α_7 mRNA levels while having no effect on other nAChR transcript levels (see also Table 6.1). These data indicate that Ca^{2+} influx through L-type Ca^{2+} channels is necessary for the induction of α_7 gene expression by membrane depolarization.

The effects of protein kinase activity on nAChR subunit expression

Next, we investigated whether the induction of α_7 gene expression by Ca^{2+} influx is mediated by the activity of a protein kinase. To test if PKA is involved, we either treated control and high K^+ cultures at day 5 with forskolin (10-50 μM) for 48 hrs to activate PKA, or treated high K^+ cultures with H-89 (1-10 μM) to inhibit PKA. Neither treatments had any effect on α_7 transcript levels (Figure 6.5). To determine if PKC is involved, we either treated control and high K^+ cultures at day 5 with phorbol-12-myristate-13-acetate (PMA; 100-300 nM) for 48 hrs to activate PKC, or treated high K^+ cultures with chelerythrin (1-20 μM) to inhibit PKC. Similarly, neither the activation nor the inhibition of PKC had any effect on α_7 transcript levels (Figure 6.5). To test for tyrosine kinase involvement, we increased the concentration of NGF 4 fold in both control and high K^+ cultures (from 25 ng/ml to 100 ng/ml), in attempt to increase signalling through *trk*A (Ma *et al.*, 1992). This treatment did not affect any of the nAChR transcript levels (Table 6.2).

In addition, we treated SCG neurons with tyrosine kinase inhibitors; neonatal SCG neurons depend on *trk* tyrosine kinase activity for survival, and treating cultures with

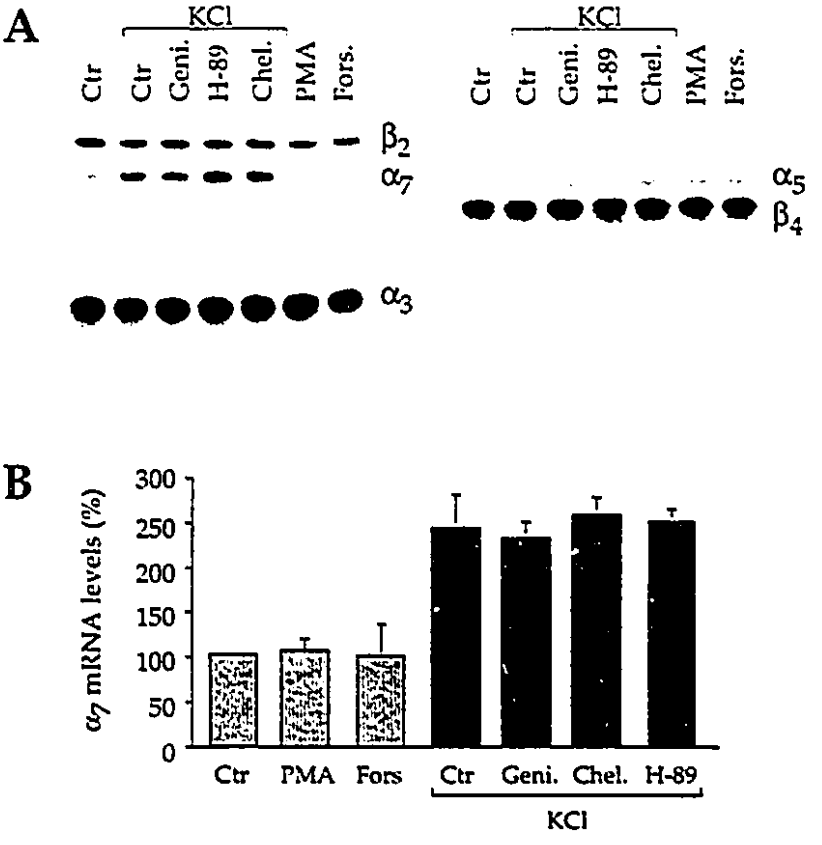

FIGURE 6.5. PKA, PKC and tyrosine kinase do not regulate nAChR subunit expression.
(A) RNase protection assays performed as in Figure 6.2 on RNA extracted from SCG neurons cultured for 7 days in control medium (Ctr), or treated at day 5 with PKC activator PMA (100 nM), PKA activator forskolin (10 μM), or with 40 mM KCl with either 0.1% DMSO (Ctr), tyrosine kinase inhibitor genistein (10 μM), PKA inhibitor H-89 (2 μM) or PKC inhibitor chelerythrin (2 μM). In addition, PMA, forskolin and NGF were added to some high K^+ cultures (not shown). None of these agents affected nAChR subunit expression (see also Tables 1 and 2).
(B) Mean (±SEM) mRNA levels for α_7 subunit relative to control (=100%); n=3 cultures. Higher doses of these agents were also tested: genistein, 100μM; H-89, 10μM; chelerythrin, 20μM; PMA, 300 nM; forskolin 30 μM; no significant differences on the nAChR subunit mRNA levels were observed at these doses (n=2).

tyrosine kinase inhibitors caused the neurons to die within 48 hrs. However, in the presence of high K^+, SCG neurons can survive for 48 hrs without *trk* activity due to the increase in $[Ca^{2+}]_i$ caused by the openings of L-type Ca^{2+} channels (Koike *et al.*, 1989; Franklin and Johnson, 1992; Franklin *et al.*, 1995). Therefore, we treated high K^+ cultures with tyrosine kinase inhibitor genistein (10-100 μM); this had no effect on the increase in α_7 transcripts or on the levels of other nAChR transcripts (Figure 6.5). We also treated high K^+ cultures with K-252a, a kinase inhibitor that inhibits *trk* activity specifically at low concentrations (10-100 nM; Koizumi *et al.*, 1988; Berg *et al.*, 1992); 100 nM K-252a had little effect on nAChR transcript levels (Table 6.2).

These results suggest that neither PKA, PKC nor tyrosine kinases are involved in the Ca^{2+} signalling cascade that affects α_7 gene expression. Furthermore, Table 6.1 and 6.2 show that the activities of these 3 classes of protein kinases appear not to be involved in the regulation of any nAChR transcript expressed by SCG neurons developing in culture.

However, we did observe that a 10 fold higher dose of K-252a as well as KT-5926 (1 μM) partially blocked the α_7 induction by high K^+ (Table 6.1); these agents inhibit a number of protein kinases at such concentration, including the multifunctional Ca^{2+}/calmodulin-dependent protein kinase II (CaM kinase II or CaM kinase) (Hashimoto *et al.*, 1991).

CaM kinase activity up-regulates α_7 gene expression

To test whether CaM kinase activity is involved in the induction of α_7 gene expression by membrane depolarization, we treated control and high K^+ cultures with KN-62, a specific CaM kinase inhibitor (Tokumistu *et al.*, 1990). In control cultures, KN-62 (10μM) for 48 hrs had no effect on nAChR transcript levels (data not shown); however, when added to high K^+ cultures, KN-62 completely blocked the increase in α_7 mRNA levels (Figure 6.6). The block by KN-62 is dose-dependent with an IC_{50} of 1.2 μM and full inhibition at 3–4 μM (Figure 6.6B), which is consistent with the dose-dependent effects of KN-62 on purified CaM kinase activity *in vitro* (Tokumistu *et al.*, 1990; Enslen *et al.*, 1994).

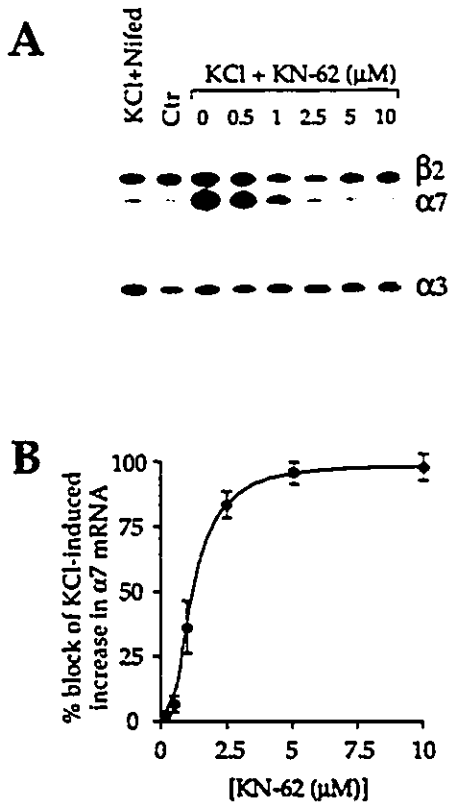

FIGURE 6.6. CaM kinase activity mediates the induction of α_7 nAChR expression by membrane depolarization.

(A) RNase protection assay performed as in Figure 6.2 on RNA extracted from neurons cultured for 7 days. High K^+ was added at day 5, either with 5 μM nifedipine, 0.1% DMSO (0), or with 0.5 to 10 μM KN-62, a CaM kinase inhibitor. In this experiment, α_3 riboprobe was added at 100 000 cpm/reaction. (B) KN-62 inhibits high K^+ induction of α_7 expression in a dose dependent manner with an IC_{50} of ~1.2 μM and full inhibition at 3-4 μM. The means (±SEM) were obtained from 3 cultures.

Table 6.1. Effects of membrane depolarization. Ca^{2+} influx and serine/threonine protein kinase activity on nAChR expression.

	40 mM KCl							
	(6)	Nifedipine (5 μM;6)	K-252a (1 μM;3)	KT-5926 (1 μM;3)	KN-62 (4 μM;6)	Chelerythrin (2 μM;3)	H-89 (1 μM;3)	PMA (100 nM;3)	Forskolin (10 μM;3)
α_3	104± 5	105± 2	95± 8	107±10	117± 7	111±10	117±10	107± 7	108±10
α_5	120±15	120± 4	ND	ND	99±17	116±15	110±23	120±28	100±20
α_7	256±15*	98± 9	166±15§	143±17§	103± 4	272±12*	257± 5*	112±20	116±15
β_2	109± 7	94± 5	100±10	123±16	106± 6	108± 7	106±14	94±12	111± 8
β_4	101± 3	109± 5	ND	ND	97±15	94±12	104± 6	98± 7	110±15

Mean (±SEM) mRNA levels, measured with RNase protection assays, expressed relative to control neurons at day 7 (=100%). All treatments were done from day 5 to day 7. *Significantly different from control neurons ($p<0.001$, t-test). §Significantly different from control neurons and high K^+-treated neurons ($p<0.05$, Duncan's multiple-range test). n is shown in parentheses; ND = not determined.

Table 6.2. Effects of NGF and tyrosine kinase activity on nAChR expression.

		40 mM KCl+			
	High NGF§ (100 ng/ml;2)	Reg. NGF+ (25 ng/ml; 6)	High NGF (100 ng/ml;2)	K-252a (100 nM;2)	Genistein (10 μM;3)
α_3	105±13	104± 5	107±12	107±13	103± 7
α_5	101±14	120±15	ND	ND	101±20
α_7	100± 8	256±15*	262±30*	230±25*	250±20*
β_2	110± 6	109± 7	99±10	100±10	114±12
β_4	95±13	101± 3	100±10	98±15	105± 9

Mean (±SEM) mRNA levels, measured with RNase protection assays, expressed relative to control neurons at day 7 (=100%). §Neurons were grown for 7 days with 100 ng/ml of NGF. +Neurons were treated with 40 mM KCl at day 5 for 48 hrs with regular or high NGF concentration, or with tyrosine kinase inhibitors. *Significantly different from control neurons ($p<0.001$, t-test). n is shown in parentheses; ND = not determined.

Lack of effects of KN-62 on L-type Ca^{2+} channels

Although the above results indicate that CaM kinase activity is involved in the Ca^{2+} signalling cascade that regulates α_7 gene expression, a potential difficulty in their interpretation could arise if, in addition to its inhibition of CaM kinase activity, KN-62 also blocked Ca^{2+} influx through the DHP-sensitive L-type Ca^{2+} channels. Therefore, we investigated this possibility by measuring Ca^{2+} currents on SCG neurons with whole-cell voltage clamp techniques. To distinguish Ca^{2+} currents flowing through L-type Ca^{2+} channels from those flowing through other Ca^{2+} channels we focused on the tail currents: several studies have shown that the Ca^{2+} tail current recorded at the end of a positive voltage step from a depolarized holding potential is due largely to DHP-sensitive L-type Ca^{2+} channels (Plummer *et al.*, 1989; Regan *et al.*, 1991; Mathie *et al.*, 1992), and can be prolonged by DHP analogues, such as Bay K 8644 or (+)202-791 (Hess *et al.*, 1984; Plummer *et al.*, 1989). Figure 6.7A shows an example of Ca^{2+} currents recorded from a neuron in the presence of TTX (1 μM), TEA (10 mM) and 4-AP (2 mM) to block voltage-dependent Na^+ and K^+ currents. Tail currents were evoked by a two step voltage protocol: first we held the neurons at -30 mV to partially inactivate non L-type Ca^{2+} channels, then we applied a 150 ms depolarizing voltage step to +30 mV, followed by a repolarizing step to -40 mV. This resulted in a large Ca^{2+} tail current (Figure 6.7A, left) which was prolonged 2-3 fold in the presence of 1 μM (+)202-791 (Figure 6.7A, right); this indicates that much of the tail current was due to the deactivation of L-type Ca^{2+} channels. In addition, as shown in Figure 6.7A, these tail currents were blocked by the DHP-antagonist, nifedipine (5 μM), but were unaffected by ω-Conotoxin GV1A (ω-CgTx; 5 μM), a specific blocker of N-type Ca^{2+} channels (Plummer *et al.*, 1989; Regan *et al.*, 1991).

To test whether KN-62 affects L-type Ca^{2+} channels, we recorded Ca^{2+} tail currents from neurons treated with 4 μM KN-62, both acutely, and for 24 hrs prior to recording. Figure 6.7A shows that KN-62 had no significant effect on L-type Ca^{2+} channels on these neurons. Therefore, we concluded that the inhibition by KN-62 on α_7 gene expression after high K^+ is due most likely to its inhibitory action on CaM kinase activity (Figure 6.6).

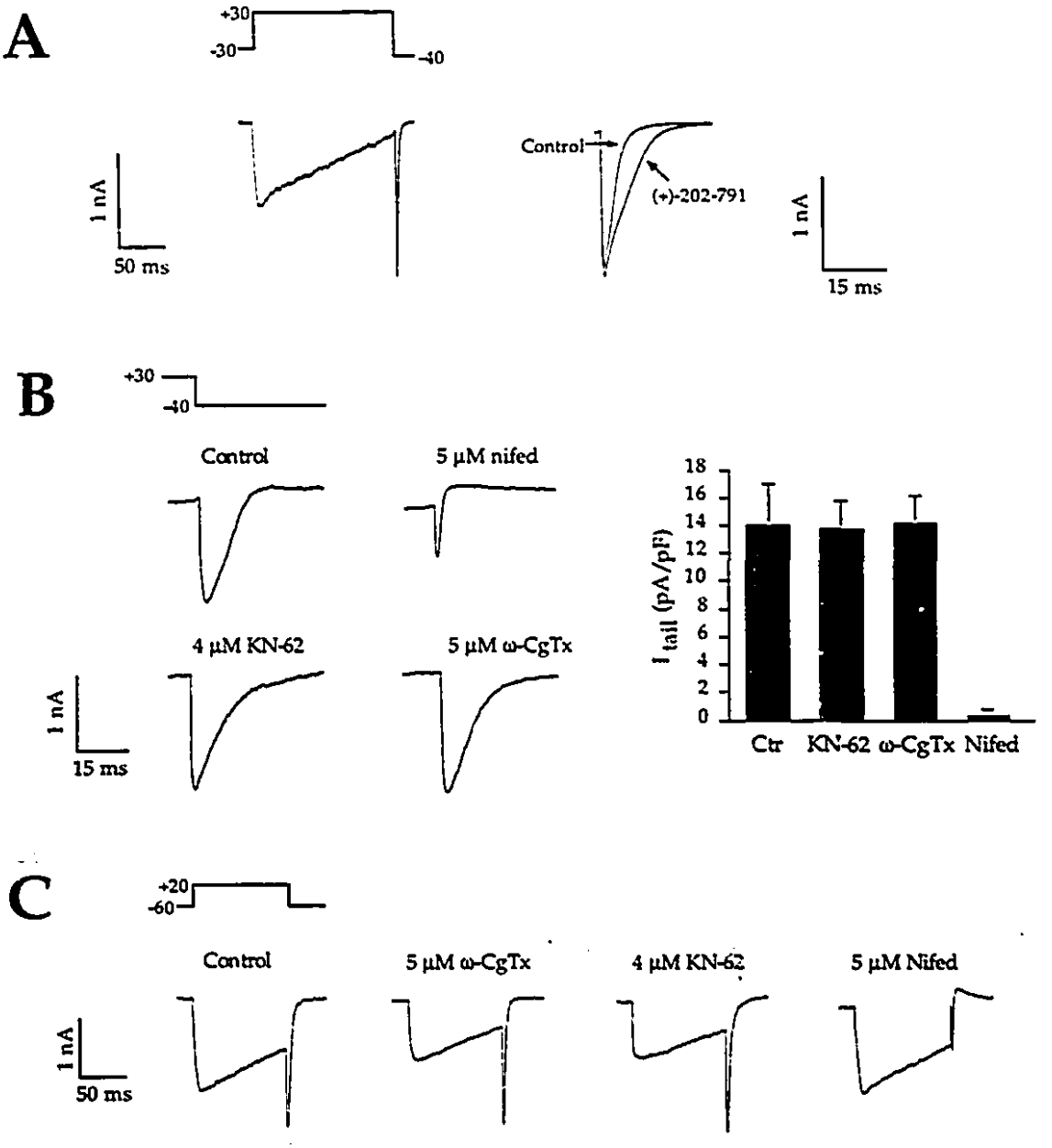

FIGURE 6.7. Effects of KN-62 on Ca^{2+} currents recorded with whole-cell voltage clamp. Leak-subtracted Ca^{2+} currents recorded in presence of 1 µM TTX, 10 mM TEA and 2 mM 4-AP. (A) The neuron was held at -30 mV to partially inactivate non L-type Ca^{2+} currents and a depolarizing step to +30 mV was applied for 150 ms. Repolarization to -40 mV at the end of the step evoked a Ca^{2+} tail current. This tail current is prolonged by DHP-agonist (+)-202-791 (1 µM; right trace). (B) Tail currents elicited as in (A) from a neuron in control medium or in presence of either 5 µM nifedipine, 5 µM ω–CgTx, or 4 µM KN-62. Nifedipine blocks the tail currents, whereas ω–CgTx and KN-62 do not. The histogram shows the mean tail current densities (±SEM) from 6 neurons in each condition, obtained by measuring the amplitude of the tail currents 3 ms after repolarization and dividing by whole-cell capacitance. (C) The neurons were held at -60 mV to remove inactivation of transient Ca^{2+}currents and a depolarizing step to +20 mV was applied for 125 ms. At least 50% of the current was blocked by ω–CgTx (5 µM); a similar blockade was observed with KN-62 (4 µM). This effect of KN-62 was observed with concentrations as low as 0.2 µM. As in (B), the tail currents were unaffected by both drugs. Nifedipine (5 µM) had a small effect on the Ca^{2+} currents during the step, while eliminating most of the tail current. All drugs were applied as in (B).Currents were filtered at 3 KHz and sampled at 5 KHz.

It had been reported, however, that KN-62 may reduce Ca^{2+} influx in other preparations (Li *et al.*, 1992). To investigate whether this could occur through other classes of Ca^{2+} channels, we recorded from neurons at more negative holding potentials (-60 mV) to remove inactivation of non-L-type Ca^{2+} currents. Figure 6.7C shows that ω-CgTx (5 μM) blocks a large portion of these Ca^{2+} currents, without any significant effect on the tail currents. We observed similar results in neurons treated with 4 μM KN-62; furthermore, even concentration as low as 0.2 μM, which had little effect on α_7 expression (Figure 6.6), also blocked these currents. Nifedipine (5 μM), on the other hand, affected only a small fraction of the current elicited by the depolarizing step, and blocked most of the tail current (Figure 6.7C); this is consistent with L-type Ca^{2+} currents representing only a small proportion of the total Ca^{2+} currents on rat SCG neurons (Plummer *et al.*, 1989; Regan *et al.*, 1991). Therefore, it appears that KN-62 can inhibit non-L-type Ca^{2+} channels.

Choline also induces α_7 expression

Several studies have shown that activation of nAChRs increases $[Ca^{2+}]_i$, either by depolarizing neurons and activating voltage-dependent Ca^{2+} channels, or by Ca^{2+} influx through nAChRs directly (Mulle *et al.*, 1992a; Vernino *et al.*, 1992; Vijayaraghavan *et al.*, 1992; Trouslard *et al.*, 1993; Rathouz and Berg, 1994). Therefore, we investigated whether application of nicotinic agonists to cultured SCG neurons, either at day 0 or day 5, would increase α_7 transcript levels. We found that neither the addition of nicotine (10-50 μM) nor carbachol (10-100 μM) for 48 hrs had any effect on the mRNA levels of the 5 nAChRs present in these neurons (data not shown), possibly because these long agonist applications desensitize the receptors.

Choline, a byproduct of ACh degradation and a weak nicotinic agonist (see Chapter 7) has been shown to cause an increase in $[Ca^{2+}]_i$ in SCG neurons, by causing Ca^{2+} release from internal stores (Koike *et al.*, 1989). To test whether an intracellular source of Ca^{2+} can up-regulate α_7, we treated neurons with 5 mM choline. Figure 6.8 shows that choline caused a moderate but significant increase in α_7 mRNA levels when added at day

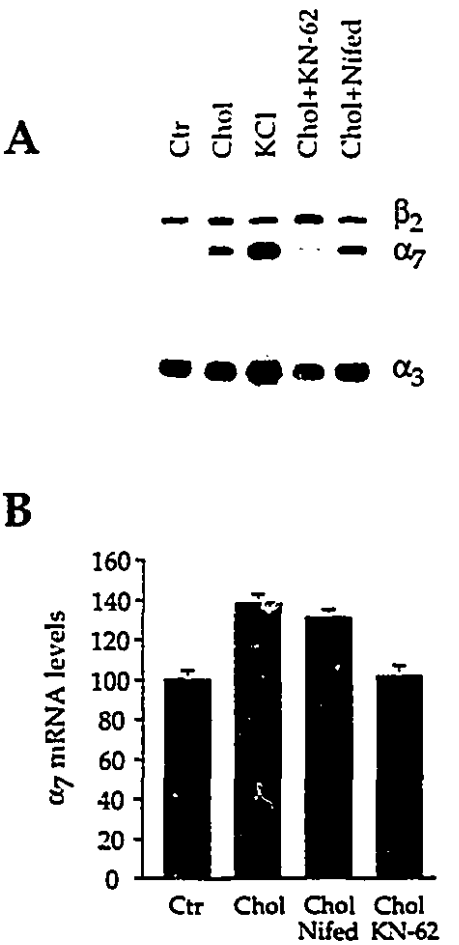

FIGURE 6.8. Choline induces α_7 expression.

RNase protection assay on RNA extracted from SCG neurons cultured for 7 days. At day 5, additional 35 mM KCl, 5 mM choline (Chol), or 5 mM choline with either KN-62 (4 μM) or nifedipine (5 μM) were added to sister cultures. Choline caused a small increase in α_7 mRNA levels without affecting the levels of α_3 and β_2; β_4 and α_5 were also unaffected (data not shown). The choline effect was not blocked by nifedipine, but was blocked by KN-62. Mean (±SEM) mRNA levels for α_7 subunit expressed relative to control (=100%); n=4 cultures.

5: the other 4 nAChR transcript levels were not affected. The choline-induced increase in α_7 transcripts was not blocked by nifedipine, indicating that Ca^{2+} influx through L-type Ca^{2+} channels was not involved. Neither was this choline effect blocked by hexamethonium (100 µM), atropine (2 µM) or α-BTX (100 nM) (data not shown), suggesting that nicotinic and muscarinic ACh receptors do not mediate this effect. Nevertheless, the increase in α_7 mRNA levels produced by choline was prevented by KN-62 (4 µM; Figure 6.8), indicating that the choline effect is mediated by a CaM kinase pathway. We did not investigate further how choline produces its effect on CaM kinase activity, but it is likely to occur by increasing Ca^{2+} release from internal stores (Koike *et al.*, 1989).

Correlation between changes in α_7 mRNA levels and changes in α-BTX-nAChRs

As the α_7 gene codes for an α-BTX-nAChR (Schoepfer *et al.*, 1990, Couturier *et al.*, 1990b; Séguéla *et al.*, 1993), we investigated whether the induction of α_7 gene expression by membrane depolarization in cultured SCG neurons results in an increase in the number of α-BTX binding sites on the surface of these neurons. Figure 6.9 shows that neurons exposed to high K^+ for 48 hrs had 3-5 fold more surface [^{125}I]α-BTX binding than control neurons. These results demonstrate a good correlation between increases in both α_7 mRNA levels and α-BTX-nAChRs on the surface of the these neurons.

Neonatal rat nodose neurons express nAChR subunit transcripts

As a first step in determining if nAChR transcripts in cultured nodose neurons are regulated in a similar way to that of cultured SCG neurons, we have measured the expression of nAChR transcripts in P1 nodose ganglia. Figure 6.10 shows an RNase protection assay for α_3, α_7, β_2, β_4 performed on mRNA extracted from P1 SCG and nodose ganglia. Nodose neurons express relatively high levels of nAChR transcripts. By comparison with SCG neurons, β_2 transcripts are expressed at similar levels, β_4 at approximately 50% lower levels, while α_3 and α_7 transcripts are expressed at even lower levels. In addition, we found that α_5 and β_3 mRNA are also present at very low levels in nodose neurons, while α_2 and α_4 transcripts are not detectable (data not shown; see also

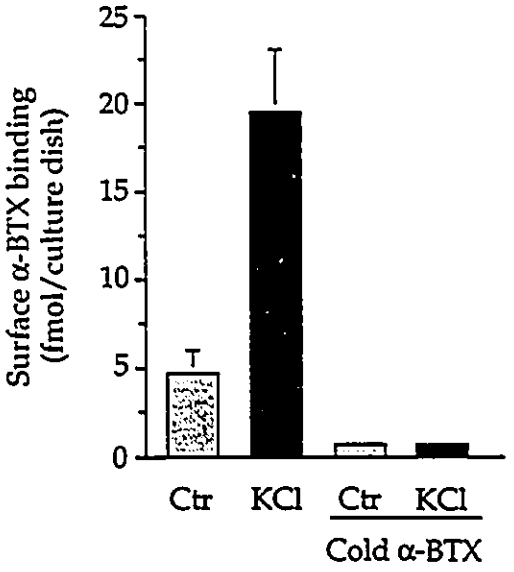

FIGURE 6.9. Membrane depolarization increases surface α-BTX binding on SCG neurons.

Mean (±SEM) surface [^{125}I]-α-BTX binding (fmol/dish) on neurons cultured for 7 days in control condition or after 48 hrs with high K^+ from day 5. Surface binding increased 3-5 fold with high K^+. Only low levels of [^{125}I]-α-BTX binding was detected when cells were pre-treated with cold α-BTX (100 nM) for 90 min. n=3.

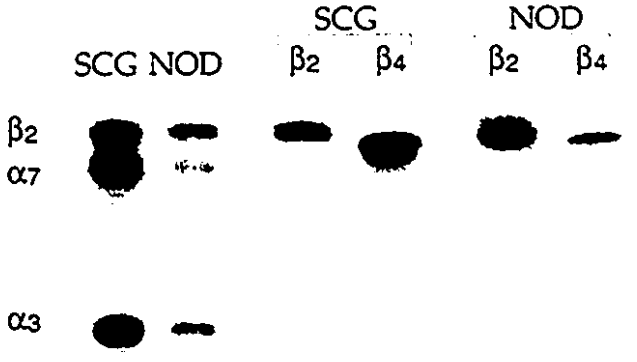

FIGURE 6.10. Nodose neurons express nAChR subunit transcripts.

RNase protection assays for α_3, α_7, β_2, and β_4 transcripts on P1 SCG and nodose neurons. Nodose neurons express β_2 mRNA at levels comparable to SCG neurons; α_3 and β_4 are expressed at lower levels in nodose neurons compared to SCG neurons. Of the 4 transcripts, α_7 is expressed at the lowest levels in nodose neurons. Each reaction contained 1 μg of total cellular RNA and 200 000 cpm for each riboprobe.

Mandelzys, 1992). These results demonstrate that even though freshly dissociated nodose neurons have small or undetectable ACh-evoked currents on their somata, they express significant levels of nAChR transcripts. These findings are consistent with the notion that a population of nodose neurons express nAChRs on their terminals. These results will be discussed further in Chapter 8.

DISCUSSION

In this chapter, we have investigated the expression of nAChRs in SCG neurons developing in culture. Our results demonstrate that when SCG neurons develop in culture, they express nAChR transcripts at levels comparable to *in vivo*, with the exception of α_7. Furthermore, the results demonstrate that membrane depolarization differentially regulates the expression of nAChR subunits by up-regulating specifically α_7. A novel aspect of this study is that it links neuronal activity with neurotransmitter receptor gene expression through a CaM kinase pathway.

Role of Ca^{2+} influx and CaM Kinase activity on α_7 subunit expression

To demonstrate that CaM kinase activity is essential for the induction of the α_7 gene by membrane depolarization, we used a potent and selective CaM kinase inhibitor, KN-62 (Tokumitsu *et al.*, 1990). Several studies have addressed the specificity of KN-62. Tokumitsu *et al.* (1990) showed that KN-62 competes with calmodulin for its binding site on CaM kinase, but does not interact with calmodulin directly. *In vitro*, KN-62 inhibits CaM kinase autophosphorylation with an IC_{50} of approximately 1.0 μM (Tokumitsu *et al.*, 1990) and inhibits phosphorylation of a purified substrate by CaM kinase with an IC_{50} of 1-2 μM (Enslen *et al.*, 1994). In contrast, 100 fold higher concentrations have little effect on calmodulin dependent kinases, such as myosin light chain kinase, phosphodiesterase, PKA or PKC (Tokumitsu *et al.*, 1990). We found that KN-62 inhibits the increase in α_7 expression induced by membrane depolarization in a dose-dependent manner with an IC_{50} of approximately 1.2 μM and full inhibition at 3-4 μM, consistent with the specific action

of KN-62 on CaM kinases (Tokumitsu *et al.*, 1990; Enslen *et al.*, 1994). In addition, high concentration (1 μM) of K-252a and KT-5926, which notably inhibit CaM kinase II (Hashimoto *et al.*, 1991), also prevented part of the increase in α_7 mRNA.

The induction of α_7 expression by membrane depolarization is due to an influx of Ca^{2+} through L-type Ca^{2+} channels. One concern was whether the effects of KN-62 were due, in part, to inhibition of Ca^{2+} influx, possibly by interfering with L-type Ca^{2+} channels directly, a concern also addressed by others (Li *et al.*, 1992; Hack *et al.*, 1993; Wyllie and Nicoll, 1994). Most of the Ca^{2+} currents in rat SCG neurons are carried through N-type channels (Plummer *et al.*, 1989; Regan *et al.*, 1991), although one can reliably measure Ca^{2+} currents through L-type channels in these neurons by recording the tail currents at the end of depolarizing voltage steps (Plummer *et al.*, 1989; Regan *et al.*, 1991; Mathie *et al.*, 1992). We used this approach to demonstrate that 4 μM KN-62 has no effect on the L-type currents on SCG neurons. Our results are consistent with those of Hack *et al.* (1993) who showed that KN-62 (2.5-10 μM) had no effect on intracellular $^{45}Ca^{2+}$ levels in rat cerebellar granule cells grown in culture with high K^+ for one week. On the other hand, we did observe some inhibition of non L-type Ca^{2+} currents by KN-62, presumably N-type currents (Plummer *et al.*, 1989; Regan *et al.*, 1991). We did not investigate this inhibition in detail, but the fact that we observed inhibition by KN-62 at doses lower than that needed to inhibit the activity of CaM kinase significantly (0.2 μM; Figure 6.4 and see Tokumitsu *et al.*, 1990; Enslen *et al.*, 1994) suggests that KN-62 affects these non-L-type Ca^{2+} channels directly. This differential effect of KN-62 on Ca^{2+} channels may explain the divergent results obtained with KN-62 on Ca^{2+} influx (Li *et al.*, 1992; Hack *et al.*, 1993; Wyllie and Nicoll, 1994).

Our finding that Ca^{2+} influx through L-type Ca^{2+} channels is essential for high K^+ induction of α_7 expression is consistent with the sustained mode of depolarization used in our experiments. Indeed, high K^+ (40 mM) raises the membrane potential to approximately -30 to -20 mV in SCG neurons (Franklin *et al.*, 1995); at such sustained

membrane potentials. L-type Ca^{2+} channels are still activated, while other types are largely inactivated (Tsien *et al.*, 1988; Plummer *et al.*, 1989). In fact, the high K^+-induced sustained elevation in $[Ca^{2+}]_i$ in rat SCG neurons (at 40 mM, the $[Ca^{2+}]_i$ =150-200 nM; Koike and Tanaka, 1991; Franklin *et al.*, 1995) is generated only by the activation of DHP sensitive L-type Ca^{2+} channels, and not by ω-CgTx-sensitive N-type Ca^{2+} channels (Vidal *et al.*, 1989; Collins *et al.*, 1991; Franklin and Johnson, 1992; Franklin *et al.*, 1995).

When this paradigm of stimulation has been used to investigate activity-mediated changes in gene expression, L-type Ca^{2+} channel activity was shown to be essential (Murphy et al, 1991; Bading *et al.*, 1993; Rosen *et al.*, 1994; Bessho et al, 1994). However, *in vivo*, membrane depolarization in neurons is not chronic, but rather pulsatile, which is likely to recruit activity of other Ca^{2+} channels; whether their activities affects gene expression is unknown. Interestingly, Murphy *et al.* (1991) demonstrated that blocking the L-type Ca^{2+} on cultured cortical neurons did not compromise the synaptic interactions and generation of action potentials on these neurons, but did inhibit the synaptic activation-dependent expression of immediate early genes. It has been found that L-type Ca^{2+} channels are preferentially targeted to the cell body and proximal dendritic membranes (Ahlijanian *et al.*, 1990; Westenbroek *et al.*, 1990). These findings suggest that L-type Ca^{2+} channels may be involved in coupling synaptic activity in distal dendrites to regulate local processes in the cell body, including gene expression (Murphy *et al.*, 1991).

CaM kinase family

Our results show that CaM kinase activity regulates α_7 gene expression. Several types of CaM kinases have been characterized and have been classified into two main groups referred to as the dedicated CaM kinases and the multifunctional CaM kinases (Schulman, 1993). Dedicated CaM kinases, which include myosin light chain kinase, phosphorylase kinase and CaM kinase III, phosphorylate unique substrates. For instance, CaM kinase III phosphorylates the eukaryotic elongation factor II. The multifunctional CaM kinases, which include CaM kinase I, II and IV activate a broad spectrum of substrates. CaM

kinase I regulates primarily neurotransmitter release by phosphorylating synaptic vesicle proteins (reviewed by Hanson and Schulman, 1992; Schulman, 1993). The two CaM kinases whose activities have been shown to affect gene expression are CaM kinase II and IV (Bading *et al.*, 1993; Enslen *et al.*, 1994; Enslen and Soderling, 1994). KN-62 has been shown to inhibit CaM kinase II (Tokumitsu *et al.*, 1990) as well as IV and V (Enslen *et al.*, 1994; Mochizuki *et al.*, 1993). While little is known about the function and distribution of CaM kinase V, CaM kinase IV has been shown to target to the nucleus (Jensen *et al.*, 1991) suggesting that it has a direct role in regulating gene expression (Enslen *et al.*, 1994). However, PKA activity has been shown to inhibit CaM kinase IV activity (Kameshita *et al.*, 1991), whereas neither activation nor inhibition of PKA has any effect on α_7 expression in SCG neurons, making it less likely that CaM kinase IV is involved. On the other hand, the biochemical properties and cellular distribution of CaM kinase II make it a more attractive candidate for mediating the effects of activity on α_7 expression (see appendix 3; Hanson *et al.*, 1994; Hanson and Schulman, 1992; Schulman, 1993).

CaM kinase II affects synaptic plasticity and gene expression

CaM kinase II (also referred simply as CaM kinase; Schulman, 1993) is a key player in the induction of LTP (Malinow *et al.*, 1989) and other forms of synaptic plasticity (Silva *et al.*, 1992a,b; Schulman, 1993; Lisman, 1994; Chapman *et al.* 1995). In brain slices from mutant mice with a null mutation in the α-subunit of CaM kinase (one of the two major brain subunits) LTP cannot be induced, and these mice are impaired in spatial learning (Silva *et al.*, 1992a,b). Thus far, the involvement of CaM kinase in regulation of synaptic function has been demonstrated to occur through post-translational processes such as modulation of ion channel activity or transmitter release (Hanson and Schulman, 1992). However, CaM kinase can phosphorylate transcription factors (Wegner *et al.*, 1992), target to the nucleus (Srinivasan *et al.*, 1994) and regulate the expression of immediate early genes (Enslen and Soderling, 1994; Bading *et al.*, 1993). Many of the immediate early gene products are believed to regulate the expression of "delayed response genes", which

may code for proteins participating in neuronal function. Our finding that activity regulates the expression of a neurotransmitter receptor subunit through a CaM kinase pathway suggests another mechanism by which CaM kinase could affect synaptic plasticity.

Mechanism of regulation of α_7 expression

How CaM kinase regulates α- expression in SCG neurons is unknown. Our data using α-amanitin suggest that the changes in α_7 mRNA levels result from altered mRNA synthesis rather than from a change in mRNA stability: the approximate rate of decay in α_7 mRNA was unaltered by α-amanitin, and was comparable to the decay of other nAChR transcripts in neurons treated with α-amanitin. However, we cannot exclude the possibility that α-amanitin blocked transcription of a gene(s) coding for a protein(s) that preferentially destabilizes α- mRNA. We have not determined the signalling events downstream of CaM kinase that are responsible for the induction of α- expression. From the relatively slow time course for α_7 mRNA levels to plateau after treatment with high K^+ (greater than 24 hrs), it seems likely that transcription of other genes, such as immediate early genes, precedes α_7 expression (Sheng and Greenberg, 1990; Bading *et al.*, 1993; Enslen and Soderling, 1994; Ghosh and Greenberg, 1995). If so, the α_7 gene could be considered a delayed response gene. Although many immediate early gene products have been shown to bind to DNA elements upstream of delayed response genes, the direct link between activity, immediate early genes induction and delayed response gene expression has not been demonstrated (Armstrong and Montminy, 1993; Morgan and Curran, 1995). The α_7 genes could represent a good model to investigate this link. The promoter elements of the α_7 gene have been identified in chick but not in rat. The promoter of chick α_7 gene has been shown to confer neuro-specific expression; however, no specific DNA binding sequence that could be responsible for an activity-mediated regulation has been identified (Matter-Sadzinski *et al.*, 1992).

It has been shown recently that α_7 and other neuronal nAChR subunits are expressed at low levels in embryonic chick skeletal muscle. Interestingly, the developmental pattern of α_7 mRNA expression follows that of the muscle α_1 subunit, reaching peak expression

prior to synaptogenesis and decreasing after synapse formation (Corriveau *et al.*, 1995). These results suggest that transcription of α- does not occur strictly in neurons (cf Matter-Sadzinski *et al.*, 1992), and that similar mechanisms that down-regulate muscle nAChR subunits during activity can also regulate α_7 in muscle. If so, this could mean that the α_7 gene contains two distinct upstream sequences that regulate transcription in opposite manner after Ca^{2+} influx, depending on the cellular context.

It is noteworthy that the increase in α_7 mRNA levels after high K^+ appears to plateau at levels equivalent to day 0, whereas *in vivo*, α_7 mRNA levels continue to increase (see Figure 6.1; Mandelzys *et al.*, 1994). These results could mean that other factors are involved in regulation of α_7 gene expression, or, alternatively, that CaM kinase activity is not optimally activated by sustained high K^+ treatment in these cultures. While several studies have shown that high K^+ activates CaM kinase activity in neurons (Fukunaga *et al.*, 1989; Ocorr and Schulman, 1991; Bading *et al.*, 1993), the biochemical properties of CaM kinase predict that pulsatile stimulations of neurons should activate CaM kinase even more effectively (Hanson *et al.*, 1994; appendix 3). Moreover, a sustained high K^+ treatment is likely to induce Ca^{2+}-activated phosphatases, such as Ca^{2+}/calmodulin-dependent phosphatase, calcineurin. Conceivably, the ratio between Ca^{2+}/calmodulin-dependent kinase and phosphatase activities is greater in neurons receiving patterned synaptic activity compared to neurons that are chronically depolarized (Hanson *et al.*, 1994; Lisman, 1994).

Effects of choline and other nicotinic agonists on α_7 expression

Nicotinic agonists, nicotine and carbachol, did not mimic the effects of high K^+, even though activation of nAChRs by these ligands causes a large increase in $[Ca^{2+}]_i$ (Mulle *et al.*, 1992a; Vernino *et al.*, 1992; Vijayaraghavan *et al.*, 1992; Trouslard *et al.*, 1993; Rathouz and Berg, 1994). However, as nAChRs desensitize, a prolonged application of nicotinic agonists may not produce a sustained increase in $[Ca^{2+}]_i$; we plan to test whether pulsatile applications of these agonists can induce α_7 expression.

Interestingly, we observed that choline produced a small but significant increase in α- expression. Choline has been shown to cause an increase in $[Ca^{2+}]_i$ in cultured SCG neurons, presumably by releasing Ca^{2+} from internal stores (Koike *et al.*, 1989). Consistent with this, we found that the choline effect on α- expression was not blocked by nifedipine, hexamethonium, α-BTX or atropine, suggesting that this effect is not due to Ca^{2+} influx nor to the activation of nicotinic or muscarinic receptors. However, the increase in α- transcript levels was blocked by KN-62, indicating that CaM kinase activity was stimulated by choline. Whether choline has a role in α- expression *in vivo* is unclear. Due to cholinesterase activity at synapses between pre-ganglionic and SCG neurons, choline could build up to considerable levels during high frequency activity, but whether it can reach high enough concentrations to influence α- expression in uncertain. Nevertheless, these results indicate that the CaM kinase-induced expression of α- may also be activated by pathways that do not require Ca^{2+} influx.

Lack of effects of PKC, PKA and tyrosine kinase inhibitors

Our results with inhibitors or activators of PKA and PKC suggest that these enzymes have little role in regulating α-. In fact, we found that none of the nAChR transcript levels were altered by these kinase inhibitors and activators. We cannot rule out, however, that some of these agents did not inhibit or activate properly the target enzymes. To reduce such possibility, we attempted to block their activity in presence of high K^+, as well as to stimulate their activity in control condition with different agents. In addition, we tested higher concentrations of these agents, without observing any effects. To stimulate PKC, we used 100 mM PMA, which could, upon prolonged treatment, down regulate PKC in SCG neurons (Matthies *et al.*, 1987). Thus, we also added PMA to high K^+ cultures, but observed no effect on the high K^+ induction of α- mRNA levels. We conclude from these experiments that PKA and PKC are not likely to be involved in the regulation of nAChR gene expression in neonatal rat SCG neurons developing in culture. This contrasts with the role of PKA and PKC on the activity-mediated expression of nAChRs by muscle extra-junctional nuclei (Klarsfeld *et al.*, 1989; Walke *et al.*, 1994).

To test for a role in tyrosine kinase activity, we used two inhibitors, genistein and K-

252a. While genistein inhibits several tyrosine kinases (Levitzki and Gazit, 1995), low concentrations of K-252a (e.g. 10-100 nM) were shown to inhibit *trk* receptors preferentially (not the EGF receptor: Koizumi *et al.*, 1988; Berg *et al.*, 1992), although higher doses can also inhibit serine/threonine protein kinases, including CaM kinase (Hashimoto *et al.*, 1991). Adding these agents to control cultures causes the neurons to die, as they need NGF and *trk*A activity to survive at this stage of development (Johnson and Deckwerth, 1993). Removal of NGF, induces apoptosis in SCG neurons (Martin *et al.*, 1988), a process that can be prevented temporarily by increasing $[Ca^{2+}]_i$ with high K^+, even though this treatment does not activate *trk*A (Koike *et al.*, 1989; Franklin *et al.*, 1995). Consistent with these findings, the neurons survived well after treatment with tyrosine kinase inhibitors in high K^+ cultures. However, the nAChR transcript levels were unaltered by these agents, suggesting that tyrosine kinases do not regulate nAChR gene expression in cultured SCG neurons, at least not under high K^+ condition. Finally, changing the concentration of NGF in the culture medium, from 25 to 100 ng/ml, a treatment that was shown to affect gene expression in cultured SCG neurons (Ma *et al.*, 1992), caused no effects on nAChR expression.

What regulates gene expression of the other nAChR subunits?

An interesting aspect of our results is that the expression of nAChR transcripts that code for subunits other than α_7 is regulated by mechanisms that appear independent of afferent innervation as well as target contact. Membrane depolarization had little effect on the expression of those transcripts, and protein kinase activity appeared not to be involved in their expression. In fact, the expression of these 4 nAChR transcripts by cultured neurons parallels closely their expression by neurons developing *in vivo* over the same time period, suggesting that the expression of these genes is governed by intrinsic mechanism related to SCG neuron phenotype. This interpretation is consistent with the observations of Zoli *et al.* (1995), which indicated that the majority of nAChR transcripts examined (i.e. α_3, α_4, β_2, and β_4) became detectable with *in situ* hybridization at a period corresponding to neurogenesis. Interestingly, Schoenherr and Anderson (1995) reported

that ligand-gated ion channel genes, including nACh, NMDA and glycine receptors, contain "Neuron-restrictive silencer element-like sequences". Thus, the release of transcription inhibition by down-regulation of a neuron-restrictive silencer factor during neurogenesis, could be a mechanism responsible for the appearance of nAChRs at this period.

When SCG neurons develop in culture, only the mRNA for α_3 increased significantly, indicating a differential regulation of the nAChR subunits during neuronal maturation. The promoter of rat α_3 nAChR subunit was recently characterized and shown to be activated by the POU domain transcription factor SCIP/Tst-1, which is believed to confer neuro-specific gene expression (Yang *et al.*, 1994). It will be interesting to determine whether this factor is also up-regulated during SCG neuron development. Incidentally, we observed a small transient decrease in α_3 mRNA levels after the first day in culture, and this decrease appeared to be reduced by high K^+ (Figure 6.2A); however, the small size and transient nature of the high K^+ effect made it difficult to investigate further. In contrast, high K^+ had no effect on α_3 mRNA levels when applied at day 5. If the α_3 mRNA levels are determined by an intrinsic mechanism related to neuronal maturation, this process may have been retarded by the dissociation of the neurons.

The levels of both β_2 and β_4 subunit transcripts appeared largely unchanged during the first two postnatal weeks of development as well as in culture for the first 7 days. β_2 mRNA is the most widespread nAChR transcript in the CNS and is expressed in all peripheral ganglia examined in the rat (Wada *et al.*, 1989; Zoli *et al.*, 1995), including the nodose ganglion (Figure 6.10). The β_2 transcript appears to be the least sensitive nAChR subunit transcript to developmental events (Hill *et al.*, 1993; Zoli *et al.*, 1995), except in the chick optic tectum (Matter *et al.*, 1990). The β_4 transcript is approximately 3 times more abundant than that of β_2 in SCG neurons and its expression seems to be largely restricted to neurons expressing α_3 (Zoli *et al.*, 1995). Interestingly, α_3 and β_4 genes, together with α_5, form a cluster in the rat (Boulter *et al.*, 1990) and chick (Couturier *et al.*, 1990a) genomes, indicating that the initiation of their expression during neurogenesis may be coordinately regulated. Downstream of β_4 and upstream of α_3 gene lies an inter-

genic sequence of more than 2 kb, which includes the α_3 promoter sequence (Boyd, 1993; Yang *et al.*, 1994); such a promoter may regulate further the expression of α_3 during neuronal maturation. Finally, the α_5 gene is oriented in the opposite direction in this cluster, suggesting a distinct regulation. Of the five nAChR transcripts, α_5 is expressed at the lowest levels; it drops transiently by approximately 30% after 3–4 days in culture. This drop is similar to what is observed after denervation *in vivo* (Mandelzys *et al.*, 1994); however, unlike for α_7, membrane depolarization did not affect α_5 mRNA levels.

Taken together, our results and those of others discussed here suggest that nAChRs in rat SCG neurons are largely controlled by intrinsic regulatory mechanisms, possibly related to neurogenesis, and neuronal maturation. One aspect of neuronal maturation that takes place during the increase in α_3, *in vivo* and in culture, is the extension of dendrites. The early expression of nAChRs may be crucial to allow rapid establishment of functional synapses when presynaptic terminals make initial contacts (Haydon and Drapeau, 1995). In addition, nAChRs may be targeted to growth cones and have a role in neuritic guidance during development (Lipton *et al.*, 1987; Pugh and Berg, 1994; Zheng *et al.*, 1994). Afterward, during synaptogenesis, another nAChR subunit, α_7, which may give rise to a homomeric α-BTX-nAChR (Schoepfer *et al.*, 1990; Couturier *et al.*, 1990b; Séguéla *et al.*, 1993), is regulated by an activity-dependent mechanism that involves CaM kinase activity. The significance of this induction is unknown, but it will occupy an important part of the next chapter.

Differences with chick autonomic neurons

Our proposal that the expression of nAChR transcripts, α_3, α_5, β_2 and β_4 is largely governed by intrinsic mechanisms in neonatal SCG neurons may not hold true for embryonic chick autonomic neurons. In culture, the transcript levels of nAChR subunits drop dramatically in ciliary neurons (Corriveau and Berg, 1994), and appear to be redundantly regulated by contacts with either their afferents or targets. However, the results obtained from studies that involved the removal of pre- and post-ganglionic interactions differ depending on whether measurements were done on nAChR transcript

levels, nAChR antibody binding, or ACh-evoked currents (Jacob and Berg, 1987; Role, 1988; Boyd *et al.*, 1988; McEachern *et al.*, 1989; Engisch and Fischbach, 1990, 1992; Gardette *et al.*, 1991; Arenella *et al.*, 1993; Moss and Role, 1993; Schwartz Levey *et al.*, 1995). For example, removal of pre-ganglionic interactions on chick ciliary neurons retarded the developmental increase in nAChR transcript levels (Schwartz Levey *et al.*, 1995), caused a large reduction in intracellular antibody binding, but not on the surface binding (Jacob and Berg, 1987; Arenella *et al.*, 1993) and caused little effects on the ACh-evoked currents (McEachern *et al.*, 1989; Engisch and Fischbach, 1992; Schwartz Levey *et al.*, 1995). Interestingly, denervation of post-hatched chick ciliary ganglia caused a 2 fold decrease in α-BTX binding in 2 days (Jacob and Berg, 1987), similar to the decrease in α_7 in cultured SCG neurons. These results suggest that extrinsic influences may regulate nAChRs at different levels of expression in chick autonomic neurons. In the next chapter, we will investigate the relationship between changes in nAChR transcripts and changes in ACh-evoked currents on SCG neurons.

Targeting of nAChR mRNA

The transport of some specific mRNAs to dendrites has been proposed to represent a strategy for regulating local supply of proteins in dendrites in response to synaptic activity (Steward and Banker, 1992). An interesting observation made from our *in situ* hybridization experiments is that nAChR transcripts remain in the somata and do not target to dendrites. However, we did not test whether we could detect transcripts that are known to be present in dendrites such as MAP2 (Bruckenstein *et al.*, 1990; Kleiman *et al.*, 1990); therefore, we cannot rule out the possibility that nAChR transcripts, localized within dendrites, were below detection. Nevertheless, similar results to ours have been reported for glutamate receptors mRNA (GluR2 and GluR3) in cultured hippocampal neurons, even though their respective proteins were found to be abundantly expressed in dendrites and dendritic spines (Craig *et al.*, 1993). Synaptosomal preparations enriched in hippocampal dendritic spines also lacked GluR1 mRNA, but contained mRNAs for MAP2 and α-CaM Kinase II (Chicurel *et al.*, 1993).

Thus far, few mRNAs have been shown to target to dendrites: MAP2, α-CaM kinase II, the immediate early gene transcript *Arc*, and the non-coding RNA neural BC1 are notable examples (Garner *et al.*, 1988; Burgin *et al.*, 1990; Bruckenstein *et al.*, 1990; Kleiman *et al.*, 1990; Chicurel *et al.*, 1993; Lyford *et al.*, 1995). The facts that these RNAs are found in dendritic spines of hippocampal neurons and that their products have been implicated in mechanisms controlling neuronal polarity or synaptic plasticity make it attractive to consider that targeting these transcripts to dendrites allows for local and rapid expression of synaptically involved proteins. If such mechanism exist, it appears that neurotransmitter receptors are not included among those proteins. In fact, there are no examples yet of a rough endoplasmic reticulum (RER)-associated mRNA (i.e. coding for a transmembrane protein) that targets to dendrites. Dendritic spines are likely to be devoid of RER (Peters *et al.*, 1991), but Steward and Reeves (1988) have found polyribosomes to be associated with membranous cisternae at the base of hippocampal neuron spines, raising the possibility that transmembrane proteins are synthesized in dendritic shafts. In the case of ligand-gated ion channels, many of them are expressed in axonal terminals, which are devoid of a translation machinery; encoding the targeting of ligand-gated ion channels in their mRNA may thus not be an efficient mechanism to discriminate targeting of receptors to axons or dendrites. In this context, it is intriguing to know if transport of ion channels to axons and dendrites is differentially regulated, or whether differential anchoring mechanisms determine their final localization.

Chapter 7

Changes in ACh-Evoked Current Densities Correlate with Changes in Transcript Levels for α_3 nAChR Subunit But Not α_7.

INTRODUCTION

In this chapter, we investigate the effects of the changes in nAChR transcript levels, described in Chapter 6, on the expression of macroscopic ACh-evoked currents on cultured SCG neurons.

To learn more about the subunit composition of nAChRs on rat SCG neurons, Mandelzys *et al.* (1995) compared the electrophysiological and pharmacological properties of ACh-evoked currents on SCG neurons with that of known nAChRs expressed in *Xenopus* oocytes (Luetje and Patrick, 1991). The major findings were that: 1) at the macroscopic level, most functional nAChRs on SCG neurons behave as a uniform population of receptors, at least with respect to agonist activation and toxin blockade; 2) the nAChRs on SCG neurons have sensitivities to nicotinic agonists and to neuronal-BTX that are intermediate to those of $\alpha_3\beta_4$ and $\alpha_3\beta_2$ receptors expressed in *Xenopus* oocytes. Based on these results and on the mRNA levels of nAChR subunits in these neurons, it was proposed that nAChRs on SCG neurons uniformly incorporate α_3, β_4 and perhaps β_2 subunits. As the mRNA levels of α_5 are less than a tenth those of α_3 in post-natal SCG neurons (Chapter 6; Mandelzys *et al.*, 1994), and because the incorporation of α_5 in functional nAChR expression is still unclear (Boulter *et al.*, 1990; Couturier *et al.* 1990b; but see Vernallis *et al.*, 1993 and McGehee and Role, 1995), our working model of the functional nAChRs in SCG neurons does not include an α_5 subunit.

The fifth nAChR subunit expressed in SCG neurons is α_7, which encodes an α-BTX-nAChR (Schoepfer *et al.*, 1990; Couturier *et al.*, 1990b; Séguéla *et al.*, 1993). Although this receptor gates a current primarily carried by Ca^{2+} in *Xenopus* oocytes, it is unclear whether this receptor gates a current on SCG neurons. α-BTX does not affect synaptic transmission between cultured sympathetic neurons (Nurse and O'Lague, 1975) and

numerous studies have shown a dissociation between α-BTX binding and nAChR blockade (Nurse and O'Lague, 1975; Duggan *et al.*, 1976; Brown and Fumagalli, 1977; Patrick and Stallcup, 1977; Carbonetto *et al.*, 1978; Ravdin and Berg, 1979; Chiappinelli, 1985; Lipton *et al.*, 1987; Mulle and Changeux, 1990; Sucher *et al.*, 1990; Zhang and Feltz, 1990). However, recently a remarkably large α-BTX sensitive current (~250 pA/pF) that desensitizes within milliseconds has been reported in chick ciliary neurons (Zhang *et al.*, 1994). In addition, Albuquerque and colleagues have observed a rapidly desensitizing ACh-evoked current sensitive to α-BTX that carries mainly Ca^{2+} (but that is at least an order of magnitude smaller than that reported in the chick ciliary ganglion) in cultured hippocampal neurons (Alkondon and Albuquerque, 1993; Castro and Albuquerque, 1995). Both of these currents could be detected by using rapid agonist applications that activate ACh-evoked currents in less than 20 ms. On SCG neurons, rapid nicotinic agonist application had not been tested, leaving the possibility that a rapidly desensitizing ACh-evoked current sensitive to α-BTX is expressed on these neurons.

Therefore, we set out to examine this possibility, particularly since the α_7 mRNA levels change in cultured SCG neurons. We already found a good correlation between the increase in α_7 transcripts and the increase in α-BTX binding on these neurons (Chapter 6). Furthermore, as the α_7 gene and the α-BTX-nAChR are regulated by an activity-dependent mechanism in SCG neurons, and perhaps by synaptic transmission *in vivo* (Mandelzys *et al.*, 1994), it is intriguing to know whether this regulation affects the properties of ACh-evoked currents on the neurons.

We observed, in the previous chapter a differential change in nAChR transcript levels in cultured SCG neurons. Only the α_3 transcript increases as the neurons develop. How does this specific increase affect the density of functional nAChRs on the neurons? Nicotinic AChRs are thought to be heteromeric pentamers formed by the assembly of 2 α and 3 ß subunits (Cooper *et al.*, 1991; Anand *et al.*, 1991). Since the mRNA levels of the ß subunits appear to have reached their plateau by P1, while the ACh-evoked current densities continue to increase postnatally (Mandelzys *et al.*, 1994), this may imply that α subunits in these neurons are rate-limiting for the assembly of functional nAChRs.

In this chapter, we developed a protocol for rapid agonist application to investigate the properties of ACh-evoked currents on SCG neurons developing in culture.

EXPERIMENTAL PROCEDURES

Neuronal cultures

SCG ganglia were dissected from postnatal P1 and P14 rats, dissociated and cultured as described in section 2.1., and in the previous chapter with respect to treatments with high K^+.

Electrophysiology

Neuronal recordings: ACh-evoked currents were measured with whole-cell patch clamp techniques as described in section 2.3.. For agonist application we used a method for rapid agonist application that provides complete change in solution around the neurons within approximately 2 ms (see Figure 2.1, section 2.3.2.). We found that our technique of rapid agonist application generally triggered unclamped voltage-dependent Na^+ currents on SCG neurons (Figure 7.1). To eliminate these currents, we included 500 nM TTX in the bath perfusion. However, we found that this was sometimes not sufficient to eliminate these unclamped Na^+ currents; the TTX had to be included also in the agonist solution. Indeed, by switching barrels, the agonist-containing solution rapidly washed out the TTX and removed the block of voltage-dependent Na^+ currents. In the presence of TTX in the bath perfusion, as well as in the control and agonist perfusion solutions we did not observe unclamped Na^+ currents (see Figure 7.3, 7.4B and 7.5A).

Sensitivity of nicotinic agonist-evoked currents to α-BTX was determined by incubating neurons with 100-500 nM α-BTX for 2-3 hrs prior to recording.

Xenopus oocyte recordings: The experiments with *Xenopus* oocytes were done in collaboration with Ali Haghighi, a graduate student in the department of physiology. The oocytes were prepared, injected and recorded as described by Bertrand *et al.* 1991. The recordings were made 2-3 days after nuclear injection of rat α_7 cDNA and co-injection

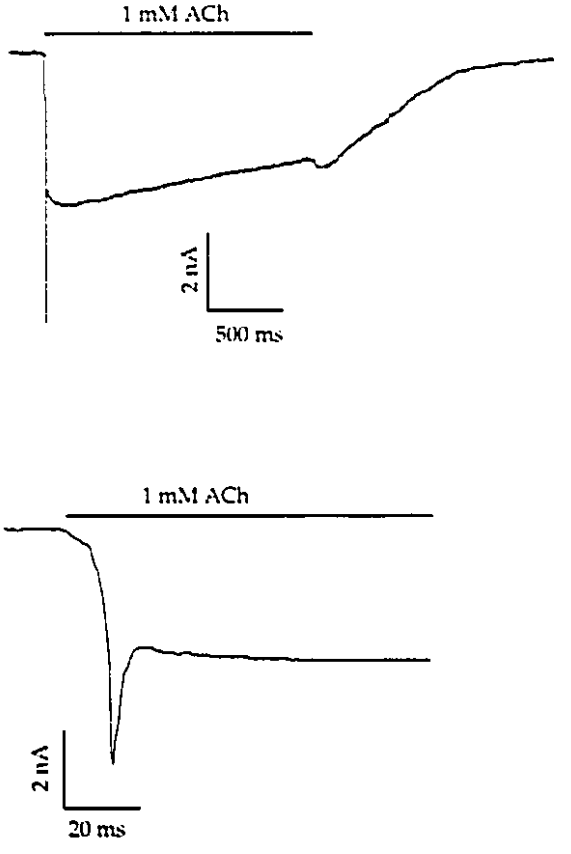

FIGURE 7.1. Unclamped voltage-dependent Na^+ currents evoked by rapid agonist application.

Top: Rapid application of 1 mM ACh on a freshly dissociated SCG neuron evokes a rapidly inactivating current followed by a slowly desensitizing current. Below: same current as above shown on a faster time scale to illustrate the initial rapidly inactivating component. This rapidly inactivating component was eliminated by addition of 0.5 μM TTX in the bath perfusion as well as in the control and agonist perfusion solutions (see Figure 7.3, 7.4B, 7.5A).

of rat $\alpha_3\beta_4$ cDNAs (kindly provided by Dr. Philippe Séguéla, Montréal Neurological Institute, McGill University) into *Xenopus* oocytes. The agonist-evoked currents were measured with a two electrode voltage clamp, built by Mr. John Knowles (Department of Physiology, McGill University). All drugs were dissolved in OR-2 solution (see below) at concentrations indicated in the text. One μM atropine was included in the perfusion solution.

Solutions: Neuronal recordings were done in regular perfusion medium (section **2.3.4.**) to which 500 nM TTX was added, as rapid application of agonists frequently evoked unclamped Na^+ currents. We used our regular intracellular perfusion solution (section **2.3.4.**) or a solution containing 150 mM CsCl, 10 mM HEPES (pH 7.4 adjusted with KOH) (Zhang *et al.*, 1994). In experiments with choline as an agonist, 1 μM atropine (Sigma) was added to the perfusion solutions.

OR-2 solution consisted of 82.5 mM NaCl, 2.5 mM KCl, 1 mM NaH_2PO_4, 1 mM $CaCl_2$, 15 mM HEPES (pH 7.4).

RESULTS

The ACh-evoked current densities increase in cultured SCG neurons and lack rapidly desensitizing kinetics.

Over 7 days of development in culture, P1 rat SCG neurons differentially regulate the expression of their nAChR subunits: the mRNA levels of α_3 increase approximately 2.5 fold; those of α_7 decrease approximately 3 fold; and those of β_2, β_4 and α_5 show little change. High K^+ treatment at day 5 causes a specific increase in α_7 mRNA, while at day 0 it sustains α_7 and causes a 30% increase in α_3 transcript levels (Figure 7.2). To investigate whether these changes in nAChR transcript levels affect the magnitude and/or kinetics of the macroscopic ACh-evoked currents, we used whole-cell voltage clamp techniques to measure ACh-evoked current densities on: 1) freshly dissociated neurons, 2) neurons cultured for 3 days with or without high K^+, and 3) neurons grown for 7 days with or without a 48 hr high K^+ treatment. For these experiments, we applied ACh with fast perfusion (see section **2.3.2.** and experimental procedures) to avoid underestimating

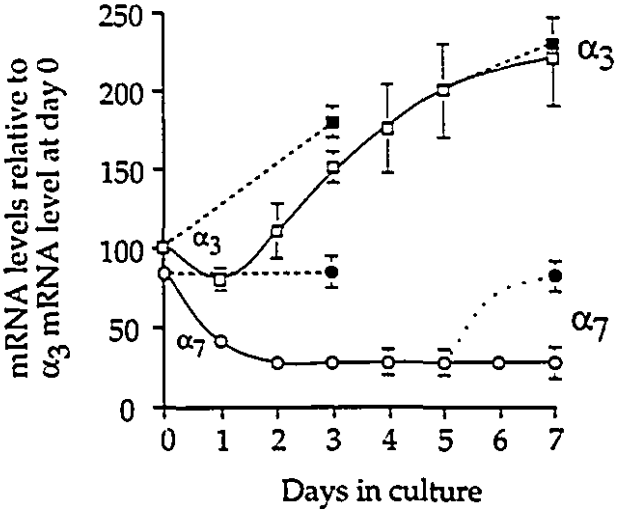

FIGURE 7.2. Summary of the changes in α_3 and α_7 nAChR subunit mRNA levels in cultured SCG neurons over 7 days of development (open symbols) and with high K^+ treatments at Day 0 and Day 5 (filled symbols). α_3 transcript levels increase 2.5 fold from day 0 to day 7, while α_7 mRNA levels decrease 3 fold within 2 days after plating. Membrane depolarization at the time of plating sustains α_7 mRNA levels, while it causes a 30% increase in α_3 mRNA levels by Day 3. Membrane depolarization at day 5 causes a 2-3 fold increase in α_7 mRNA levels, while it has little effect on α_3 mRNA levels. The other nAChR subunits remain unchanged during that time (see Chapter 6).

any rapidly desensitizing components. For measurement of ACh-evoked current densities, we used 100 μM ACh; we also tested 1 mM ACh as it was shown to activate a rapidly desensitizing current on chick ciliary neurons (Zhang *et al.*, 1994).

Figure 7.3 shows the response of a freshly dissociated P1 SCG neuron upon rapid application of 1 mM ACh with whole-cell voltage clamp, and demonstrates that the activation of the current was achieved within less than 5 ms (Figure 7.3; below). The rising phase can be described by first order kinetics, while the desensitizing phase can be described by a double exponential time course with time constants 2 and 3 orders of magnitude slower than that for the rising phase. No rapidly desensitizing component was observed. We found that the peak current densities evoked by 100 μM ACh were not significantly different from those evoked by 1 mM ACh, although the currents evoked by 1 mM ACh activated 4-5 fold faster (Table 7.1).

Figure 7.4A shows the mean ACh-evoked current densities measured over time in culture, either at day 0, 3 and 7. We observed a 2.5 fold increase in the density of ACh-evoked currents on SCG neurons that had developed from day 0 to day 7 in culture. This increase correlates well with the increase in α_3 subunit, but not with the decrease in α_7. In addition, the ACh-evoked current densities measured at day 3 were significantly larger in high K^+-treated neurons than in control neurons, as were the α_3 mRNA levels (Figure 7.2). However, when the neurons were treated with high K^+ at day 5, we observed no difference in the average magnitude of the ACh-evoked current compared to control neurons (Figure 7.4A), despite the 2-3 fold increase in α_7 and the 3-5 fold increase in α-BTX-nAChRs (Chapter 6).

Figure 7.4B shows examples of ACh-evoked currents from a control neuron in culture for 7 days, and from a neuron in culture for the same time but exposed to 40 mM KCl for 48 hrs starting at day 5. We observed no significant difference in the rate of desensitization of the currents evoked from neurons under both culture conditions.

These results indicate that changes in α_7 transcript levels have little effect on the size of the macroscopic ACh-evoked currents on SCG neurons, suggesting that α_7 subunits play little role in these currents. However, the results suggest that α_3 plays an important role in the developmental increase in ACh-evoked currents in culture. A similar

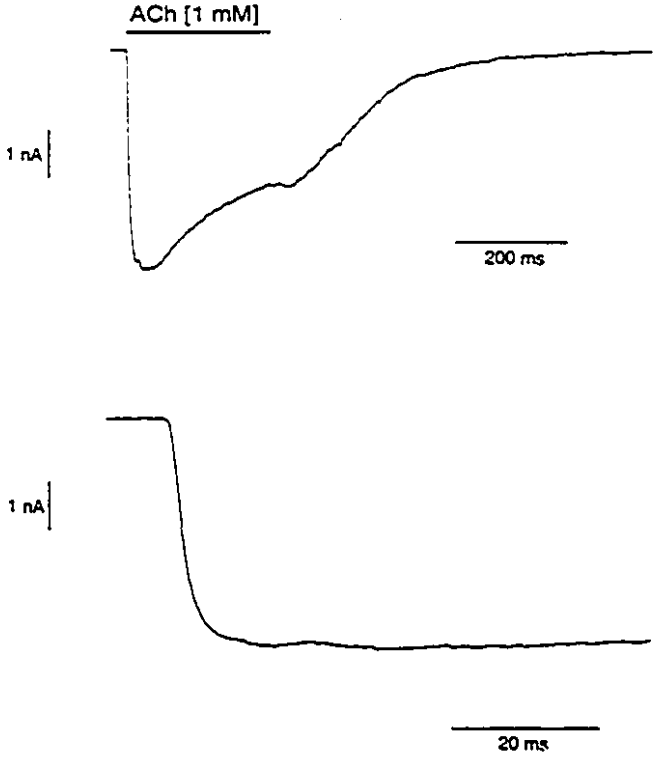

FIGURE 7.3. Whole-cell currents evoked by rapid application of ACh.

Two consecutive whole-cell currents from a P7 SCG neuron, evoked by rapidly applying 1 mM ACh. The ACh was applied for 250 ms; the lower trace shows only the first 80 msec. The currents were recorded at 2 min intervals, filtered at 3 KHz and sampled at 5 KHz. TTX at 0.5 μM was added to both the ACh and perfusion solutions to eliminate unclamped voltage-gated Na^+ currents.

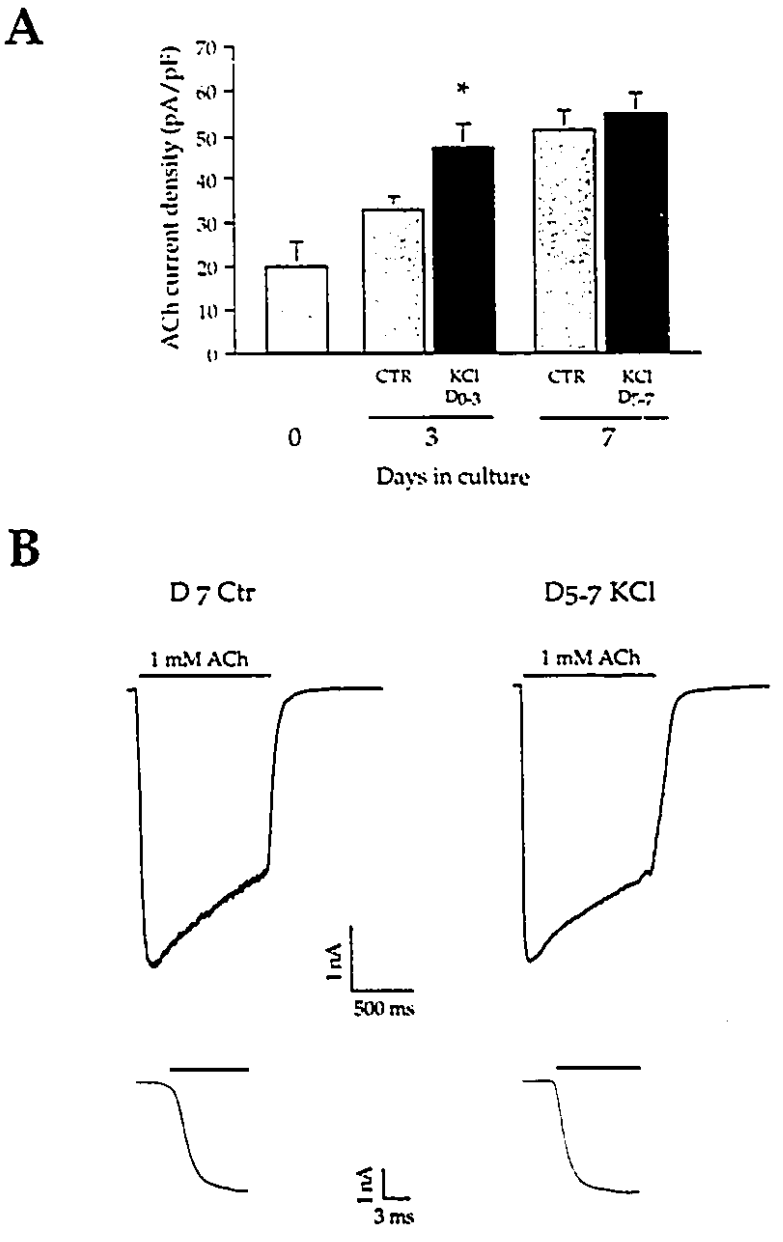

FIGURE 7.4. ACh-evoked current densities correlate with changes in α3 but not α7 transcript levels.

Whole-cell voltage clamp recording from freshly plated neurons (3-16 hrs; n=10), or neurons that have developed for 3 (n=12) and 7 (n=12) days in control culture. Some cultures were treated with high K^+ either at the time of plating (n=12) or at day 5 (n=10). (A) Mean (±SEM) ACh-evoked current densities increase over time in culture at a rate similar to the increase in α3 mRNA (see Figure 7.1). No significant differences between 7 day old control neurons and neurons treated with high K^+ for 48 hrs at day 5. *Neurons treated with high K^+ at the time of plating have significantly larger ACh current densities compared to control neurons ($p<0.005$, t-test), similar to the differences seen in α3 mRNA levels. 100 μM ACh was used to measure ACh-evoked current densities. (B) Representative currents evoked by fast application of 1 mM ACh. Lower traces show the first 15 ms of the response on a faster time scale to illustrate the speed of activation. ACh-evoked currents usually reached 90 % of maximal value within 5-10 ms. No rapidly desensitizating components were observed in the currents either in control- or high K^+-treated neurons at any time in culture or from freshly dissociated neurons. Currents were filtered at 3 KHz and sampled at 5 KHz.

correlation between α_3 mRNA levels and ACh-evoked current densities exists for these neurons during postnatal development *in vivo* (Mandelzys *et al.*, 1994).

Lack of inhibition by α-BTX

The expression of rat α_7 subunit in *Xenopus* oocytes gives rise to a channel whose order of ligand potency is: nicotine > cytisine > DMPP > ACh and whose current is blocked by α-BTX (Séguéla *et al.*, 1993). In chick ciliary neurons and in some rat hippocampal neurons, which both express α_7 (Corriveau and Berg, 1993; Séguéla *et al.*, 1993), an α-BTX sensitive nicotine- and ACh-evoked current has been reported (Alkondon and Albuquerque, 1993; Zhang *et al.*, 1994; Castro and Albuquerque, 1995).

To determine whether a component of the nicotinic-evoked response on SCG neurons is sensitive to α-BTX, we applied 10 to 100 μM nicotine and 100 μM to 1 mM ACh onto control neurons, or neurons that were pre-incubated with 100-500 nM α-BTX for 2-3 hrs (Figure 7.5A). As rat SCG neurons express 3 fold more α_7 mRNA at P14 compared to P1 (Mandelzys *et al.*, 1994), we used neurons from P14 SCG neurons for these experiments.

Figure 7.5B shows that no significant difference was observed in the agonist-evoked current densities between control and α-BTX-treated neurons. Neither did we detect any significant difference in the kinetics for activation or desensitization of the agonist-evoked currents (Table 7.1) between control and α-BTX-treated neurons.

The peak current densities evoked by 100 μM nicotine were 2.5 fold larger than those evoked by 20 μM nicotine, and were comparable to those evoked by 100 μM ACh. As with ACh, the nicotine-evoked currents activated more rapidly with higher concentrations (Table 7.1). All ACh- and nicotine-evoked currents desensitized with a double exponential time course. The faster time constants ranged from 150-250 ms and the slower time constants ranged from 6-10 sec; none of the agonist-evoked currents had rapidly desensitizing kinetics (Table 7.1).

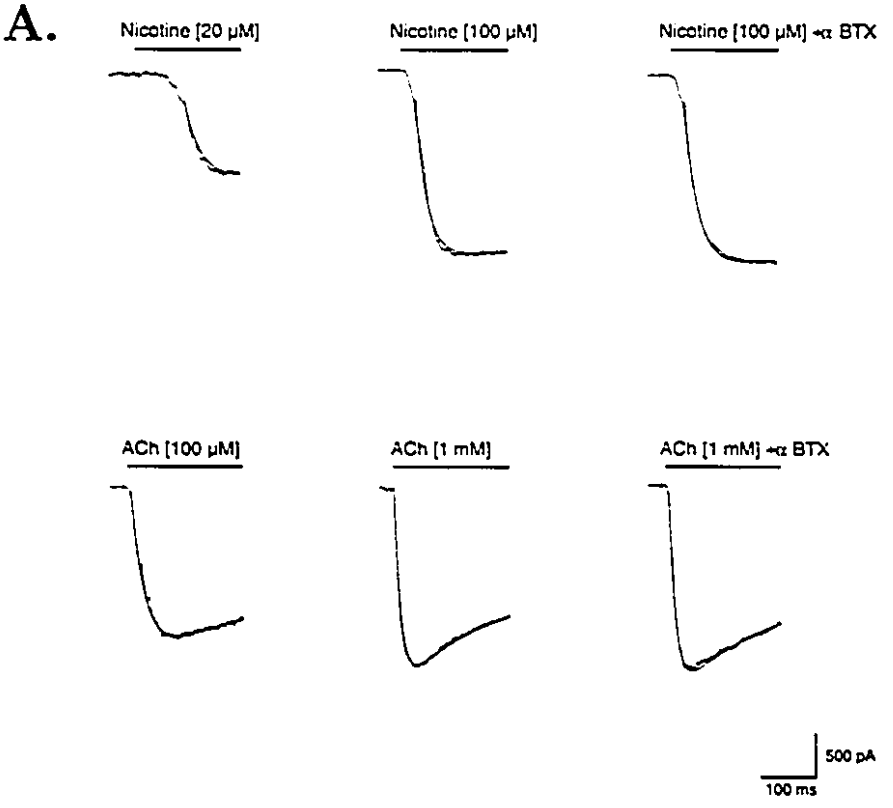

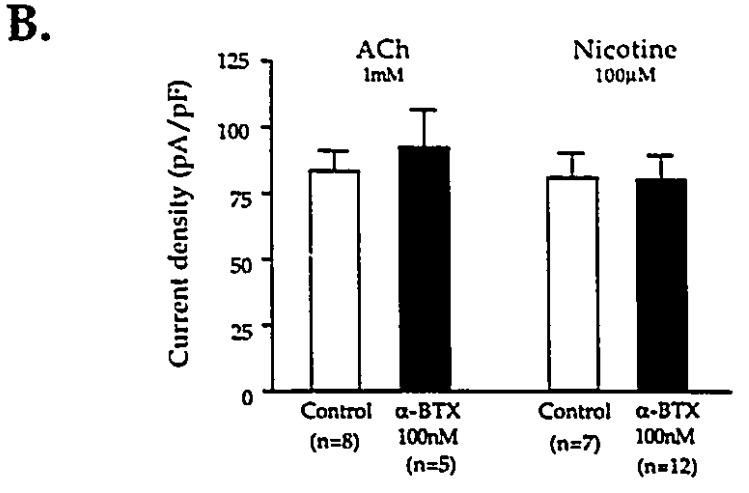

FIGURE 7.5. Lack of effect by α-BTX on ACh- and nicotine-evoked currents. **A.** Whole-cell currents from 6 different neurons; four currents are from neurons in control perfusion and evoked by rapid application of: 20 μM nicotine, 100 μM nicotine, 100 μM ACh, and 1 mM ACh; two currents are from neurons incubated with 10-7M α-BTX for 2 hrs and evoked by rapid application of: 1 mM ACh; and 100 μM nicotine. Each current has been superimposed with a single rising exponential and a double decaying exponential function: A1* (exp[-t/τ1]-1)*(A2*exp[t/τ2]+A3*exp[t/τ3]), where, A1=600pA, τ1=43ms, τ2=185ms, τ3=10815ms, and A2/A3=0.55, for 20 μm nicotine; A1=1920pA, τ1=30ms, τ2=185ms, τ3=10715ms, and A2/A3=0.17, for 100 μm nicotine; A1=1600pA, τ1=34ms, τ2=185ms, τ3=10815ms, and A2/A3=0.31 for 100 μm nicotine and 100 nM α-BTX; A1=1570pA, τ1=27ms, τ2=1725ms, τ3=10825ms, and A2/A3=0.46 for 100 μm ACh; A1=1170pA, τ1=12ms, τ2=162ms, τ3=10825ms, and A2/A3=0.5 for 1 mM ACh; A1=1190pA, τ1=12ms, τ2=175ms, τ3=10715ms, and A2/A3=0.5 for 1 mM ACh and 100 nM α-BTX. The currents were filtered at 2 KHz and sampled at 5 KHz. TTX (0.5 μM) was added to the agonist and perfusion solutions. **B.** Mean ACh and nicotine-evoked current densities with or without preincubation of 100 nM α-BTX. In one group the currents were evoked with 1 mM ACh and in the other with 100 μM nicotine. Bars represent the S.E.M. No significant differences were observed between control and α-BTX- treated neurons.

Table 7.1. Time course of activation and desensitization of ACh- and nicotine-evoked currents with or without α-BTX.

Agonist	Activation		Desensitization			
	Control	10^{-7} M α-BTX	Control		10^{-7} M α-BTX	
	τ	τ	(Af)τf	(As)τs	(Af)τf	(As)τs
ACh 100 μM (n=5)	23 ± 4.4	nd	(0.18) 181 ± 12	(0.82) 8307 ± 154	nd	nd
ACh 1 mM (n=9)	6.9 ± 0.9	6.2 ± 1.4	(0.33) 153 ± 9	(0.67) 7836 ± 187	(0.35) 168 ± 17	(0.65) 7448 ± 254
Nicotine 20 μM (n=6)	38 ± 1.4	nd	nd	nd	nd	nd
Nicotine 100 μM (n=6)	23 ± 3.2	22 ± 3.8	(0.11) 172 ± 24	(0.89) 6327 ± 214	(0.10) 158 ± 29	(0.90) 6432 ± 278

The values (τ) represent the mean (± S.E.M.) time constants (in msec) from equations used to describe the activation and desensitization of the agonist-evoked currents with or without α-BTX (see Figure 7.5). The desensitization kinetics are described by a double exponential decay where (A) represents the relative amplitude for the fast (f) and slow (s) components, respectively.

Choline as an agonist for α_7 receptors in *Xenopus* oocytes

The above results suggest that the α-BTX-nAChR does not gate significant ACh- or nicotine-evoked currents on SCG neurons. One possibility is that another ligand activates preferentially this receptor. The α-BTX-nAChR is believed to be expressed primarily in non-synaptic membranes or perhaps "peri-synaptically" in chick ciliary neurons (Jacob and Berg, 1983; Loring *et al.*, 1985; Sargent and Wilson, 1995). Thus, synaptically released ACh may not be able to activate this receptor, even if the ACh diffuses outside the synaptic cleft, as it is rapidly degraded by acetylcholinesterase. One of the byproduct of ACh degradation is choline; during high frequency activity, choline may accumulate and perhaps diffuse outside of the cleft. We hypothesized that choline could be a ligand for the α-BTX-nAChR. To test this hypothesis, we expressed a cDNA for α_7 into *Xenopus* oocytes, and measured their sensitivity to choline.

Figure 7.6A shows that 5 mM choline activates α_7 receptors expressed in *Xenopus* oocytes and is at least as potent as 100 μM ACh (see also Table 7.2); these currents are blocked by 100 nM α-BTX. It is noteworthy that much of the initial desensitizing component of these currents is likely to arise from a Ca^{2+}-activated Cl^- conductance (Séguéla *et al.*, 1993; Gerzanich *et al.*, 1994).

In contrast to α_7 receptors, choline was a poor agonist for $\alpha_3\beta_4$ receptors expressed in

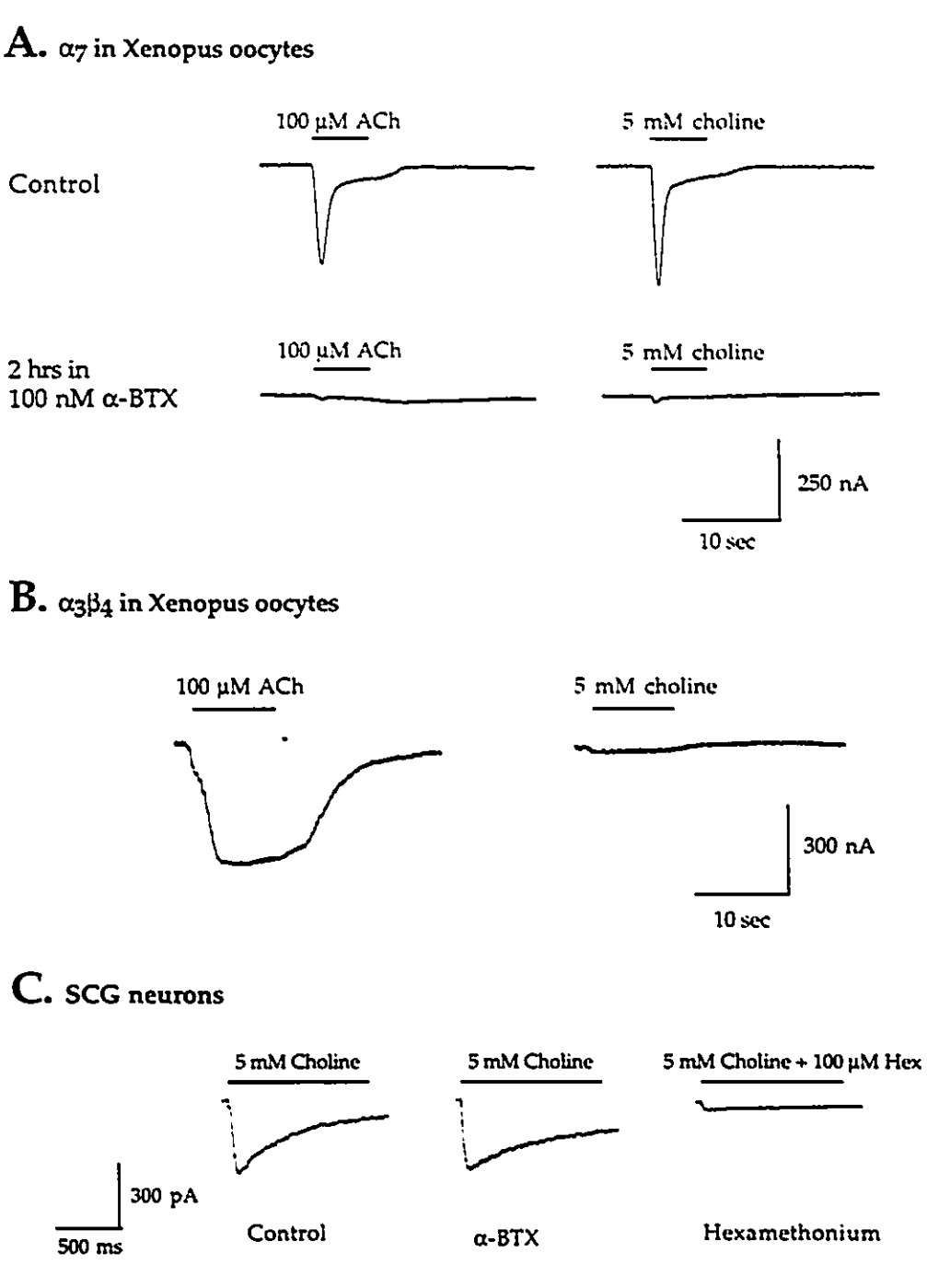

FIGURE 7.6. Choline as an agonist on α7 receptors in Xenopus oocytes and on nAChRs in SCG neurons.

(A) Inward currents recorded from a Xenopus oocyte injected 2 days before with cDNA encoding α7. The currents were evoked with 100 μM ACh or 5 mM choline and recorded with two electrode voltage-clamp at -60mV holding potential. Both the ACh- and choline-evoked currents were blocked by incubating the oocyte in 100 nM α-BTX for 2 hrs. (B) Inward currents recorded from a Xenopus oocyte co-injected 2 days before with cDNAs encoding α3 and β4. Currents were evoked as in A. Currents were sampled at 100 Hz. (C) Currents evoked by 5 mM choline on SCG neurons. Whole-cell recordings from 3 different neurons; left: control; middle: after 2hrs of preincubation with 100 nM α-BTX; right: with 100 μM hexamethonium in the perfusion and agonist solutions. The holding potential for all three neurons was -60mV. The currents were filtered at 3 KHz and sampled at 5 KHz. TTX (0.5 μM) was included in the agonist and perfusion solutions.

Xenopus oocytes, whereas ACh evoked large inward currents: choline is approximately 20 fold less potent on $\alpha_3\beta_4$ receptors than is 100 μM ACh (Figure 7.5B: Table 7.2).

Choline as an agonist on SCG neurons

As choline is a better agonist on α_7 receptors than on α_3/β_4 receptors in *Xenopus* oocytes, we tested the action of choline on voltage-clamped SCG neurons to determine if we can detect an α-BTX sensitive choline-evoked current on these neurons. Figure 7.6C shows that 5 mM choline activates inward currents on rat SCG neurons with a time course significantly slower than that activated by ACh. The peak choline-evoked current densities were only approximately 5-15% of those activated by 100 μM ACh, which is similar to the ratios that we observe for $\alpha_3\beta_4$ receptors expressed in *Xenopus* oocytes (Table 7.2). Pre-treatment with 100 nM α-BTX for 2-3 hrs had no effect on these choline-evoked inward currents, whereas 100 μM hexamethonium reduced the peak current by 80% (Figure 7.6C). These results indicate that most if not all of the choline-evoked currents on SCG neurons are gated by nAChRs that are insensitive to α-BTX.

Table 7.2 Ratios of choline/ACh sensitivity on α_7 and α_3/β_4 nAChRs in *Xenopus* oocytes and on SCG neuron nAChRs.

	Xenopus oocytes*		SCG neurons+	SCG neurons#	
	α_7	α_3/β_4	nAChR	control	α-BTX
Ratio Choline-/ACh-evoked currents	1.3 ±0.2 (7)	0.06 ±0.015 (6)	0.10 ±0.05 (10)	0.13 ±0.02 (15)	0.14 ±0.02 (14)

* 5 mM choline and 100 μM ACh were applied on the same *Xenopus* oocytes expressing either α_7 or α_3/β_4 nAChRs. + 5 mM choline was applied on P1 SCG neurons with fast perfusion, and the mean evoked current density was divided by the mean ACh (100 μM)-evoked current density on P1 SCG neurons (Figure 7.4A). # For the experiment with α-BTX, 1 mM choline and 30 μM ACh were co-applied sequentially by pressure ejection from a double-barrel puffer on control neurons and on neurons treated with 500 nM α-BTX. This table shows that choline is a better ligand for α_7 receptors than for α_3/β_4 receptors in *Xenopus* oocytes, while choline is a poor ligand for SCG neuron nAChRs. In the presence of α-BTX, the ratio of choline/ACh sensitivity on the neurons is not significantly different compared to control neurons ($P>0.1$, t-test).

Low concentration of ACh (e.g. 30 μM) was shown not to activate α-BTX sensitive currents on chick ciliary neurons (Zhang *et al.* 1994), and choline activates α_7 receptors better than $\alpha_3\beta_4$ receptors on *Xenopus* oocytes (Figure 7.6A and 7.6B). Therefore, we tested whether the ratio of ACh (30 μM)/choline (1 mM)-evoked currents would be affected by pre-incubation of α-BTX. We found no significant difference in this ratio between control neurons and neurons pre-incubated with α-BTX (Table 7.2). These results suggest either that 1) SCG neurons do not express currents that behave similar to α_7 receptors in *Xenopus* oocytes, or 2) this current is too small to resolve with our recordings, and is masked by the large ACh-evoked currents that are insensitive to α-BTX.

DISCUSSION

In this chapter we have measured the relationship between the changes in nAChRs observed at the mRNA level with changes in macroscopic ACh-evoked currents on cultured SCG neurons. Our major findings are that the increase in ACh-evoked current densities correlate well with the increase in α_3 transcript, while changes in α_7 transcript cause little, or no, effect on the macroscopic ACh-evoked currents. Finally, the nicotinic agonist-evoked currents on SCG neurons have little or no sensitivity to α-BTX.

Relationship between α_3 nAChR subunit transcript levels and ACh-evoked currents.

The only nAChR transcript that increases significantly in cultured SCG neurons is α_3, and we find a similar increase in ACh-evoked current densities. This finding suggests that the increase in α_3 gene expression causes an increase in functional nAChRs: if so then the α_3 subunit may be rate-limiting for the assembly of nAChRs on neonatal SCG neurons. A similar correlation exists *in vivo* (Mandelzys *et al.*, 1994). In addition, we observed that the mean ACh-evoked current density on neurons cultured for 3 days with high K^+ was 1.4 fold larger than that on control neurons (Figure 7.4A), and we observed a 1.3 fold increase in α_3 transcript levels in neurons

treated with high K^+ at day 1 (Figure 7.2). This additional correlation adds further support to the concept that expression of α_3 in these neurons is a rate-limiting event for the expression of functional nAChRs.

As nAChRs are believed to comprise 2 α and 3 ß subunits (Anand *et al.*, 1991; Cooper *et al.*, 1991), the concept that α_3 is rate-limiting for nAChR appearance implies that the ß subunits are expressed in excess in these neurons at this stage of development. Interestingly, Hill *et al.* (1993) found that the $ß_2$ protein is localized in large excess in the cytoplasm compared to the plasma membrane of CNS neurons. In ciliary and choroid cells of chick ciliary ganglia, prevalent intracellular staining with MAb35 nAChR antibody has been observed (Jacob *et al.*, 1986; Jacob, 1991). In fact, a large proportion of the intracellular pool of nAChR subunits is degraded without ever reaching the surface membrane of cultured muscle cells (Merlie, 1984) or chick ciliary neurons (Stollberg and Berg, 1987). These internal pools could, in part, consist of excess single nAChR subunits that have not assembled into functional receptors, due to the limited availability of an essential subunit. The existence of a rate-limiting subunit in ligand-gated multimeric ion channels would allow neurons to modify the functional expression of their ligand-gated receptors by controlling only one gene.

Lack of relationship between changes in α_7 transcript levels and ACh-evoked currents and lack of α-BTX sensitivity of these currents.

While the ACh-evoked currents increase 2.5 fold over a week in culture, the levels of α_7 mRNA decrease 3 fold, suggesting that the α_7 subunit does not contribute significantly to the macroscopic ACh-evoked currents in rat SCG neurons. In addition, increasing α_7 mRNA levels by 2-3 fold with membrane depolarization at day 5 had no effect on the magnitude or kinetics the ACh-evoked currents on these neurons. Even though these neurons express an α-BTX-nAChR (Chapter 6; Fumagalli *et al.*, 1976), we did not detect any effect by α-BTX on the ACh-evoked currents on these neurons. Several studies have reported a similar dissociation between α-BTX binding and nAChR blockade (Nurse and O'Lague, 1975; Duggan *et al.*, 1976; Brown and

Fumagalli, 1977; Patrick and Stallcup, 1977; Carbonetto *et al.*, 1978; Ravdin and Berg, 1979; Chiappinelli, 1985; Lipton *et al.*, 1987; Mulle and Changeux, 1990; Sucher *et al.*, 1990; Zhang and Feltz, 1990). However, a recent study has indicated that a rapidly desensitizing α-BTX sensitive ACh-evoked current could be detected on chick ciliary neurons (Zhang *et al.*, 1994); this would suggest that previous studies had missed such a current because of the use of slow agonist applications. However, by using a rapid agonist application system, we did not detect such a current on neonatal rat SCG neurons.

Thus, our results contrast those of chick ciliary neurons (Zhang *et al.*, 1994), which have been shown to contain the same 5 subunits as SCG neurons, including significant levels of α_7 mRNA (Corriveau and Berg, 1993), and to contain α-BTX-nAChRs (Jacob and Berg, 1983; Loring *et al.*, 1985); it is unclear where the discrepancy lies. In chick ciliary neurons, α_7 does not associate with any of the known nAChR subunits (Vernallis *et al.*, 1993), but possibly associates with other unidentified proteins. There is precedent evidence that α_7 can co-assemble with other subunits. In chick brain and retina, α_7 has been shown to co-assemble with an α_8 subunit, a subunit not yet found in rats (Schoepfer *et al.*, 1990; Keyser *et al.*, 1993; Gotti *et al.*, 1994). In chick sympathetic neurons, the ACh-evoked currents are insensitive to α-BTX, but treatment with antisense α_3 oligonucleotides produced ACh-evoked currents on these neurons that could be partially blocked by α-BTX, suggesting that α_7 had assembled with other subunits to form nAChRs (Listerud *et al.*, 1991). In addition, in *Xenopus* oocytes, the α_7 subunit can replace the muscle α subunit and co-assemble with the other muscle nAChR subunits (ß,γ and σ) to form a functional receptor (e.g. α_7/ß/γ/σ; Helekar *et al.*, 1994).

Another possibility is that α-BTX-nAChRs on SCG neurons are functionally different on SCG neurons. It has been shown that prolyl isomerase activity is essential for the formation of functional homomeric ligand-gated ion channels in *Xenopus* oocytes (e.g. α_7 nAChRs or 5-HT_3 receptors; Helekar *et al.*, 1994).

Therefore, it is conceivable that by co-assembling with different proteins, or by

undergoing differential post-translational modifications. α_7 assembles into receptors with different functions.

However, the report by Zhang *et al.* (1994) of such a large α-BTX sensitive ACh-evoked current, with such rapid desensitization kinetics is surprising. The peak current for the rapidly desensitizing component evoked by 20 μM nicotine was 5-10 nA (249 pA/pF), an order of magnitude larger than for the slowly desensitizing component (around 0.3-1 nA, or 26 pA/pF). The slowly desensitizing component was accounted for by heteromeric nAChRs on these neurons (Zhang *et al.*, 1994). The time constant of desensitization of this α-BTX sensitive component was 11 ms. On these neurons, the α-BTX-nAChRs were shown to be localized on extra-synaptic or peri-synaptic membranes (Jacob and Berg, 1983; Loring *et al.*, 1985; Sargent and Wilson, 1995). Being away from the synapse suggests that it is not likely to receive synaptically released ACh rapidly. Thus, the functional significance of this rapidly desensitizing current is unclear.

It should be noted that the α_7 receptor expressed in *Xenopus* oocytes does not desensitize very rapidly (Séguéla *et al.*, 1993; Figure 7.6A). The Ca^{2+}-activated Cl^- conductance inactivates within hundreds of msec, but the remaining inward current still flows for several hundreds of milliseconds to seconds during ACh application. Thus, if the α-BTX sensitive current on chick ciliary neurons is gated by an α_7 receptor, it means that this receptor has a remarkably faster rate of desensitization than in *Xenopus* oocytes.

Furthermore, it should be pointed out that when we omitted to add TTX in the perfusion solution, we observed in the ACh responses a large rapidly inactivating component that was very similar to that reported by Zhang *et al.* (1994) (Figure 7.1). However, in the presence of TTX this current disappeared indicating that is was due to unclamped voltage-dependent Na^+ currents. Moreover, if we added TTX in the perfusion solution, but omitted the TTX in the agonist solution, we still evoked unclamped Na^+ currents, since the rapid perfusion system washed off the TTX

containing solution around the recorded neuron. Zhang *et al.* (1994) tested the TTX sensitivity of this rapidly desensitizing current on 5 neurons and showed that it was not affected; however the authors did not state that they included the TTX in the agonist solution. It is therefore possible that this current was evoked by unclamped Na^+ currents. On the other hand, the fact that α-BTX blocked this current would be inconsistent with it being an unclamped Na^+ current. However, Zhang *et al.* (1994) also reported the surprising finding that α-BTX blocked 30–45 % of the slowly desensitizing nicotine-evoked current on these neurons. It has been shown that some lots of α-BTX can be contaminated with neuronal-BTX (see Loring and Zigmond, 1988), which is a potent blocker of nicotinic synaptic transmission on these neurons. Conceivably, the lot of α-BTX used in this study contained some neuronal-BTX, and by blocking part of the nicotine-evoked response, the threshold for activating unclamped Na^+ currents was not reached.

In cultured rat hippocampal neurons, a much smaller rapidly desensitizing α-BTX sensitive current (e.g. 100–400 pA) has been observed with fast perfusion (Zorumski *et al.*, 1992; Alkondon and Albuquerque, 1993), and has been shown to be carried largely by Ca^{2+} (Castro and Albuquerque, 1995). This current was found on approximately 80% of the neurons and to have a desensitization time constant of approximately 27 ms (Alkondon and Albuquerque, 1993). Interestingly, the neurons that expressed this current had little if any slowly desensitizing ACh-evoked current. If the α-BTX sensitivity of this current is due to α_7, this finding suggests either that only α_7 is expressed on these neurons, or that α_7 co-assembles with other nAChR subunits expressed in the rat hippocampus, such as α_2, α_4 and/or β_2 (Wada *et al.*, 1989). The difference in the types of nAChR subunits expressed by hippocampal neurons compared to SCG neurons might favour incorporation of α_7 into heteromeric nAChRs that are consequently sensitive to α-BTX.

This possibility is consistent with the results obtained by Puchacz *et al.* (1994) who over-expressed the rat α_7 gene in SH-SY5Y cell lines. These cells express nAChRs

and α-BTX-nAChRs at low levels, and express small nicotine-evoked currents (e.g. 100-250 pA) that activate and desensitize slowly and are insensitive to α-BTX. After over-expression of α_7, these cells had 30 fold more α-BTX binding; they also had nicotine-evoked currents (100-1000 pA) that rapidly desensitized and that were blocked by α-BTX. However, they no longer expressed slowly desensitizing nicotine-evoked currents. These results suggest that α_7 co-assembled with other native subunits to give rise to a rapidly desensitizing current, sensitive to α-BTX.

What is the role of α_7 in SCG neurons?

The role for the α_7 gene product in rat sympathetic neurons remains unclear. It seems likely that it codes for a subunit that contributes to the α-BTX-nAChR (Chapter 6; Shoepfer *et al.*, 1990; Couturier *et al.*, 1990b; Séguéla *et al.*, 1993). However, α-BTX does not block cholinergic transmission at synapses on rat SCG neurons (Nurse and O'Lague 1975; Brown and Fumagalli 1977; Chiappinelli 1985); furthermore, the α-BTX-nAChRs are not preferentially localized at synapses, but have an extrasynaptic distribution (Jacob and Berg 1983; Fumagalli and DeRenzis 1984; Loring *et al.* 1985; Loring *et al.* 1988; Sargent and Wilson, 1995). Taken together, this suggests that the α-BTX-nAChR may not be directly involved in one to one synaptic transmission between pre-ganglionic and post-ganglionic neurons. One possibility, however, is that the α-BTX-nAChR plays a modulatory role by activating Ca^{2+}-dependent processes. The α_7 receptors expressed in *Xenopus* oocytes are highly permeable to Ca^{2+} (Séguéla *et al.*, 1993), and the α-BTX-nAChR in chick ciliary neurons promotes Ca^{2+} influx, which in turn may affect process outgrowth (Vijayaraghavan *et al.*, 1992; Pugh and Berg, 1994). As a result of acetylcholinesterase in the synaptic cleft, it is possible that, after a burst of synaptic activity, choline accumulates transiently (possibly reaching mM concentrations), diffuses outside the cleft, and acts on the α-BTX-nAChRs in the extrasynaptic membrane. However, we did not resolve a choline gated-current that could be blocked by α-BTX on SCG neurons; nonetheless, we show that choline gates α_7 receptors in *Xenopus* oocytes (Figure 7.6).

If the α-BTX-nAChR on SCG neurons does gate a small Ca^{2+} current, it is possible that this current was not resolved in our recordings because the α-BTX-insensitive ACh response on SCG neurons is so large. α-BTX takes time to block the α-BTX-nAChRs, so we could not measure ACh-evoked currents with or without α-BTX on the same neurons. Thus, if the current flowing through the α-BTX-nAChR was less than 5% that of the current flowing through the other nAChR, and had slow kinetics, it would be difficult to detect. Further work needs to be done to determine whether this receptor gates a current on SCG neurons, and whether its activation affects Ca^{2+}-dependent processes. Measuring changes in Ca^{2+} levels by Ca^{2+} imaging on voltage-clamped neurons may allow resolution of such potential current.

It is attractive to consider that activation of α-BTX-nAChRs by choline in the vicinity of active synapses would result in a local increase in intracellular Ca^{2+} concentration post-synaptically, which could selectively modulate the efficacy of these activated synapses. Similarly, if α-BTX-nAChRs are located on the presynaptic cholinergic terminals, choline could act on these presynaptic receptors to elevate Ca^{2+} concentrations in the terminals and affect transmitter release.

Incidentally, the α_7 transcript levels were up-regulated by choline treatment on these neurons (Chapter 6). However, α-BTX did not block the choline effect indicating that choline does not up-regulate α_7 by causing Ca^{2+} influx through the α-BTX-nAChR. Instead, it is likely that choline promotes Ca^{2+} release from internal stores through an unknown mechanism (Koike *et al.*, 1989).

The regulation of α_7 mRNA by membrane depolarization in SCG neurons, its regulation during synaptogenesis in muscle (Corriveau *et al.*, 1995), its developmental increase during critical stages of synaptogenesis in the vertebrate brain (Couturier *et al.*, 1990b), and the high permeability to Ca^{2+} of the α_7 receptor (Séguéla *et al.*, 1993) suggest that this receptor plays a role in cellular events related to synapse formation. Determining its precise function may help elucidate the role of nicotinic synaptic transmission in the CNS where this subunit is highly expressed.

Chapter 8

General Discussion and Conclusion

In my thesis, I investigated factors that control the extension of dendrites and the expression of nAChRs on peripheral neurons. My main findings are: 1) satellite cells inhibit sensory neurons of the rat nodose ganglion from extending dendrites and induce them to acquire a unipolar morphology; 2) P1 nodose neurons are capable of extending dendrites in culture in the absence of ganglionic satellite cells and in the presence of NGF; 3) in the presence of BDNF and/or NT-3, nodose neurons retain properties of sensory neurons; 4) as nodose neurons extend dendrites the density of functional nAChRs on their somatodendritic domains increase; 5) in cultured rat neonatal sympathetic neurons, four nAChR subunit transcripts and functional nAChRs are expressed as *in vivo*; 6) the α_7 nAChR subunit expression is dependent on membrane depolarization and is regulated through a CaM kinase pathway; 7) changes in ACh-evoked current densities on SCG neurons correlate with changes in mRNA levels for α_3; 8) changes in α_7 transcript levels correlate with changes in α-BTX-nAChRs on the surface of the neurons but do not affect macroscopic ACh-evoked currents.

I have already discussed these results in details in previous chapters, therefore, in this discussion, I would like to conclude with a hypothesis for one of the mechanisms that up-regulates neurotransmitter receptor expression on neurons.

In Chapter 4, I showed that the increase in ACh-evoked current densities on nodose neurons correlated with the extent of dendrite outgrowth. Furthermore, we find a temporal correlation in the expression of these two postsynaptic elements (Chapter 3; Mandelzys *et al.*, 1990; Mandelzys and Cooper, 1992). In the presence of different neurotrophins, nodose neurons express nAChRs at a density that also correlates with the extent of dendrite outgrowth (Chapter 5). For example, in the presence of BDNF, nodose neurons express low density of ACh-evoked currents and do not extend much dendrites, whereas

NGF induces many neurons to extend dendrites and to express large ACh-evoked currents (Chapter 5). These observations provide circumstantial evidence that dendrite outgrowth and up-regulation of nAChR expression are, in some way, linked together.

The issue is whether 1) dendrite extension and nAChR expression are two separate processes and that the extrinsic factors, such as NGF, influence each process separately; or 2) the two processes are not independent, but in some way, the expression of the postsynaptic receptors is a consequence of the extension of dendrites.

Based on the results from my thesis, I favour the latter, that is, that the extrinsic influence, NGF, does not influence nAChR expression directly, but rather causes the neurons to extend dendrites, and as a result, this triggers some intrinsic mechanism that leads to an up-regulation of nAChRs and maybe other proteins needed for synapse formation.

Before discussing this hypothesis, I discuss the findings that nodose neurons express significant levels of nAChR transcripts *in vivo* in order to emphasize that the initial expression of nAChRs on nodose neurons is likely to occur by a different mechanism than the one that up-regulates the receptor density when the neurons acquire a dendritic-axonal polarity.

ACh-evoked currents and nAChR transcript levels in neonatal nodose neurons

We showed that nodose neurons express nAChR genes *in vivo*: at birth, the neurons contain 6 different nAChR transcripts: α_3, α_5, α_7, β_2, β_3 and β_4 (Chapter 6; see also Mandelzys, 1992). Surprisingly, most freshly dissociated neurons did not have ACh-evoked currents, and in those that did, the currents were small. A number of possibilities can be offered to explain this difference. First, as discussed in Chapter 5, there is good evidence to indicate that sensory neurons express nAChRs on their terminals (Diamond, 1955, 1959; Gray, 1959; Paintal, 1964; Esplin *et al.*, 1972; Chesselet, 1984; Rowell *et al.*, 1987; Swanson *et al.*, 1987; Nordberg *et al.*, 1989; Mulle *et al.*, 1991). Therefore, the fact that little or no ACh-evoked currents were detected on the cell bodies might be due to the lack of nAChR targeting to somata membranes in these neurons *in vivo*. The nAChR transcripts in nodose neurons are expressed at lower levels compared to SCG neurons,

except for β_2. The presence of low levels of nAChR transcripts in the neurons may be sufficient to supply nAChRs for the axonal terminals.

Second, it is also possible that nAChR transcript levels have little correspondence to the number of functional receptors on the cell surface. For example, the evidence of a large intracellular pool of receptors (see Jacob *et al.*, 1986; Stollberg and Berg, 1987; Hill *et al.*, 1993) and of silent receptors on the plasma membrane (see Margiotta *et al.*, 1987b) provide good reasons to believe that differences in mRNA levels may not reflect in similar differences in functional receptors. However, we found a good correlation between the increase in ACh-evoked currents and the increase in α_3 mRNA levels in SCG neurons (Chapters 6 and 7). This finding emphasizes the problem of regulating gene expression of multimeric ligand-gated receptors, and offers the possibility that neurons control functional expression of these multimeric receptors by regulating expression of a rate-limiting subunit.

A third possibility is that nAChRs are not preferentially targeted to the terminals and are destined to cell body membranes, but their number is limited by the low amount of α_3 subunits compared to the total amount of ß subunits. Indeed, the levels of α_3 transcripts in nodose neurons were much lower than in SCG neurons (Chapter 6). Therefore, α_3 may be a rate limiting subunit for the assembly of functional nAChRs on nodose neurons.

A fourth possibility is that nodose neurons are heterogeneous with respect to nAChR expression, and only those neurons which have detectable small ACh-evoked currents are those that express nAChR genes. Heterogeneity may also exist in the types of nAChR transcripts that are present in different nodose neurons; for instance, all neurons could express β_2, but only a few express α_3. Therefore, the nodose neurons that express both subunits (and/or β_4) could be the ones that have small ACh-evoked currents, whereas those that lack ACh-evoked currents would be missing one essential nAChR subunit, such as α_3.

If the expression of nAChR transcripts in sensory neurons (see also Boyd *et al.*, 1991; Zoli *et al.*, 1995) does not plays a role in nicotinic function, the activation of their transcription may have been a consequence of a common mechanism that turned on

nAChR gene expression in most peripheral neurons during neurogenesis (Zoli *et al.*, 1995; see Schoenherr and Anderson, 1995). Afterward, the lack of developmental increase in the transcription of some of these genes (particularly α_3) during neuronal maturation of sensory neurons could have rendered this initial low level expression irrelevant to nicotinic function.

What increases functional nAChR expression on somatodendritic domains of nodose neurons?

In Chapter 5, I proposed 5 possible mechanisms that could increase the functional density of nAChRs on nodose neurons. Below, I discuss each of these possibilities, and incorporate in this discussion some of my findings on the regulation of nAChR gene expression in SCG neurons (Chapter 6 and 7).

1) *Receptor modulation:* NGF affects the modulation of nAChRs, such as an increase in gated currents due to protein kinase activity, or an increase in receptor incorporation, which gives rise to larger ACh-evoked currents.

2) *Activity increases nAChR gene expression:* As nodose neurons form functional synapses in these cultures, electrical activity up-regulates receptor expression.

3) *NGF increases nAChR gene expression:* NGF directly regulates nAChR gene expression through a *trk*A-mediated pathway.

4) *Change in receptor targeting:* the removal of satellite cells alters the morphology of the neurons, which in turn changes the targeting of nAChRs to somatodendritic domains, instead of the nerve terminals, without affecting nAChR gene expression.

5) *Intrinsic regulation of nAChR genes associated with dendrite outgrowth:* The elaboration of dendrites by nodose neurons produces some intrinsic signals in the neurons to express more nAChRs to supply the increasing postsynaptic membrane.

1) Receptor modulation

A number of studies have shown that changes in the magnitude of macroscopic ACh-evoked currents can arise from receptor modulation (Berg *et al.*, 1989). Margiotta *et al.*

(1987b) demonstrated that a cAMP-dependent mechanism can increase ACh sensitivity by 2-3 fold within minutes to hours in cultured chick ciliary neurons. Role and colleagues showed that soluble factor released by pre-ganglionic neurons gives rise to a 10 fold increase in ACh sensitivity within 1-4 days in cultured chick sympathetic neurons (Role, 1988; Gardette *et al.*, 1991). These changes in ACh sensitivity could be accounted for by changes in single channel properties, as well as an increase in functional receptor incorporation at the surface membrane. Furthermore, Haivorsen *et al.*, (1991) showed that an eye extract regulates ACh sensitivity, whereas it does not affect nAChR transcript levels (Corriveau and Berg, 1994).

Similar extrinsic influences are likely to modulate nAChR function in nodose neurons. However, the increase in ACh-evoked current densities observed on nodose neurons developing in culture is slow. The neurons must develop for several days before this increase in macroscopic ACh-evoked currents becomes significant. This time course seems inconsistent with an event like phosphorylation of the receptors. We cannot exclude, however, that protein kinase activity changes slowly in these neurons as they develop in culture. Measuring ACh-evoked currents at the single channel level may help determine whether receptor function is changed in these neurons as they develop dendrites.

2) **Activity and nAChR expression**

We found that membrane depolarization of cultured SCG neurons had little effect on the magnitude of the ACh-evoked currents. In addition, the transcript levels of α_3, α_5, β_2 and β_4 were not significantly changed. As nodose neurons express the same subunits, we might expect that activity does not regulate expression of those nAChR subunit genes in nodose neurons. In contrast to the lack of effect of membrane depolarization on α_3, α_5, β_2 and β_4 expression, we found that α_7 mRNA levels and α-BTX binding increased with membrane depolarization. The levels of α_7 in nodose neurons are much lower compared to SCG neurons; it will be interesting to determine whether synaptic activity in nodose cultures increases α_7 mRNA levels and α-BTX binding. However, based on the lack of significant difference in macroscopic ACh-evoked currents on SCG neurons, with or without high K^+ (Chapter 7), I do not expect that this potential increase in α_7 will affect

the macroscopic ACh-evoked currents on nodose neurons.

3) NGF and nAChR gene expression

We find an 8 fold increase in the mean ACh-evoked currents on nodose neurons grown with NGF compared to neurons grown in absence of neurotrophin (Chapter 5; see also Mandelzys and Cooper, 1992). Does this mean that NGF regulates nAChR gene expression directly in nodose neurons? In Chapter 6, we did not observe any change in the expression of nAChR transcripts in SCG neurons when we increased NGF concentration, or when we treated the neurons for 48 hrs with an inhibitor to *trk* receptors. These results suggest that NGF does not regulate nAChR gene expression in SCG neurons, at least not in the short term (48 hrs). In the long term, it is difficult to determine whether NGF regulates nAChR expression in SCG neurons, as they depend highly on NGF for survival. From these results, it is tempting to consider that NGF does not *per se* regulate nAChR gene expression in nodose neurons as well. If so, how might NGF increase nAChRs on nodose neurons? I speculate that the effects of NGF on nAChR expression are indirect: NGF promotes nodose neurons to acquire a dendritic-axonal polarity; this change in polarity affects gene expression and perhaps targeting of nAChRs (see below).

4) Change in receptor targeting

As mentioned above, there is good evidence that sensory neurons have nAChRs on their nerve terminals, consistent with the fact that they have little ACh-evoked currents on their somata. One possibility is that the change in neuronal morphology of nodose neurons cultured without satellite cells alters the targeting of nAChRs: when the neurons become multipolar and acquire a dendritic-axonal polarity, the nAChRs are targeted to the somatodendritic domains rather than to the terminals. Indeed, targeting mechanisms are intimately related to neuronal polarity (Kelly and Grote, 1993). In the presence of satellite cells, the cytoskeletal properties of a pseudo-unipolar neuron may promote the delivery of transport vesicles containing nAChRs to the bifurcating axon. When satellite cells are removed, nodose neurons extend several axons, and begin to express more nAChRs on

the surface of their cell body, even without adding NGF (Mandelzys and Cooper, 1992). Conceivably, the cytoskeletal properties of these multi-axonal neurons have been altered, so that delivery of transport vesicles containing nAChRs is no longer preferentially targeted to axonal terminals.

If sensory neurons express nAChRs at their terminals, and if a change in targeting is involved in re-directing nAChRs to somatodendritic domains of these newly polarized nodose neurons, one question remains: Can the amount of receptors made to supply the terminals of sensory neurons be sufficient to supply the somatodendritic domains of these newly polarized neurons? Considering the difference in surface area of both regions, it would appear that the supply might be insufficient without an increased production of nAChRs.

5) **Intrinsic regulation of nAChR genes associated with dendrite outgrowth**

When P1 SCG neurons develop in culture, the expression pattern of nAChR transcripts parallels the one that occurs *in vivo* over the same period, with the exception of α_7. This occurs even though the neurons have been disconnected from their pre- and post-ganglionic interactions and separated from their satellite cells (Chapter 6); furthermore, the macroscopic ACh-evoked currents increase over this period in culture (Chapter 7). In addition, our attempts at inhibiting protein kinase activity in these neurons did not affect nAChR expression. A reasonable interpretation from these results is that nAChR expression in SCG neurons is governed largely by intrinsic mechanisms. These intrinsic mechanisms could be related early on to neurogenesis, since the first appearance of nAChR transcripts, in most peripheral neurons and in many brain regions occurs at a time that corresponds to neurogenesis (Zoli *et al.*, 1995; see also Schoenherr and Anderson; 1995). Afterward, during neuronal maturation and specialization, the expression of some nAChRs may be further modulated, or consolidated. One aspect of neuronal maturation is the extension of dendrites; neurons must express ligand-gated receptors on their dendrites in order to allow them to receive functional synapses. Therefore, one possibility is that dendrite extension provides intrinsic signals to produce more receptors. In neonatal SCG neurons, the developmental increase, *in vivo* and in culture, in the density of

functional nAChRs (and α_3 transcripts) corresponds to a period of extensive dendrite outgrowth (Voyvodic, 1987; Brusckenstein and Higgins 1988b; Mandelzys *et al.*, 1994). In nodose neurons, it is possible that the increase in ACh-evoked current densities on neurons that extend dendrites is, in fact, due to an intrinsic demand by these neurons to fill their dendritic membranes with nAChRs.

Conclusion

Figure 8.1 illustrates how I view the developmental changes that occur in nodose neurons with respect to the relationship between neuronal polarity and nAChR expression. (A) *In vivo*, and possibly in culture with satellite cells, a large proportion of nodose neurons express nAChR transcripts at relatively low levels, sufficient to supply nAChRs to their terminals. These receptors may have a modulatory role in cholinergic transmission or axonal guidance. (B) Upon conversion from a pseudo-unipolar morphology to a multipolar morphology, nAChRs are no longer targeted preferentially to the terminals but are inserted in the soma membrane. At this stage, nodose neurons possess the potential to develop a dendritic-axonal polarity and to increase expression of nAChRs. (C) When provided with NGF, these neurons undergo further maturation and develop this dendritic-axonal polarity. This maturation phase could promote further targeting of nAChRs to the somatodendritic domains (compared to B), but, in addition, the expression of nAChR genes is increased during this maturation phase. A good candidate gene to be primarily induced is α_3 which is expressed at low levels in (A), and which increases specifically when SCG neurons undergo similar maturation. The intrinsic mechanism that would link dendritic outgrowth and the control of ligand-gated ion channel gene expression is unknown. Retrograde signals from growing dendrites may carry information that influences gene expression of receptors. In addition, some genes that are essential for dendritic extension and that are up-regulated during dendritic outgrowth may be linked with nAChR subunit genes, so that their expression is coordinately regulated.

In conclusion, I propose that, among the factors that control neurotransmitter receptor expression during neuronal development, one of them is derived from the extension of

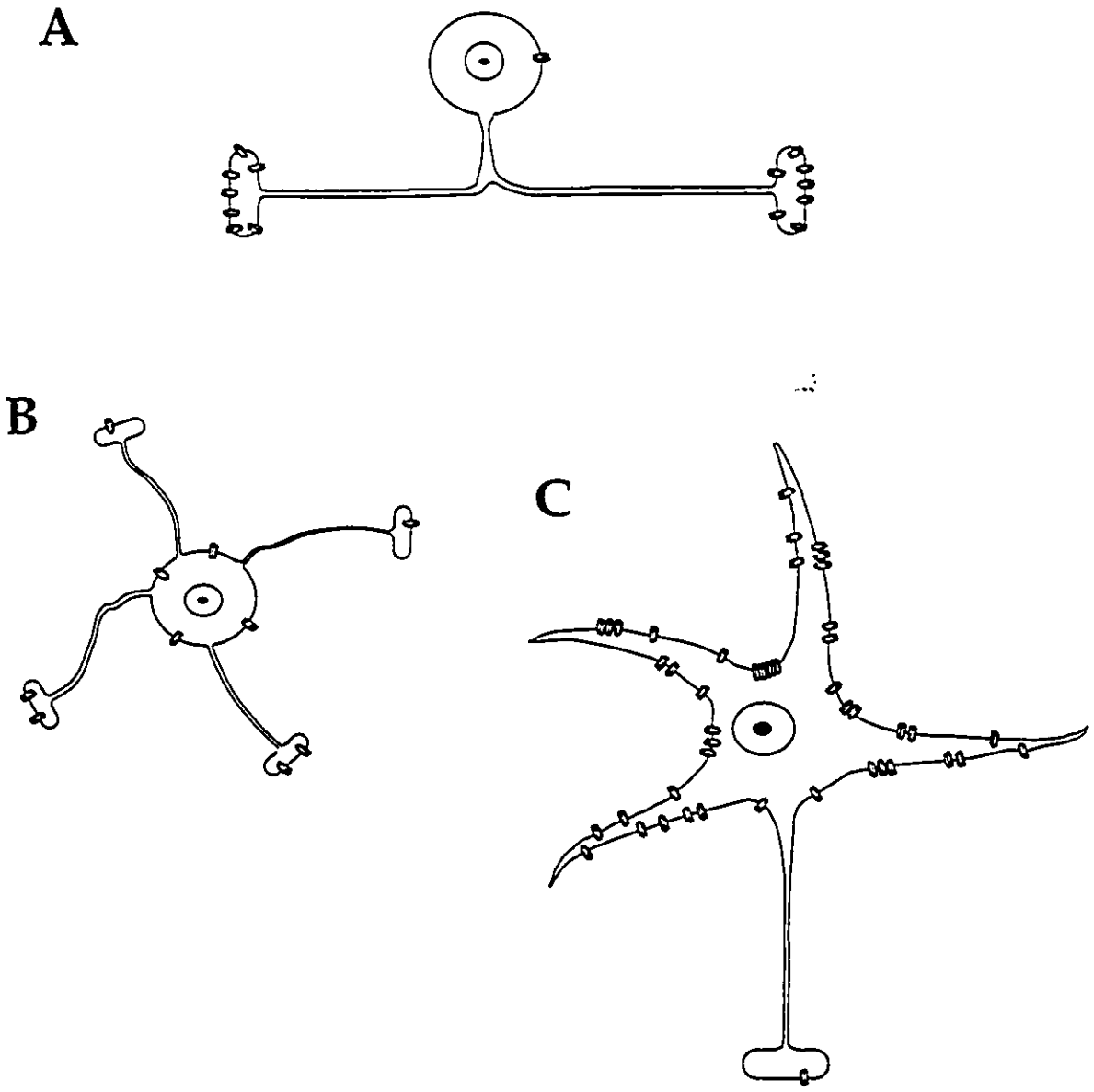

FIGURE 8.1. Model of relationship between neuronal polarity of nodose neurons and nAChR expression.

(A) Sensory neuron, developing *in vivo* or in culture in the presence of satellite cells, express low levels of nAChRs and target them to their terminals. (B) After separating nodose neurons from their ganglionic satellite cells, the neurons extend multiple axons and begin to target nAChRs to their cell body membrane. (C) In the presence of NGF, nodose neurons extend dendrites; this elaboration of dendrites may further promote targeting of receptors to somatodendritic domains; furthermore, the extension of dendrites activates some intrinsic signals that up-regulate nAChR genes, giving rise to a high density of nAChRs on their somatodendritic domains. See text for more details.

dendrites. This hypothesis and the working model of nodose neuron differentiation should stimulate future experiments to learn more about mechanisms that control neuronal polarity and synaptogenesis.

The remarkably elaborated neuronal architectures in the brain add much complexity for neurons to regulate their multiple functions. The synthetic machinery of the neuron has to supply all of its specialized domains with the appropriate elements in order to succeed in communicating with other neurons. Furthermore, the neuron must be able to adjust to changes in the needs of any of these domains, in order to modify its communications with other neurons, and, presumably, to provide the brain with the ability to learn.

Bibliography

Acheson A., Conover J.C., Fandl J.P., Dechiara T.M., Russell M., Thadani A., Squinto S.P., Yancopoulos G.D. and Lindsay R.M. (1995). A BDNF autocrine loop in adult sensory neurons prevents cell death. Nature 374: 450-453.

Ahlijanian M.K., Westenbroek R.E. and Catterall A. (1990). Subunit structure and localization of dihydropyridine-sensitive calcium channels in mammalian brain, spinal cord, and retina. Neuron 4: 819-832.

Alkondon M. and Albuquerque E.X. (1993). Diversity of nicotinic acetylcholine receptors in rat hippocampal neurons. I. Pharmacological and functional evidence for distinct structural subtypes. J. Pharmacol. Exp. Ther. 265: 1455-1473.

Altman J. and Bayer S.A. (1982). Development of the cranial nerve ganglia and related nuclei in the rat. In Advances in Anatomy, Embryology and Cell Biology, Volume 74. Springer-Verlag, New York.

Anand R., Conroy W.G., Schoepfer R., Whiting P. and Lindstrom J. (1991). Neuronal nicotinic acetylcholine receptors expressed in Xenopus oocytes have a pentameric quarternary structure. J. Biol. Chem. 266: 11192-11198.

Arenella L.S., Oliva J.M. and Jacob. M.H. (1993). Reduced levels of acetylcholine receptor expression in chick ciliary ganglion neurons developing in the absence of innervation. J. Neurosci. 13: 4525-4537.

Armstrong R.C. and Montminy M.R. (1993). Transsynaptic control of gene expression. Annu. Rev. Neurosci. 16: 17-29.

Ausubel F.M., Brent R., Kingston R.E., Moore D.D., Seidman J.G., Smith J.A. and Struhl K. (1989). Current protocols in molecular biology. Greene Publishing Associates with Wiley-Interscience, New York.

Autillo-Touati A., Chamak B., Araud D., Vuillet J., Seite R. and Prochiantz. A. (1988). Region-specific neuro-astroglial interactions: ultrastructural study of the in vitro expression of neuronal polarity. J. Neurosci. Res. 19: 326-342.

Baas P.W., Sinclair G. and Heideman S. (1987). Role of microtubules in the cytoplasmic

compartmentation of neurons. Brain Res. 420: 73-81.

Baas P.W., Deitch J.S. and Black M.M. (1988). Polarity orientation of microtubules in hippocampal neurons: uniformity in the axon and nonuniformity in the dendrite. Proc. Natl. Acad. Sci. USA 85: 8335-8339.

Baccaglini P.I. and Cooper E. (1982). Influences on the expression of acetylcholine receptors on rat nodose neurons in cell culture. J. Physiol. 324: 441-451.

Bading H., Ginty D.D. and Greenberg M.E. (1993). Regulation of gene expression in hippocampal neurons by distinct calcium signaling pathways. Science 260: 181-186.

Barbacid M. (1994). The trk family of neurotrophin receptors. J. Neurobiol. 25: 1386-1403.

Barde Y.-A., Edgar D. and Thoenen H. (1982). Purification of a new neurotrophic factor from mammalian brain. EMBO 1: 549-553.

Barde Y.-A. (1989). Trophic factors and neuronal survival. Neuron 2: 1525-1534.

Barker P.A., Lomen-Hoerth C., Gensch E.M., Meakin S.O., Glass D.J. and Shooter E.M. (1993). Tissue-specific alternative splicing generates two isoforms of the trkA receptor. J. Biol. Chem. 268: 15150-15157.

Barker P.A. and Shooter E.M. (1994). Disruption of NGF binding to the low affinity neurotrophin receptor $p75^{LNTR}$ reduces NGF binding to trkA on PC12 cells. Neuron 13: 203-215.

Barrett G.L. and Bartlett P.F. (1994). The p75 receptor mediates survival or death depending on the stage of sensory neurone development. Proc. Natl. Acad. Sci. USA 91: 6501-6505.

Bartlett W.P. and Banker G.A. (1984a). An electron microscopy study of the development of axons and dendrites by hippocampal neurons in culture. I. Cells which develop without intercellular contacts. J. Neurosci. 4: 1944-1953.

Bartlett W.P. and Banker G.A. (1984b). An electron microscopy study of the development of axons and dendrites by hippocampal neurons in culture. II. Synaptic relationships. J. Neurosci. 4: 1954-1965.

Battleman D.S., Geller A.I. and Chao M.V. (1993). HSV-1 vector mediated gene transfer of the human nerve growth factor receptor $p75^{hNGFR}$ defines high affinity NGF binding. J. Neurosci. 13: 941-951.

Bear M.F. and Malenka R.C. (1994). Synaptic plasticity: LTP and LTD. Curr. Opin. Neurobiol. 4: 389-399.

Beck K.D., Lamballe F., Klein R., Barbacid M., Schauwecker P.E., McNeill T.H., Finch C.E., Hefti F. and Day J.R. (1993). Induction of noncatalytic trkB neurotrophin receptors during axonal sprouting in the adult hippocampus. J. Neurosci. 13: 4001-4014.

Benedetti M., Levi A. and Chao M.V. (1993). Differential expression of nerve growth factor receptors leads to altered binding affinity and neurotrophin responsiveness. Proc. Natl. Acad. Sci. USA 90: 7859-7863.

Benes F.M., Parks T.N. and Rubel E.W. (1977). Rapid dendritic atrophy following deafferentation: an EM morphometric analysis. Brain Res. 122: 1-13.

Bennett M.K. and Scheller R.H. (1994). Molecular correlates of synaptic vesicle docking and fusion. Curr. Opin. Neurobiol. 4: 324-329.

Berg D.K., Boyd R.T., Halvorsen S.W., Higgins L.S., Jacob M.H. and Margiotta J.F. (1989). Regulating the number and function of neuronal acetylcholine receptors. Trends Neurosci. 12: 16-21.

Berg M.M., Sternberg D.W., Hempstead B.L. and Chao M.V. (1991). The low-affinity p75 nerve growth factor (NGF) receptor mediates NGF-induced tyrosine phosphorylation. Proc. Natl. Acad. Sci. USA 88: 7106-7110.

Berg M.M., Sternberg D.W., Parada L.F. and Chao M.V. (1992). K-252a inhibits nerve growth factor-induced trk proto-oncogene tyrosine phosphorylation and kinase activity. J. Biol. Chem. 267: 13-16.

Bergzon J., Kokaia Z., Ernfors P., Kokaia M., Leanza G., Nilsson O.G., Persson H. and Lindvall O. (1993). Regulation of neurotrophin and trkA, trkB and trkC tyrosine kinase receptor messenger RNA expression in kindling. Neuroscience 53: 433-446.

Berkemeier L.R., Winslow J.W., Kaplan D.R., Nikolics K., Goeddel D.V. and Rosenthal A. (1991). Neurotrophin-5: a novel neurotrophic factor that activates trk and trkB. Neuron 7: 857-866.

Bernhardt R. and Matus A. (1984). Light and electron microscopic studies of the distribution of microtubule-associated protein 2 in rat brain a difference between dendritic and axonal cytoskeletons. J. Comp. Neurol. 226: 203-221.

Bernardt R., Huber G. and Matus A. (1985). Differences in the developmental patterns of three microtubule-associated proteins in the rat cerebellum. J. Neurosci. 5: 977-991.

Bertrand D., Cooper E., Valera S., Rungger D. and Ballivet M. (1991). Electrophysiology of neuronal nicotinic acetylcholine receptors expressed in Xenopus oocytes following nuclear injections of genes or cDNAs. In: Conn PM editor. Methods in Neurosciences. vol 4. San Diego: Academic Press Inc. pp 174-193.

Berry M. and Bradley P. (1976). The growth of the dendritic trees of Purkinje cells in irradiated agranular cerebellar cortex. Brain Res. 116: 361-387.

Bessho Y., Nawa H. and Nakanishi S. (1994). Selective up-regulation of an NMDA receptor subunit mRNA in cultured cerebellar granule cells by K^+-induced depolarization and NMDA treatment. Neuron 12: 87-95.

Bevan S. and Geppetti P. (1994). Protons: small stimulants of capsaicin-sensitive sensory nerves. TINS 17: 509-512.

Binder L.I., Frankfurter A. and Rebhun L.I. (1985). The distribution of tau in the mammalian central nervous system. J. Cell Biol. 101: 1371-1378.

Birren S., Lo J. and Anderson D.J. (1993). Sympathetic neurons undergo a developmental switch in trophic dependence. Development 119: 597-610.

Black M.M. and Baas P.W. (1989). The basis of polarity in neurons. TINS 12: 211-214.

Bliss T.V.P. and Collingridge G.L. (1993). A synaptic model of memory: Long-term potentiation in the hippocampus. Nature 361: 31-39.

Bocchini V. and Angeletti P.U. (1969). The nerve growth factor purification as a 30.000-molecular

weight protein. Proc. Natl. Acad. Sci. USA 64: 787-794.

Bossy B., Bossy-Wetzel E. and Reichardt L.F. (1991). Characterization of the integrin alpha8 subunit: a new integrin beta 1-associated subunit, which is prominently expressed on axons and on cells in contact with basal laminae in chick embryos. EMBO 10: 2375-2385.

Bothwell M. (1995). Functional interactions of neurotrophins and neurotrophin receptors. Annu. Rev. Neurosci. 18: 223-253.

Boulter J., O'Shea-Greenfield A., Duvoisin R.M., Connolly J.G., Wada E., Jensen A., Gardner P.D., Ballivet M., Deneris E.S., McKinnon D., Heinemann S. and Patrick J. (1990). α3, α5, and ß4: three members of the rat neuronal nicotinic acetylcholine receptor-related gene family form a gene cluster. J. Biol. Chem. 265: 4472-4482.

Boyd R.T., Jacob M.H., Couturier S., Ballivet M. and Berg D.K. (1988). Expression and regulation of neuronal acetylcholine receptor mRNA in chick ciliary ganglia. Neuron 1: 495-502.

Boyd R.T., Jacob M.H., McEachern A.E., Caron S. and Berg D.K. (1991). Nicotinic acetylcholine receptor mRNA in DRG neurons. J. Neurobiol. 22: 1-14.

Boyd R.T. (1993). Sequencing and promoter analysis of the genomic region between the rat neuronal nicotinic acetylcholine receptor ß4 and α3 genes. J. Neurobiol. 25: 960-973.

Bradley P. and Berry M. (1978). The Purkinje cell dendritic tree in mutant mouse cerebellum. A quantitative Golgi study of weaver and staggerer mice. Brain Res. 142: 135-141.

Brenner H.R. and Martin A.R. (1976). Reduction in acetylcholine sensitivity of axotomized ciliary ganglion cells. J. Physiol. 260: 159-176.

Brown D.A. and Fumagalli L. (1977). Dissociation of α-bungarotoxin binding and receptor block in the rat superior cervical ganglion. Brain Res. 129: 165-168.

Bruckenstein D.A. and Higgins D. (1988a). Morphological differentiation of embryonic rat sympathetic neurons in tissue culture. I Conditions under which neurons form axons but not dendrites. Dev. Biol. 128: 324-336.

Bruckenstein D.A. and Higgins D. (1988b). Morphological differentiation of embryonic rat

sympathetic neurons in tissue culture. II Serum promotes dendritic growth. Dev. Biol. 128: 337-348.

Bruckenstein D., Johnson M.I. and Higgins D. (1989). Age-dependent changes in the capacity of rat sympathetic neurons to form dendrites in tissue culture. Dev. Brain Res. 46: 21-32.

Bruckenstein D.A., Lein P.J., Higgins D. and Fremeau R.T.Jr. (1990). Distinct spatial localization of specific mRNAs in cultured sympathetic neurons. Neuron 5: 809-819.

Buchman V.L. and Davies A.M. (1993). Different neurotrophins are expressed and act in a developmental sequence to promote the survival of embryonic sensory neurons. Development 118: 989-1001.

Buj-Bello A.M., Pinon L. and Davies A.M. (1994). The survival of NGF-dependent but not BDNF-dependent cranial sensory neurons is promoted by several different neurotrophins early in their development. Development 120: 1573-1580.

Bunge R.P. and Wood P.M. (1987). Tissue culture studies of interactions between axons and myelinating cells of the central and peripheral nervous system. Prog. Brain Res. 71: 143-152.

Burgin K.E., Waxham M.N., Rickling S., Westgate S.A., Mobley W.C. and Kelly P.T. (1990). In situ hybridization histochemistry of Ca^{2+}/calmodulin-dependent protein kinase in developing rat brain. J. Neurosci. 10: 1788-1798.

Burridge K., Fath K., Kelly T., Nuckolls G. and Turner C. (1988). Focal adhesions: transmembrane junctions between the extracellular matrix and the cytoskeleton. Annu. Rev. Cell. Biol. 4: 487-525.

Burton P.R. (1988). Dendrites of mitral cell neurons contain microtubules of opposite polarity. Brain Res. 473: 107-115.

Caceres A., Binder L.I., Payne M.R., Bender P., Rebhun L. and Steward O. (1984). Differential subcellular localization of tubulin and the microtubule-associated protein MAP2 in brain tissue as revealed by immunocytochemistry with monoclonal hybridoma antibodies. J. Neurosci. 4: 394-410.

Caceres A., Banker G. and Binder L. (1986). Immunocytochemical localization of tubulin and microtubule-associated protein during development of hippocampal neurons in culture. J. Neurosci.

6: 714-722.

Caceres A. and Kosik K.S. (1990). Inhibition of neurite polarity by tau antisense oligonucleotides in primary cerebellar neurons. Nature 343: 461–463.

Caceres A., Mautino J. and Kosik K.S. (1992). Suppression of MAP2 in cultured cerebellar macroneurons inhibits minor neurite formation. Neuron 9: 607-618.

Cajal S. Ramón y (1955). Histologie du système nerveux de l'homme et des vertébrés. Vol. I p.639. French translation by L. Azoulay. Instituto Ramón y Cajal. Madrid.

Cajal S. Ramón y (1989). Recollections of my life. pp. 1-638. Cambridge: MIT.

Campenot R.B. (1994). NGF and the local control of nerve terminal growth. J. Neurobiol. 25: 599-611.

Carbonetto S.T., Fambrough D.M. and Muller K.J. (1978). Nonequivalence of α-bungarotoxin receptors and acetylcholine receptors in chick sympathetic neurons. Proc. Natl. Acad. Sci. USA 75: 1016-1020.

Carbonetto S. and Fambrough D.M. (1979). Synthesis, insertion into the plasma membrane, and turnover of α-bungarotoxin receptors in chick sympathetic neurons. J. Cell Biol. 81: 555-569.

Carbonetto S. and Stach R.W. (1982). Localization of nerve growth factor bound to neurons growing nerve fibers in culture. Brain Res. 255: 463–473.

Castro N.G. and Albuquerque E.X. (1995). α-bungarotoxin-sensitive hippocampal nicotinic receptor channel has a high calcium permeability. Biophys. J. 68: 516-524.

Chamak B., Fellous A., Glowinski J. and Prochiantz A. (1987). MAP2 expression and neuritic outgrowth and branching are coregulated through region-specific neuro-astroglial interactions. J. Neurosci. 7: 3163-3170.

Chamak B. and Prochiantz A. (1989). Influence of extracellular matrix proteins on the expression of neuronal polarity. Development 106: 483–491.

Chang H.T. (1952). Cortical neurons with particular reference to the apical dendrites. Cold Spring

Harbor Symp. Quant. Biol. 17: 189-202.

Changeux J.-P. (1991). Compartmentalized transcription of acetylcholine receptor genes during motor endplate epigenesis. New Biol. 3: 413-429.

Chao M.V., Bothwell M.A., Ross A.H., Koprowski H., Lanahan A.A., Buck C.R. and Sehgal A. (1986). Gene transfer and molecular cloning of the human NGF receptor. Science 232: 518-521.

Chao M.V. (1994). The p75 neurotrophin receptor. J. Neurobiol. 25: 1373-1385.

Chapman P.F., Frenguelli B.G., Smith A., Chen C.-M. and Silva A.J. (1995). The α-Ca^{2+}/calmodulin kinase II: a bidirectional modulator of presynaptic plasticity. Neuron 14: 591-597.

Chesselet M.F. (1984). Presynaptic regulation of neurotransmitter release in the brain: facts and hypotheses. Neuroscience 12: 347-375.

Chiappinelli V.A. (1985). Actions of snake venom toxins on neuronal nicotinic receptors and other neuronal receptors. Pharmacol. Ther. 31: 1-32.

Chicurel M.E., Terrian D.M. and Potter H. (1993). mRNA at the Synapse: analysis of a synaptosomal preparation enriched in hippocampal dendritic spines. J. Neurosci. 13: 4054-4063.

Chomczynski P. and Sacchi N. (1987). Single-step method of RNA isolation by acid guanidinium thiocyanate-phenol-chloroform extraction. Anal. Biochem. 162: 156-159.

Chu G.C., Moscoso L.M., Sliwkowski and Merlie J.P. (1995). Regulation of the acetylcholine receptor ε subunit gene by recombinant ARIA: an in vitro model for transynaptic gene regulation. Neuron 14: 329-339.

Clapham D.E. (1995). Calcium signaling. Cell 80: 259-268.

Clarke P.B.S. and Pert A. (1985). Autoradiographic evidence for nicotine receptors on nigrostriatal and mesolimbic dopaminergic neurons. Brain Res. 348: 355-358.

Clarke P.B.S., Schwartz R.D., Paul S.M., Pert C.B. and Pert A. (1985). Nicotinic binding in rat brain: autoradiographic comparison of [^{3}H]acetylcholine, [^{3}H]nicotine, and [^{125}I]-α-bungarotoxin. J. Neurosci. 5: 1307-1315.

Clarke P.B.S. (1992). The fall and rise of neuronal α-bungarotoxin binding proteins. TIPS 13: 407-413.

Clarke P.B.S. (1993). Nicotinic receptors in mammalian brain: localization and relation to cholinergic innervation. Prog. Brain Res. 98: 77-83.

Clendening B. and Hume R.I. (1990). Cell interactions regulates dendritic morphology and response to neurotransmitters in embryonic chick sympathetic preganglionic neurons in vitro. J. Neurosci. 10: 3992-4005.

Cohen G.B., Ren R. and Baltimore D. (1995). Modular binding domains in signal transduction proteins. Cell 80: 237-248.

Cohen M.W., Anderson M.J., Zorychta E and Weldon P.R. (1979). Accumulation of acetylcholine receptors at nerve-muscle contacts in culture. Prog. Brain Res. 49: 335-349.

Cohen M.W., Jones O.T. and Angelides K.J. (1991). Distribution of Ca^{2+} channels on frog motor nerve terminals revealed by fluorescent ω-conotoxin. J. Neurosci. 11: 1032-1039.

Collins F., Schmidt M.F., Guthrie P.B. and Kater S.B. (1991). Sustained increase in intracellular calcium promotes neuronal survival. J. Neurosci. 11: 2582-2587.

Conroy W.G., Vernallis A.B. and Berg D.K. (1992). The α5 gene product assembles with multiple acetylcholine receptor subunits to form distinctive receptor subtypes in brain. Neuron 9: 679-691.

Cooper E. (1984). Synapse formation among developing sensory neurons from rat nodose ganglia grown in tissue culture. J. Physiol. 351: 263-274.

Cooper E. and Lau M. (1986). Factors affecting the expression of acetylcholine receptors on rat sensory neurons in culture. J. Physiol. 377: 409-420.

Cooper E., Couturier S. and Ballivet M. (1991). Pentameric structure and subunit stoichiometry of a neuronal acetylcholine receptor. Nature 350: 235-238.

Cordon-Cardo C., Tapley P., Jing S.Q., Nanduri V., O'Rourke E., Lamballe F., Kovary K., Klein R., Jones K.R., Reichardt L.F. and Barbacid M. (1991). The trk tyrosine protein kinase mediates the mitogenic properties of nerve growth factor and neurotrophin-3. Cell 66: 173-183.

Corfas G., Rosen K.M., Aratake H., Krauss R. and Fischbach G.D. (1995). Differential expression of ARIA isoforms in the rat brain. Neuron 14: 103-115.

Corriveau R.A. and Berg D.K. (1993). Coexpression of multiple acetylcholine receptor genes in neurons: quantification of transcripts during development. J. Neurosci. 13: 2662-2671.

Corriveau R.A. and Berg D.K. (1994). Neurons in culture maintain acetylcholine receptor levels with far fewer transcripts than in vivo. J. Neurobiol. 25: 1579-1592.

Corriveau R.A., Romano S.J., Conroy W.G., Oliva L. and Berg D.K. (1995). Expression of neuronal acetylcholine receptor genes in vertebrate skeletal muscle during development. J. Neurosci. 15: 1372-1383.

Couturier S., Erkman L., Valera S., Rungger D., Bertrand S., Boulter J., Ballivet M. and Bertrand D. (1990a). α_5, α_3, and non-α_3: three clustered avian genes encoding neuronal nicotinic acetylcholine-related subunits. J. Biol. Chem. 256: 17560-17567

Couturier B.D., Matter J.-M., Hernandez M.-C., Bertrand S., Millar N., Valera S., Barkas T. and Ballivet M. (1990b). A neuronal nicotinic acetylcholine receptor subunit (α_7) is developmentally regulated and forms a homo-oligomeric channel blocked by α-Btx. Neuron 5: 847-856.

Covernton P.J.O., Kojima H., Sivilotti L.G., Gibb A.J. and Colquhoun D. (1994). Comparison of neuronal nicotinic receptors in rat sympathetic neurones with subunit pairs expressed in Xenopus oocytes. J. Physiol. 481: 27-34.

Craig A.-M., Jareb M. and Banker G. (1992). Neuronal polarity. Curr. Opin. Neurobiol. 2: 602-606.

Craig A.-M., Blackstone C.D., Huganir R.L. and Banker G. (1993). The distribution of glutamate receptors in cultured rat hippocampal neurons: postsynaptic clustering of AMPA-selective subunits. Neuron 10: 1055-1068.

Craig A.-M. and Banker G. (1994). Neuronal polarity. Annu. Rev. Neurosci. 17: 267-310.

Crick F. (1982). Do dendritic spines twitch? TINS 5: 44-46.

Crowley C., Spencer S.D., Nishimura M.C., Chen K.S., Pitts-Meek S., Armanini M.P., Ling L.H.,

McMahon S.B., Shelton D.L., Levinson A.D. and Phillips H.S. (1994). Mice lacking nerve growth factor display perinatal loss of sensory and sympathetic neurons yet develop basal forebrain cholinergic neurons. Cell 76: 1001-1011.

D'Amico-Martel A. and Noden D.M. (1983). Contributions of placodal and neural crest cells to avian cranial peripheral ganglia. Am. J. Anat. 166: 445–468.

Davies A.M., Lee K.-F. and Jaenisch R. (1993). p75-deficient trigeminal sensory neurons have an altered response to NGF but not to other neurotrophins. Neuron 11: 565-574.

Davies A.M. (1994). The role of neurotrophins in the developing nervous system. J. Neurobiol. 25: 1334-1348.

Davis L., Banker G.A. and Steward O. (1987). Selective dendritic transport of RNA in hippocampal neurons in culture. Nature 330: 477–479.

Davis L., Burger B., Banker G.A. and Steward O. (1990). Dendritic transport: quantitive analysis of the time course of somatodendritic transport of recently synthesized RNA. J. Neurosci. 10: 3056-3068.

Davis S., Gale N.W., Aldrich T.H., Maisonpierre P.C., Lhotak V., Pawson T., Goldfarb M. and Yancopoulos G.D. (1994). Ligands for EPH-related receptor tyrosine kinases that require membrane attachment or clustering for activity. Science 266: 816-819.

De Camilli P., Miller P.E., Navone F., Theurkauf W.E. and Vallee R.B. (1984). Distribution of microtubule-associated protein 2 in the nervous system of the rat studied by immunofluorescence. Neurosci 11: 819-846.

Deitch J.S. and Rubel E.W. (1984). Afferent influences on brainstem auditory nuclei of the chicken: time course and specificity of dendritic atrophy following deafferentation. J. Comp. Neurol. 229: 66-79.

De Koninck P., Carbonetto S. and Cooper E. (1993). NGF induces neonatal rat sensory neurons to extend dendrites in culture after removal of satellite cells. J. Neurosci. 13: 577-585.

De Koninck P. and Cooper E. (1995). Factors controlling nicotinic acetylcholine receptor expression on rat sympathetic neurons. In: Effects of Nicotine on Biological Systems II. Advances

in Pharmacological Sciences. Birkhäuser. Verlag. Basel. pp 137-143.

Deltoro E.D., Juiz J.M., Peng X., Lindstrom J. and Criado M. (1994). Immunocytochemical localization of the α-7 subunit of the nicotinic acetylcholine receptor in the rat central nervous system. J. Comp. Neurol. 349: 325-342.

Deneris E.S., Connolly J., Rogers S.W. and Duvoisin R. (1991). Pharmacological and functional diversity of neuronal nicotinic acetylcholine receptors. TIPS 12: 34-40.

Denis-Donini S., Glowinski J. and Prochiantz A. (1984). Glial heterogeneity may define the three-dimensional shape of mouse mesencephalic dopaminergic neurons. Nature 307: 641-643.

Desmond N.L. and Levy W.B. (1988). Anatomy of associative long-term synaptic modification. In: long term potentiation: from biophysics to behavior (Landfield P.W., Deadwyler SA. eds). pp 265-305. New York: Liss.

Devay P., Qu X. and Role L.W. (1994). Regulation of nAChR subunit gene expression relative to the development of pre- and postsynaptic projections of embryonic chick sympathetic neurons. Dev. Biol. 162: 56-70.

Diamond J. (1955). Observations on the excitation by acetylcholine and by pressure of sensory receptors in the cat's carotid sinus. J. Physiol. 130: 513-532.

Diamond J. (1959). The effects of injecting acetylcholine into normal and regenerating nerves. J. Physiol. 145: 611-629.

DiCicco-Bloom E., Friedman W.J. and Black I.B. (1993). NT-3 stimulates sympathetic neuroblast proliferation by promoting precursor cell survival. Neuron 11: 1101-1111.

Diez-Gaza F.J. and Avila J. (1993). MAP2 phosphorylation parallels dendrite arborization in hippocampal neurones in culture. Dev. Neurosci. 4: 419-422.

Dinsmore J.H. and Solomon F. (1991). Inhibition of MAP2 expression affects both morphological and cell division phenotypes of neuronal differentiation. Cell 64: 817-826.

Dodge F.A. and Rahamimoff R. (1967). Co-operative action of calcium ions in transmitter release at the neuromuscular junction. J. Physiol. 193: 419-432.

Dotti C.G. and Banker G.A. (1987). Experimentally induced alteration in the polarity of developing neurons. Nature 330: 254-256.

Dotti C.G., Sullivan C.A. and Banker G.A. (1988). The establishment of polarity by hyppocampal neurons in culture. J. Neurosci. 8: 1454-1468.

Dryer S.E. and Chiappinelli V.A. (1987). Analysis of quantal content and quantal conductance in two populations of neurons in the avian ciliary ganglion. Neuroscience 20: 905-910.

Duggan A.W., Hall J.G. and Lee C.Y. (1976). α-bungarotoxin, cobra neurotoxin and excitation of Renshaw cells by acetylcholine. Brain Res. 107: 166-170.

Eccles J.C. (1964). The physiology of synapses. Springer, Berlin.

Egan S.E. and Weinberg R.A. (1993). The pathway to signal achievement. Nature 365: 781-782.

Elgoyhen A.B., Johnson D.S., Boulter J., Vetter D.E. and Heinemann S. (1994). α9: an acetylcholine receptor with novel pharmacological properties expressed in rat cochlear hair cells. Cell 79: 705-715.

Elson E. (1993). Barriers to diffusion Curr. Biol. 3:152-153.

Engisch K.L. and Fischbach G.D. (1990). The development of ACh- and GABA-activated currents in normal and target-deprived embryonic chick ciliary ganglia. Dev. Biol. 139: 417–426.

Engisch K.L. and Fischbach G.D. (1992). The development of ACh- and GABA-activated currents in embryonic chick ciliary ganglion neurons in the absence of innervation in vivo. J. Neurosci. 12: 1115-1125.

Enslen H. and Soderling T.R. (1994). Roles of Calmodulin-dependent protein kinase and phosphatase in calcium-dependent transcription of immediate early genes. J. Biol. Chem. 269: 20872-20877.

Enslen H., Sun P., Brickey D., Soderling S., Klamo E. and Soderling T.R. (1994). Characterization of Ca^{2+}/calmodulin-dependent protein kinase IV. J. Biol. Chem. 269: 15520-15527.

Ernfors P., Ibánez C.F., Ebendal T., Olson L. and Persson (1990). Molecular cloning and

neurotrophic activities of a protein with structural similarities to nerve growth factor: developmental and topographical expression in the brain. Proc. Natl. Acad. Sci. USA 87: 5454-5458.

Ernfors P., Merlio J.-P. and Persson H. (1992). Cells expressing mRNA for neurotrophins and their receptors during embryonic rat development. Eur. J. Neurosci. 4: 1140-1158.

Ernfors P., Lee K.-F. and Jaenisch R. (1994a). Mice lacking brain-derived neurotrophic factor develop with sensory deficits. Nature 368: 147-150.

Ernfors P., Lee K.-F., Kucera J. and Jaenisch R. (1994b). Lack of neurotrophin-3 leads to deficiencies in the peripheral nervous system and loss of limb proprioception. Cell 77: 503-512.

Esplin D.W., Capek R. and Esplin B.A. (1972). Pharmacological studies on dorsal root responses produced by ventral root stimulation in the cat. Can. J. Physiol. 50: 119-122.

Falls D.L., Rosen K.M., Corfas G., Lane W.S. and Fischbach G.D. (1993). ARIA, a protein that stimulates acetylcholine receptor synthesis, is a member of the neu ligand family. Cell 72: 801-815.

Fariñas I., Jones K.R., Backus C. and Wang X.-Y. (1994). Severe sensory and sympathetic deficits in mice lacking neurotrophin-3. Nature 369: 658-661.

Ferreira A. and Caceres A. (1989). The expression of acetylated microtubules during axonal and dendritic growth in cerebellar macroneurons which develop in vitro. Dev. Brain Res. 49: 205-213.

Fitzgerald M. (1983). Capsaicin and sensory neurones-a review. Pain 15: 1109-1130.

Fletcher T.L., Cameron P., De Camilli P. and Banker G. (1991). The distribution of synapsin I and synaptophysin in hippocampal neurons developing in culture. J. Neurosci. 11: 1617-1626.

Fletcher T.L., De Camilli P. and Banker G. (1994). Synaptogenesis in hippocampal cultures: evidence indicating that axons and dendrites become competent to form synapses at different stages of neuronal development. J. Neurosci. 14: 6695-6706.

Flores C.M., Rogers S.W., Pabreza L.A., Wolfe B.B. and Kellar K.J. (1992). A subtype of nicotinic cholinergic receptor in rat brain is comprised of α-4 and ß-2 subunits and is up-regulated

by chronic nicotine treatment. Mol. Pharm. 41: 31-37.

Forehand C.J. (1985). Density of somatic innervation on mammalian autonomic ganglion cells is inversely related to dendritic complexity and preganglionic convergence. J. Neurosci. 5: 3403-3408.

Franklin J.L. and Johnson E.M. (1992). Suppression of programmed neuronal death by sustained elevation of cytoplasmic calcium. TINS 15: 501-508.

Franklin J.L., Sanz-Rodriguez C., Juhasz A., Deckwerth T.L. and Johnson E.M. Jr. (1995). Chronic depolarization prevents programmed death of sympathetic neurons in vitro but does not support growth: Requirement for Ca^{2+} influx but not trk activation. J. Neurosci. 15: 643-664.

Frey U., Huang Y.Y. and Kandel E.R. (1993). Effects of cAMP simulate a late stage of LTP in hippocampal CA1 neurons. Science 260: 1661-1664.

Frisén J., Verge V.M.K., Fried K., Risling M., Persson H., Trotter J., Hökfelt T. and Lindholm D. (1993). Characterization of glial trkB receptors: differential response to injury in the central and peripheral nervous systems. Proc. Natl. Acad. Sci. USA 90: 4971-4975.

Froehner S.C. (1993). Regulation of ion channel distribution at synapses. Annu. Rev. Neurosci. 16: 347-368.

Fuchs P.A. nad Murrow B.W. (1992). Cholinergic inhibition of short (outer) hair cells of the chick's cochlea. J. Neurosci. 12: 800-809.

Fujiwara M., Kurahashi K., Mizuno N. and Nakamura Y. (1978). Involvement of nicotinic and muscarinic receptors in synaptic transmission in cat superior cervical ganglion reinnervated by vagal primary afferent axons. J. Pharmacol. Exp. Ther. 205: 77-99.

Fukunaga K., Rich D.P. and Soderling T.R. (1989). Generation of the Ca^{2+}-independent form of Ca^{2+}/calmodulin-dependent protein kinase II in cerebellar granule cells. J. Biol. Chem. 264: 21830-21836.

Fumagalli L., De Renzis G. and Miani N. (1976). Acetylcholine receptors: number and distribution in intact and deafferented superior cervical ganglion of the rat. J. Neurochem. 27: 47-52.

Fumagalli L. and DeRenzis G. (1984). Extrasynaptic localization of α-bungarotoxin receptors in the rat superior cervical ganglia. Neurochem. Int. 6: 355-364.

Furshpan E.J., MacLeish P.R., O'Lague, P.H. and Potter D.D. (1976). Chemical transmission between rat sympathetic neurons and cardiac myocytes developing in microcultures: evidence for cholinergic, adrenergic and dual-function neurons. Proc. Natl. Acad. Sci. USA 73: 4225-4229.

Furshpan E.J., Landis S.C., Matsumoto S.G. and Potter D.D. (1986). Synaptic functions in rat sympathetic neurons in microcultures. I. Secretion of norepinephrine and acetylcholine. J. Neurosci. 6: 1061-1079.

Gaese F., Kolbeck R. and Barde Y.-A. (1994). Sensory ganglia require neurotrophin-3 early in development. Development 120: 1613-1619.

Gardette R., Listerud M.D., Brussaard A.B. and Role L.W. (1991). Developmental changes in transmitter sensitivity and synaptic transmission in embryonic chicken sympathetic neurons innervated in vitro. Dev. Biol. 147: 83-95.

Garner A.S. and Large T.H. (1994). Isoforms the avian trkC receptor: a novel kinase insertion dissociates transformation and process outgrowth from survival. Neuron 13: 457-472.

Garner C.C. and Matus A. (1988). Different forms of microtubule-associated protein 2 are encoded by separated mRNA transcripts. J. Cell Biol. 106: 79-783.

Garner C.C., Tucker R.P. and Matus A. (1988). Selective localization of messenger RNA for cytoskeletal protein MAP2 in dendrites. Nature 336: 674-677.

Gaudin-Chazal G., Portalier P., Puizillout J.J. and Vigier D. (1983). Simultaneous visualization of aortic and [^{3}H]5-hydroxytryptamine-accumulating cells bodies in the nodose ganglion of the cat. J. Physiol. Lond. 337: 321-330.

Gerzanich V., Anand R. and Lindstrom J. (1994). Homomers of α8 and α7 subunits of nicotinic receptors exhibit similar channel but contrasting binding site properties. Mol. Pharmacol. 45: 212-220.

Ghosh A., Carnahan J. and Greenberg M.E. (1994). Requirement for BDNF in activity-dependent survival of cortical neurons. Science 263: 1618-1623.

Ghosh A. and Greenberg M.E. (1995). Calcium signaling in neurons: molecular mechanisms and cellular consequences. Science 267: 239-247.

Ginty D.D., Glowacka D., Bader D.S., Hidaka H. and Wagner J.A. (1991). Induction of immediate early genes by Ca^{2+} influx requires cAMP-dependent protein kinase in PC12 cells. J. Biol. Chem. 266: 17454-17458.

Glass D.J., Nye S.H., Hantzopoulos P., Macchi M.J., Squinto S.P., Goldfarb M. and Yancopoulos G.D. (1991). trkB mediates BDNF-NT-3-dependent survival and proliferation in fibroblasts lacking the low affinity NGF receptor. Cell 66: 405–413.

Goedert M., Crowther R.A. and Garner C.C. (1991). Molecular characterization of microtubule-associated protein tau and MAP2. TINS 14: 193-199.

Goelet P., Castellucci V.F., Schacher S. and Kandel E.R. (1986). The long and the short of long-term memory - a molecular framework. Nature 322: 419–422.

Goslin K., Schreyer D.J., Skene J.H.P. (1988). Development of neuronal polarity: GAP–43 distinguishes axonal from dendritic growth cones. Nature 336: 672-677.

Goslin K., Schreyer D.J., Skene J.H.P. and Banker G. (1990). Changes in the distribution of GAP-43 during the development of neuronal polarity. J. Neurosci. 10: 588-602.

Gotti C., Hanke W., Maury K., Moretti M., Ballivet M., Clementi F. and Bertrand D. (1994). Pharmacology and biophysical properties of α_7 and α_7-α_8 α-bungarotoxin receptor subtypes immunopurified from the chick optic lobe. Eur. J. Neurosci. 6: 1281-1291.

Götz R., Koster R., Winkler C., Raulf F., Lottspeich F., Scharti M. and Thoenen H. (1994). Neurotrophin-6 is a new member of the nerve growth factor family. Nature. 372: 266-269.

Gray V.A.B. (1959). Initiation of impulses at receptors. In *Handbook of Physiology*, vol. 1, sect. 1, J. Field and H.W. Magoun, eds. pp. 123-145. American Physiological Society. Baltimore. MD.

Greene L.A. and Tischler A.S. (1976). Establishment of a noradrenergic clonal line of rat adrenal pheochromocytoma cells which respond to nerve growth factor. Proc. Natl. Acad. Sci. USA 73: 2424-2428.

Greene L.A. and Tischler A.S. (1982) PC12 pheochromocytoma cell in neurobiology research. Adv. Cell Neurobiol. 3. 373–414.

Greene L.A., Sobeih M.M. and Tenk K.K. (1991). Methodologies for the culture and experimental use of the PC12 rat pheochromocytoma cell line. In Culturing Nerve Cells ed. G. Banker K. Goslin. pp. 207-226. Cambridge: MIT.

Gumbiner B.M. (1993). Proteins associated with the cytoplasmic surface of adhesion molecules. Neuron 11: 551-564.

Hack N., Hidaka H., Wakefield M.J. and Balazs R. (1993). Promotion of granule cell survival by high K^+ or excitatory amino acid treatment and Ca^{2+}/calmodulin-dependent protein kinase activity. Neuroscience 57: 9-20.

Hall Z.W. and Sanes J.R. (1993). Synaptic structure and development: the neuromuscular junction. Cell. 72/ Neuron 10: 99-121.

Hallböök F., Ibánez C.F. and Persson H. (1991). Evolutionary studies of the nerve growth factor family reveal a novel member abundantly expressed in xenophus ovary. Neuron 6: 845-858.

Halvorsen S.W. and Berg D.K. (1987). Affinity labeling of neuronal acetylcholine receptor subunits with an α-neurotoxin that blocks receptor function. J. Neurosci. 7: 2547-2555.

Halvorsen S.W., Schmid H.A., McEachern A.E. and Berg D.K. (1991). Regulation of acetylcholine receptors on chick ciliary ganglion neurons by components from the tissue. J. Neurosci. 11: 2177-2186.

Hamill O.P., Marty A., Neher E., Sakmann B. and Sigworth F.J. (1981). Improved patch-clamp techniques for high resolution current recording from cells and cell-free membrane patches. Pflügers Archiv. 391: 85-100.

Hammond C. and Tritsch D. (1990). Neurobiologie cellulaire. ed. Doin. Paris pp. 1-631.

Hanson P.I. and Schulman H. (1992). Neuronal Ca^{2+}/calmodulin-dependent protein kinases. Annu. Rev. Biochem. 61: 559-601.

Hanson P.I., Meyer T., Stryer L. and Schulman H. (1994). Dual role of calmodulin in

autophosphorylation of multifunctional CaM kinase may underlie decoding of calcium signals. Neuron 12: 943-956.

Hantzopoulos P.A., Suri C., Glass D.J., Goldfarb M.P. and Yancopoulos D. (1994). The low affinity NGF receptor, p75, can collaborate with each of the trks to potentiate functional responses to the neurotrophins. Neuron 13: 187-201.

Harris K.M. and Stevens J.K. (1989). Dendritic spines of CA1 pyramidal cells in the rat hippocampus: serial electron microscopy with reference to their biophysical characteristics. J. Neurosci. 9: 2982-2997.

Hashimoto Y., Nakayama T., Teramoto T., Kato H., Watanabe T., Kinoshita M., Tsukamoto K., Tokunaga K., Kurokawa K., Nakanishi S., Matsuda Y. and Nonomura Y. (1991). Potent and preferential inhibition of Ca^{2+}/calmodulin-dependent protein kinase II by K252a and its derivative, KT 5926. Biochem. Biophys. Res. Comm. 181: 423-429.

Hawrot, E. (1980). Cultured sympathetic neurons: effects of cell-derived and synthetic substrata on development. Dev. Biol. 74: 136-151.

Hawrot E. and Patterson P.H. (1979). Long-term cultures of dissociated sympathetic neurons. Meth. Enzym. 58: 574-584.

Haydon P.G. and Drapeau P. (1995). From contact to connection: early events during synaptogenesis. TINS 18: 196-201.

Helekar S.A., Char D., Neff S. and Patrick J. (1994). Prolyl isomerase requirement for the expression of functional homo-oligomeric ligand-gated ion channels. Neuron 12: 179-189.

Hempstead B.L., Patil N., Thiel B. and Chao M.V. (1990). Deletion of cytoplasmic sequences of the nerve growth factor receptor leads to a loss of high affinity ligand binding. J. Biol. Chem. 265: 9595-9598.

Hempstead B.L., Martin-Zanca D., Kaplan D.R., Parada L.F. and Chao M.V. (1991). High affinity binding requires co-expression of the trk proto-oncogene and the low affinity NGF receptor. Nature. 350: 678-683.

Hendry I.A. and Campbell J. (1976). Morphometric analysis of rat superior cervical ganglion after

axotomy and nerve growth factor treatment. J. Neurocytol. 5: 351-360.

Hess P., Lansman J.B. and Tsien R.W. (1984). Different modes of Ca channel gating behavior favoured by dihydropyridine Ca agonists
and antagonists. Nature 311: 538-544.

Higgins D., Waxman A. and Banker G. (1988). The distribution of microtubule-associated protein 2 changes when dendritic growth is induced in rat sympathetic neurons in vitro. Neurosci. 24: 583-592.

Higgins D., Lein P.J., Osterhout D.J. and Johnson M.I. (1991). Tissue culture of mammalian autonomic neurons. In Culturing Nerve Cells ed. G. Banker K. Goslin, pp. 177-205. Cambridge: MIT.

Hill C.S. and Treisman R. (1995). Transcriptional regulation by extracellular signals: mechanisms and specificity. Cell 80: 199-211.

Hill J.A., Zoli M., Bourgeois J.P. and Changeux J.-P. (1993). Immunocytochemical localization of a neuronal nicotinic receptor: the ß2 subunit. J. Neurosci. 13: 1551-1568.

Hirai H., Maru Y., Hagiwara K., Nishida J. and Takaku F. (1987). A novel putative tyrosine kinase receptor encoded by the EPH gene. Science 238: 1717-1720.

Hirokawa N., Shiomura Y., Okabe S. (1988a). Tau proteins: the molecular structure and mode of binding on microtubules. J. Cell. Biol. 107: 1449-1459.

Hirokawa N., Hisanaga S. and Shiomura Y. (1988b). MAP2 is a component of crossbridges between microtubules and neurofilaments in the neural cytoskeleton: quick-freeze, deep-etch immunoelectron microscopy and reconstitution studies. J. Neurosci. 8: 2769-2779.

Hofer M.M. and Barde Y.-A. (1988). Brain-derived neurotrophic factor prevents neuronal death in vivo. Nature 331: 261-262.

Hohn A., Leibrock J., Bailey K. and Barde Y.-A. (1990). Identification and characterization of a novel member of the nerve growth factor/brain-derived neurotrophic factor family. Nature 344: 339-341.

Holtzman D.M., Li Y. Parada L.F., Kinsman S., Chen C.-K., Valletta J.S., Zhou J., Long J.B. and Mobley W.C. (1992). p140^{trk} mRNA marks NGF-responsive forebrain neurons: evidence that trk gene expression is induced by NGF. Neuron 9: 465-478.

Holtzman D.M., Kilbridge J., Li Y., Cunningham E.M. Jr., Lenn N.J., Clary D.O., Reichardt L.F. and Mobley W.C. (1995). trkA expression in the CNS: evidence for the existence of several novel NGF-responsive CNS neurons. J. Neurosci. 15: 1567-1576.

Housley G.D. and Ashmore J.F. (1991). Direct measurement of the action of acetylcholine on isolated outer hair cells of the guinea pig cochlea. Proc. R. Soc. Lond. (B) 244: 161-167.

Huber G., Alaimo-Beuret D. and Matus A. (1985). MAP3: characterization of a novel microtubule-associated protein. J. Cell Biol. 100: 496-507.

Hunter T. (1995). Protein kinases and phosphatases: the yin and yang of protein phosphorylation and signaling. Cell 80: 225-236.

Ibánez C.F., Ebendal T., Barbany G., Murray-Rust J., Blundell T.L. and Persson H. (1992). disruption of the low affinity receptor-binding site in NGF allows neuronal survival and differentiation by binding to the trk gene product. Cell 69: 329-341.

Ibánez C.F. (1994). Structure-function relationships in the neurotrophin family. J. Neurobiol. 25: 1349-1361.

Ip N.Y., Ibánez C.F., Nye S.H., McClain J., Jones P.F., Gies D.R., Belluscio L., Le B.M., Espinosa R., Squinto S.P., Persson H. and Yancopoulos G.D. (1992). Mammalian neurotrophin-4: structure, chromosomal localization, tissue distribution, and receptor specificity. Proc. Natl. Acad. Sci. USA 89: 3060-3064.

Ip N.Y., Li Y., Yancopoulos G.D. and Lindsay R.M. (1993a). Cultured hippocampal neurons show responses to BDNF, NT-3, and NT-4, but not NGF. J. Neurosci. 13: 3394-3405.

Ip N.Y., Stitt T.N., Tapley P., Klein R., Glass D.J., Fandl J., Greene L.A., Barbacid M. and Yancopoulos G.D. (1993b). Similarities and differences in the way the trk receptors in neuronal and nonneuronal cells. Neuron 10: 137-149.

Ip N.Y. and Yancopoulos G.D. (1994). Neurotrophic factor receptors: just like other growth factor

and cytokine receptors? Curr. Opin. Neurobiol. 4: 400-405

Jacob M.H. and Berg D.K. (1983). The ultrastructural localization of α-bungarotoxin binding sites in relation to synapses on chick ciliary ganglion neurons. J. Neurosci. 3: 260-271.

Jacob M.H., Berg D.K. and Linstrom J. (1984). Shared antigenic determinant between the Electrophorus acetylcholine receptor and a synaptic component on chicken ciliary ganglion neurons. Proc. Natl. Acad. Sci. USA 81: 3223-3227.

Jacob M.H., Lindstrom J.L. and Berg D.K. (1986). Surface and intracellular distribution of a putative neuronal nicotinic acetylcholine receptor. J. Cell Biol. 103: 205-214.

Jacob M.H. and Berg D.K. (1987). Effects of preganglionic denervation and postganglionic axotomy on acetylcholine receptors in the chick ciliary ganglion. J. Cell Biol. 105: 1847-1854.

Jacob M.H. and Berg D.K. (1988). The distribution of acetylcholine receptors in chick ciliary ganglion neurons following disruption of ganglionic connections. J. Neurosci. 8: 3838-3849.

Jacob M.H. (1991). Acetylcholine receptor expression in developing chick ciliary ganglion neurons. J. Neurosci. 11: 1701-1712.

Jelsma T.N., Friedman H.H., Berkelaar M., Bray G.M. and Aguayo A.J. (1993). Different forms of the neurotrophin receptor trkB mRNA predominate in rat retina and optic nerve. J. Neurobiol. 24: 1207-1214.

Jensen K.F., Ohmstede C.-A., Fisher R.S. and Sahyoun N. (1991). Nuclear and axonal localization of Ca^{2+}/calmodulin-dependent protein kinase type Gr in rat cerebellar cortex. Proc. Natl. Acad. Sci. USA 88: 2850-2853.

Jessell T.M., Siegel R.E. and Fischbach G.D. (1979). Induction of acetylcholine receptors on cultured skeletal muscle by a factor extracted from brain and spinal cord. Proc. Natl. Sci. USA 76: 5397-5401.

Jing S., Tapley P. and Barbacid M. (1992). Nerve growth factor mediates signal transduction through trk homodimer receptors. Neuron 9: 1067-1079.

Johnson E.M. Jr. and Deckwerth T.L. (1993). Molecular mechanisms of developmental neuronal

death. Annu. Rev. Neurosci. 16: 31-46.

Johnson M.I., Higgins D. and Ard M.D. (1989). Astrocytes induce dendritic development in cultured sympathetic neurons. Dev. Brain Res. 47: 289-292.

Jonakait G.M. (1993). Neural-immune interactions in sympathetic ganglia. TINS 16: 419-423.

Jones K.R. and Reichardt L.F. (1990). Molecular cloning of a human gene that is a member of the nerve growth factor family. Proc. Natl. Acad. Sci. USA 87: 8060-8064.

Jones K.R., Farinas R., Backus C. and Reichardt L.F. (1994). Targeted disruption of the BDNF gene perturbs brain and sensory neuron development but not motor neuron development. Cell 76: 989-999.

Kalcheim C. and Gendreau M. (1988). Brain-derived neurotrophic factor stimulates survival and neuronal differentiation in cultured avian neural crest. Brain Res. 469: 79-86.

Kameshita I. and Fujisawa H. (1991). Phosphorylation and functional modification of calmodulin-dependent protein kinase IV by cAMP-dependent protein kinase. Biochem. Biophys. Res. Comm. 180: 191-196.

Kang H. and Schuman E.M. (1995). Long-lasting neurotrophin-induced enhancement of synaptic transmission in the adult hippocampus. Science 267: 1658-1662.

Kaplan D.R., Martin-Zanca D. and Parada L.F. (1991a). Tyrosine phosphorylation and tyrosine kinase activity of the trk proto-oncogene product induced by NGF. Nature 350: 158-160.

Kaplan D.R., Hempstead B.L., Martin-Zanca D., Chao M.V. and Parada L.F. (1991b). The trk proto-oncogene product: a signal transducing receptor for nerve growth factor. Science 252: 554-558.

Kaplan D.R. and Stephens R.M. (1994). Neurotrophin signal transduction by the trk receptor. J. Neurobiol. 25: 1404-1417.

Katz B. and Miledi R. (1968). The role of calcium in neuromuscular facilitation. J. Physiol. 195: 481-492.

Katz D.M., Markey K.A., Goldstein M. and Black I.B. (1983). Expression of catecholaminergic characteristics by primary sensory neurons in the normal adult rat in vivo. Proc. Natl. Acad. Sci. USA 80: 3526-3530.

Katz D.M., Erb M., Lillis R. and Neet K. (1990). Trophic regulation of nodose ganglion cell development: evidence for an expanded role of nerve growth factor during embryogenesis in the rat. Exp. Neurol. 110: 1-10.

Kelly R.B. and Grote E. (1993). Protein targeting in the neuron. Annu. Rev. Neurosci. 16: 95-127.

Kennedy M.B. (1989). Regulation of neuronal function by calcium. TINS 12: 417-420.

Kennedy, M.B. (1992). Second messengers and neuronal function. In: An introduction to molecular neurobiology. Ed. Hall, Z., Sinauer associates, inc. pp. 207-246.

Kessler J.A., Adler J.E., Bell W.O. and Black I.B. (1983). Substance P and somatostatin metabolism in sympathetic and special sensory ganglia in vitro. Neuroscience 9: 309-318.

Keyser K.T., Britto L.R.G., Schoepfer R., Whiting P., Cooper J., Conroy W., Borozozowska-Prechtl A., Karten H.J. and Lindstrom J. (1993). Three subtypes of α-bungarotoxin-sensitive nicotinic acetylcholine receptors are expressed in chick retina. J. Neurosci. 13: 442-454.

Kim S.U., Hogue-Angeletti R. and Gonatas N.K. (1979). Localization of nerve growth factor receptors in sympathetic neurons cultured in vitro. Brain Res. 168: 602-608.

Kirby M.L. (1988). Nodose placode contributes autonomic neurons to the heart in the absence of cardiac neural crest. J. Neurosci. 8: 1089-1095.

Klarsfeld A., Laufer R., Fontaine B., Devillers-Thiéry A., Dubreuil C. and Changeux J.-P. (1989). Regulation of muscle AChR α subunit gene expression by electrical activity: Involvement of protein kinase C and Ca^{2+}. Neuron 2: 1229-1236.

Kleiman R., Banker G. and Steward O. (1990). Differential subcellular localization of particular mRNAs in hippocampal neurons in culture. Neuron 5: 821-830.

Klein R., Parada L.F., Coulier F. and Barbacid M. (1989). trkB, a novel tyrosine protein kinase receptor expressed during mouse neural development. EMBO 8: 3701-3709.

Klein R., Conway D., Parada L.F. and Barbacid M. (1990a). The trkB tyrosine protein kinase gene codes for a second neurogenic receptor that lacks the catalytic kinase domain. Cell 61: 647-656.

Klein R., Martin-Zanca D.Barbacid M. and Parada L.F. (1990b). Expression of the tyrosine kinase receptor gene trkB is confined to the murine embryonic and adult nervous system. Development 109: 845-850.

Klein R., Jing S.Q., Nanduri V., O'Rourke E. and Barbacid M. (1991a). The trk proto-oncogene encodes a receptor for nerve growth factor. Cell 65: 189-197.

Klein R., Nanduri V., Jing S.Q., Lamballe F., Tapley P., Bryant S., Cordon-Cardo C., Jones K.R., Reichardt L.F. and Barbacid M. (1991b). The trkB tyrosine protein kinase is a receptor for brain-derived neurotrophic factor and neurotrophin-3. Cell 66: 395–403.

Klein R., Lamballe F., Bryant S. and Barbacid M. (1992). The trkB tyrosine protein kinase is a receptor for neurotrophin-4. Neuron 8: 947-956.

Klein R., Smeyne R.J., Wurst W., Long L.K., Auerbach B.A., Joyner A.L. and Barbacid M. (1993). Targeted disruption of the trkB neurotrophin receptor gene results in nervous system lesions and neonatal death. Cell 75: 113-122.

Klein R., Silos-Santiago I., Smeyne R.J., Lira S., Brambrilla R., Bryant S., Zhang L., Snider W.D. and Barbacid M. (1994). Disruption of the neurotrophin-3 receptor gene trkC eliminates Ia muscle afferents and results in abnormal movements. Nature 368: 249-251.

Koch C.A., Anderson D., Moran M.F., Ellis C. and Pawson T. (1991). SH2 and SH3 domains: elements that control interactions of cytoplasmic signaling proteins. Science 252: 668-674.

Koch C.A. and Zador A. (1993). The function of dendritic spines: devices subserving biochemical rather than electrical compartmentalization. J. Neurosci. 13: 413–422.

Koike T., Martin D.P. and Johnson E.M. Jr. (1989). Role of Ca^{2+} channels in the ability of membrane depolarization to prevent neuronal death induced by trophic-factor deprivation: Evidence that levels of internal Ca^{2+} determine nerve growth factor dependence of sympathetic ganglion cells. Proc. Natl. Acad. Sci. USA 86: 6421-6425.

Koike T., Tanaka S. (1991). Evidence that nerve growth factor dependence of sympathetic neurons

for survival in vitro may be determined by levels of cytoplasmic free Ca^{2+}. Proc. Natl. Acad. Sci. USA 88: 3892-3896.

Koizumi S., Contreras M.L. Matsuda Y., Hama T., Lazarovici L. and Guroff G. (1988). K-252a: a specific inhibitor of the action of nerve growth factor on PC12 cells. J. Neurosci. 8: 715-721.

Korsching S. and Thoenen H. (1983a). Nerve growth factor in sympathetic ganglia and corresponding target organs of the rat: correlation with density of sympathetic innervation. Proc. Natl. Acad. Sci. USA 80: 3513-3516.

Korsching S. and Thoenen H. (1983b). Quantitative demonstration of the retrograde axonal transport of endogenous nerve growth factor. Neurosci. Lett. 39: 1-4.

Korsching S. (1993). The neurotrophic factor concept: a reexamination. J. Neurosci. 13: 2739-2748.

Kosik K.S. and Finch E.A. (1987). MAP2 and tau segregate into dendritic and axonal domains after the elaboration of morphologically distinct neurites, an immunocytochemical study of cultured rat cerebellum. J. Neurosci. 7: 3142-3153.

Kraner S., Chong J.A., Tsay H.-J. and Mandel G. (1992). Silencing the type II sodium channel gene: a model for neural-specific gene regulation. Neuron 9: 37-44.

Krieg P.A. and Melton D.A. (1987). In vitro RNA synthesis with SP6 polymerase. Methods in Enzymology 155: 397-415.

Lai C. and Lemke G. (1991). An extended family of protein-tyrosine kinase genes differentially expressed in the vertabrate nervous system. Neuron 6: 691-704.

Lafont F., Rouget M., Triller A., Prochiantz A. and Rousselet A. (1992). In vitro control of neuronal polarity by glycosaminoglycans. Development 114: 17-29.

Lamballe F., Klein R. and Barbacid M. (1991). trkC, a new member of the trk family of tyrosine protein kinases, is a receptor for neurotrophin-3. Cell 66: 967-979.

Lamballe F., Tapley P. and Barbacid M. (1993). trkC encodes multiple neurotrophin-3 receptors with distinct biological properties and substrate specificities. EMBO 12: 3083-3094.

Landis S.C. (1976). Rat sympathetic neurons and cardiac myocytes developing in microcultures: correlation of the fine structure of endings with neurotransmitter function in single neurons. Proc. Natl. Acad. Sci. USA 73: 4220-4224.

Landreth G.E., Smith D.S., McCabe C. and Gittinger C. (1990). Characterization of a nerve growth factor-stimulated protein kinase in PC12 cells which phosphorylates microtubule-associated protein 2 and pp250. J. Neurochem. 55: 514-523.

Larkman A.U. (1991). Dendritic morphology of pyramidal neurons of the visual cortex of the rat: III. Spine distribution. J. Comp. Neurol. 306: 332-343.

Le Douarin N.M. (1986). Cell line segragation during peripheral nervous system ontogeny. Science 231: 1515-1522.

Le Douarin N.M. and Ziller C. (1993). Plasticity in neural crest cell differentiation. Curr. Opin. Cell Biol. 5: 1036-1043.

Lee K.F., Li E., Huber L.J., Landis S.C., Sharpe A.H., Chao M.V. and Jaenisch R. (1992). Targeted mutation of the gene encoding the low affinity NGF receptor p75 leads to deficits in the peripheral sensory nervous system. Cell 69: 737-749.

Lee K.F., Davies A.M. and Jaenish R. (1994). p75-deficient embryonic dorsal root sensory and neonatal sympathetic neurons display a decreased sensitivity to NGF. Development 120: 1027-1033.

Leibrock J., Lottspeich F., Hohn A., Hofer M., Hengerer B., Masiakowski P., Thoenen H. and Barde Y.-A. (1989). Molecular cloning and expression of brain-derived neurotrophic factor. Nature 341: 149-152.

Lein P.J. and Higgins D. (1989). Laminin and a basement membrane extract have different effects on axonal and dendritic outgrowth from embryonic rat sympathetic neurons in vitro. Dev. Biol. 136: 330-345.

Lein P.J. and Higgins D. (1991). Protein synthesis is required for the initiation of dendritic growth in embryonic sympathetic neurons in vitro. Dev. Brain Res. 60: 187-196.

Lein P.J., Higgins D., Turner D.C., Flier L.A. and Terranova V.P. (1991). The NC1 domain of

type IV collagen promotes axonal growth in sympathetic neurons through interaction with the α ß/ integrin. J. Cell Biol. 113: 417–428.

Lein P.J., Banker G. and Higgins D. (1992). Laminin selectively enhances axonal growth and accelerates the development of polarity by hippocampal neurons in culture. Dev. Brain Res. 69: 191-197.

Lein P., Johnson M., Guo X., Rueger D. and Higgins D. (1994). Osteogenic protein-1 (OP-1) induces dendritic growth in cultured sympathetic neurons. Soc. Neurosci. Abs. 20: 680.

Le Roux P.D. and Reh T.A. (1994). Regional differences in glial-derived factors that promote dendritic outgrowth from mouse cortical neurons in vitro. J. Neurosci. 14: 4639–4655.

Levi-Montalcini R. (1987). The nerve growth factor 35 years later. Science 237: 1154-1162.

Levitzki A. and Gazit A. (1995). Tyrosine kinase inhibition: an approach to drug development. Science 267: 1782-1788.

Li G., Hidaka H. and Wollheim C.B. (1992). Inhibition of voltage-gated Ca^{2+} channels and insulin secretion in hit cells by the Ca^{2+}/calmodulin-dependent protein kinase II inhibitor KN-62: comparison with antagonists of calmodulin and L-type Ca^{2+} channels. Mol. Pharmacol. 42: 489-498.

Lieberman A.R. (1976). Sensory ganglia. In: The peripheral nerve (LANDON. DN ed). London. Chapman and Hall.

Linden D.J. (1994). Long-term synaptic depression in the mammalian brain. Neuron 12: 457–472.

Lindholm D., Castrén E., Berzaghi M., Blöchi A. and Thoenen H. (1994). Activity-dependent and hormonal regulation of neurotrophin mRNA levels in the brain -implications for neuronal plasticity. J. Neurobiol. 25: 1362-1372.

Lindsay R.M., Rohrer H. (1985). Placodal sensory neurons in culture: nodose ganglion neurons are unresponsive to NGF, lack NGF receptors but are supported by liver-derived neurotrophic factor. Dev. Biol. 112: 30–48.

Lindsay R.M., Thoenen H. and Barde Y.-A. (1985). Placode and neural crest-derived sensory

neurons are responsive at early developmental stages to brain-derived neurotrophic factor. Dev. Biol. 112: 319-328.

Lindvall O., Ernfors P., Bengzon J., Kokaia Z., Smith M.-L., Siesjö B.O. and Persson H. (1992). Differencial regulation of mRNAs for nerve growth factor, brain-derived neurotrophic factor, and neurotrophin-3 in the adult rat brain following cerebral ischemia and hypoglycemic coma. Proc. Natl. Acad. Sci. USA 89: 648-652.

Lindvall O., Kokaia Z., Bengzon J., Elmér E. and Kokaia M. (1994). Neurotrophins and brain insults. TINS 17: 490–486.

Lipton S.A., Aizenman E. and Loring R.H. (1987). Neural nicotinic acetylcholine responses in solitary mammalian retinal ganglion cells. Pflugers Archives 410: 37–43.

Lipton S.A. and Kater S.B. (1989). Neurotransmitter regulation of neuronal outgrowth, plasticity and survival. TINS 12: 265-270.

Lisman J. (1994). The CaM kinase II hypothesis for the storage of synaptic memory. TINS 17: 406–412.

Listerud M., Brussaard A.B., Devay P., Colman D.R. and Role L.W. (1991). Functional contribution of neuronal AChR subunits revealed by antisense oligonucleotides. Science 254: 1518-1521.

Litman P., Barg J., Rinzoonski L. and Ginzburg I. (1993). Subcellular localization of tau mRNA in differentiating neuronal cell culture: implications for neuronal polarity. Neuron 10: 627-638.

Litman P., Barg J. and Ginzburg I. (1994). Microtubules are involved in the localization of tau mRNA in primary neuronal cell cultures. Neuron 13: 1463-1474.

Lochter A. and Schachner M. (1993). Tenascin and extracellular matrix glycoproteins: from promotion to polarization of neurite growth in vitro. J. Neurosci. 13: 3986–4000.

Loeb D.M., Maragos J., Martin-Zanca D., Chao M.V., Parada L.F. and Greene L.A. (1991). The trk proto-oncogene rescues NGF responsiveness in mutant NGF-nonresponsive PC12 cell lines. Cell 66: 961-966.

Loeb D.M., Tsao H., Cobb M.H. and Greene L.A. (1992). NGF and other growth factors induce an association between ERK1 and the NGF receptor, gp140^{prototrk}. Neuron 9: 1053-1065.

Loring R.H., Dahm L.M. and Zigmond R.E. (1985). Localization of α-bungarotoxin binding sites in the ciliary ganglion of the embryonic chick: an autoradiographic study at the light and electron microscopic level. Neuroscience 14: 645-660.

Loring R.H., Sah D.W.Y., Landis S.C. and Zigmond R.E. (1988). The ultrastructural distribution of putative nicotinic receptors on cultured neurons from the rat superior cervical ganglion. Neuroscience 24: 1071-1080.

Loring R.H. and Zigmond R.E. (1988). Characterization of neuronal nicotinic receptors by snake venom neurotoxins. TINS 11: 73-78.

Luetje C.W. and Patrick J. (1991). Both α- and ß-subunits contribute to the agonist sensitivity of neuronal nicotinic acetylcholine receptor. J. Neurosci. 11: 837-845.

Lyford G.L., Yamagata K., Kaufmann W.E., Barnes C.A., Sanders L.K., Copeland N.G., Gilbert D.J., Jenkins N.A., Lanahan A.A. and Worley P.F. (1995). *Arc*, a growth factor and activity-regulated gene, encodes a novel cytoskeleton-associated protein that is enriched in neuronal dendrites. Neuron 14: 433–445.

Ma Y., Campenot R.B. and Miller F.D. (1992). Concentration-dependent regulation of neuronal gene expression by nerve growth factor. J. Cell Biol. 117: 135-141.

Mahadeo D., Kaplan L., Chao M.V. and Hempstead B.L. (1994). High affinity nerve growth factor binding displays a faster rate of association than p140trk binding. Implications for multi-subunit polypeptide receptors. J. Biol. Chem. 269: 6884-6891.

Mains R.E. and Patterson P.H. (1973). Primary cultures of dissociated sympathetic neurons. I. Establishment of long-term growth in culture and studies of differentiated properties. J. Cell Biol. 59: 329-345.

Maisonpierre P.C., Belluscio L., Squinto S., Ip N.Y., Furth M.E., Lindsay R.M. and Yancopoulos G.D. (1990). Neurotrophin-3: a neurotrophin factor related to NGF and BDNF. Science 247: 1446-1451.

Malinow R., Schulman H. and Tsien R.W. (1989). Inhibition of post-synaptic PKC or CaMKII blocks induction but not expression of LTP. Science 245: 862-866.

Mandel G. and McKinnon D. (1993). Molecular basis of neural-specific gene expression. Annu. Rev. Neurosci. 16: 323-345.

Mandelzys A., Cooper E., Verge M.K. and Richardson P.M. (1990). Nerve growth factor induces functional nicotinic acetylcholine receptors on rat sensory neurons in culture. Neuroscience 37: 523-530.

Mandelzys A. (1992). Postnatal expression of nicotinic acetylcholine receptors by rat peripheral neurons. Ph.D. Thesis. Department of Physiology. McGill University.

Mandelzys A. and Cooper E. (1992). Effects of ganglionic satellite cells and NGF on the expression of nicotinic acetylcholine currents by rat sensory neurons. J. Neurophysiol. 67: 1213-1221.

Mandelzys A., Piè B., Deneris E.S. and Cooper E. (1994). The developmental increase in ACh current densities on rat sympathetic neurons correlates with changes in nicotinic ACh receptor α-subunit gene expression and occurs independent of innervation. J. Neurosci. 14: 2357-2364.

Mandelzys A., De Koninck P. and Cooper E. (1995). Agonist and toxin sensitivities of ACh-evoked currents on neurons expressing multiple nicotinic ACh receptor subunits. J. Neurophysiol. in press

Margiotta J.F., Berg D.K. and Dionne V.E. (1987a). The properties and regulation of functional acetylcholine receptors on chick ciliary ganglion neurons. J. Neurosci. 7: 3612-3622.

Margiotta J.F., Berg D.K. and Dionne V.E. (1987b). Cyclic AMP regulates the proportion of functional acetylcholine receptors on chicken ciliary ganglion neurons. Proc. Natl. Acad. Sci. USA 84: 8155-8159.

Margiotta J.F. and Gurantz D. (1989). Changes in the number, function, and regulation of nicotinic acetylcholine receptors during neuronal development. Dev. Biol. 135: 326-339.

Marsh S.J., Stansfeld C.E., Brown D.A., Davey R. and McCarthy D. (1987). The mechanism of action of capsaicin on sensory C-type neurons and their axons in vitro. Neuroscience 23: 275-289.

Marshall C.J. (1995). Specificity of receptor tyrosine kinase signaling: transient versus sustained extracellular signal-regulated kinase activation. Cell 80: 179-185.

Marshall J., Molloy R., Moss G.W.J., Howe J.R. and Hughes T.E. (1995). The jellyfish green fluorescent protein: a new tool for studying ion channel expression and function. Neuron 14: 211-215.

Marshall L.M. (1981). Synaptic localization of α-bungarotoxin binding which blocks nicotinic transmission at frog sympathetic neurons. Proc. Natl. Acad. Sci. USA 78: 1948-1952.

Martin D.P., Schmidt R.E., DiStefano P.S., Lowry O.H., Carter J.G. and Johnson E.M. Jr. (1988). Inhibitors of protein synthesis and RNA synthesis prevent neuronal death caused by nerve growth factor deprivation. J. Cell Biol. 106: 829-844.

Martinou J.-C. and Merlie J.P. (1991). Nerve-dependent modulation of acetylcholine ε-subunit gene expression. J. Neurosci. 11: 1291-1299.

Martin-Zanca D., Barbacid M. and Parada L.F. (1990). Expression of the trk proto-oncogene is restricted to the sensory cranial and spinal ganglia of neural crest origin in mouse development. Genes & Devel. 4: 683-694.

Mathie A., Bernheim L and Hille B. (1992). Inhibition of N-type calcium channels by muscarinic receptor activation in rat sympathetic neurons. Neuron 8: 907-914.

Mathieu C., Moisand A. and Weber M.J. (1984). Acetylcholine metabolism by cultured neurons from rat nodose ganglia: regulation by a macromolecule from muscle-conditioned medium. Neuroscience 13: 1373-1386.

Matsumura M. and Koelle G.B. (1961). The nature of synaptic transmission in the superior cervical ganglion following reinnervation by the afferent vagus. J. Pharmacol. Exp. Ther. 134: 28-46.

Matter J.-M., Matter-Sadzinski L. and Ballivet M. (1990). Expression of neuronal nicotinic acetylcholine receptor genes in the developing chick visual system. EMBO 9: 1021-1026.

Matter-Sadzinski L., Hernandez M.-C., Roztocil T., Ballivet M. and Matter J.-M. (1992). Neuronal specificity of the α7 nicotinic acetylcholine receptor promoter develops during morphogenesis of

the central nervous system. EMBO 11: 4529–4538.

Matthies H.J.G., Palfrey H.C., Hirning L.D. and Miller R.J. (1987). Down regulation of protein kinase C in neuronal cells: effects on neurotransmitter release. J. Neurosci. 7: 1198-1206.

Mattson M.P. (1988). Neurotransmitters in the regulation of neuronal cytoarchitecture. Brain Res. 472: 179-212.

Matus A. (1988). Microtubule-associated proteins: their potential role in determining neuronal morphology. Annu. Rev. Neurosci. 11: 29–44.

Matus A. (1994). Stiff microtubules and neuronal morphology. TINS 17: 19-22.

Maue R.A., Kraner S.D., Goodman R.H. and Mandel G. (1990). Neuron-specific expression of the rat brain type II sodium channel gene is directed by upstream regulatory elements. Neuron 4: 223-231.

McCormick F. (1993). How receptors turn ras on Nature 363: 15-16.

McEachern A.E., Jacob M.H. and Berg. D.K. (1989). Differential effects of nerve transection on the ACh and GABA receptors of chick ciliary ganglion neurons. J. Neurosci. 9: 3899-3907.

McGehee D.S. and Role L.W. (1995). Physiological diversity of nicotinic acetylcholine receptors expressed by vertebrate neurons. Annu. Rev. Physiol. 57: 521-546.

McMahan. U.J. (1990). The agrin hypothesis. Cold Spring Harbor Symp. Quant. Biol. 55:407–418.

McMahon S.B., Armanini M.P., Ling L.H. and Phillips H.S. (1994). Expression and coexpression of trk receptors in subpopulations of adult primary sensory neurons projecting to identified peripheral targets. Neuron 12: 1161-1171.

Merlie J.P. (1984). Biogenesis of the acetylcholine receptor, a multisubunit integral membrane protein. Cell 36:573-575.

Meyer T., Hanson P.I., Stryer L. and Schulman H. (1992). Calmodulin traping by calcium/calmodulin-dependent protein kinase. Science 256: 1199-1202.

Middlemas D.S., Lindberg R.A. and Hunter T. (1991). trkB, a neural receptor protein-tyrosine kinase: evidence for a full-lenght and two truncated receptors. Mol. Cell Biol. 11: 143-153.

Milbrandt J. (1986). Nerve growth factor rapidly induces c-*fos* mRNAin PC12 rat pheochromacytoma cells. Proc. Natl. Acad. Sci. USA 83: 2374-2378.

Miller F.D., Speelman A., Mathew T.C., Fabian J., Pozniak C. and Toma J.G. (1994). Nerve growth factor derived from terminals selectively increases the ratio of p75 to trkA NGF receptors on mature sympathetic neurons. Dev. Biol. 161: 206-217.

Miyasaka T., Chao M.V., Sherline P. and Saltied A.R. (1990). Nerve growth factor stimulates a protein kinase in PC-12 that phosphorylates microtubule-associated protein-2. J. Biol. Chem. 265: 4730-4735.

Mochizuki H., Ito T. and Hidaka H. (1993). Purification and characterization of Ca^{2+}/calmodulin-dependent protein kinase V from rat cerebrum. J. Biol. Chem. 268: 9143-9147.

Morgan J.I. and Curran T. (1995). Immediate-early genes: ten years on. TINS 18: 66-67.

Moss B.L. and Role L.W. (1993). Enhanced ACh sensitivity is accompanied by changes in ACh receptor channel properties and segregation of ACh receptor subtypes on sympathetic neurons during innervation in vivo. J. Neuroscience 13: 13-28.

Mu X., Silos-Santiago I., Caroll S.L. and Snider W.D. (1993). Neurotrophin receptor genes are expressed in distinct patterns in developing dorsal root ganglia. J.Neurosci. 13: 4029-4041.

Mudge A.W. (1984). Schwann cells induce morphological transformation of sensory neurones in vitro. Nature 309: 367-369.

Mulle C. and Changeux J.-P. (1990). A novel type of nicotinic receptor in the rat CNS characterized by patch clamp techniques. J. Neurosci. 10: 169-175.

Mulle C., Vidal C., Benoit P. and Changeux J.-P. (1991). Existence of different subtypes of nicotinic acetylcholine receptors in the rat habenulo-interpeduncular system. J. Neurosci. 11: 2588-2597.

Mulle C., Choquet D., Korn H. and Changeux J.-P. (1992a). Calcium influx through nicotinic

receptor in rat central neurons: Its relevance to cellular regulation. Neuron 8: 135-143.

Mulle C., Léna C. and Changeux J.-P. (1992b). Potentiation of nicotinic receptor response by external calcium in rat central neurons. Neuron 8: 937-945.

Murphy T.H., Worley P.F. and Baraban J.M. (1991). L-type voltage-sensitive calcium channels mediate synaptic activation of immediate early genes. Neuron 7: 625-635.

Nguyen P.V., Abel T. and Kandel E.R. (1994). Requirement of a critical period of transcription for induction of a late phase of LTP. Science 265: 1104-1107.

Nordberg A., Nilsson-Hakansson L., Adem A., Hardy J., Alafuzoff I., Lai Z., Herrera-Marschitz M. and Winblad B. (1989). The role of nicotinic receptors in the pathophysiology of Alzheimer's disease. Prog. Brain Res. 79: 353-362.

Nurse C.A. and O'Lague P.H. (1975). Formation of cholinergic synapses between dissociated sympathetic neurons and skeletal myotubes of the rat in cell culture. Proc. Natl. Acad. Sci. USA 72: 1955-1959.

Ocorr K.A. and Shulman H. (1991). Activation of multifunctional Ca^{2+}/calmodulin-dependent kinase in intact hippocampal slices. Neuron 6: 907-914.

Ohmichi M., Decker S. and Saltiel A. (1991). Nerve growth factor induces the association of a 130 Kd phosphoprotein with its receptor in PC12 pheochromocytoma cells. Cell Reg. 2: 691-697.

Ohmichi M., Decker S.J. and Saltiel A.R. (1992). Activation of phosphadylinositol-3 kinase by nerve growth factor involves indirect coupling of the trk proto-oncogene with src homology 2 domains. Neuron 9: 769-777.

Okazawa H., Nishiyama K., Kamei M., Washizaki K., Murayama S., Kwak S. and Kanazawa I. (1993). trk immunoreactivity at neuronal dendrite and cell body. Biochem. Biophys. Res. Comm. 194: 683-690.

Olmsted J.B. (1986). Microtubule-associated proteins. Annu. Rev. Cell Biol. 2: 421-457.

Oppenheim R.W. (1991). Cell death during development of the nervous system. Annu. Rev. Neurosci. 14: 453-501.

Ortells M.O. and Lunt G.G. (1995). Evolutionary history of the ligand-gated ion-channel superfamily of receptors. TINS 18: 121-127.

Osterberg A.-J. C., Raisman G., Field P.M., Iversen L.L. and Zigmond R.E. (1976). A quantitative comparison of the formation of synapses in the rat superior cervical ganglion by its own and by foreign nerve fibers. Brain Res. 107:445-470.

Osterhout D.J., Frazier W.A. and Higgins D. (1992). Thrombospondin promotes process outgrowth in neurons from the peripheral and central nervous systems. Dev. Biol. 150: 256-265.

Ozkaynak E., Rueger D.C., Drier E.A., Corbett C., Ridge R.J., Sampath T.K. and Opperman H. OP-1 cDNA encodes an osteogenic protein in the TGF-beta family. EMBO 9: 2085-2093.

Paintal A.S. (1964). Effects of drugs on vertebrate mechanoreceptors. Pharmacol. Rev. 16: 341-380.

Paintal A.S. (1973). Vagal sensory receptors and their reflex effects. Physiol. Rev. 53: 159-227.

Palouzier B., Barrit-Chamoin M.C., Portalier P. and Ternaux J.P. (1987). Cholinergic neurons in the rat nodose ganglia. Neurosci. Lett. 80: 147-152.

Pannese E. (1981). The satellite cells of the sensory ganglion. Advances in Anatomy, Embryology and Cell Biology. 65: 1-111.

Papke R.L. (1993). The kinetic properties of neuronal nicotinic receptors: genetic basis of functional diversity. Prog. Neurobiol. 41: 509-531.

Patrick J. and Stallcup W.B. (1977). Immunological distinction between acetylcholine receptor and the α-bungarotoxin-binding component on sympathetic neurons. Proc. Natl. Acad. Sci. USA 74: 4689-4692.

Patrick J., Séquéla P., Vernino S., Amador M., Luetje C. and Dani J.A. (1993). Functional diversity of neuronal nicotinic acetylcholine receptors. Prog. Brain Res. 98: 113-120.

Patterson P.H. and Chun L.L.Y. (1977). The induction of acetylcholine synthesis in primary cultures of dissociated rat sympathetic neurons. I. Effects of conditioned medium. Dev. Biol. 56: 263-280.

Pawson T. (1995). Protein modules and signalling networks. Nature 373: 573-580.

Peng I., Binder L.I. and Black M.M. (1986). Biochemical and immunological analyses of cytoskeletal domains of neurons. J. Cell Biol. 102: 252-262.

Persohn E. and Schachner M. (1987). Immunoelectron-microscopic localization of the neural cell adhesion molecules L1 and N-CAM during postnatal development of the mouse cerebellum. J. Cell Biol. 105: 569-576.

Persohn E. and Schachner M. (1990). Immunohistological localization of the neural adhesion molecules L1 and N-CAM in the developing hippocampus of the mouse. J. Neurocytol. 19: 807-819.

Peters A., Palay S.L. and Webster H. (1991). The fine structure of the nervous system: The neurons and supporting cells. Oxford University Press, Inc. 3rd ed.

Plummer M.R., Logothesis D.E. and Hess P. (1989). Elementary properties and pharmacological sensitivities of calcium channels in mammalian peripheral neurons. Neuron 2: 1453-1463.

Prochiantz A., Rousselet A. and Chamak B. (1990). Adhesion and the in vitro development of axons and dendrites. Prog. Brain Res. 86: 331-336.

Puchacz E., Buisson B., Bertrand D. and Lukas R.J. (1994). Functional expression of nicotinic acetylcholine receptors containing rat α7 subunitsin human SH-SY5Y neuroblastoma cells. FEBS 354: 155-159.

Pugh P.C. and Berg D.K. (1994). Neuronal acetylcholine receptors that bind α-bungarotoxin mediate neurite retraction in a calcium-dependent manner. J. Neurosci. 14: 889-896.

Purves D., Hadley R.D. and Voyvodic J.T. (1986a). Dynamic changes in the dendritic geometry of individual neurons visualized over periods of up to three months in the superior cervical ganglion of living mice. J. Neurosci. 6: 1051-1060.

Purves D., Rubin E., Snider W.D. and Lichtman (1986b). Relation of animal size to convergence, divergence, and neuronal number in peripheral sympathetic pathways. J. Neurosci. 6: 158-163.

Purves D., Snider W.D. and Voyvodic J.T. (1988). Trophic regulation of nerve cell morphology

and innervation in the autonomic nervous system. Nature 336: 123-128.

Qian J., Bull M.S. and Levitt P (1992). Target-derived astroglia regulate axonal outgrowth in a region-specific manner. Dev. Biol. 149: 278-294.

Rabizadeh S., Oh J., Zhong L.-T., Yang J., Bitler C.M., Butcher L.L. and Bredesen D.E. (1993). Induction of apoptosis by the low-affinity NGF receptor. Science 261: 345-348.

Radeke M.J., Misko T.P., Hsu C., Herzenberg L.A. and Shooter E.M. (1987). Gene transfer and molecular cloning of the rat nerve growth factor receptor. Nature 325: 593-597.

Rakic P. and Sidman R.L. (1973). Organization of cerebellar cortex secondary to deficit of granule cells in weaver mutant mice. J. Comp. Neurol. 152: 133-162.

Rao A. and Steward O. (1991). Evidence that protein constituents of post-synaptic membrane specializations are locally synthesized: analysis of proteins synthesized in synaptosomes. J. Neurosci. 11: 2881-2895.

Rall W. (1970). Cable properties of dendrites and effects of synaptic location. In: excitatory synaptic mechanisms (Anderson P., Jansen J.K.S. eds). pp175-187. Oslo: Universitetsforlaget.

Rathouz M.M. and Berg D. (1994). Synaptic-type acetylcholine receptors raise intracellular calcium levels in neurons by two mechanisms. J. Neurosci. 14: 6935-6945.

Ravdin P.M. and Berg D.K. (1979). Inhibition of neuronal acetylcholine sensitivity by α-toxins from *Bungarus multicinctus* venom. Proc. Natl. Acad. Sci. USA 76: 2072-2076.

Regan L.J., Sah D.W.Y. and Bean B.P. (1991). Ca^{2+} channels in rat central and peripheral neurons: high-threshold current resistant to dihydropyridine blockers and ω-conotoxin. Neuron 6: 269-280.

Regehr W.G. and Tank D.W. (1994). Dendritic calcium dynamics. Curr. Opin. Neurobiol. 4: 373-382.

Richardson P.M. and Riopelle R.J. (1984). Uptake of nerve growth factor along peripheral and spinal axons of primary sensory neurons. J. Neurosci. 4: 1683-1689.

Robitaille R., Adler E.M. and Charlton M.P. (1990). Strategic location of calcium channels at transmitter release sites of frog neuromuscular synapses. Neuron 5: 773-779.

Robitaille R., Garcia M.L., Kaczorowski G.J. and Charlton M.P. (1993). Functional colocalization of calcium and calcium-gated potassium channels in control of transmitter release. Neuron 11: 645-655.

Rodriguez-Tébar A., Dechant G. and Barde Y.-A. (1990). Binding of brain-derived neurotrophic factor to the nerve growth factor receptor. Neuron 4: 487–492.

Rodriguez-Tébar A., Dechant G., Gotz R. and Barde Y.-A. (1992). Binding of neurotrophin-3 to its neuronal receptors and interactions with nerve growth factor and brain-derived neurotrophic factor. EMBO 11: 917-922.

Rogers S.W., Mandelzys A., Deneris E.S., Cooper E. and Heinemann S. (1992). The expression of nicotinic acetylcholine receptors by PC12 cells treated with NGF. J. Neurosci. 12: 4611–4623.

Role L.W. (1988). Neural regulation of acetylcholine sensitivity in embryonic sympathetic neurons. Proc. Natl. Acad. Sci. 85: 2825-2829.

Rosen L.B., Ginty D.D., Weber M.J. and Greenberg M.E. (1994). Membrane depolarization and calcium influx stimulate MEK and MAP kinase via activation of ras. Neuron 12: 1207-1221.

Rosenthal A., Goeddel D.V., Nguyen T., Lewis M., Shih A., Laramee G.R., Nikolics K. and Winslow J.W. (1990). Primary stucture and biological activity of a novel human neurotrophic factor. Neuron 4: 767-773.

Rothwell N.J. and Hopkins S.J. (1995a). Cytokines and the nervous system I: expression and recognition. TINS 18: 83-88.

Rothwell N.J. and Hopkins S.J. (1995b). Cytokines and the nervous system II: actions and mechanisms of action. TINS 18: 130-136.

Rousselet A., Fetler L., Chamak B. and Prochaintz A. (1988). Rat mesencephalic neurons in culture exhibit different morphological traits in the presence of media conditioned on mesencephalic or striatal astroglia Paris. Dev. Biol. 129: 495-504.

Rousselet A., Autillo-Touati A., Araud D. and Prochiantz A. (1990). In vitro regulation of neuronal morphogenesis and polarity by astrocyte-derived factors. Dev. Biol. 137: 33-45.

Rowell P.P., Carr L.A. and Garner A.C. (1987). Stimulation of [^{3}H]dopamine release gy nicotine in rat nucleus accumbens. J. Neurochem. 49: 1449-1454.

Rubin E. (1985a). Development of the rat superior cervical ganglion: ganglion cell maturation. J. Neurosci. 5: 673-684.

Rubin E. (1985b). Development of the rat superior cervical ganglion: Initial stages of synapse formation. J. Neurosci. 5: 697-704.

Ruit K.G. and Snider W.D. (1991). Administration or deprivation of nerve growth factor during development permanently alters neuronal geometry. J. Comp. Neurol. 314: 106-113.

Sah D.W.Y. Loring R.H. and Zigmond R.E. (1987). Long-term blockade by toxin F of nicotinic synaptic potentials in cultured sympathetic neurons. Neuroscience 20: 867-874.

Sambrook J., Fritsch. E.F., Maniatis. T. (1989). Molecular Cloning: a laboratory manual. 2nd ed. Nolan C. editor. Cold Spring Harbor Lab. Press.

Sanes J.R. (1989). Extracellular matrix molecules that influence neural development. Annu. Rev. Neurosci. 12: 491-516.

Sargent P.B. and Pang D.Z. (1988). Denervation alters the size, number, and distribution of clusters of acetylcholine receptor-like molecules on frog cardiac ganglion neurons. Neuron 1: 877-886.

Sargent P.B. and Pang D.Z. (1989). Acetylcholine receptor-like molecules are found in both synaptic and extrasynaptic clusters on the surface of neurons in the frog cardiac ganglion. J. Neurosci. 9: 1062-1072.

Sargent P.B., Bryan G.K., Streichert L.C. and Garrett E.N. (1991). Denervation does not alter the number of neuronal bungarotoxin binding sites on autonomic neurons in the frog cardiac ganglion. J. Neurosci. 11: 3610-3623.

Sargent P.B. (1993). The diversity of neuronal nicotinic acetylcholine receptors. Annu. Rev.

Neurosci. 16: 403-443.

Sargent P.B. and Wilson H.L. (1995). Distribution of nicotinic acetylcholine receptor subunit immunoreactivities on the surface of chick ciliary ganglion neurons. In Effects of Nicotine on Biological Systems II. Advances in Pharmacological Sciences. Birkhäuser. Verlag. Basel. pp 355-361.

Schafer T., Schwab M.E. and Thoenen H. (1983). Increased formation of preganglionic synapses and axons due to a retrograde trans-synaptic action of nerve growth factor in the rat sympathetic nervous system. J. Neurosci. 3: 1501-1510.

Schanen-King C., Nel A., Williams L.K. and Landreth G. (1991). Nerve growth factor stimulates the tyrosine phosphorylation of MAP2 Kinase in PC12 cells. Neuron 6: 915-922.

Schecterson L.C. and Bothwell M. (1992). Novel roles for neurotrophins are suggested by BDNF and NT-3 mRNA expression in developing neurons. Neuron 9: 449-463.

Scheibe R.J. and Wagner J.A. (1992). Retinoic acid regulates both expression of the nerve growth factor receptor and sensitivity to nerve growth factor. J. Biol. Chem. 267: 17611-17616.

Schilling K., Dickinson M.H., Connor J.A. and Morgan J.I. (1991). Electrical activity in cerebellar cultures determines Purkinje cell dendritic growth patterns. Neuron 7: 891-902.

Schlessinger J. and Ullrich A. (1992). Growth factor signaling by receptor tyrosine kinases. Neuron 9: 383-391.

Schlessinger J. and Bar-Sagi D. (1995). Activation of ras and other signaling pathways by tyrosine receptor kinases. In symposia on quantitative biology: molecular genetics of cancer. vol. 60 (cold spring harbor. New York: cold spring harbor laboratory press). in press.

Schoenherr C.J. and Anderson D.J. (1995). The neuron-restrictive silencer factor (NRSF): a coordinate repressor of multiple neuron-specific genes. Science 267: 1360-1363.

Schoepfer R., Halvorsen S.W., Conroy W.G., Whiting P. and Lindstrom J. (1989). Antisera against an acetylcholine receptor α3 fusion protein bind to ganglionic but not brain nicotinic acetylcholine receptors. FEBS Letters 257: 393-399.

Schoepfer R., Conroy W.G., Whiting P., Gore M. and Lindstrom J. (1990). Brain α-bungarotoxin binding protein cDNAs and MAbs reveal subtypes of this branch of the ligand-gated ion channel gene superfamily. Neuron 5: 35-48.

Schulman H. (1993). The multifunctional Ca^{2+} calmodulin-dependent protein kinases. Curr. Opin. Cell Biol. 5: 247-253.

Schwartz J.P., Pearson J. and Johnson E.M. (1982). Effect of exposure to anti-NGF on sensory neurons of adults rats and guinea pigs. Brain Res. 244: 378-381.

Schwartz Levey M., Brumwell C.L., Dryer S.E. and Jacob M.H. (1995). Innervation and target tissue interactions differentially regulate acetylcholine receptor subunit mRNA levels in developing neurons in situ. Neuron 14: 153-162.

Séguéla P., Wadiche J., Dineley-Miller K., Dani J. and Patrick J.W. (1993). Molecular cloning, functional properties, and distribution of rat brain α7 nicotinic cation channel highly permeable to calcium. J. Neurosci. 13: 596-604.

Shelton D.L. and Reichardt L.F. (1984). Expression of the beta nerve growth factor gene correlates with the density of sympathetic innervation in effector organs. Proc. Natl. Acad. Sci. USA 81: 7951-7955.

Sheng M. and Greenberg M.E. (1990). The regulation and function of c-fos and other immediate early genes in the nervous system. Neuron 4: 477-485.

Sheng M., Thompson M.A. and Greenberg M.E. (1991). CREB: a Ca^{2+}-regulated transcription factor phosphorylated by calmodulin-dependent kinases. Science 252: 1427-1430.

Shepherd M.G. (1994). Neurobiology. 3rd ed. Oxford University press. New York. pp. 1-760.

Sieber-Blum M. (1991). Role of the neurotrophic factors BDNF and NGF in the commitment of pluripotent neural crest cells. Neuron 6: 949-955.

Silva A.J., Stevens C.F., Tonegawa S. and Wang Y. (1992a). Deficient hippocampal long-term potentiation in α-calcium-calmodulin kinase II mutant mice. Science 257: 201-206

Silva A.J., Paylor R., Wehner J.M. and Tonegawa S. (1992b). Impaired spatial learning in α-

calcium-calmodulin kinase II mutant mice. Science 257: 206-211.

Small D.H., Reed G., Whitefield B. and Nurcombe V. (1995). Cholinergic regulation of neurite outgrowth from isolated chick sympathetic neurons in culture. J. Neurosci. 15: 144-151.

Smeyne R.J., Klein R., Schnapp A., Long L.K., Bryant S., Lewin A., Lira S.A. and Barbacid M. (1994). Severe sensory and sympathetic neuropathies in mice carrying a disrupted TRK/NGF receptor gene. Nature 368: 246-249.

Smolen A.J. and Raisman G. (1980). Synapse formation in the rat superior cervical ganglion during normal development and after neonatal deafferentation. Brain Res. 181: 315-323.

Smolen A.J. and Beaston-Wimmer P. (1986). Dendritic development in the rat superior cervical ganglion. Dev. Brain Res. 29: 245-252.

Snider W.D. (1988). Nerve growth factor enhance arborization of sympathetic ganglion cells in developing mammals. J. Neurosci. 8: 2628-2634.

Soppet D., Escandon E., Maragos J., Middlemas D.S., Reid S.W., Blair J., Burton L.E., Stanton B.R., Kaplan D.R., Hunter T., Nikolics K. and Parada L.F. (1991). The neurotrophic factors brain-derived neurotrophic factor and neurotrophin-3 are ligands for the trkB tyrosine kinase receptor. Cell 65: 895-903.

Squinto S.P., Stitt T.N., Aldrich T.H., Davis S., Bianco S.M., Radziejewski. Glass D.J., Masiakowski P., Furth M.E., Valenzuela D.M., DiStefano P.S. and Yancopoulos G.D. (1991). trkB encodes a functional receptor for brain-derived neurotrophic factor and neurotrophin-3 but not nerve growth factor. Cell 65: 885-893.

Srinivasan M., Edman C.F and Schulman H. (1994). Alternative splicing introduces a nuclear localization signal that targets multifunctional CaM kinase to the nucleus. J. Cell. Biol. 126: 839-852.

Stahl N. and Yancopoulos G.D. (1994). The tripartite CNTF receptor complex: activation and signaling involves components shared with other cytokines. J. Neurobiol. 25: 1454-1466.

Stephens R.M., Loeb D.M., Copeland T.D., Pawson T., Greene L.A. and Kaplan D.R. (1994). trk receptors use redundant signal transduction pathways involving SHC and PLC-γ1 to mediate NGF

responses. Neuron 12: 691-705.

Sternberger L.A. and Sternberger N.H. (1983). Monoclonal antibodies distinguish phosphorylated and non-phosphorylated forms of neurofilaments in situ. Proc. Natl. Acad. Sci. USA 80: 6126-6130.

Steward O. and Falk P.M. (1986). Protein-synthetic machinery at postsynaptic sites during synaptogenesis: a quantitive study of the association between polyribosomes and developing synapses. J. Neurosci. 6: 412-423.

Steward O. and Reeves T.M. (1988). Protein-synthetic machinery beneath postsynaptic sites on CNS neurons: association between polyribosomes and other organelles at the synaptic site. J. Neurosci. 8: 176-184

Steward O. and Banker G.A. (1992). Getting the message from the gene to the synapse: sorting and intracellular transport of RNA in neurons. TINS 5: 180-186.

Stollberg J. and Berg D.K. (1987). Neuronal acetylcholine receptors: fate of surface and internal pools in cell culture. J. Neurosci. 7: 1809-1815.

Streichert L.C. and Sargent P.B. (1992). The role of acetylcholinesterase in denervation supersensitivity in the frog cardiac ganglia. J. Physiol. 445: 249-260.

Stuart G.J. and Sakmann B. (1994). Active propagation of somatic action potentials into neocortical pyramidal cell dendrites. Nature 367: 69-72.

Sucher N.J., Cheng T.P.O. and Lipton S.A. (1990). Neural nicotinic acetylcholine responses in sensory neurons from postnatal rat. Brain Res. 533: 248-254.

Sumal K.K., Blessing W.W., Joh T.H., Reis D.J. and Pickel V.M. (1983). Synaptic interaction of vagal afferents and catecholaminergic neurons in the rat nucleus tractus solitarius. Brain Res. 277: 31-40.

Swanson L.W., Simmons D.M., Whiting P.J. and Lindstrom J. (1987). Immunohistochemical localization of neuronal nicotinic receptors in the rodent central nervous system. J. Neurosci. 7: 3334-3342.

Tanaka C. and Nishizuka Y. (1994). The protein kinase C family for neuronal signaling. Annu. Rev. Neurosci. 17: 551-567.

Talman W.T., Perrone M.H. and Reis D.J. (1980). Evidence for L-glutamate as the neurotransmitter of baroreceptor afferent nerve fibres. Science 209: 813-815.

Tartaglia L.A. and Goeddel D.V. (1992). Two TNF receptors. Immunol. Today 13: 151-153.

Tartaglia, L.A., Ayres, T.M., Wong, G.H.w. and Goeddel, D.V. (1993). A novel domain within the 55 kd TNF receptor signals cell death. Cell 73: 213-216.

Tennyson V.M. (1965). Electron microscopic study of the developing neuroblast of the dorsal root ganglion of the rabbit embryo. J. Comp. Neur. 124: 267-318.

Ternaux J.P., Falempin M., Palouzier B., Chamoin M.C. and Portalier P. (1989). Presence of cholinergic neurons in the vagal afferent system: biochemical and immunohistochemical approaches. J. Auton. Nerv. Syst. 28: 233-242.

Tiedge H., Fremeau R.T., Weinstock P.H., Arancio O. and Brosius J. (1991). Dendritic location of neural BC1 RNA. Proc. Natl. Acad. Sci. USA 88: 2093-2097.

Tokumitsu H., Chijiwa T., Hagiwara M., Mizuntani A., Terasawa M. and Hidaka H. (1990). KN-62, 1-[*N,O*-Bis(5-isoquinolinesulfonyl)-*N*-methyl-L-tyrosyl]-4-phenylpiperizine, a specific inhibitor of Ca^{2+}/calmodulin-dependent protein kinase II. J. Biol. Chem. 265: 4315-4320.

Torre E.R. and Steward O. (1992). Demonstration of local protein synthesis within dendrites using a new cell culture system that permits the isolation of living axons and dendrites from their cell bodies. J. Neurosci. 12: 762-772.

Traverse S., Seedorf K., Paterson H., Marshall C.J., Cohen P. and Ullrich A. (1994). EGF triggers neuronal differentiation of PC12 cells that overexpress the EGF receptor. Curr. Biol. 4: 694-701.

Triller A., Cluzeaud F., Pfeiffer F., Betz H. and Korn H. (1985). Distribution of glycine receptors at central synapses: an immunoelectron microscopy study. J. Cell Biol. 101: 683-688.

Tropea M., Johnson M.I. and Higgins D. (1988). Glial cells promote dendritic development in rat sympathetic neurons in vitro. Glia 1: 380-392.

Trouslard J., Marsh S.J. and Brown D.A. (1993). Calcium entry through nicotinic receptor channels and calcium channels in cultured rat superior cervical ganglion cells. J. Physiol. Lond. 468: 53-71

Tsien R.W., Lipscombe D., Madison D.V., Bley K.R. and Fox A.P. (1988). Multiple types of neuronal calcium channels and their selective modulation. TINS 11: 431-438.

Tsoulfas P., Soppet D., Escandon E., Tessarollo L., Mendoza-Ramirez J.-L., Rosenthal A., Nikolics K. and Parada L.F. (1993). The rat trkC locus encodes multiple neurogenic receptors that exhibit differential response to neurotrophin-3 in PC12 cells. Neuron 10: 975-990.

Tucker R.P., Binder L.I. and Matus A.I. (1988). Neuronal microtubule-associated proteins in the embryonic avian spinal cord. J. Comp. Neurol. 271: 44-55.

Turner D.C., Flier L.A. and Carbonetto S. (1989). Identification of a cell-surface protein involved in PC12 cell-substratum adhesion and neurite outgrowth on laminin and collagen. J. Neurosci. 9: 3287-3296.

Vale R.D., Banker G. and Hall Z. (1992). The neuronal cytoskeleton. In: An introduction to molecular neurobiology. Ed. Hall, Z., Sinauer associates, inc. pp. 247-280.

Valenzuela D.M., Maisonpierre P.C., Glass D.J., Rojas E., Nunez L., Kong Y., Gies D.R., Stitt T.N., Ip N.Y. and Yancopoulos G.D. (1993). Alternative forms of rat trkC with different functional capabilities. Neuron 10: 963-974.

Vallee R.B. and Bloom G.S. (1991). Mechanisms of fast and slow axonal transport. Annu. Rev. Neurosci. 14: 59-92.

van der Geer P., Hunter T. and Lindberg R.A. (1994). Receptor protein-tyrosine kinases and their signal transduction pathways. Ann. Rev. Cell Biol. 10: 251-337.

Vaughn J.E. (1989). Review: fine structure of synaptogenesis in the vertebrate central nervous system. Synapse 3: 255-285.

Verdi J.M., Birren S.J., Ibánez C.F., Persson H., Kaplan D.R., Benedetti M., Chao M.V. and Anderson D.J. (1994). $p75^{LNGFR}$ regulates trk signal transduction and NGF-induced neuronal differentiation in MAH cells. Neuron 12: 733-745.

Verdi J.M. and Anderson D.J. (1994). Neurotrophins regulate sequential changes in neurotrophin receptor expression by sympathetic neuroblasts. Neuron 13: 1359-1372.

Verge V.M.K., Merlio J.-P., Grondin J., Ernfors P., Persson H., Riopelle R.J., Hökfelt T. and Richardson P.M. (1992). Colocalization of NGF binding sites, trk mRNA, and low-affinity NGF receptor mRNA in primary sensory neurons: responses to injury and infusion of NGF. J. Neurosci. 12: 4011-4022.

Vernino S., Amador M., Luetje C.W., Patrick J. and Dani J.A. (1992). Calcium modulation and high calcium permeability of neuronal nicotinic acetylcholine receptors. Neuron 8: 127-134.

Vernino S., Rogers M., Radcliffe K.A. and Dani J.A. (1994). Quantitative measurement of calcium flux through muscle and neuronal nicotinic acetylcholine receptors. J. Neurosci. 14: 5514-5524.

Vernallis A.B., Conroy W.G. and Berg D.K. (1993). Neurons assemble acetylcholine receptors with as many as three kinds of subunits while maintaining subunit segregation among receptor subtypes. Neuron 10: 451-464.

Vidal S., Raynaud B. and Weber M.J. (1989). The role of Ca^{2+} channels of the L-type in neurotransmitter plasticity of cultured sympathetic neurons. Mol. Brain Res. 6: 187-196.

Vijayaraghavan S., Schmid H.A., Halvorsen S.W. and Berg D.K. (1990). Cyclic AMP-dependent phosphorylation of a neuronal acetylcholine receptor α-type subunit. J. Neurosci. 10: 3255-3262.

Vijayaraghavan S., Pugh P.C., Zhang Z.-w., Rathouz M.M. and Berg D.K. (1992). Nicotinic receptors that bind α-bungarotoxin on neurons raise intracellular free calcium. Neuron 8: 353-362.

Vogel K.S. and Davies A.M. (1991). The duration of neurotrophic factor independence in early sensory neurons is matched to the time course of target field innervation. Neuron 7: 819-830.

Volonte C., Angelastro J.M. and Greene L.A. (1993a). Association of protein kinases ERK1 and ERK2 with p75 nerve growth factor receptors. J. Biol. Chem. 268: 21410-21415.

Volonte C., Ross A.H. and Greene L.A. (1993b). Association of a purine-analog-sensitive protein kinase activity with p75 nerve growth factor receptors. Mol. Biol. Cell 4: 71-78.

Voyvodic J.T. (1987). Development and regulation of dendrites in the rat superior cervical

ganglion. J. Neurosci. 7: 904-912.

Wada E., Wada K., Boulter J., Deneris E., Heinemann S., Patrick J. and Swanson L.W. (1989). Distribution of α2, α3, α4, and ß2 neuronal nicotinic receptor subunit mRNAs in the central nervous system: a hybridization histochemical study in the rat. J. Comp. Neurol. 284: 314-335.

Walke W., Staple J., Adams L., Gnedy M., Chahine K. and Goldman D. (1994). Calcium-dependent regulation of rat and chick muscle nicotinic acetylcholine receptor (nAChR) gene expression. J. Biol. Chem. 269: 19447-19456.

Walpole, R.E. (1982). Introduction to statistics. 3rd ed. Macmillian Publishing Co., Inc. pp. 1-521.

Wegner M., Zhaodan C. and Rosenfeld M.G. (1992). Calcium-regulated phosphorylation within the leucine zipper of C/EBPß. Science 256: 370-373.

Westenbroek R.E., Merrick D.K. and Catterall W.A. (1989). Differential subcellular localization of the RI and RII Na^+ channel subtypes in central neurons. Neuron 3: 695-704.

Westenbroek R.E., Ahlijanian M.K. and Catterall W.A. (1990). Clustering of L-type Ca^{2+} channels at the base of major dendrites in hippocampal pyramidal neurons. Nature 347: 281-284.

Whiting P.J. and Lindstrom J.M. (1986). Purification and characterization of a nicotinic acetylcholine receptor from chick brain. Biochemistry 25: 2082-2093.

Wingate R.J.T and Thompson I.D. (1994). Targeting and activity-related dendritic modification in mammalian retinal ganglion cells. J. Neurosci. 14: 6621-6637.

Winter J., Forbes C.A., Sternberg J. and Lindsay R.M. (1988). Nerve growth factor (NGF) regulates adult rat cultured dorsal root ganglion neuron responses to the excitotoxin capsaicin. Neuron 1: 973-981.

Wong R.O.L., Herrmann K. and Shatz C.J. (1991). Remodelling of retinal ganglion cell dendrites in the absence of action potential activity. J. Neurobiol. 22: 685-697.

Wright E.M., Vogel K.S. and Davies A.M. (1992). Neurotrophic factors promote the maturation of developing sensory neurons before they become dependent on these factors for survival. Neuron 9: 139-150.

Wyllie D.J.A. and Nicoll R.A. (1994). A role for protein kinases ans phosphatases in the Ca^{2+}-induced enhancement of hippocampal AMPA receptor-mediated synaptic responses. Neuron 13: 635-643.

Yamamori T., Fukada K., Aebersold R., Korsching S., Fann M.J. and Patterson P.H. (1989). The cholinergic neuronal differentiation factor from heart cells is identical to leukemia inhibitory factor [published erratum appears in Science 1990 Jan 19:247(4940):271]. Science 246: 1412-1416.

Yan Q. and Johnson E.M. Jr. (1988). An immunohistochemical study of the nerve growth factor receptor in developing rats. J. Neurosci. 8: 3481-3498.

Yang X., McDonough J., Fyodorov D., Morris M., Wang F. and Deneris E.S. (1994). Characterization of an acetylcholine receptor α3 gene promoter and its activation by the POU domain factor SCIP/Tst-1. J. Biol. Chem. 269: 10252-10264.

Yawo H. (1987). Changes in the dendritic geometry of mouse superior cervical ganglion cells following postganglionic axotomy. J. Neurosci. 7: 3703-3711.

Zhang Z.-w. and Feltz P. (1990). Nicotinic acetylcholine receptors in porcine hypophyseal intermediate lobe cells. J. Physiol. 422: 83-101.

Zhang Z.-w., Vijayaraghavan S. and Berg D.K. (1994). Neuronal acetylcholine receptors that bind α-bungarotoxin with high affinity function as ligand-gated ion channels. Neuron 12: 167-177.

Zheng J.Q., Felder M., Connor J.A. and Poo M.-m. (1994). Turning of nerve growth cones induced by neurotransmitters. Nature 368: 140-144.

Zoli M., Le Novère N., Hill J.A. Jr. and Changeux J.-P. (1995). Developmental regulation of nicotinic ACh receptor subunit mRNAs in the rat central and peripheral nervous systems. J. Neurosci. 15: 1912-1939.

Zorumski C.F., Thio L.L., Isenberg K.E. and Clifford D.B. (1992). Nicotinic acetylcholine currents in cultured postnatal rat hippocampal neurons. Mol. Pharmacol. 41: 931-936.

Appendix 1

Diversity of the Neurotrophins and Their Receptors

NGF, the first member of the neurotrophin family, was discovered over 4 decades ago (Levi-Montalcini, 1987), and only 30 years later was the second neurotrophin, brain-derived neurotrophic factor (BDNF), discovered (Barde *et al.*, 1982). The BDNF gene was then cloned (Leibrock *et al.*, 1989) and screening for homologs led to the identification of genes encoding three additional neurotrophins termed NT-3, NT-4/5 and NT-6 (Ernfors *et al.*, 1990; Hohn *et al.*, 1990; Jones and Reichardt, 1990; Maisonpierre *et al.*, 1990; Rosenthal *et al.*, 1990; Berkemeier *et al.*, 1991; Hallböök *et al.*, 1991; Ip *et al.*, 1992; Götz *et al.*, 1994).

The first neurotrophin receptor to be identified was originally termed the NGF receptor (Chao *et al.*, 1986; Radeke *et al.*, 1987). However, its binding affinity to NGF was 2 orders of magnitude lower than the high affinity [I^{125}]-NGF binding observed on nerve cells, and it did not appear to contain an intracellular signalling domain. In 1991, the *trk* proto-oncogene, originally described in 1986 as an oncoprotein in human colon carcinoma, was shown to serve as the signalling receptor for NGF (Kaplan *et al.*, 1991a,b; Klein *et al.*, 1991a). Soon after *trk*B was recognized as the primary receptor for BDNF (Klein *et al.*, 1991b; Soppet *et al.*, 1991; Squinto *et al.*, 1991) and NT-4/5 (Berkemeier *et al.*, 1991; Klein *et al.*, 1992; Ip *et al.*, 1992), while *trk*C was recognized as the primary receptor for NT-3 (Lamballe *et al.*, 1991) (Figure A.1.1). However, NT-3 has been shown to interact also with *trk*A and *trk*B in transfected cell lines (Cordon-Cardo *et al.*, 1991, Klein *et al.*, 1991b; Soppet *et al.*, 1991; Squinto *et al.*, 1991). The recently identified NT-6, a neurotrophin found in fish, has been shown promote survival of NGF-responsive chick neurons and therefore may bind to *trk*A, albeit with a lower affinity (Götz *et al.*, 1994) (see Figure A.1.1.).

The molecular diversity of *trk* receptors is greatly extended by alternative splicing: to date, we know 2 variants of *trk*A (Barker *et al.*, 1993), 8 variants of *trk*B (Klein *et al.*,

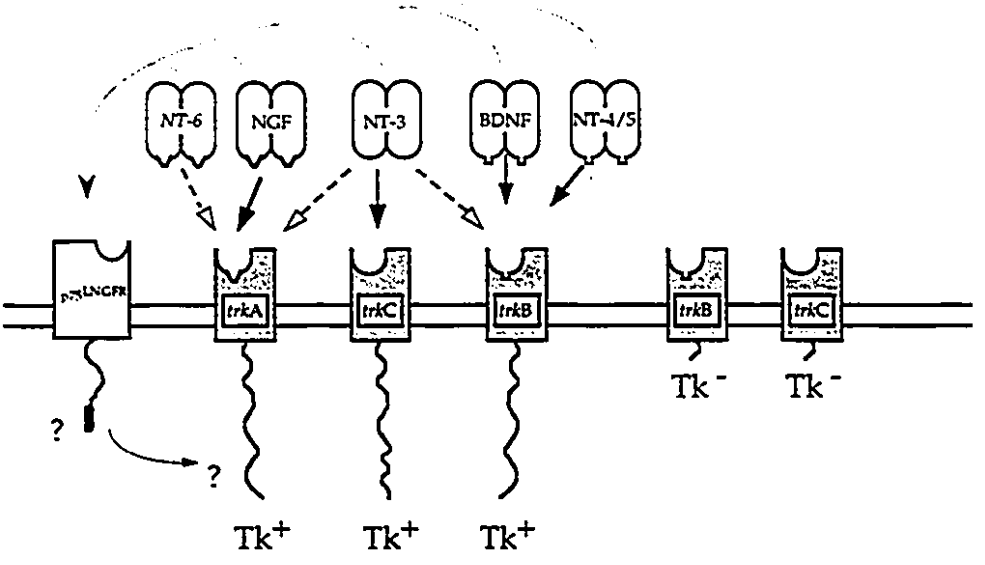

FIGURE A.1.1. Diversity of neurotrophins and neurotrophin receptors

Tk^+= with tyrosine kinase domain

Tk^-= splice variant without a tyrosine kinase domain

Dashed arrows indicate that binding is either at low affinity or has been observed in non-neuronal context.

$p75^{LNGFR}$ binds with similar affinities all neurotrophins. Its role in signallin poorly understood

1989; 1990a; Middlemas *et al.*, 1991), and 8 variants of *trk*C (Lamballe *et al.*, 1991, 1993; Tsoulfas *et al.*, 1993; Valenzuela *et al.*, 1993). The 2 *trk*A variants (796 and 790 amino acids) differ by only 6 amino acids in the extracellular domain; while no differences in their biological properties have been reported, the shorter isoform has been detected mainly in nonneuronal cells (Barker *et al.*, 1993). The 8 isoforms of *trk*B can be classified in two groups designated *trk*B^{TK+} (n=6) and *trk*B^{TK-} (n=2), based on the presence or absence of the intracellular tyrosine kinase (TK) catalytic domain. The same classification can be used for *trk*C isoforms: 4 *trk*C^{TK+}s and 4 *trk*C^{TK-}s. While both truncated isoforms (*trk*B^{TK-} and *trk*C^{TK-}) appear not to transduce signals upon neurotrophin binding, alternative splicing in the TK catalytic domains of *trk*B^{TK+} and *trk*C^{TK+} may confer differential functional properties in these receptors (Valenzuela *et al.*, 1993; Tsoulfas *et al.*, 1993; Garner and Large, 1994). Interestingly, both classes of truncated isoforms have been detected in glial cells but not in neurons (Beck *et al.*, 1993; Frisén *et al.*, 1993; Jelsma *et al.*, 1993; Valenzuela *et al.*, 1993). The role of these truncated isoforms is unknown, although the induction of *trk*B^{TK-} expression in glial cells after injury in the CNS has led to the proposal that they might be involved in ligand recruitment or presentation (Beck *et al.*, 1993; Frisén *et al.*, 1993). A brief description of what is known about the signalling cascades that tyrosine kinase *trk* receptors activate is presented in the following appendix.

$p75^{LNGFR}$

The low-affinity NGF receptor turned out to be a low-affinity pan neurotrophin receptor, and is now referred to as p75 or $p75^{LNGFR}$ (Chao *et al.*, 1986; Radeke *et al.*, 1987; Rodriguez-Tébar *et al.*, 1990, 1992). It has been generally assumed that $p75^{LNGFR}$ is not capable of signalling (Chao, 1994); however, recent experiments have raised the possibility that $p75^{LNGFR}$ is, in fact, capable of mediating intracellular signals (Ohmichi *et al.*, 1991; Tartaglia and Goeddel, 1992; Battleman *et al.*, 1993; Volonte *et al.*, 1993a,b). Protein kinase activities have been found to be associated with $p75^{LNGFR}$ (Ohmichi *et al.*, 1991; Volonte *et al.*, 1993a), including MAPK activity (Volonte *et al.*, 1993b). $p75^{LNGFR}$

exhibits structural resemblance with the TNF receptor family, which are capable of cytoplasmic signalling, and may include a signal for apoptosis (Tartaglia *et al.*, 1993; Rabizadeh *et al.*, 1993; Chao, 1994; Barrett and Bartlett, 1994). An ability of $p75^{LNGFR}$ to promote apoptosis cannot be widespread however, as many cells that express $p75^{LNGFR}$ do not undergo programmed cell death.

However, a number of experiments have shown that $p75^{LNGFR}$ is not essential for NGF mediated signalling through *trk*A (Glass *et al.*, 1991; Ibánez *et al.*, 1992; Jing *et al.*, 1992; Ip *et al.*, 1993b). Nevertheless, several lines of evidence suggest that $p75^{LNGFR}$ plays a role in neurotrophin's action on nerve cells. In summary, $p75^{LNGFR}$ is believed to influence both 1) high-affinity binding of neurotrophins, particularly NGF, and 2) neurotrophin mediated signalling, although not through a $p75^{LNGFR}$-*trk*A dimerization (Milbrandt, 1986; Berg *et al.*, 1991; Hempstead *et al.*, 1991; Rodriguez-Tébar *et al.*, 1992; Scheibe and Wagner, 1992; Davies *et al.*, 1993; Battleman *et al.*, 1993; Benedetti *et al.*, 1993; Barker and Shooter, 1994; Chao, 1994; Ibánez, 1994; Verdi *et al.*, 1994). Moreover, the fact that $p75^{LNGFR}$ is expressed primarily in projection neurons, rather than in local circuit neurons, suggests that $p75^{LNGFR}$ could promote retrograde NGF transport. The underlying mechanisms for these putative functions have not been resolved. The numerous functions that have been proposed for $p75^{LNGFR}$ suggest that it associates with different auxiliary molecules that are differentially expressed during development and in distinct cell types (Chao, 1994).

Appendix 2

Signal Transduction by Neurotrophin Receptors and Ca^{2+} Influx Leading to Gene Expression

Extensive progress has been made over the past few years in elucidating the signal transduction by receptor tyrosine kinases (RTKs). Activation of these receptors by the binding of their ligands is known to affect the expression of many genes via partially identified cascades of phosphorylation events (on tyrosine, serine and threonine residues) propagated down to transcription factors. To date, many of the identified signalling events are shared by most RTKs (e.g. EGF, LIF, NGF receptors); some specificity, however, between the various signals is beginning to unravel (Marshall, 1995). The complexity of these mechanisms is increased by the fact that Ca^{2+} influx during neuronal activity also affects the expression of many of the same genes that are regulated by RTK activity (Sheng and Greenberg, 1990). Moreover, Ca^{2+} influx has been shown to up-regulate neurotrophin and neurotrophin receptor expression (Lindvall *et al.*, 1992, 1994; Bergzon *et al.*, 1993; Merlio *et al.*, 1993; Lindhom *et al.*, 1994).

In nerve cells, genes that are regulated by RTK activity and Ca^{2+} influx have been classified in two groups: the immediate early genes (IEGs) whose transcription occurs rapidly (e.g. min) and transiently, and the delayed response genes (or late response genes) whose expression is modified more slowly (e.g. hours, days) (Ghosh and Greenberg, 1995). The products of these delayed response genes could include proteins that are involved in a variety of neuro-specific functions (Armstrong and Montminy, 1993). Many of the known IEGs (e.g. *c-fos*, *c-jun*) code for transcription factors that bind, often as heterodimers, to DNA sequences (e.g. AP-1 site) that are found in promoter elements of delayed response genes. Therefore, it has been proposed that IEG products control the expression of delayed response genes; in this way, induction of IEG expression constitutes an upstream event in the signalling pathway leading to expression of delayed response gene. However, a direct link between IEG expression and transcriptional activation of

delayed response genes during synaptic activity or upon growth factors activation has not yet been established (Armstrong and Montminy, 1993; Morgan and Curran, 1995). Most of our understanding on these signalling pathways comes from experiments with cultures of cell lines and, in some instances, have been confirmed in primary neurons.

Figure A.2.1 makes a naive attempt at summarizing some of the intracellular signalling events triggered by transynaptic activity and NGF receptor activity. This sketch makes, by no means, a fair representation of everything that is known (or not known) about signal transduction via Ca^{2+} and NGF. This diagram emphasizes primarily the most characterized pathway that NGF use to regulate neuronal differentiation and gene expression. It also describes in parallel a Ca^{2+}/calmodulin-dependent protein kinase pathway which is relevant to the results presented in Chapter 6. This diagram also illustrates some of the potential cross talks between NGF- and Ca^{2+}-induced signalling events. Despite the apparent redundancy and convergence in these pathways, specificity among these signals may reside in the time courses, cellular locations, intensities or frequencies at which these converging pathways are stimulated (Sheng and Greenberg, 1990; Schulman, 1993; Marshall, 1995; Ghosh and Greenberg, 1995). As overwhelming as they may seem, these multiple interactions provide neurons with the capacity to regulate the expression of the appropriate genes at the appropriate time, while using a limited set of molecules.

However, a major aspect that this figure fails to illustrate is how genes are turned off. Indeed, negative regulation may actually play a much greater role in regulating neuronal function than currently appreciated (Mandel and McKinnon, 1993). A growing number of neuro-specific genes have been shown to contain promoter elements that restrict their expression in their appropriate neuronal context (Maue *et al.*, 1990; Kraner *et al.*, 1992; Schoenherr and Anderson, 1995). The mechanisms underlying negative regulation of neuro-specific genes are, for the most part, enigmatic; however, a neuro-restrictive silencer factor (NRSF) was recently identified. This factor, which represses multiple neuro-specific genes, is expressed in non-neuronal cells and in undifferentiated neuronal progenitors, while its expression disappears in neurons (Schoenherr and Anderson, 1995). Beyond these mechanisms that determine neuro-specific genes (e.g. from liver-specific genes), may

exist others that restrict expression to a particular subset of neurons. Although this should hold for any tissue, the complex mosaic of phenotypically distinct cells in the brain requires a more elaborated assortment of positive and negative regulators. There seems to be an unusually diverse array of transcriptional activators that are activated by external stimuli; silencing elements should be in place in the nervous system in order to obtain some specificity in gene regulation (Mandel and McKinnon, 1993).

Figure A.2.1 was based on the following references:
Sheng and Greenberg, 1990; Koch *et al.*, 1991; Ginty *et al.*, 1991; Hanson and Schulman, 1992; Wegner *et al.*, 1992; Egan and Weinberg, 1993; McCormick, 1993; Schulman, 1993; Enslen and Soderling, 1994; Kaplan and Stephens, 1994; Rosen *et al.*, 1994; Srinivasan *et al.*, 1994; Tanaka and Nishizuka, 1994; Cohen *et al.*, 1995; Ghosh and Greenberg, 1995; Hill and Treisman, 1995; Hunter, 1995; Marshall, 1995; Pawson, 1995.

Figure description: The binding of NGF dimers to *trk*A induces dimerization and autophosphorylation of *trk*A creating 5 phosphotyrosine sites on the receptors. These residues then become "docking sites" for SH2 domain-containing proteins; *src* homology (SH) regions 2 and 3, referred as to SH2 and SH3 domains, are non-catalytic domains conserved among many cytoplasmic signalling proteins. SH2 domains bind specifically to tyrosine phosphoproteins. Three SH2 domain-containing signalling molecules are known to associate with autophosphorylated *trk*A, and in turn become phosphorylated: SHC, phospholipase C-γ1 (PLC-γ1) and phosphatidylinositol-3 or PI-3 kinase. An adaptor protein (e.g. Grb2), binds to phosphorylated SHC via its SH2 domain. This adaptor protein also possess SH3 domains, which bind to specific proline-rich motifs, such as those of the guanine nucleotide exchange factor (GEF) named SOS. Consequently, Grb2 recruits SOS near the plasma membrane where Ras activation is presumed to take place. SOS presents a guanine nucleotide to the inactive Ras-GDP (also called $p21^{ras}$), which converts it to an active Ras-GTP. The active Ras turns on a cascade of phosphorylations from kinase to kinase ending by the activation of MAPK (mitogen-activated-protein- or microtubule-associated-protein-2- kinase). Briefly, a MAPK kinase (MEK) is activated by a MEK kinase (e.g. Raf or MEKK) that has been activated by Ras. MAPK (also termed ERK) is a multifunctional kinase with many substrates, including *rsk*, transcription factors (TFs) and MAP2. MAPK can translocate into the nucleus to phosphorylate TFs or phosphorylate proteins such as *rsk* which themselves translocate into the nucleus to phosphorylate TFs. This signalling cascade is turned off by the rapid hydrolysation of Ras-GTP back to its inactive form by an intrinsic GTPase activity. In addition, GTPase activating proteins (GAPs) will catalyse this inactivation. GAPs also possess SH2 domains, therefore they may also be activated by RTK activity, and thus counteract accumulation of Ras-GTP induced by a GEF. Perhaps then, effective signal transmission through the Ras route occurs only when GAPs are inhibited. This signalling cascade is likely to be intercepted by several signals, either positive or negative, or there may be shorter routes, such as the direct association between *trk*A and MAPK. Such association could occur when *trk*A is internalized; retrogradely transported *trk*A could remain autophosphorylated, while NGF resides inside the transport vesicles. Internalized *trk*A can therefore possibly travel near the nucleus and activate signalling proteins such as MAPK. PI-3 kinase also associates with autophosphorylated *trk*A via its SH2 domain. Its function is poorly understood, although it may have a role in protein sorting and trafficking, which could include the targeting of internalized *trk*A. PLC-γ1 also associates with *trk*A; it catalyses the hydrolysis of PI 4,5-bisphosphate to the potent second messengers inositol triphosphate (IP_3) and diacylglycerol (DAG). DAG activates PKC, while IP_3 triggers release of Ca^{2+} from internal stores. It is possible that PKC phosphorylates a GEF directly, which would activate the ras-MAPK cascade. Finally, *trk*A activation leads to tyrosine phosphorylation of the protein SNT which is found primarily in the nucleus. Its role is unknown, but to date it is the only identified target of RTK activity that is specific for *trk*A, therefore its activity may underlie some of the specificity in neurotrophin action.

When Ca^{2+} flows inside the cell, it activates, among several targets, protein kinases, such as CaM kinases, PKCs and adenylate cyclase (AC). AD produces second messenger cAMP that activates PKA, which can phosphorylate the CRE binding protein CREB, a TF for genes that contain Ca^{2+} response elements (CaRE and CRE or Ca/CRE; found notably in IEGs). PKC, via an unknown pathway can activate a TF, named serum response factor (SRF), which binds to the serum response element (SRE) of IEGs, such as *c-fos*. CaM kinase IV is a monomeric enzyme that can penetrate into the nucleus and phosphorylate CREB. CaM kinase II is multimeric and can remain active for a prolonged period, because of inter-subunits phosphorylation. CaM kinase II can phosphorylate CREB and other TFs. Ca^{2+} may activate gene expression via activation of Ras-MAPK cascade. The signal that activates Ras by Ca^{2+} is unknown; it may involve a protein kinase, such as CaM kinase or PKC, which could phosphorylate GEF thereby activating the Ras-MAPK cascade, or phosphorylate GAP, which may decrease hydrolysation of active Ras-GTP into inactive Ras-GDP. Another appealing possibility, purely speculative, is that phosphorylation of Ca^{2+} channels, such as voltage dependent Ca^{2+} channels (particularly L-type Ca^{2+} channels) and ligand-gated channels (NMDAR and nAChR) occurs when Ca^{2+} flows through the channel. This could provide a substrate for the SH2 domains of GRB2 and thus trigger the GEF-Ras cascade. Conceivably, such a mechanism may necessitate the spatial arrangement of the Ca^{2+} channels with the Ras activators, in order to confer specificity in the induction by Ca^{2+} influx.

Few examples of delayed response genes being regulated by external signals have been described in neurons, and we know very little about how these signals operate to induce their expression. The identification α7 nAChR gene as a candidate delayed response gene and the identification of a CaM kinase pathway leading to α7 up-regulation provide a good model for investigating the relationship between activity, kinase activity, IEG expression and delayed response gene expression in neurons (Chapter 6).

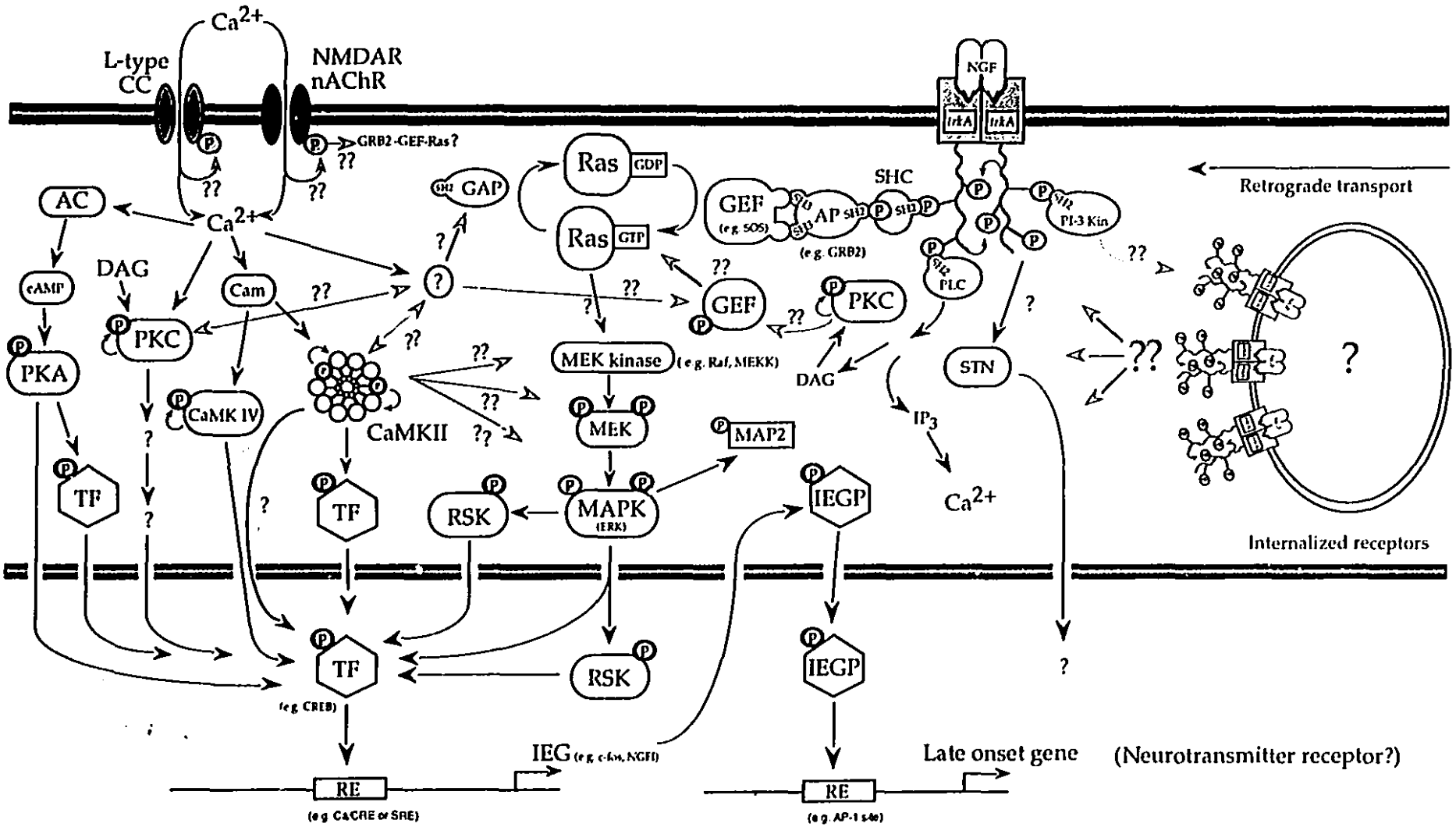
Ca2+
L-type CC
NMDAR nAChR
NGF
trkA
GRB2-GEF-Ras?
AC
cAMP
PKA
DAG
PKC
Cam
CaMK IV
Ca2+
GAP
Ras GDP
Ras GTP
GEF (e.g. SOS)
AP
SHC
(e.g. GRB2)
PI-3 Kin
PLC
Retrograde transport
MEK kinase (e.g. Raf, MEKK)
MEK
MAPK (ERK)
MAP2
CaMKII
RSK
TF
IP3
STN
IEGP
Internalized receptors
(e.g. CREB)
IEG (e.g. c-fos, NGFI)
RE
(e.g. CaCRE or SRE)
Late onset gene
(e.g. AP-1 site)
(Neurotransmitter receptor?)
P = Serine/Threonine phosphorylated
R = Tyrosine phosphorylated
? = Identified pathway through unknown mechanism
?? = Possible pathway, still speculative (dashed arrow)

Appendix 3

The Multifunctional Ca^{2+}/Calmodulin-Dependent Protein Kinase II

CaM kinase II is part of a large group of enzymes that are activated by the Ca^{2+} receptor, calmodulin. While CaM kinase I, III, and the myosin-light chain kinase have narrow and relatively specialized substrate protein specificities, CaM kinase II phosphorylates a wide scope of substrates that are important in almost every major cellular activity (Hanson and Schulman, 1992). In nerve cells, it has been shown to regulate neurotransmitter synthesis and release, ion channels, cytoskeletal function and gene expression (Hanson and Schulman, 1992). Two CaM Kinase II subunits, α and β, are highly expressed in the nervous system: for example, they comprise as much as 2% of total hippocampal proteins (Kennedy, 1992). Both subunits are abundant in dendrites, and the mRNA coding for the α subunit is targeted to dendrites (Burgin *et al.*, 1990). Furthermore, CaM kinase II may comprise as much as 20-30% of the postsynaptic densities (Kennedy, 1992).

The most interesting features of CaM kinase II are its regulatory properties that may confer to the enzyme the ability to translate synaptic activity into biochemical signals. CaM kinase II is a multimeric holoenzyme formed by 8-10 subunits arranged in a "rosette", with the catalytic and regulatory domain on the outside and the association domain in the center (Schulman, 1993; see Figure A.3.1). Activation of the kinase occurs by trapping of Ca^{2+}-bound calmodulin onto the autoinhibitory site of a subunit, which then autophosphorylates itself (Meyer *et al.*, 1992). This converts the subunit into a Ca^{2+}-independent enzyme that still remains active beyond the duration of the activating Ca^{2+} signal. Autophosphorylation also occurs between neighbouring subunits within the holoenzyme; therefore two calmodulin molecules are needed, one to activate a subunit and the other to present an autoinhibitory domain of its neighbouring subunit for autophosphorylation. This means that phosphorylation of only one or two subunits may be sufficient to produce activation of all other subunits. This process is highly cooperative

and may render activation of the enzyme dependent on the frequency of Ca^{2+} oscillations (Hanson and Schulman, 1992; Schulman, 1993; Hanson *et al.*, 1994).

Likewise, CaM kinase II appears to be a major player in generation of LTP. Its role was first demonstrated by application of specific CaM kinase II inhibitors, which completely blocked LTP induction, but not its maintenance (Malinow *et al.*, 1989). Also, Ocorr and Schulman (1991) showed that LTP increases the level of Ca^{2+}-independent CaM kinase II activity in hippocampal slices. More recently, mutant mice lacking the CaM kinase II α subunit were generated (Silva *et al.*, 1992a); these mice developed apparently normally with no obvious anatomical change in their brain. The synaptic currents measured by whole-cell recording in hippocampal neurons of mutant mice also appeared normal. However, in most experiments hippocampal slices from these mice displayed no LTP, providing strong support for CaM kinase II playing a critical role in LTP.

In addition Silva *et al.* (1992b) showed, in a following study, that these mutant mice had impaired spatial learning. Although these mice appeared to have normal vision and the ability to navigate, they could not use spatial visible cues to locate a hidden platform in a "Morris water task". These results also add support to the hypothesis that phenomena such as LTP and LTD underlie some forms of learning and memory.

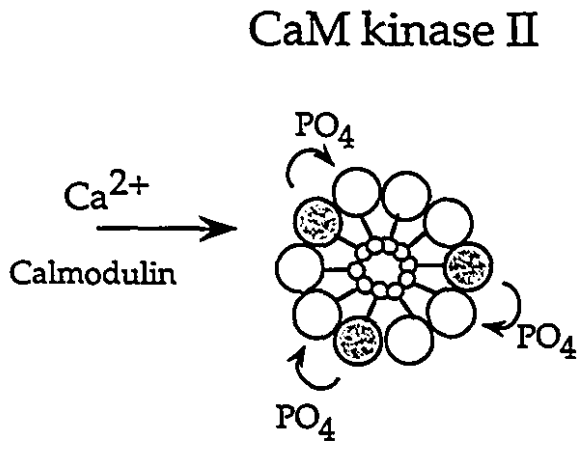

FIGURE A.3.1 Multimeric CaM kinase II. Autophosphorylation of CaM kinase II involves intra- and inter-subunit phosphorylations. This provide to the multimeric enzyme with the ability to remain active long periods after Ca^{2+} stimulation. Furthermore, differences in stimulation frequency may produce distinct levels of autophosphorylation of the multimeric enzyme, which may confer Ca^{2+} spike frequency decoding properties to CaM kinase II.